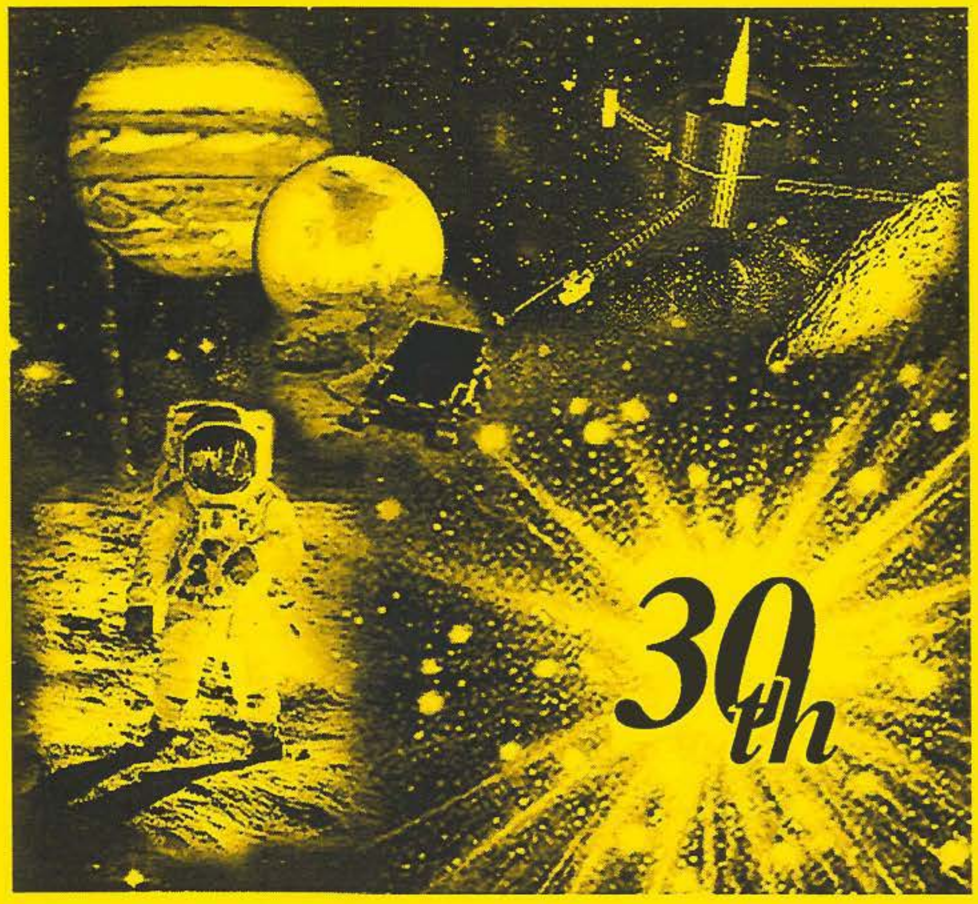


# Lunar and Planetary Science Conference

## March 15–19, 1999
## Houston, Texas

Sponsored by

National Aeronautics and Space Administration
Lunar and Planetary Institute
NASA Johnson Space Center

LPI

## Program to Technical Sessions

# THIRTIETH LUNAR AND PLANETARY SCIENCE CONFERENCE

**March 15–19, 1999**

**Houston, Texas**

### Sponsored By

National Aeronautics and Space Administration
Lunar and Planetary Institute
NASA Johnson Space Center

### Program Committee

Carl Agee, Co-Chair, *NASA Johnson Space Center*
David Black, Co-Chair, *Lunar and Planetary Institute*
Conel Alexander, *Carnegie Institution of Washington*
Carlton Allen, *Lockheed Martin*
Donald Bogard, *NASA Johnson Space Center*
Harold Connolly, Jr., *California Institute of Technology*
Cassandra Coombs, *College of Charleston*
John Grant, *NASA Headquarters*
Friedrich Hörz, *NASA Johnson Space Center*
Michael Kelley, *Rensselaer Polytechnic Institute*
Walter Kiefer, *Lunar and Planetary Institute*
David Kring, *University of Arizona*
Renu Malhotra, *Lunar and Planetary Institute*
Timothy Parker, *Jet Propulsion Laboratory*
Frans Rietmeijer, *University of New Mexico*
Graham Ryder, *Lunar and Planetary Institute*
Susan Sakimoto, *NASA Goddard Space Flight Center*
Paul Spudis, *Lunar and Planetary Institute*
Meenakshi Wadhwa, *Field Museum of Natural History, Chicago*

LPI

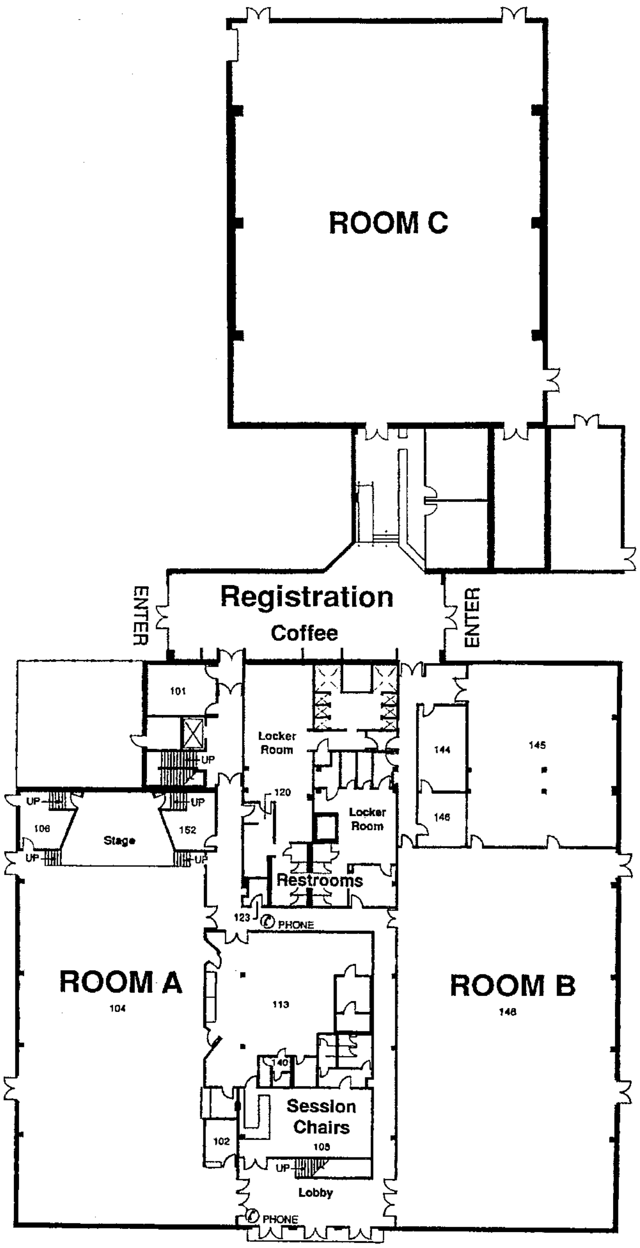


**FIRST FLOOR**
**Robert R. Gilruth Recreation Facility**
**Building 207**

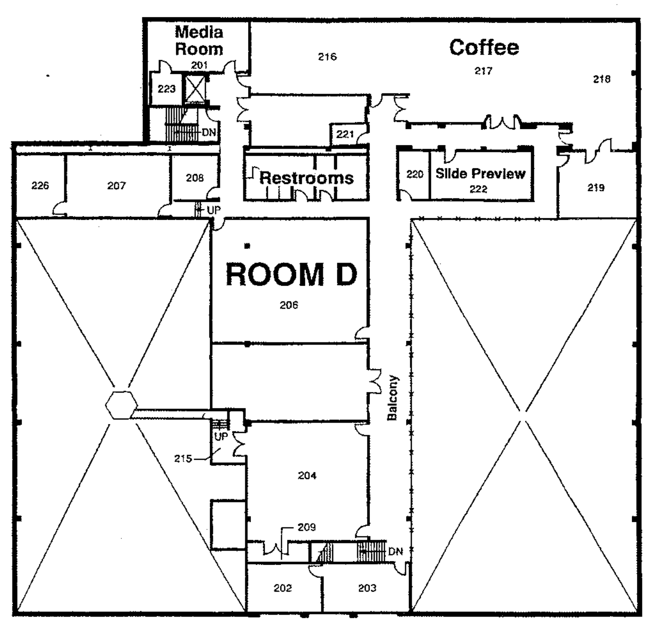


**SECOND FLOOR**
**Robert R. Gilruth Recreation Facility**
**Building 207**

# CONFERENCE INFORMATION

## Registration—LPI Open House

A combination Registration/Open House will be held Sunday, March 14, 1999, from 5:00 p.m. until 8:00 p.m. at the Lunar and Planetary Institute. Registration will continue in the Gilruth Center, Monday through Thursday, 8:00 a.m. to 5:00 p.m. A shuttle bus will be available to transport participants between the LPI and local hotels Sunday evening from 4:45 p.m. to 8:30 p.m.

## Message Center

A message center will be established in the registration area in the Gilruth Center during the oral sessions. People who need to contact attendees during the conference may call 281-483-0321. The message center will be open Monday through Thursday from 8:00 a.m. to 5:00 p.m. and Friday from 8:00 a.m. until noon. A fax machine will be located at the staff desk for **incoming messages only**. Faxes should be sent to 281-483-8722. Telephone messages and faxes will be posted on a bulletin board near the registration desk.

## Transportation Assistance

Assistance with arranging airline reservations is available from the Omega World Travel Office in Room 130 of Building 1 (phone 281-483-3305). Conference badges must be worn for entrance to this building. This service will be available each day of the conference from 8:00 a.m. to 5:00 p.m.

## Shuttle Bus Service

A shuttle bus service between JSC, LPI, University of Houston–Clear Lake, and various hotels will operate daily. A detailed schedule of the shuttle routes is in your registration packet and is available at the registration desk.

## Badges

During the week of the conference, your conference badge will allow access to JSC at all gates, the first floor of Building 1 (Travel Office), and the Gilruth Center. Please be aware that this badge does not allow access to those areas or buildings not open to the general public except those specifically outlined above.

## Space Center Houston

Space Center Houston is open from 10:00 a.m. until 7:00 p.m. daily. Major attractions are the Mission Status Center, Starship Gallery, tour of JSC, Space Shuttle Mock-Up, Space Center Theater, Manned Maneuvering Unit, and Space Center Plaza. Restaurants and gift shops are available. The ticket prices are $12.95 for adults and $8.95 for children. For further information call 281-244-2105.

## GUIDE TO TECHNICAL SESSIONS AND ACTIVITIES

**Monday Morning, 8:30 a.m.**

| | |
|---|---|
| Room A | Presolar Grains |
| Room B | Lunar Volcanos: From the Inside Out |
| Room C | Mars Lander Science |
| Room D | Impacts I |

**Monday Afternoon, 1:30 p.m.**

Room C **PLENARY SESSION**

Presentations to the 1998 GSA Stephen E. Dwornik Student Paper Award Winners followed by

**Harold Masursky Lectures**

**Monday Afternoon, 3:00 p.m.**

| | |
|---|---|
| Room A | Venus Geology and Geophysics |
| Room B | Planetary Interior Processes |
| Room C | Mars Surface Chemistry |
| Room D | SPECIAL SESSION — NEAR at Eros |

**Tuesday Morning, 8:30 a.m.**

| | |
|---|---|
| Room A | Early Solar System Processes and Timescales |
| Room B | SPECIAL SESSION — New Moon I: Hot Spots, Gravity, and Magnetism |
| Room C | SPECIAL SESSION — Mars Global Surveyor (MGS): A New Chapter |
| Room D | Icy Satellites |

**Tuesday Noontime, 12:15 p.m.**

Room C SPECIAL SESSION — Future Planetary Missions

**Tuesday Afternoon, 1:30 p.m.**

| | |
|---|---|
| Room A | Calcium-Aluminum-rich Inclusions (CAIs) |
| Room B | SPECIAL SESSION — New Moon II: Major Lunar Terrains |
| Room C | Mars Global Surveyor (MGS): Oceans, Basins, and More |
| Room D | Cosmic Dust |

**Tuesday Evening, 7:00–9:30 p.m.**

UHCL Bayou Bldg. Poster Session I

*Mars Global Surveyor (MGS) and Pathfinder*
*Lunar Volcanos from the Inside Out*
*New Moon Views*
*Venus Geology and Geophysics*
*Europa*
*Small Bodies*
*Origins of Planetary Systems*
*Presolar Grains*
*Calcium-Aluminum-rich Inclusions (CAIs) and Chondrules*
*Chondrites*
*Astrobiology: Precursors, Origins, and Martians*
*Cosmic Dust*
*Planetary Interior Processes*
*Impacts I*
*Special Session — Future Missions: Science and Technology*

**Wednesday Morning, 8:30 a.m.**

| | |
|---|---|
| Room A | Martian Meteorites I: The Newest and the Oldest |
| Room B | Impacts II |
| Room C | Mars Global Surveyor (MGS): Volcanics and Surfaces |
| Room D | Origins of Planetary Systems |

**Wednesday Afternoon, 1:30 p.m.**

| | |
|---|---|
| Room A | Chondrules |
| | ***Session dedicated to the memory of Elbert King*** |
| Room B | Lunar Structure, Evolution, and Highlands |
| Room C | Mars Tectonics, Volcanism, and Interior |
| Room D | Small Bodies |

**Wednesday Evening, 6:00–9:30 p.m.**

Conference Social Event, Campbell Hall, Pasadena Fairgrounds

**Thursday Morning, 8:30 a.m.**

| | |
|---|---|
| Room A | Martian Meteorites II: Shergottites, Nakhlites, and Chassigny |
| Room B | Chondrites I: Alteration and Processing |
| Room C | Mars Climate, Polar Caps, and Hydrology |
| Room D | Lunar Poles and Regolith |

**Thursday Afternoon, 1:30 p.m.**

| | |
|---|---|
| Room A | Astrobiology: Precursors, Origins, and Martians |
| Room B | Achondrites and Anomalous Meteorites |
| Room C | Io |
| Room D | Planetary Surface Processes |

**Thursday Evening, 7:00–9:30 p.m.**

UHCL Bayou Bldg. Poster Session II

*Education: Fun in the Classroom*
*Outer Planet Satellites*
*Small Icy Bodies*
*Achondrites*
*Iron Meteorites*
*Meteorite Mélange*
*Cosmogenic Nuclides*
*Martian Meteorites*
*Mars: General Science*
*Future Mars Missions*
*Recipes for Lunar Rocks*
*Lunar Missions and Data*
*Lunar Poles and Regolith*
*Mercury*
*Impacts II*
*Planetary Surface Processes*
*New Instruments and Techniques*
*Digital Datasets*

**Friday Morning, 8:30 a.m.**

| | |
|---|---|
| Room A | Near-Future Mars Missions |
| Room B | Iron Meteorites and Platinum-Group Elements |
| Room C | Europa |
| Room D | Chondrites II: Portales Valley and Others |

** Designates Speaker*

***Room A – Gilruth Room 104***
***Room B – Gilruth Old Gym***
***Room C – Gilruth New Gym***
***Room D – Gilruth Room 206***
***UCHL – Bayou Building, University of Houston–Clear Lake***

## Monday, March 15, 1999
## PRESOLAR GRAINS
## 8:30 a.m. Room A

**Chairs: D. D. Clayton**
**A. M. Davis**

Nittler L. R.* Alexander C. M. O'D.
*Automatic Identification of Presolar Al- and Ti-rich Oxide Grains from Ordinary Chondrites* **[#2041]**
We report the use of a fully automated $^{17}O/^{16}O$ and $^{18}O/^{16}O$ mapping technique to locate twenty-four new presolar oxide grains, including the first report of a presolar titanium oxide grain, in a mixed acid residue of four ordinary chondrites.

Liu W.* Clayton D. D.
*Condensation of Carbon in Supernovae: 1. Basic Chemistry* **[#1108]**
Contrary to the conventional wisdom on cosmic dust condensation based on thermochemical equilibrium theory, kinetic chemistry demonstrates that carbon condenses in supernovae even if C<O because radioactivity destroys the CO trap.

Bernatowicz T.* Bradley J. Amari S. Messenger S. Lewis R.
*New Kinds of Massive Star Condensates in a Presolar Graphite from Murchison* **[#1392]**
We report the discovery of two new kinds of presolar condensates (kamacite and cohenite) in a presolar graphite originating in a supernova.

Braatz A.* Ott U. Henning Th. Jäger C. Jeschke G.
*Nitrogen Configuration in Presolar Diamonds* **[#1551]**
The different optical features of diamonds depend predominantly on their nitrogen contents and configurations. We have tried to deduce the nitrogen configuration of diamonds from the Murchison meteorite, using combined IR and EPR measurements.

Meshik A. P.* Pravdivtseva O. V. Hohenberg C. M.
*Separation of Xe-H and Xe-L by Selective Laser Absorption in Murchson Diamonds* **[#1621]**
Selective laser absorption experiments in meteoritic diamonds are continued. Heating by pulsed lasers at 1064 nm and, to a lesser extent, 266 nm seems to selectively separate Xe-H from Xe-HL in Murchison diamond separates, while 533 nm does not.

Verchovsky A. B.* Fisenko A. V. Semjonova L. F. Wright I. P. Pillinger C. T.
*Presolar Diamonds from Efremovka & Boriskino: C, N and Noble Gas Isotopes in Grain Size Fractions and Implications for the Origin of Diamonds* **[#1746]**
In addition to the four grain size fractions of diamonds separated from the Efremovka (CV3) meteorite reported earlier, six more diamond size-fractions from the same meteorite have been generated with sizes both coarser and finer than the original set.

Fahey A. J.* Messenger S.
*Isotopic Measurements of Murchison and Semarkona Residues by TOF-SIMS* **[#1101]**
We have developed a method to measure isotopic ratios in individual articles by and have measured numerous terrestrial materials for their Si and Mg isotopic ratios as well as individual grains from Murchison and Semarkona.

Hoppe P.* Strebel R. Amari S. Lewis R. S.

*Silicon-isotopic Compositions of Individual, Submicrometer-sized Presolar Silicon Carbide Grains* **[#1256]**

We report Si-isotopic compositions of 69 individual, submicrometer-sized presolar SiC grains. The Si-isotope systematics resembles that of the micron-sized grains except that the fraction of the rare type Y/Z grains is significantly higher.

Lugaro M. Gallino R. Zinner E.* Amari S.

*Si Isotopic Ratios in Mainstream Presolar SiC Grains Revisited* **[#1403]**

We present a Monte Carlo model for local heterogeneities in the Si isotopic composition due to the stochastic nature of contributions from different types of supernovae. This model successfully reproduces the Si isotopic ratios of mainstream presolar SiC grains.

Amari S.* Nittler L. R. Zinner E. Lewis R. S.

*Titanium Isotopic Ratios in Presolar SiC Grains of Type A and B* **[#1009]**

Titanium isotopic ratios of presolar SiC grains of type A and B from Murchison show 4 distinct patterns, reflecting complexities of the origin of grains of these types and of nuclear reactions responsible for the observed patterns throughout the history of the galaxy.

Pellin M. J.* Davis A. M. Lewis R. S. Amari S. Clayton R. N.

*Molybdenum Isotopic Composition of Single Silicon Carbide Grains from Supernovae* **[#1969]**

Measurement of Mo isotopic compositions of single presolar SiC grains from supernovae show a signature of r-process nucleosynthesis, but a different one from that responsible for solar system Mo.

Meyer B. S.* Nichols R. H. Podosek F. A. Jennings C. L.

*Subtleties in Computing Anomalies from Late Nucleosynthetic Additions to the Proto-Solar Nebula* **[#1904]**

Computing isotopic anomalies from late addition of massive star ejecta into solar material is subject to error due to systematic flaws in stellar yields. More realistic anomaly estimates come from admixture of stellar yields with compositions from chemical evolution models.

Robert F.* Hanon P. Chaussidon M.

*A Summary of the Li-Be-B Isotopic Compositions and Elemental Ratios in Chondrites: Implications for Light Element Nucleosynthesis* **[#1188]**

LiBeB elemental and isotopic ratios in chondrites are compared with the theoretical predictions which can be made from nuclear reaction rate ratios. The agreement between the prediction and the data from carbonaceous chondrites is almost perfect.

**Monday, March 15, 1999**
**LUNAR VOLCANOS: FROM THE INSIDE OUT**
**8:30 a.m. Room B**

**Chairs: C. Coombs**
**G.A. Snyder**

Warren P. H.* Ulff-Møller F.
*Lunar Meteorite EET96008: Paired with EET87521, but Rich in Diverse Clasts* **[#1450]**
We have studied the bulk composition and petrology of the EET96008 lunar meteorite. This fragmental breccia is nearly pure VLT mare basalt and paired with EET87521. However, the sample is rich in diverse clasts, e.g., highland impact melt breccia.

Snyder G. A.* Neal C. R. Ruzicka A. M. Taylor L. A.
*Lunar Meteorite EET 96008, Part II: Whole-Rock Trace-Element and PGE Chemistry, and Pairing with EET 87521* **[#1705]**
Mineral-chemical and trace-element data on the "new" lunar meteorite EET 96008 suggest pairing with EET 87521 and indicate little affinity with VLT mare basalt.

Shih C.-Y.* Nyquist L. E. Bogard D. D. Reese Y. Wiesmann H. Garrison D.
*Rb-Sr, Sm-Nd and $^{39}Ar$-$^{40}Ar$ Isotopic Studies of an Apollo 11 Group D Basalt* **[#1787]**
Rb-Sr, Sm-Nd and $^{39}Ar$-$^{40}Ar$ age data for Apollo 11 Group D basalt 10002,1003 will be presented. Its source isotopic composition will be discussed.

Neal C. R.* Jain J. C. Snyder G. A. Taylor L. A.
*Platinum Group Elements from the Ocean of Storms: Evidence of Two Cores Forming?* **[#1003]**
PGE data are presented for 7 Apollo 12 basalts to investigate the PGE budget of their source regions.

Elkins L. T.* Grove T. L.
*Origin of Lunar Ultramafic Green Glasses: Constraints from Phase Equilibrium Studies* **[#1035]**
The compositional variability displayed in Apollo 14 and 11 green glasses was produced by fractional crystallization of olivine and orthopyroxene combined with assimilation of sunken high-Ti lunar magma ocean cumulates at 440 km depth.

Papike J. J.* Fowler G. W. Adcock C. T. Shearer C. K.
*Systematics of Ni and Co in Olivine from Planetary Melt Systems: Lunar Mare Basalts* **[#1006]**
Olivine Co/Ni systematics in Apollo 12 basalts were studied by SIMS and correlated with EMP data. Our results, along with previous studies, show that (12009) was extruded onto the lunar surface and is parental to five other cumulates (12075,-020,-018,-040,-035).

McKay G. A.* Le L.
*Partitioning of Tungsten and Hafnium Between Ilmenite and Mare Basaltic Melt* **[#1996]**
Early results from an experimental study of W partitioning between ilmenite and melt suggest that ilmenite has significant capacity to fractionate W from Hf.

Hess P. C.* Parmentier E. M.
*Asymmetry and Timing of Mare Volcanism* **[#1360]**
Mare volcanism is long-lived but unevenly distributed in space and time. The cumulate overturn model helps to explain the longevity, the sparse volcanic output, the timing and possibly the nearside-farside asymmetry in mare volcanism.

Zhong S.* Parmentier E. M. Zuber M. T.
*Early Lunar Evolution and the Origin of Asymmetric Distribution of Mare Basalts* **[#1789]**
We demonstrate that the hemispheric asymmetry in the distribution of mare basalts may be explained as a result of instability of the illmenite cumulate layer above the metallic core, as long as the metallic core is relatively small.

Hiesinger H.* Head J. W. III Jaumann R. Neukum G.

*Lunar Mare Volcanism* **[#1199]**

We present lunar mare basalt ages and relate them to the titanium concentration. We also provide volume estimates and discuss the influence of crustal thickness on basalt eruptions.

Hawke B. R.* Giguere T. G. Blewett D. T. Lucey P. G. Peterson C. A. Taylor G. J. Spudis P. D.

*Remote Sensing Studies of Ancient Mare Basalt Deposits* **[#1956]**

The purposes of this report are to examine the way that multiple data sets were used to investigate ancient lunar volcanism and to present the most recent results of our studies of cryptomare using Galileo, Clementine, and Lunar Prospector data.

Gillis J. J.* Spudis P. D.

*Preflow Structure and Topography Controlling Mare Basalt Flows* **[#2019]**

Remote sensing observations of how preflow structure and topography influence the process of rille formation. Volcanic features examined within the Orientale and Australe basin support rille formation as primarily a constructional process.

Clark P. E.* Evans L.

*Determining Lunar Titanium Abundance on the Basis of Combined Remote Sensing Techniques* **[#1824]**

Lunar Ti derived from Apollo gamma-ray and Clementine spectral reflectance are compared, both showing unimodal distribution. CSR Ti values are correlated with bulk Fe estimates, an effect now noted for all spectral reflectance derived Ti maps.

**Monday, March 15, 1999**
**MARS LANDER SCIENCE**
**8:30 a.m. Room C**

**Chairs: P. A. Bland**
**J. W. Rice**

Golombek M. P.*
*Erosion Rates at the Mars Pathfinder Landing Site and Climate Change on Mars* **[#1387]**
Aeolian features at the Pathfinder site limit the deflation rate to <0.1 nm/yr (or m/Ga) and argues for the present cold and dry environment since 3.5–1.8 Ga. Growing evidence suggests an earlier wetter environment with erosion rates orders of magnitude higher.

Kuzmin R. O.* Greeley R.
*Local and Regional Aeolian Geomorphology at the Mars Pathfinder Landing Site Area: Evidence for Paleowind Regime* **[#1415]**
Images from the Mars Pathfinder and Global Surveyor missions for the MPF site show a complex aeolian history with evidence for a change in the climate/wind regime from ESE-WNW to the current NE-SW wind.

Bridges N. T.* Parker T. J. Kramer G. M.
*Rock Abrasion on Mars: Clues from the Pathfinder and Viking Landing Sites* **[#1907]**
Ventifact morphology and statistics at the three Mars landing sites are examined using new "super-resolution" IMP and Viking Lander images.

Stefanis M. S.* Moore H. J.
*Impact Crater Deposits at the Mars Pathfinder Landing Site: Updated Results Considering Effects of Aerodynamic Drag on Ejecta* **[#1409]**
When effects of aerodynamic drag are considered, conclusions regarding material at the MPF site can be drawn. Impactites from distant craters are unlikely, even with the new calculations of mu ratios. Thus, the majority of materials would be locally derived.

Bland P. A.* Smith T. B.
*Meteorite Accumulations on Mars* **[#1673]**
We identify a narrow range of small-mass meteoroids which should impact Mars surface at survivable speeds. With oxidative weathering $\sim 10^{-3}$ lower than Earth, this small flux could give rise to large accumulations: $\sim 10^4$ meteorites > 10 g per $km^2$.

Hörz F.* Cintala M. J.
*Collisionally Processed Rocks on Mars* **[#1641]**
Pathfinder photos suggest that specific surface features and overall shapes of some boulders reflect collisional processes on sub-meter scales on the martian surface.

Rice J. W. Jr.* Lemmon M. T. Smith P. H. Yingst R. A.
*Sedimentary Structures at the Mars Pathfinder Landing Site* **[#2063]**
Fluvial geomorphic investigations show that a rich and complex history of events has occurred at the Pathfinder landing site.

Parker T. J.* Kirk R. L. Davies M. E.
*Location and Geologic Setting for the Viking 1 Lander* **[#2040]**
Super res. of the horizon at VL-1 has revealed "new" features we use for triangulation. We propose an alternative landing site location for which we believe the confidence is very high. Super res. of VL-1 images also reveals much of the drift material at the site to consist of gravel-size deposits.

Larsen K. W.* Arvidson R. E. Jolliff B. L. Clark B. C.

*Comparisons of Soils and Rocks at the Viking Lander 1 and Pathfinder Landing Sites* **[#1443]**

Comparison of images taken at the Viking 1 and Pathfinder landing sites indicates a greater abundance of dark granules at the Pathfinder site. Correspondence analysis applied to the chemical data obtained at these sites supports this conclusion.

McSween H. Y. Jr.* Ghosh A.

*Sulfur Mixing Relationships in Martian Soils, and Possible Implications for a Globally Homogeneous Dust Layer* **[#1083]**

Linearities in plots of Viking and Pathfinder soil compositions may arise from cementation by sulfate. Viking sulfur-poor dust is similar to Pathfinder average soil, but differences in some elements argue against a globally homogeneous dust layer.

Brückner J. Dreibus G.* Lugmair G. W. Rieder R. Wänke H. Economou T.

*Chemical Composition of the Martian Surface as Derived from Pathfinder, Viking, and Martian Meteorite Data* **[#1250]**

New APXS data of C (< 0.8 wt.%), Mn, Cr, and K. Element systematics of Pathfinder samples and SNC are matching. A mixing diagram of rocks, soils, and mean SNC values indicates an about 1:1 abundance ratio of felsic and mafic rocks for soil.

McLennan S. M.*

*Sedimentary Geochemistry on Mars: Major Element Evidence from Pathfinder and Viking* **[#1700]**

Martian soil and rock chemistry may be influenced by sedimentary processes such as weathering and mineral fractionation during transport. Soils provide an estimate of the martian upper crust which approximates to typical basaltic shergottites.

Morris R. V.* Shelfer T. D. Ming D. W. Golden D. C.

*Magnetic Properties Experiments with a Pathfinder Magnet Array on Mauna Kea Volcano: Evidence the Martian Magnetic Mineralogy is Fe-Ti Spinel* **[#1802]**

Magnetic properties experiments on Mauna Kea volcano with a copy of the Pathfinder Magnet Array and palagonitic aeolian dust show Fe-Ti spinels are a viable interpretation of the Pathfinder magnetic properties experiment.

**Monday, March 15, 1999**
**IMPACTS I**
**8:30 a.m. Room D**

**Chairs: B. M. French**
**D. A. Kring**

Mazur M. J.* Stewart R. R. Hildebrand A. R.
*Seismic Characterization of Buried Possible Impact Structures* **[#1393]**
We have examined several seismic datasets collected within the Western Canadian Sedimentary Basin over circular subsurface features. Many features diagnostic of impact craters such as raised rims, troughs, terraces, inferred breccia infill, and faults have been observed.

French B. M.* Cordua W. S.
*Intense Fracturing of Quartz at the Rock Elm (Wisconsin) "Cryptoexplosion" Structure: Evidence for Meteorite Impact* **[#1123]**
Quartz grains from uplifted sandstones in the center of a 6-km-diameter "cryptoexplosion" structure at Rock Elm, WI, show intense fracturing and other features that indicate that the structure formed by meteorite impact in Ordovician or later time.

Therriault A. M.* Fowler A. D. Grieve R. A. F.
*The Sudbury Igneous Complex: Mineralogy and Petrology of a Differentiated Impact Melt Sheet* **[#1801]**
The SIC is a layered body within the Sudbury Structure, Canada. A detailed mineralogical and petrological study reveals that the original SIC melt crystallized in a water-rich environment. Its unusual petrology is evidence of its derivation from an impact melt.

Pope K. O.* Ocampo A. C.
*The Chicxulub Continuous Ejecta Blanket and Its Implications for Fluidized Ejecta Blankets on Mars* **[#1380]**
Comparisons of the Chicxulub continuous ejecta blanket with crater scaling relationships and analyses of Chicxulub ejecta from Belize and Mexico indicate that the ejecta are part of a fluidized ejecta blanket, perhaps similar to fluidized ejecta blankets on Mars.

Sharpton V. L.* Corrigan C. M. Marín L. E. Urrutia-Fucugauchi J. Vogel T. A.
*Characterization of Impact Breccias from the Chicxulub Impact Basin: Implications for Excavation and Ejecta Emplacement* **[#1515]**
An initial geophysical and geochemical characterization of impact core samples from Chicxulub provide new constraints on the excavation and ejecta emplacement processes that occurred during the formation of one of the largest impact basins known on Earth.

Schultz P. H.* Zárate M. Hames W. E.
*Three New Argentine Impact Sites: Implications for Mars* **[#1898]**
Three new impact sites have been discovered in Argentine loessoid deposits dating back to the Miocene. This discovery has implications for impact derived glass deposits on Mars where low sedimentation rates over 3 Ga enhances their concentrations.

Koeberl C.* Plescia J. B. Hayward C. L. Reimold W. U.
*Impactites at the Upheaval Dome Structure, Utah?* **[#1094]**
We studied quartz nodules at Upheaval Dome, previously interpreted as impactites, and found no indication of a high-temperature history. The samples have high contents of elements that indicate fluid interaction and are interpreted as normal low-temperature quartz.

See T. H.* Galindo C. Golden D. C. Yang V. Mittlefehldt D. Hörz F.
*Major-Element Composition of Ballistically Dispersed Melts from Meteor Crater, AZ* **[#1633]**
Studies of the composition of Meteor Crater impact melts, with the primary objective being to correlate the melt compositions with the major target lithologies and their stratigraphic positions within the target.

Koeberl C. Simonson B. M.* Reimold W. U.
*Geochemistry and Petrography of a Late Archean Spherule Layer in the Griqualand West Basin, South Africa* **[#1755]**
Samples from a late Archean spherule layer in drill cores from the Pering Mine were studied and show enrichments in siderophile elements, which may represent an extraterrestrial component.

Dass J. D. Glass B. P.*
*Geographic Variations in Concentration of Mineral Inclusions in Muong Nong-type Australasian Tektites: Implications Regarding the Location of the Australasian Tektite Source Crater* **[#1081]**
Mineral inclusions (primarily zircon and an $Al_2SiO_5$ phase) were found in 19 of 32 layered Australasian tektites. The highest concentrations are in samples from Muong Phin, Laos. Our prelimary data are consistent with a source crater in southern Laos or adjacent area.

Ebel D. S.* Grossman L.
*Condensation in a Model Chicxulub Fireball* **[#1906]**
Spinel and silicate liquid compositions and $fO_2$ paths are calculated for condensation of impact vapor for four Chicxulub scenarios, with and without admixed air, along realistic P-T paths. Ni-metal, liquid, Ca-silicate and Fe-Mg spinel result in most cases.

Robin E.* Rocchia R. Lefèvre I. Pierrard O. Dupuis C. Smit J. Zaghbib-Turki D. Matmati F.
*Local Variations in Spinel Compositions at the K/T Boundary in Tunisia: Evidence for Long Range Dispersion of Impact Debris* **[#1601]**
Local variations in spinel compositions are observed at the K/T boundary in Tunisia, consistent with the idea of a long range dispersion of impact debris. Their atmospheric reentry might have generated a series of environmental stresses contributing to the K/T crisis.

Pierrard O.* Robin E. Rocchia R. Lefevre I. Smit J. Vonhof H.
*Late Eocene Ni-rich Spinel from LL44-GPC3 (Central Pacific), ODP Site 689B (Maud Rise, Antarctic), DSDP Sites 94 (Gulf of Mexico) and 612 (US East Coast)* **[#1674]**
The Ni-rich spinel anomaly, previously reported in the E/O Stratotype at Massignano in Italy, is recorded worldwide in upper Eocene sediments. We show that this anomaly derives from the same event as the one that produced microkrystites, probably a comet impact.

**Monday, March 15, 1999**
**PLENARY SESSION**
**MASURSKY LECTURES**
**1:30 p.m. Room C**

**Chairs: C. B. Agee**
**D. C. Black**

Presentation of the 1998 GSA Stephen F. Dwornik Student Paper Award Winners

Belton M. J. S.*
*Galileo: Mission of a Lifetime* **[#1225] [invited]**
I illustrate some of the more significant scientific and technical accomplishments that have so far been made during the Galileo Mission through my experiences and recollections as the Leader of the Imaging Science Team for the past twenty years.

Porco C. C.*
*The Summer of '04: Cassini's Exploration of the Saturn System* **[invited]**

## Monday, March 15, 1999
## VENUS GEOLOGY AND GEOPHYSICS
## 3:00 p.m. Room A

**Chairs: R. J. Phillips**
**A. T. Basilevsky**

Basilevsky A. T.* Kryuchkov V. P. Ivanov M. A. Head J. W. III
*Craters on the Geologic Units of Northern Venus* **[#1249]**
For 200 impact craters north of 30°N we determined on what geologic units they are superposed. Of 64 craters seen on units older than regional plains, 54 to 59 influence this plain and younger units too, implying rapid formation of the older units.

Herrick R. R.* Sharpton V. L.
*There are a Lot More Embayed Craters on Venus than Previously Thought* **[#1696]**
We created DEMs of 70 craters with stereo data. Rim heights and rim-floor depths are less for craters with dark vs. bright floors. Exteriors and interiors of dark-floored craters are embayed. Previous estimates of recent Venusian resurfacing are too low.

Kreslavsky M. A.* Head J. W. III
*Estimation of the Thickness of Regional Volcanic Plains on Venus* **[#1192]**
The thickness was estimated in several sites through (1) height statistics of flooded and unflooded small shield volcanoes; and (2) flooding of impact craters. Correlation between the thickness of plains material and wrinkle ridge patterns was found.

Ghail R. C.*
*50 Ma Old Tesserae in South-East Thetis Regio?* **[#1257]**
The area of tesserae in southeast Thetis Regio is modeled as a fold-and-thrust compressional belt and a basin-and-range type plateau collapse, respectively, similar to that proposed for the Himalayas and the Tibetan plateau.

Ivanov M. A.* Head J. W. III
*Ridge-Ribbon Age Relationships in Northeast Ovda Regio, Venus* **[#1232]**
The sequence of formation of ridges, ribbons, and graben has been established in NE Ovda: Contractional features (ridges) — emplacement of intratessera plains — formation of extensional features (ribbons).

Head J. W. III* Basilevsky A. T.
*A Model for the Geological History of Venus from Stratigraphic Relationships: Comparison to Geophysical Mechanisms* **[#1390]**
The geological history of Venus is examined and found to be consistent with a geophysical mechanism involving depleted mantle layer overturn.

Dubuffet F.* Rabinowicz M. Monnereau M.
*Multi-Scales of Mantle Convection: Implications on Venus* **[#1733]**
Comparison between the Geoid to Topography Ratio of Venus highlands and the GTR given by a 3D convection model. Implications on the viscosity of the mantle of Venus. Thermal instabilities and volcanism.

Phillips R. J.* Bullock M. A.

*Coupled Climate and Interior Evolution on Venus* **[#1385]**

Climate-interior evolution coupling is investigated by merging a partial melting/parameterized convection model with a gray radiative-convective atmospheric model. For Venus, the coupled model produces a 3 to 4-fold increase in volcanic production.

Hashimoto G. L.* Abe Y.

*Impact of Variation in Atmospheric Water Abundance on Surface Temperature of Venus* **[#1867]**

Using the Venus climate model, we examine the influence of the variation in the atmospheric water abundance on the surface temperature. If our proposed mechanism of chemical-albedo feedback is operating, the change in surface temperature is small.

**Monday, March 15, 1999**
**PLANETARY INTERIOR PROCESSES**
**3:00 p.m. Room B**

**Chairs:** **V. J. Hillgren**
**N. L. Chabot**

Chabot N. L.* Drake M. J.
*The Effect of Silicate Composition on the Solubility of K in Metal* **[#1001]**
[D(K)] metal/silicate increases by ~100 with increasing depolymerization of the silicate melt. At 15 kb and 1900°C D(K) for the Earth yields a present day heat generation ~100 lower than needed to drive the Earth's geodynamo. Higher P and T will be studied.

Hillgren V. J.* Boehler R.
*A Case Against Si as the Sole or Major Light Element in the Core* **[#1650]**
We examine the viability of Si as the light element in the core in conjunction with the results of high pressure experiments on the interactions between silicates and Si-rich metals.

Pike W. A.* Bertka C. M. Fei Y.
*Melting Temperatures in the Fe-Ni-S System at High Pressures: Implications for the State of the Martian Core* **[#1489]**
The eutectic temperature of a model martian core in the Fe-Ni-S system at core-mantle boundary pressures is significantly lower than that found in previous Ni-free models. The melting curve determined in this study suggests an entirely liquid core.

Lauer H. V. Jr.* Jones J. H.
*Tungsten and Nickel Partitioning Between Solid and Liquid Metal; Implications for High-Pressure Metal/Silicate Experiments* **[#1617]**
Experiments show that W enters metallic liquids more readily when they contain carbon. This effect must be taken into account, especially in high-pressure experiments that are often performed in graphite capsules.

Holzheid A.* Grove T. L.
*Sulfur Solubility in Silicate Melts Saturated with Metal Sulfide at Elevated Pressure and Temperature: Implications for Core-Mantle Interactions* **[#1013]**
The bulk silicate Earth's sulfur content is ~7× higher than the expected sulfur solubility of a silicate liquid. Sulfur-saturated core-forming metal segregation event is not supported by the expected and observed S abundances in the Earth's mantle.

Holder D. H. Colson R. O.* Floden A. M. Hendrickson T. R. Malum K. M. Nermoe M. K. B.
*The Effects of CO on the Activity of Nickel and Zinc in Silicate Melts, with Implications for Ni Partitioning and Petrogenesis of Apollo 15 Green Glass B* **[#1482]**
Our present experiments continue to demonstrate that CO does have an effect on Ni activity, and in fact indicate that the interaction between CO and Ni is much stronger in green glass analog compositions than in the diopsidic compositions studied previously.

Borisov A.*
*Noble Metal Reaction with Solid Oxides or a Melt Components: A New Representation of Binary Phase Diagrams* **[#1263]**
I suggest a new representation of binary phase diagrams, which is useful for consideration of very reducing conditions, where interaction of PGEs with solid oxides or melt components becomes important and may result in melting of initially solid noble metals.

Jacobsen S. B.*

*Accretion and Core Formation Models Based on Extinct Radionuclides* **[#1978]**

Tungsten isotope data show that the Moon must have formed at ~25 Ma assuming a giant impact origin. At least 20% of the Earth must have accreted subsequent to the formation of the Moon to effectively erase the $\varepsilon_W$ anomaly in the silicate Earth.

Woolum D. S.* Cassen P. Porcelli D. Wasserburg G. J.

*Incorporation of Solar Noble Gases from a Nebula-derived Atmosphere during Magma Ocean Cooling* **[#1518]**

To test the idea that solar gases were acquired by the Earth by dissolution in a magma ocean from a nebula-derived atmosphere, we calculate the cooling history of such a system. Preliminary results constrain the conditions under which this could have occurred.

**Monday, March 15, 1999**
**MARS SURFACE CHEMISTRY**
**3:00 p.m. Room C**

**Chairs: J. F. Mustard**
**E. A. Cloutis**

Wallendahl A.* Treiman A. H.
*Geochemical Models of Low-Temperature Alteration of Martian Rocks* **[#1268]**
Alteration of martian basalt, T < 150°C, at high high rock/water will yield: clay + carbonate + qz and near neutral pH water if $CO_2$ = 6 Mbar; and clay + serpentine + diopside, gas rich in $H_2$, and alkaline water (to pH ~12) if $CO_2$ is not externally buffered.

Newsom H. E.* Hagerty J. J. Goff F.
*Mixed Hydrothermal Fluids and the Origin of the Martian Soil: A New Quantitative Model* **[#1262]**
A combination of neutral-chloride hydrothermal fluids (providing Cl) and acid-sulfate fluids (providing S) can quantitatively explain the abundances of S, Cl, and other mobile elements in the soil, but not the Fe in soil magnetic minerals.

Mustard J. F.*
*Mapping Unique Spectral Materials in Valles Marineris* **[#1484]**
A partial unmixing algorithm is used to map the distribution and abundance of materials with subtle spectral differences in Valles Marineris. This approach will be applied to both mafic and altered materials.

Cloutis E. A.* Bell J. F. III
*Spectral Reflectance Properties of Aluminum Hydroxides and Implications for Mars* **[#1945]**
Reflectance spectra of diaspores (AlOOH) exhibit a number of absorption features associated with Al-OH and OH vibrations near 1.8, 2.0, 3.33 and 3.42 microns. The latter two bands are outside the range exhibited by other hydrated minerals.

Eiler J. M.* Kitchen N.
*Experimental Study of the Stable-Isotope Systematics of $CO_2$ Ice/Vapor Systems and Relevance to the Study of Mars* **[#1309]**
Experimental measurements of the fractionation of C and O isotopes between $CO_2$ ice and vapor at conditions relevant to the near-surface of Mars constrain isotopic variability that can be generated by cycles of sublimation and condensation.

Yen A. S.* Grunthaner F. J. Kim S. S. Hecht M. H.
*Ultraviolet Radiation Induced Defects in Silicates: A Precursor to the Martian Oxidants* **[#1924]**
Recent experiments show that lattice defects can be created in silicates by short exposures to UV radiation at the martian surface. Subsequent reactions with the atmosphere at these sites may explain the unusual reactivity of the soil.

Bishop J. L.*
*Hydrothermal Alteration Products as Key to Formation of Duricrust and Rock Coatings on Mars* **[#1887]**
A model is presented for the formation of duricrust and rock coatings on Mars. Hydrothermal alteration of volcanic tephra may produce a corrosive agent that attacks rock surfaces and binds dust particles to form duricrust.

Johnson J. R.*
*Thermal Infrared Reflectance and Emission Spectra of Mars-like Dust Coatings on Basalt Substrates* **[#1214]**
Laboratory hemispherical reflectance and emissivity spectra of basalts coated with Mars analog soils show a reduction in spectral contrast (relative to uncoated basalts) in the 8-14-μm region, linearly related to coating thickness until ~60-μm thickness.

Wang A.* Jolliff B. L. Haskin L. A. Kuebler K.
*Raman Spectral Features of Pyroxene — Application to Martian Meteorites Zagami & EETA79001* **[#1666]**
Raman peak positions of basaltic pyroxenes provide structural information and cation ratios, as illustrated for Zagami and EETA79001.

Farrand W. H.* Lane M. D.
*Reflectance and Emittance Properties of Spring-formed Ferricretes and Acid Mine Drainage Materials: Relevance to Remote Sensing of Mars* **[#1936]**
The reflectance and emittance properties of minerals associated with spring formed ferricretes and acid mine drainage materials is described. It is suggested that they may be appropriate analog materials for certain regions on Mars.

**Monday, March 15, 1999**
**SPECIAL SESSION**
**NEAR AT EROS**
**3:00 p.m. Room D**

**Chairs: S. Murchie**
**M. Robinson**

Cheng A.*
*Overview of NEAR's Flyby of Eros* **[invited]**

Veverka J.*
*NEAR Imaging Science Results at Eros* **[invited]**

Thomas P.*
*The Shape of Eros as Determined from NEAR Images* **[invited]**

Murchie S.*
*NEAR Spectroscopic Results at Eros* **[invited]**

Yeomans D.*
*NEAR Radio Science Results at Eros* **[invited]**

**Tuesday, March 16, 1999**
**EARLY SOLAR SYSTEM PROCESSES AND TIMESCALES**
**8:30 a.m. Room A**

**Chairs: M. Wadhwa**
**R. H. Nichols Jr.**

Srinivasan G.* Papanastassiou D. A. Wasserburg G. J. Bhandari N. Goswami J. N.
*$^{26}Al$-$^{26}Mg$ and $^{53}Mn$-$^{53}Cr$ Systematics in the Piplia Kalan Eucrite* **[#1730]**
We report TIMS on $^{26}$Al-$^{26}$Mg and $^{53}$Mn-$^{53}$Cr in the Piplia Kalan eucrite. We appear to confirm the ion microprobe evidence for $^{26}$Al in this planetary differentiate, when it formed. We do not find evidence for $^{53}$Mn. The apparent conflict will be addressed.

Srinivasan G. Papanastassiou D. A.* Wasserburg G. J. Bhandari N. Goswami J. N.
*Sm-Nd Systematics and Initial $^{87}Sr/^{86}Sr$ in the Piplia Kalan Eucrite* **[#1718]**
We report Sm-Nd data on the Piplia Kalan eucrite. We obtain isochrons which yield a $^{147}$Sm-$^{143}$Nd age of 4.57±0.10 Ga, initial $(^{143}Nd/^{144}Nd)_{CHUR} = -0.71 \pm 3.6$ εu, and initial $^{146}Sm/^{144}Sm = (4.4 \pm 1.2) \times 10^{-3}$. Some discrepancies in short-lived dating systems are discussed.

Walker R. J.* Becker H. Morgan J. W.
*Comparative Re-Os Isotope Systematics of Chondrites: Implications Regarding Early Solar System Processes* **[#1208]**
Variations in the modern Os isotopic compositions of carbonaceous, ordinary and enstatite chondrites highlight the different nebular processing of highly siderophile elements affecting the precursor materials of these chondrite groups.

Becker H.* Walker R. J. Morgan J. W.
*Re-Os Isotopic Systematics of Matrix, Chondrules, Metal and More CAIs from the Allende Meteorite* **[#1086]**
Re-Os isotopic data on matrix, chondrules, metal grains and CAIs from Allende reveal substantial variations between some of these components. The range in $^{187}$Os/$^{188}$Os covered by Allende components is larger than the range observed for bulk chondrites.

Shukolyukov A.* Lugmair G. W.
*The $^{53}Mn$-$^{53}Cr$ Isotope Systematics of the Enstatite Chondrites* **[#1093]**
We studied the Mn-Cr isotope systematics in the E-chondrites Abee and Khainpur and found that the original $^{53}$Mn abundance in E-chondrite material is lower than that in ordinary chondrites. This indicates that the original $^{53}$Mn distribution in the nebula was heterogeneous.

Wadhwa M.* Shukolyukov A. Davis A. M. Lugmair G. W.
*Origin of Silicate Clasts in Mesosiderites: Trace Element Microdistributions and Mn-Cr Systematics Tell the Tale* **[#1707]**
We report the results of a study of trace element distributions and Mn-Cr systematics in several basaltic clasts and one diogenitic clast from Vaca Muerta. The goal of this study is to ascertain whether these clasts are related to the HEDs.

Nyquist L. E.* Shih C.-Y. Wiesmann H. Reese Y. Ulyanov A. A. Takeda H.
*Towards a Mn-Cr Timescale for the Early Solar System* **[#1604]**
Mn-Cr analyses give the following timescale: (i) Type B CAI to chondrules: 5.8±1.6 Ma; (ii) Chondrules to HED PB differentiation: 6.3±2.6 Ma; (iii) Chondrules to Ibitira eucritic basalt: 14±4 Ma; (iv) Chondrules to LEW86010 angrite: 10.0±1.2 Ma.

Dougherty J. R.* Brannon J. C. Nichols R. H. Jr. Podosek F. A.
*Thoroughly Anomalous Cr in the Ordinary Chondrite Semarkona* **[#1451]**
We present Cr isotopic compositions in successive dissolution fractions of the OC Semarkona. The anomaly patterns are similar to those observed in carbonaceous chondrites, but differ in detail, and are discussed in light of the proposed heliocentric gradient in $^{53}$Cr.

Nichols R. H. Jr.* Podosek F. A. Meyer B. S. Jennings C. L.

*Collateral Consequences of Inhomogeneous Distribution of Short-lived Radionuclides in the Solar Nebula* **[#1790]**

We present the collateral isotopic consequences in stable and long-lived isotopes if massive stars are responsible for the late injection of short-lived radionuclides at their canonical abundances.

Pravdivtseva O. V.* Hohenberg C. M.

*Observations of Mineral-Specific I-Xe Ages in Ordinary Chondrites* **[#2047]**

I-Xe ages for separated minerals from H-, L- and LL-chondrites correlate with melting temperatures of the host phases, demonstrating the utility of the I-Xe system for the study of post-formational processes.

Choi B.-G.* Huss G. R. Wasserburg G. J.

*Search for a Correlation Between $^{60}$Fe and $^{26}$Al in Chondrites* **[#1862]**

The Ni isotopic compositions of spinels and sulfide in an Allende CAI and olivines in chondrules of ordinary chondrites were measured. The data imply that the initial ($^{60}Fe/^{56}Fe$) was less than 2E-6 when this object formed.

Bogard D. D.* Garrison D. H.

*$^{39}$Ar-$^{40}$Ar Dating of Thermal Events on Meteorite Parent Bodies* **[#1104]**

A summary of $^{39}$Ar-$^{40}$Ar ages reveals the impact and thermal history of several meteorite parent bodies, i.e., eucrites, chondrites, mesosiderites, acapulcoites/lodranites, winonaites, enstatites, and IAB and IIE irons.

Tanimizu M.* Tanaka T.

*La-Ce Decay System of the Eucrite Millbillillie* **[#1181]**

We established a new technique for Ce isotope measurement. After determining the decay constant of $^{138}$La, we applied La-Ce system to an eucrite. The obtained age is younger than the Sm-Nd age. La-Ce system seems more sensitive to thermal annealing.

**Tuesday, March 16, 1999**
**SPECIAL SESSION**
**NEW MOON I: HOT SPOTS, GRAVITY, AND MAGNETISM**
**8:30 a.m. Room B**

**Chairs: B. L. Jolliff**
**P. G. Lucey**

Haskin L. A.* Gillis J. J. Jolliff B. L. Korotev R. L.
*On the Distribution of Th in Lunar Surface Materials* **[#1858]**
Th concentrations in the surface materials of the feldspathic highlands as estimated from Lunar Prospector data are generally consistent with the hypothesis that most of the Th was emplaced there as Imbrium ejecta.

Wieczorek M. A.* Phillips R. J.
*Thermal Modeling of Mare Volcanism and the "Procellarum KREEP Terrane"* **[#1547]**
The Procellarum/Imbrium region of the Moon likely contains a large portion of the Moon's incompatible elements. We show that the heat production of this province may be the cause of the bulk of lunar volcanism.

Jolliff B. L.* Gillis J. J. Haskin L. A. Korotev R. L. Wieczorek M. A.
*Major Lunar Crustal Terranes: Surface Expressions and Crust-Mantle Origins* **[#1670]**
Global data show that the Moon's crust consists of 3 major geologic terranes (Feldspathic Highlands, Procellarum KREEP, South Pole-Aitken). Each represents the surface expression of a geologic province with distinctive character at depth and geologic history.

Korotev R. L.*
*The "Great Lunar Hot Spot" and the Composition and Origin of "LKFM" Impact-Melt Breccias* **[#1305]**
Apollo KREEP-rich, mafic melt breccias (LKFM) are products of impacts into the Great Lunar Hot Spot, not the feldspathic highlands. The breccias consist mainly of KREEP norite and olivine from the mantle and feldspathic upper crust.

Elphic R. C.* Maurice S. Lawrence D. J. Feldman W. C. Barraclough B. L. Binder A. B. Lucey P. G.
*Lunar Prospector Measurements of the Distribution of Incompatible Elements Gadolinium, Samarium, and Thorium* **[#1109]**
Lunar Prospector neutron spectrometer (NS) and gamma ray spectrometer (GRS) observations have been used to map out the distribution of incompatible elements on the lunar surface.

Lawrence D. J.* Feldman W. C. Barraclough B. L. Binder A. B. Elphic R. C. Maurice S. Miller M. C. Prettyman T. H.
*Delineating the Major KREEP-bearing Terranes on the Moon with Global Measurements of Absolute Thorium Abundances* **[#2024]**
We are presenting new results regarding the global thorium abundances on the Moon using LP GRS data. Specifically, we are presenting a map of absolute thorium abundances along with thorium abundances for various lunar terranes.

Feldman W. C.* Lawrence D. J. Maurice S. Elphic R. C. Barraclough B. L. Binder A. B. Lucey P. G.
*Classification of Lunar Terranes Using Neutron and Thorium Gamma-Ray Data* **[#2056]**
Lunar Prospector neutron flux data are combined with thorium gamma-ray line intensities to classify the various lunar terranes. Although our analysis is preliminary, the method shows promise of delineating low from high titanium regions on the Moon.

Konopliv A. S.* Yuan D. N.
*Lunar Prospector 100th Degree Gravity Model Development* **[#1067]**
The latest Lunar Prospector gravity results will be presented. Currently under development is a 100th degree and order model that has higher resolution and more accurately represents the uncertainties on the farside and nearside than previous models.

Freed A. M.* Melosh H. J. Solomon S. C.

*Tectonics of Mascon Loading: Resolution of the Strike-Slip Fault Paradox* **[#1691]**

Previous numerical models predict an annulus of conjugate strike-slip faults around axisymmetric surface loads, though few such faults are observed. We offer a resolution to this paradox based on planet radius, load radius, and lithospheric thickness.

Kiefer W. S.*

*Lunar Gravity Models: Large, Near Side Impact Basins* **[#1995]**

Lunar mascon gravity highs and surrounding lows are generally due to mare basalt fill, flanked by impact basin ejecta. Super-isostatic moho uplift is important for some impact basins and is possibly due to non-Newtonian lower crustal flow during the impact event.

Mitchell D. L.* Halekas J. S. Lin R. P. Anderson K. A. Acuña M. H. Binder A.

*High Resolution Mapping of the Lunar Crustal Magnetic Field* **[#1959]**

We present high resolution mapping of the large lunar crustal magnetic field anomaly antipodal to the Mare Crisium impact basin and smaller magnetic anomalies to the north of this region.

Halekas J. S.* Mitchell D. L. Lin R. P. Anderson K. A. Acuña M. H. Binder A.

*Global Mapping of the Lunar Crustal Magnetic Field* **[#1949]**

We present the first global maps of the lunar crustal magnetic field. We confirm results from the Apollo missions showing strong magnetic fields in impact basin antipodes, and also extend the mapping to higher latitude regions.

Lin R. P.* Mitchell D. L. Harrison L. Halekas J. S. Hood L. L. Acuña M. H. Binder A.

*Miniature Magnetospheres on the Moon and Their Relation to Albedo Swirls* **[#1930]**

Observations by the Magnetometer/Electron Reflectometer experminent onboard Lunar Prospector show the presence of crustal magnetic fields capable of shielding the surface from solar wind ion implantation in regions containing albedo swirls.

**Tuesday, March 16, 1999**
**SPECIAL SESSION**
**MARS GLOBAL SURVEYOR (MGS): A NEW CHAPTER**
**8:30 a.m. Room C**

**Chairs: A. L. Albee**
**J. A. Grant**

Albee A. L.*
*The Surprising Saga of Mars Global Surveyor — A New Chapter* **[#1084]**
During the 18 months since orbit insertion at Mars, MGS has aerobraked from the original 45-hr elliptical orbit to the 2-hr circular mapping orbit. Despite spacecraft problems a wealth of unique observational data has been collected during the year's delay.

Malin M. C.* Edgett K. S.
*MGS MOC the First Year: Geomorphic Processes and Landforms* **[#1028]**
Presentation of new MGS MOC results regarding Mars volcanism, Valles Marineris, lakes and oceans, northern plains, valleys and channels, fretted terrain, polar regions, and layered materials. Sedimentology results are described in a companion paper.

Edgett K. S.* Malin M. C.
*MGS MOC the First Year: Sedimentary Materials and Relationships* **[#1029]**
New MGS MOC results regarding Mars eolian sediments and landforms, mass wasting, layers in the Valles Marineris, and sedimentary structures in the polar layered deposits. Other MOC geomorphology results are described in a companion paper.

Hartmann W. K.* Berman D. C. Esquerdo G. A. McEwen A. S.
*Recent Martian Volcanism: New Evidence from Mars Global Surveyor* **[#1270]**
Evidence for very young martian volcanism is reported. Ages of a few hundred My are found from crater counts. In addition, evidence is reported for deformation of km-scale craters and softening of martian terrain by isostatic adjustment in permafrost.

Smith D. E.* Zuber M. T. MOLA Science Team
*MOLA's First Observations of the Southern Hemisphere Topography of Mars* **[#1631]**
MOLA is expected to obtain its first observations of Mars' southern hemisphere in the couple of weeks just prior to the LPSC. Preliminary results of this early mapping will be presented.

Zuber M. T.* Smith D. E.
*Effect of Mars' Present-Day North Polar Cap on the Moment of Inertia and Planetary Dynamics* **[#1589]**
We use recent observations of the topography and gravity of Mars' north polar cap to calculate the effects of the cap on planetary dynamics. We also address potential effects of the cap at different times in Mars' obliquity cycle.

Johnson C. L.* Solomon S. C. Head J. W. III Smith D. E. Zuber M. T.
*Lithospheric Loading by the Northern Polar Cap on Mars* **[#1345]**
Loading of the martian lithosphere by the northern polar cap is investigated using elastic and viscoelastic models and constraints from MOLA data and geology. Implications for basement topography, polar cap volume and the gravity field are discussed.

Christensen P. R.* Bandfield J. Clark R. Edgett K. S. Hamilton V. Lane M. Kieffer H. H. Malin M. Morris D. Ruff S. Roush T. Smith M.
*The Composition of Martian Surface Materials: Mars Global Surveyor Thermal Emission Spectrometer Observations* **[#1461]**
The MGS TES has detected crystalline hematite within a localized zone ~300 km in diameter near ~0N, ~5° W. Low albedo surfaces indicate the presence of basaltic materials; the spectra are best fit by a mixture of pyroxene, plagioclase, ±olivine.

Bandfield J. L.* Christensen P. R. Hamilton V. E.
*Isolation and Analysis of Martian Low Albedo Surface Spectra from the MGS Thermal Emission Spectrometer* **[#1725]**
A technique for performing a surface-atmosphere separation using TES data and a preliminary analysis of surface spectral signatures from several martian low albedo regions will be described.

Mellon M. T.* Jakosky B. M. Varnes E. S. Kieffer H. H. Christensen P. R.
*Thermal Inertia from Mars Global Surveyor for Aerobraking and Science Phasing Missions* **[#1117]**
We use newly acquired Thermal Emission Spectrometer data from the Mars Global Surveyor spacecraft to derive the thermal inertia of the martian surface. Results are mapped and compared with Viking-based thermal inertias.

Simpson R. A.*
*Search for Bistatic Surface Echoes at Highly Oblique Angles in Mars Global Surveyor Radio Occultation Data* **[#1939]**
Surface echoes, captured during acquisition of radio occultation data, are both interference during extraction of atmospheric temperature-pressure profiles and information about the surface in their own right. This report summarizes 1998 results from Mars Global Surveyor.

Connerney J. E. P. Acuña M. H.* Ness N. F. MGS MAG/ER Science Investigation Team
*Martian Magnetic Anomalies* **[invited]**

Brain D. A.* Bagenal F. Acuña M. H. Connerney J. E. P. Cloutier P. A. Crider D. H. Law C. C. Walker P. W. Chen Y. Lin R. P. Mitchell D. Reme H. Mazelle C. Vignes D. Ness N. F.
*Implications of Mars Global Surveyor MAG/ER Data for Atmospheric Water Loss at Mars* **[invited]**

**Tuesday, March 16, 1999**
**ICY SATELLITES**
**8:30 a.m. Room D**

**Chairs: S. A. Fagents**
**W. B. McKinnon**

Hendrix A. R.* Barth C. A. Stewart A. I. F. Hord C. W. Lane A. L.
*Hydrogen Peroxide on the Icy Galilean Satellites* **[#2043]**
The Galileo Ultraviolet Spectrometer detects hydrogen peroxide on Europa, Ganymede and Callisto.

Martin P. D.* McCord T. B. Hansen G. B. Hibbitts C. A. Carlson R. W. Johnson T. V. Matson D. L. Galileo NIMS Team
*Ganymede's Surface: Less Water-Ice on the Leading Hemisphere?* **[#1947]**
We conclude from this analysis that there is an hemispherical dichotomy of the distribution of icy constituents on Ganymede, within the range of latitude of our investigation, implying more water-ice in the trailing hemisphere than in the leading hemisphere.

Hibbitts C. A.* McCord T. B. Hansen G. B. Klemaszewski J. E.
*Possible Exogenic and Impact Origins for Carbon Dioxide on the Surface of Callisto* **[#1540]**
$CO_2$ is ubiquitous on the surface of Callisto. The leading hemisphere: $CO_2$ is concentrated in ice-rich impact craters. Trailing hemisphere: a global distribution as a sinusoid centered on the equator at 270° longitude suggests effects from Jupiter's magnetic field.

Hogenboom D. L.* Kargel J. S. Pahalawatta P. V.
*Densities and Phase Relationships at High Pressures of the Sodium Sulfate–Water System* **[#1793]**
Study of the pressure dependence of density and eutectic melting in the $Na_2SO_4$-$H_2O$ system. Unlike $MgSO_4$, $Na_2SO_4$ causes melting point depression of ice-I that increases with pressure to 200 MPa. Effects on icy satellite geochemistry expected.

Baron J. E.* Tyler G. L. Simpson R. A.
*Long-Wavelength Scattering from Buried Craters and Refractive Lenses: Implications for Remote Sensing of Icy Galilean Satellites* **[#1940]**
We revisit the buried crater and refraction scattering models for the unusual radar properties of the icy Galilean satellites. Using 3-D numerical simulations, we examine the ability of these models to reproduce observational data at long wavelengths.

Black G. J.* Campbell D. B. Nicholson P. D.
*Europa, Ganymede and Callisto: Modeling of Subsurface Structure from Multi-Wavelength Radar Observations* **[#1711]**
A model of the coherent backscatter effect is applied to the radar reflectivities of the Galilean satellites. The model is formulated in terms of a power law distributed number density of scatterers and the loss tangent of the surrounding medium.

Schenk P. M.* Moore J. M.
*On the Importance of Being Lofn: Geology of Large Impact Basins on Callisto* **[#1786]**
The crater Lofn has a diameter of 330 km, is analogous to central dome craters on Ganymede, and probably reflects a stiffening of the lithosphere of Callisto with time.

Dombard A. J.* McKinnon W. B.
*A Re-Examination of Crater Relaxation on Ganymede and Callisto Using an Elastoviscoplastic Rheological Model* **[#2006]**
New finite element studies show that while elastic stress storage in a lithosphere permits long time-scale crater retention, relaxation is more rapid than once estimated, and that the style of plastic failure may be an important heat flow diagnostic.

Zahnle K.* Levison H. Dones L. Schenk P.

*Cratering Rates in the Outer Solar System* **[#1776]**

This paper extends our revision of cratering rates to Saturn, Uranus, Infinity, and Beyond. Estimated surface ages will be listed for every moon where we have data. But the emphasis will be on Triton. We will also question the existence of small comets.

Stern A. S. McKinnon W. B.*

*Triton's Surface Age and Impactor Population Revisited (Evidence for an Internal Ocean)* **[#1766]**

We combine crater counts on Triton with much improved estimates of impact rates, dominated by Kuiper Belt objects. We find surface ages are no greater than ~0.1–0.3 Gyr. Given recent volcanic activity on Triton is deep-seated, a logical lava source is an internal ocean.

## Tuesday, March 16, 1999
## SPECIAL SESSION
## FUTURE PLANETARY MISSIONS
## 12:15 p.m. Room C

**Chairs:** **C. F. Chyba**
**C. B. Pilcher**

McCleese D.*
*Evolution of Earth-Like Environments Campaign Strategy Working Group* **[invited]**

Stofan E. R.* Banerdt W. B. Bogard D. D. Campbell B. A. Grinspoon D. Haberle R. M. Lucey P. G. Peterson C. Phillips R. J. Pieters C. M. Saunders R. S. Smrekar S. E. Spudis P. D.
*The Campaign Strategy Working Group for the Formation and Dynamics of Earth-like Planets: Seeking to Determine How Earth-like Planets Form and Evolve* **[#1339] [invited]**
The Formation and Dynamics of Earth-like Planets CSWG focuses on understanding how habitable worlds form through study of our neighboring planets. This mission planning activity concentrates on Mercury, Venus, Moon and geophysical networks on Mars.

Veverka J.* Ahrens T. Belton M. Binzel R. Boynton W. Feldman P. Soderblom L. Yelle R. Wolf A. Gershman B.
*Exploring Comets, Asteroids, and Related Bodies: A Report from the Campaign Strategy Working Group on Building Blocks and Chemical Origins of the SSES* **[#1739] [invited]**
Exploring comets, asteroids, and related bodies: A report from the Campaign Strategy Working Group on building blocks and chemical origins of the SSES.

Chyba C. F. McKinnon W. B.* Coustenis A. Johnson R. E. Kovach R. L. Khurana K. Lorenz R. McCord T. B. McDonald G. D. Pappalardo R. T. Race M. Thomson R.
*Europa and Titan: Preliminary Recommendations of the Campaign Science Working Group on Prebiotic Chemistry in the Outer Solar System* **[#1537] [invited]**
The Prebiotic Chemistry in the Outer Solar System CSWG is establishing science objectives for subsequent missions to Europa and Titan. Here we report the preliminary results of this process, and solicit further input from the scientific community.

Porco C. C.* Brown R. H. Del Genio A. Dowling T. Harris A. Horanyi M. Lin D. Nicholson P. Spencer J. Spilker T.
*Astrophysical Analogs in the Solar System: A Campaign for Solar System Exploration* **[#1800] [invited]**
This presentation will describe the science objectives for the Astrophysical Analogs Campaign Strategy Working Group of the Solar System Exploration Subcommittee, and the mission set being considered by this group.

## Tuesday, March 16, 1999
## CALCIUM-ALUMINUM-RICH INCLUSIONS (CAIs)
## 1:30 p.m. Room A

**Chairs: H. C. Connolly Jr.**
**T. LaTourrette**

Guan Y.* Huss G. R. MacPherson G. J. Wasserburg G. J.
*Calcium-Aluminum-rich Inclusions in Unequilibrated Enstatite Chondrites: A Preliminary Petrologic and Isotopic Study* **[#1391]**
CAIs in three enstatite chondrites resemble those in carbonaceous and ordinary chondrites; one, a hibonite-bearing CAI, contains Al/Mg-correlated excess $^{26}$Mg and thus provides further evidence that $^{26}$Al was widespread in the early solar nebula.

Fagan T. J.* Krot A. N. Keil K.
*Are Ca,Al-rich Inclusions in EH3 and EL3 Chondrites Native to the Enstatite Chondrite-forming Regions?* **[#1944]**
We report mineralogy of 10 Ca,Al-rich inclusions in EH3 and EL3 chondrites. The CAis are spinel-rich and often contain osbornite (TiN) and/or heideite ($FeTi_2S_4$). Based on the presence of these Ti-bearing phases, we infer that the CAIs are native to the EC-forming region.

Connolly H. C. Jr.* Burnett D. S.
*Minor Element Distributions in Spinels from Type B, CAIs: An Experimental Study* **[#1459]**
We determined spinel/liquid D's for Ti and V for average type B CAI composition at the C-CO buffer curve. Measured D for Ti and V in spinel fail to account for observed compositions in type B CAIs, requiring a complex igneous history or relict grains.

Simon S. B.* Davis A. M. Grossman L.
*Complex Zoning in Fassaite: A Recorder of Growth and Resorption in Type B1 CAIs* **[#1727]**
Complex zoning patterns within single crystals of fassaite in Type B1 CAIs are probably indicators of reheating events. Patchy and complex zoning was investigated by SEM, EMP and IMP to improve our understanding of CAI crystallization histories.

Krot A. N.* Weber D. Greshake A. Ulyanov A. A. McKeegan K. D. Hutcheon I. Sahijpal S. Keil K.
*Relic Ca,Al-rich Inclusions in Chondrules from the Carbonaceous Chondrites Acfer 182 and Acfer 094* **[#1511]**
We describe the discovery of two relic CAIs inside chondrules. The relic CAIs and host chondrules contain phases, plagioclase and hibonite, suitable for Al-Mg isotopic study, and may provide information on the time difference between CAI and chondrule formation.

Beckett J. R.* Paque J. M. Stolper E.
*The Use of Melilite Compositions to Constrain the Thermal History and Liquid Line of Descent of Type B CAIs* **[#1920]**
We calculate compositions of melilite coexisting with silicate melts based on experimental data and determine the temperatures of crystallization for melilite and clinopyroxene in Type B inclusions.

LaTourrette T.* Hutcheon I. D.
*Mg Diffusion in Melilite: Thermal Histories for CAIs and Their Parent Bodies* **[#2003]**
Experimentally measured Mg diffusion coefficients in åkermanite are used to constrain the thermal history of isotopically disturbed CAIs.

Ushikubo T.* Hiyagon H. Sugiura N. Ulyanov A. A.
*Combined Ion Microprobe Studies of O and Mg Isotopes in an Efremovka CAI* **[#1320]**
Combined ion microprobe studies of O and Mg isotopes were performed for an Efremovka CAI. It is found that anorthite has an anomalous O isotopic composition of ~–40‰, but still shows disturbance in the Mg isotopes.

Ito M.* Yurimoto H. Nagasawa H.
*Oxygen Isotope Micro-Distribution vs. Composition in Melilite/Fassaite in the Allende CAI 7R-19-1: A New Evidence for Multiple Heating* **[#1538]**
The heterogeneous distributions of O within a fassaite, and between gehlenitic and akermanite-rich melilite in 7R-19-1, an Allende CAI measured by micro-analysis with SIMS, showed evidence for multiple heating in the primitive solar nebula.

Campbell A. J.* Simon S. B. Humayun M. Grossman L.
*Microanalysis of Siderophile Elements in Fremdlinge Using Laser Ablation ICP-MS* **[#1609]**
Laser ablation ICP-MS was used to measure siderophile element distributions in Fremdlinge with a spatial resolution of 15 microns. PGE ratios that are not always chondritic were established in Fremdlinge prior to their incorporation into CAIs.

Hiyagon H.* Hashimoto A.
*An Ion Microprobe Study of Oxygen Isotopes in Various Types of Inclusions in Y-82050 (CO3), ALH-77307 (CO3) and Y-86009 (CV3) Chondrites* **[#1319]**
In-situ ion microprobe analyses were performed for various types of inclusions in two CO (Y-82050 and ALH-77307) and one CV (Y-86009) chondrite, and the newly obtained results are presented and discussed.

Davis A. M. Hashimoto A.* Parsad N.
*Trace Element Fractionation During Evaporation in Reducing Atmospheres* **[#2023]**
We have evaporated melts of CAI composition doped with trace elements in 0.0001 atm $H_2$. The lack of Ce anomalies in residues shows that CAIs with large negative Ce anomalies cannot have evaporated in the solar nebula.

Richter F. M.* Parsad N. Davis A. M. Hashimoto A.
*CAI Cosmobarometry* **[#1989]**
We report new experimental data on the mass loss kinetics and associated isotope fractionation of residues of molten Type B1 CAI samples evaporated at different temperatures, pressures, and gas compositions.

## Tuesday, March 16, 1999
## SPECIAL SESSION
## NEW MOON II: MAJOR LUNAR TERRAINS
## 1:30 p.m. Room B

**Chairs: P. D. Spudis**
**M. S. Robinson**

Storrs A. D.* Caldwell J. J. Hawke B. R. Bell J. F. Smith G. A.
*Imaging Observations of the Moon with the Hubble Space Telescope* **[#1880]**
We have observed the Moon with the Hubble Space Telescope. We compare the images and mineralogical maps made from this data with those from other sources. The data are complimentary to existing data sets.

Robinson M. S.* McEwen A. S. Eliason E. Lee E. M. Malaret E. Lucey P. G.
*Clementine UVVIS Global Mosaic: A New Tool for Understanding the Lunar Crust* **[#1931]**
A 100 m/pixel 5 band mosaic of the Moon from Clementine UVVIS data has been completed. A summary of the data along with potential errors due to topographic slopes, scattered light, and phase angle variations will be presented.

Le Mouélic S.* Langevin Y. Erard S.
*Discrimination Between Olivine and Pyroxene from Clementine NIR Data: Application to Aristarchus Crater* **[#1098]**
We present new results obtained with Clementine NIR data on Aristarchus crater. UVVIS data are used to discriminate between maturity effects and mineralogy. NIR data complement this information by discriminating olivine from pyroxene within identified mare basalts.

Pinet P. C.* Chevrel S. Daydou Y. H. Le Mouélic S. Langevin Y. Erard S.
*Aristarchus Crater Spectroscopic Heterogeneity from Clementine UV-VIS-NIR Data* **[#1555]**
The spectroscopic mapping reflects petrology changes. The deepest material exposed in the peak indicates an anorthositic horizon, overlain by an ol/px-rich horizon, with a progressive change in the ratio, the px abundance increasing as the depth decreases.

Raitala J.* Kreslavsky M. A. Shkuratov Yu. G. Starukhina L. V. Kaydash V. G.
*Nonmare Volcanism on the Moon: Characteristics from the Clementine Data* **[#1457]**
We study spectra of nonmare domes (Hansteen alpha, Gruithuisen gamma, delta, Mairan T) with UVVIS data. The domes are bright, red, and have a specific spectral feature in IR. Some other formations (e.g. Mons La Hire) have the same spectral signature.

Pieters C. M.* Tompkins S.
*The Distribution of Lunar Olivine/Troctolite Outcrops: Mineralogical Evidence for Mantle Overturn?* **[#1286]**
Olivine/troctolite has been identified in central peaks of 7 large craters (of 109). This mineralogy is found only with anorthosite. The distinctly equatoral distribution of such outcrops suggests an origin linked to early global scale processes.

Tompkins S.* Hawke B. R. Pieters C. M.
*Distribution of Materials Within the Crater Tycho: Evidence for Large Gabbroic Bodies in the Highlands* **[#1573]**
A variety of remote sensing data suggests that Tycho Crater may have exposed a gabbroic pluton during the impact process. A detailed study of the composition and distribution of geologic units at Tycho is underway.

Heather D. J.* Dunkin S. K.
*Multispectral Analysis of the Lunar Farside Crater King Using Clementine Data* **[#1179]**
This study utilises Clementine multispectral data to investigate the geology of the farside lunar crater King.

Spudis P. D.* Bussey D. B. J. Hawke B. R.
*Deposits of the Imbrium Basin: Montes Alpes and Caucasus* **[#1348]**
We continue our ongoing study of the composition of basin deposits by examining the northern ejecta of the Imbrium basin using Clementine and Lunar Prospector coverage to map the chemical composition of Imbrium ejecta in this region of the Moon.

Peterson C. A.* Hawke B. R. Lucey P. G. Taylor G. J. Blewett D. T. Spudis P. D.
*Remote Sensing Studies of Highland Units on the Lunar Farside* **[#1624]**
The interior of South Pole-Aitken (SPA) basin shows elevated levels of FeO, $TiO_2$, Th, and K. The original anorthosite crust was covered by a thick blanket of mafic ejecta from SPA near the basin rim and by lesser amounts farther to the north.

Blewett D. T.* Taylor G. J. Lucey P. G. Hawke B. R. Gillis J. J.
*High-Resolution, Quantitative Remote Sensing of South Pole-Aitken Basin* **[#1438]**
SPA has uniform FeO (~11 %). Northern SPA has elevated Ti and Th contents, likely due to admixed mare basalt. The south has low Ti like the surrounding highlands, but a distinct Th anomaly. This is not consistent with any known pure rock type.

Grier J. A.* McEwen A. S. Lucey P. G. Strom R. G. Milazzo M.
*Relative Ages of Large Rayed Lunar Craters — Implications* **[#1910]**
The relative ages of large lunar craters can be inferred from spectral estimates ejecta maturity. The radiometric ages of Tycho, Copernicus, and Autolycus help constrain the relative ages of other large craters, such as Lichtenberg.

Lawson S. L.* Jakosky B. M.
*Brightness Temperatures of the Lunar Surface: The Clementine Long-Wave Infrared Global Data Set* **[#1892]**
LWIR measurements reveal that (1) nadir-looking observations of the lunar surface are adequately fit by a Lambertian temperature model and (2) the dayside lunar thermal emission is largely governed by albedo and by the emission angle of observations.

**Tuesday, March 16, 1999**
**MARS GLOBAL SURVEYOR (MGS): OCEANS, BASINS, AND MORE**
**1:30 p.m. Room C**

**Chairs: S. E. H. Sakimoto**
**O. Aharonson**

Smith D. E.* Zuber M. T. Neumann G. A.
*Preliminary Global Topographic Model of Mars Based on MOLA Altimetry, Earth-based Radar, and Viking, Mariner and MGS Occultations* **[#1845]**
Laser altimetry, Earth based radar, Mariner, Viking and MGS occultations, and lander locations have been used to derive a new long wavelength topography model for Mars.

Aharonson O.* Zuber M. T. Neumann G. A.
*Second Order Statistics of Topography of the Northern Hemisphere of Mars from MOLA* **[#1792]**
Recent measurements of the topography of Mars made by MOLA allow quantification of surface properties in a statistically robust way. These include surface roughness, characteristic correlation length, and RMS slope.

Kreslavsky M. A.* Head J. W. III
*Kilometer-scale Roughness of Geological Units on Mars: Initial Results from MOLA Data* **[#1191]**
Scale dependence of the median slope is studied for a number of geological units. Similarity of km-scale roughness of Vastitas Borealis Formation subunits and the circumpolar mantling deposits suggests similarity of their origin.

Frey H.* Sakimoto S. E. H. Roark J.
*MOLA Topographic Structure of the Isidis and Utopia Impact Basins* **[#1500]**
MOLA data show the Utopia Basin to be far more symmetric and bowl-like than previously believed, consistent with an impact origin. MOLA profiles through the Isidis Basin are used to find the basin center, inner ring diameter and rim height.

Thomson B. J.* Head J. W. III
*Utopia Basin, Mars: a New Assessment Using Mars Orbiter Laser Altimeter (MOLA) Data* **[#1894]**
We have reexamined Utopia Basin with MOLA topographic data. We found that the maximum ponded volume in the basin corresponds to a water level of –4350 m. We also found a distinctive terrace at this elevation, suggestive of a standing body of water.

Head J. W. III* Kreslavsky M. Hiesinger H. Pratt S.
*Northern Seas and Oceans in the Past History of Mars: New Evidence from Mars Orbiter Laser Altimeter (MOLA) Data* **[#1352]**
MOLA data show that polygonal ground and low onset diameters of craters with lobate ejecta correspond to basins in the northern hemisphere.

Tanaka K. L.* MacKinnon D. J.
*Basins and Sedimentation Within the Martian Northern Plains* **[#1217]**
MOLA data show that six basins and sedimentary plains make up the northern plains of Mars. Four types of plains units are deposited in them, in the following stratigraphic order: marginal, level-top, basin-floor, and downslope units.

Garvin J. B.* Sakimoto S. E. H.
*Ice-associated Impact Craters on Mars: Implications from MOLA Observations* **[#2026]**
Impact craters adjacent to the North Polar Cap on Mars are observed to display anomalously large amounts of infill, with 10–20 m scale layering in some cases. This suggests dynamic modification of these features.

Sakimoto S. E. H.* Garvin J. B.
*Topography of Impact Structures on the Northern Polar Cap of Mars* **[#1993]**
Viking image data and MOLA topography are used to investigate possible craters and their modification precesses on the N. Polar Cap of Mars.

Fishbaugh K. E.* Head J. W. III
*North Polar Region of Mars: Topography of Circumpolar Deposits and Sediments Based on Mars Orbiter Laser Altimeter (MOLA) Data* **[#1401]**
New topography data are interpreted to indicate that Olympia Planitia overlies ice, mantled cratered plains underlie mantled smooth plains, the cap was once larger, and significant circumpolar sediments originated from previous polar deposits.

Williams R. M.* Phillips R. J.
*Flow Rates and Duration Within Kasei Valles, Mars* **[#1417]**
Derived maximum discharges for Kasei Valles based on elevations from MOLA are orders of magnitude lower than previously estimated. Morphological relationships within the system suggest a gradual formation including several periods of fluvial activity.

Sullivan R.* Daubar I. Fenton L. Malin M. Veverka J.
*Mass-Movement Considerations for Dark Slope Streaks Imaged by the Mars Orbiter Camera* **[#1809]**
Dark streak formation on martian slopes is similar to small mass-movements on debris-covered steep slopes elsewhere on Mars; dark streak features result where small mass-movements occur in the presence of a thin, potentially mobile dust mantle.

Bulmer M. H.* McGovern P. J.
*Emplacement Kinematics of the Northern Olympus Mons Aureole Deposit* **[#2016]**
Five MOLA tracks have collected over Olympus Mons and the surrounding aureole deposits. These topographic profiles allows us to make quantitative comparisons between the different aureole deposits and with mass movement products on Earth, Venus and the Moon.

**Tuesday, March 16, 1999**
**COSMIC DUST**
**1:30 p.m. Room D**

**Chairs:** **K. Kehm**
**S. J. Clemett**

Campins H.*
*Interstellar Signatures in Cometary Solids* **[#1542]**
Comets are believed to be the most primitive bodies in the solar system. However, clear evidence that comets retain a record of the presolar environment has only emerged in the past three years. This paper summarizes these recent results.

Flynn G. J.* Keller L. P. Jacobsen C. Wirick S.
*Organic Carbon in Cluster IDPs from the L2009 and L2011 Collectors* **[#1091]**
Carbon-XANES spectroscopic measurements demonstrate the presence of organic carbon in four cluster fragments from L2009 and L2011, with the one high deuterium cluster showing three distinctly different spectra over a 5×5 micron region.

Clemett S. J.* Messenger S. Keller L. P. Zare R. N.
*Are Aromatic Hydrocarbons the Carriers for D/H and $^{15}N/^{14}N$ Isotope Anomalies in IDPs?* **[#1783]**
Aromatic hydrocarbons are investigated as possible carriers of D/H and $^{15}N/^{14}N$ isotope anomalies in IDPs. In the case of D/H ratios a significant correlation is found for $^{14}N/^{14}N$ ratios, however, more data is still required.

Bradley J. P. Keller L. P. Gezo J.* Snow T. Flynn G. J. Brownlee D. E. Bowey J.
*The 10 and 18 Micrometer Silicate Features of GEMS: Comparison with Astronomical Silicates* **[#1835]**
Comparison of infrared absorption/emission features of submicrometer silicate grains with astronomical silicates.

Brownlee D. E.* Joswiak D. J. Bradley J. P.
*High Spatial Resolution Analyses of GEMS and Other Ultrafine Grained IDP Components* **[#2031]**
Ultrathin microtome sections,using new techniques, has permitted elemental analysis of IDP components that are smaller than 100 nm. These studies indicate the glass component of GEMS has very low Fe content and the residual Fe content may reside in nm-size sulfides.

Rietmeijer F. J. M.*
*Evolution of Condensed Pre-Solar Dust with Metastable Eutectic Smectite Dehydroxylate Compositions: Truly GEMS* **[#1060]**
Ultrafine-grained, metastable eutectic, serpentine dehydroxylate principal components (PCs) with modal Fe = 0.7 in chondritic aggregate IDPs form by thermal annealing of coarse-grained, smectite dehydroxylate PCs and condensed Fe-oxide grains.

Engrand C.* McKeegan K. D. Leshin L. A. Bradley J. P. Brownlee D. E.
*Oxygen Isotopic Compositions of Interplanetary Dust Particles: $^{16}O$-Excess in a GEMS-rich IDP* **[#1690]**
The oxygen isotopic compositions of 4 individual IDPs were measured by ion microprobe. One GEMS-rich IDP is relatively enriched in $^{16}O$. This is the first observation of a significant $^{16}O$-enrichment in a "whole-rock" measurement of a chondritic particle.

Pepin R. O.* Palma R. L. Schlutter D. J.
*Evidence for a Dominant Component of Solar-Energetic-Particle (SEP) Helium and Neon in a Suite of Interplanetary Dust Particles* **[#1864]**
Most of the 12 IDPs analyzed in this study are surprisingly rich in SEP gases, unaccompanied by a significant component due to solar-wind irradiation. Estimates of the SEP/SW fluence ratio from these data are $10^{-3}$ to $10^{-4}$.

Kehm K.* Flynn G. J. Hohenberg C. M. Palma R. L. Pepin R. O. Schlutter D. J. Sutton S. R. Walker R. M.
*A Consortium Investigation of Possible Cometary IDPs* **[#1398]**
We have formed a consortium to study the Messenger and Walker hypothesis that cluster IDPs from June/July 1991 originate from comet SW-3. Initial results from this study do not confirm the anomalous He previously reported as ubiquitous in these IDPs.

Joswiak D. J.* Brownlee D. E. Bradley J. P.
*Amphibole and Disordered Pyriboles in a 10 μm IDP: A Link to Carbonaceous Chondrites?* **[#1987]**
We report the first occurrence of amphibole and disordered pyriboles in an IDP. Similar phases were observed in chondrules in Allende and therefore this IDP may have links with certain carbonaceous chondrites.

Llorca J. Casanova I.*
*Experimental Studies on Sulfide, Carbide and Hydrocarbon Formation in IDPs* **[#1395]**
Experimental reactions between metal and different gas mixtures under nebular P,T,X show no sulfur poisoning effects on the metal-catalyzed hydrocarbon formation. Partial sulfurization of metal results in the formation of primary pyrrhotite prior to troilite.

Genge M. J.* Grady M. M.
*Thermal Heteorogeneity in Micrometeoroids During Entry Heating* **[#1578]**
Evidence for thermal heterogeneity in micrometeorites is presented and its implications for entry heating discussed.

Bernhard R. P.* Warren J. See T. H. Hörz F.
*Optical Analysis of Aerogel Collectors Exposed on Mir* **[#1806]**
The capture of both man-made and natural particles by ODC, combined with experimental evidence, demonstrate that aerogel is a superb and unsurpassed medium to soft-capture high-velocity particles.

**Tuesday, March 16, 1999**
**POSTER SESSION I**
**7:00 p.m. UHCL**

## Mars Global Surveyor (MGS) and Pathfinder

Arvidson R. Guinness E. Slavney S. Springer R.
*Archiving and Release of Data from Mars Surveyor Program Missions* **[#1408]**
The Mars Surveyor Program has adopted a set of guidelines for producing archives from its missions, from Mars Global Surveyor through 2008. MGS data acquired during orbit insertion will be released by April 1999, and thereafter every 6 months.

Caplinger M. A. Jensen E. Edgett K. Eliason E. M. Garcia P. A.
*An Archive of MGS/MOC Imaging Data* **[#1659]**
The Mars Orbiter Camera Imaging Team for the MGS Mission has released an archive of digital image data for distribution to the science community available through the Planetary Data System.

Tracadas P. W. Zuber M. T. Smith D. E.
*Probing the Martian Upper Atmosphere and Exosphere with Orbital Analysis of Mars Global Surveyor During the Science Phasing Orbits* **[#1957]**
The Mars Global Surveyor (MGS) spacecraft experiences measurable drag due to Mars' exosphere (where the science phasing orbits (SPO) had their perifocus). A measurable decrease in both semi-major axis (60 km) and eccentricity (0.002) is measured over the 290 orbits of SPO.

Garvin J. B. Frawley J. J. Sakimoto S. E. H.
*North Polar Dunes on Mars: MOLA Measurements and Implications for Sediment Volumes* **[#1721]**
martian near-polar transverse dunes have been quantified using MOLA topographic data. They are typically 20 m high, 1.5 km wide, and 2.5 km apart. Polar dune sediment volumes probably exceed 10,000 cubic km, a factor of ten larger than previously suspected.

Matias A. Garvin J. B. Sakimoto S. E. H.
*Mid-Latitude vs. Polar-Latitude Transitional Impact Craters: Geometric Properties from Mars Orbiter Laser Altimeter (MOLA) Observations and Viking Images* **[#2008]**
MOLA topography is used to investigate mid- and polar-latitude crater morphology differences.

Garvin J. B. Baloga S. M.
*Inferences on the Emplacement Dynamics of Martian Impact Crater Ejecta: Constraints from MOLA Topography* **[#1735]**
A continuum flow model using cylindrical geometry is developed for analyzing ejecta emplacement for martian rampart craters. New constraints on the behavior of ejecta are suggested.

Frey H. Sakimoto S. E. H. Roark J.
*MOLA Topographic Variations Along the Crustal Dichotomy Boundary Zone in Eastern and Western Mars* **[#1501]**
MOLA profile data reveal differences in the topographic character of the crustal dichotomy boundary zone both along the boundary and between the boundaries in eastern (Deuteronilus-Ismenius Lacus) and western (Tempe) Mars.

Frey H. Roark J. Sakimoto S. E. H. McGovern P.
*The Crustal Dichotomy Boundary West of Tempe Terra: Speculation on Where It Lies Beneath Alba Patera Based on MOLA Topography* **[#1798]**
Based on MOLA topographic data we suggest that Alba sits astride the ancient crustal dichotomy boundary, not adjacent to it, and that its eastern half lies on old cratered terrain.

Frey H. Sakimoto S. E. H. Roark J.
*Discovery of a New Cassini-Size Basin on Mars from MOLA Topographic Data* **[#1497]**
MOLA profile and gridded data provide clear evidence for a previously unknown 450-km-wide, 2-km-deep basin (as large as, and deeper than, the Cassini impact basin) which is not apparent in either Viking imagery or Viking-era topography.

Kreslavsky M. A. Head J. W. III
*Frequency Distribution of Kilometer-scale Slopes on Mars: Initial Results from MOLA Data* **[#1190]**
Slopes on 0.4-25 km baselines were calculated. Steep-slope tails of the slope-frequency distributions are compared for highland plateau, Vastitas Borealis Formation and the North polar cap. Approaches to study of km-scale roughness are discussed.

Hiesinger H. Head J. W. III
*Polygonal Terrain of Utopia Planitia, Mars: The First MOLA Results* **[#1354]**
We present results on the morphology, topography, and the position of polygonal terrain within the Utopia basin and discuss models for the formation.

Lanagan P. D. McEwen A. S.
*Genesis of Young Martian Channels Observed in MOC Images* **[#1814]**
High-resolution images from the Mars Orbiter Camera have revealed several relatively small but young outflow channels in close proximity to volcanic features. These young channels may mark locations of shallow crustal ice.

Hamilton V. E.
*The Effect of Particle Size on Rock Spectra in the Thermal Infrared: Implications for TES Data Analysis* **[#2001]**
The surface of Mars is covered by a wide range of particle sizes, all of which are likely to represent multimineralic mixtures. Accurate deconvolution of TES surface spectra will be aided by an understanding of particle size effects in mixtures.

Edgett K. S. Malin M. C.
*Low Albedo Sediment Transported by Eolian Suspension on Mars: Wind Streaks in Western Arabia Terra* **[#1135]**
A single image from Mars Global Surveyor solves the long-standing question about the origin of low-albedo wind streaks in west Arabia Terra. The dark material is a mantle deposit caused by deposition of dark grains from eolian suspension.

Banerdt W. B. Neumann G. A.
*The Topography (and Ephemeris) of Phobos from MOLA Ranging* **[#2021]**
We have used feature correlation and matching of topography models to correct MOLA ranging data for Phobos to the proper coordinate system, which provides a tight constraint on the ephemeris of Phobos.

Metzger S. M. Carr J. R. Johnson J. R. Lemmon M. Parker T. J.
*Sediment Flux from Dust Devils on Mars — Initial Calculations* **[#2022]**
Spectral differencing techniques have enhanced five dust devil plumes from MPF. The dust devils are 14–79 m wide, 46–350 m tall, and travel over ground at 0.5–4.6 m/s. Their dust loading was approximately 5E–4 kg $m^{-3}$, relative to the general haze of 1.8E–7 kg $m^{-3}$.

Kraft M. D. Greeley R.
*Aeolian Abrasion and the Preservation of Rock Coatings at the Mars Pathfinder Landing Site* **[#1686]**
Ventifacts and rock coatings coexist at the Mars Pathfinder site. Coatings may be salt-cemented, varnish-like, or silica. Experiments show that coatings abrade more easily than rock. The soil layer has deflated. Recent aeolian abrasion is minimal.

Kirk R. L   Howington-Kraus E.   Hare T.   Barrett J.   Becker K.   Cook D.   Sucharski T.   Thompson K.   Blue J.   Galuszka D.   Redding B.   Isbell C.   Lee E.   Rosanova T.   Gaddis L.   Johnson J.   Soderblom L.   Ward W.   Parker T.   Dorrer E.   Holzapfel A.

*Mapping the Sagan Memorial Station Site: Progress and Plans* **[#1844]**

Progress in USGS mapping the Sagan Station site in 1998 has included completion of a supixel-accurate control network and creation of a digital terrain model containing ~500,000 digitally measured points. Eight mapping tasks for 1999 are described.

Basilevsky A. T.   Markiewicz W. J.   Thomas N.   Keller H. U.

*Morphology of the APXS Analyzed Rocks at the Pathfinder Site: Implications for Their Weathering Rate and Distance of Transportation* **[#1313]**

Morphologic studies of APXS analyzed rocks showed that pits on them were resulted from weathering with the rate ~10-2 mm/m.y. Many of the rocks are "broken pebbles" that takes off constraints on the distance of their in-current transportation.

Bridges N. T.   Crisp J. A.

*Constraints on Martian Soil Composition as Inferred from Viking XRFS and Pathfinder APXS and IMP Data* **[#1927]**

Viking XRFS and Pathfinder APXS soil analyses are compared. Images of APXS soil sites are used to infer geologic context. Using these methods, explanations for the differences in soil composition between the Pathfinder and Viking sites are explored.

Komatsu G.   Righter K.

*Salt Weathering of Volcanic Rocks with Xenolith Inclusions: An Alternative Interpretation to "Conglomerate" at the Pathfinder Landing Site* **[#1068]**

The pebble and socket morphology of some rock surfaces in Pathfinder images, which has been interpreted to be conglomerate, may be explained by a combination of salt weathering and xenolith inclusions in volcanic rocks.

Yingst R. A.   Reid R. J.   Smith P. H.   Rice J. W. Jr.

*Spectral Analysis of the Mini-Matterhorn Region, Sagan Memorial Station, Mars* **[#1912]**

We use multispectral analysis of rocks and soils at Mini-Matterhorn to determine whether rock types indicate separate flood events. Two types of rocks are seen which may represent weathering differences incurred from two catastrophic outflows.

Minitti M. E.   Rutherford M. J.

*Genesis of the Mars Pathfinder Sulfur-free Rock from a SNC Parental Magma* **[#1198]**

We investigated the genesis of the sulfur-free rock by conducting experiments on a SNC basaltic starting material under both dry and hydrous conditions. Crystallization of the SNC basalt containing ~ 1.5 wt% $H_2O$ yields the sulfur-free rock.

## Lunar Volcanos from the Inside Out

Spohn T.   Konrad W.   Breuer D.   Ziethe R.

*Lunar Volcanism Induced by Heat Advected from the Lower Mantle: Results of 2D and 3D Mantle Convection Calculations* **[#1768]**

Lunar thermal histories from 2d and 3d convection calculations are presented that study the partial remelting of the magma ocean. The melt zone forms at the likely source depth of the mare basalts and may exist well into the Eratosthenian period.

Taylor L. A.   Patchen A.   Morris R. V.   Taylor D.   Pieters C.   Keller L. P.   McKay D. S.   Wentworth S.

*Chemical and Mineralogical Characterization of the 44–20, 20–10, and <10 Micron Fractions of Lunar Mare Soils* **[#1885]**

The Lunar Soil Characterization Consortium has chemically and modally characterized the fine fractions of mare soils, including separation of pyroxenes data into four groups. $I_s$/FeO data are also presented.

Shearer C. K. Papike J. J.
*Origin of Lunar Mare High-Titanium Basalts. Melting of a Deep Hybridized Source or Shallow Assimilation of High-Ti Cumulates?* **[#1365]**
Shallow assimilation and source hybridization that have been favored by many lunar petrologists as models for the origin of high-Ti mare basalts. These two models are mechanically different, yet their final products are surprisingly similar.

Giguere T. A. Taylor G. J. Hawke B. R. Lucey P. G.
*Distribution of the Titanium Contents of Lunar Mare Basalts: Not Bimodal* **[#1465]**
Remote sensing measurements show that the Ti contents of mare basalts do not form a bimodal distribution, in contrast to data on samples. Maria with intermediate Ti contents (4–7.5 wt% $TiO_2$) are more abundant than are those with high Ti contents.

Snyder G. A. Taylor L. A. Patchen A. Nazarov M. A. Semenova T. S.
*Volcanism at Mare Crisium: Mineralogy and Petrology of "New" Luna 24 Basalts* **[#1496]**
We present petrologic, mineral-chemical, and $^{40}Ar$-$^{39}Ar$ data for Luna 24 mare basalts, including the most primitive olivine vitrophyre analyzed to date.

Van Orman J. A. Elkins L. T. Grove T. L.
*Origin of High-Ti Lunar Ultramafic Glasses: Experimental Evidence from Melting of Magma Ocean Cumulates and Depths of Positive Buoyancy for Melts of Varying Ti Content* **[#1807]**
Experimental melts of high-Ti magma ocean cumulates do not resemble high-Ti ultramafic glasses. Densities of lunar high-Ti melts constrain depth of origin.

Petrycki J. A. Wilson L.
*Volcanic Features and Age Relationships Associated with Lunar Graben* **[#1335]**
We have documented a variety of volcanic features and deposits associated with lunar graben. These imply that graben were commonly formed by shallow dyke emplacement in Imbrian and Eratosthenian times.

Dunkin S. K. Heather D. J.
*The Marius Hills Volcanic Complex: A Stratigraphic Study* **[#1180]**
Clementine analysis of sinuous rilles and impact craters is used to determine the stratigraphy of the Marius Hills region.

Antonenko I.
*Global Estimates of Cryptomare Deposits: Implications for Lunar Volcanism* **[#1703]**
A global survey of cryptomare areas, volumes and ages was conducted. Results show that volcanism may have been more voluminous in early lunar history than previously believed, suggesting a hotter interior and earlier formation of melt source regions.

Gaddis L. R. Hawke B. R. Robinson M. S. Coombs C. R.
*Juvenile Materials in Lunar Pyroclastic Deposits* **[#1732]**
This abstract reports on a comparison of the compositional characteristics of small and large lunar pyroclastic deposits as viewed with Clementine UVVIS data.

Lindstrom M. M. Mittlefehldt D. W. Martinez R. R.
*Basaltic Lunar Meteorite EET96008 and Evidence for Pairing with EET87521* **[#1921]**
Geochemical study of lunar meteorite EET96008 shows that it is a heterogeneous basaltic breccia containing matrix and clasts of variable composition. Comparison with EET87521 shows that the two breccias are almost certainly paired meteorites.

Mikouchi T.
*Mineralogy and Petrology of a New Lunar Meteorite EET96008: Lunar Basaltic Breccia Similar to Y-793274, QUE94281 and EET87521* **[#1558]**
This abstract presents the mineralogy and petrology of EET96008, a new lunar meteorite. It is a basaltic breccia (mainly VLT and low-Ti basalts) similar to Y793274, QUE94821 and EET87521. All of them probably share the same source crater on the Moon.

## New Moon Views

Hood L. L. Lin R. P. Mitchell D. L. Acuna M. A. Binder A. B.
*Initial Maps of the Crustal Magnetic Field of the Moon Using Lunar Prospector Magnetometer Data* **[#1382]**
Across a broad section of the southern far side mapped at high altitudes using data from February through May of 1998, the largest concentrations of crustal fields occur near the antipodes of the crisium, Serenitatis, and Imbrium basins.

Gillis J. J. Haskin L. A. Spudis P. D.
*An Empirical Calibration to Calculate Thorium Abundances from the Lunar Prospector Gamma-Ray Data* **[#1699]**
We offer a preliminary calibration for the Prospector gamma-ray data, to calculate ppm Th from the map of Th gamma-ray count rate. We then correlate Th concentrations with specific geologic units to yield information about local geologic processes.

Ojakangas G. W.
*Luni-solar Tidal Signatures in 2000 Ma Rhythmic Tidal Sedimentary Sequences and Implications for the Ancient Lunar Orbit* **[#1694]**
The oldest tidal sedimentary cyclicities presently known (~2Ga) are described. Although degraded, lamina sequences display neap-spring and other cycles that constrain the lunar orbit to semimajor axis values > ~20 earth radii ~2Ga ago.

Gasnault O. d'Uston C.
*A Numerical Code for Fast Neutron Planetary Emission in Surface Analysis* **[#1717]**
Neutron detectors are used in composition mapping. A code was developed to allow a thorough study of the leakage neutron flux in planetary surfaces. Quantified Fe impact on lunar fast neutrons is evaluated and appears consistent with measurements.

Wieczorek M. A. Phillips R. J. Korotev R. L. Jolliff B. L. Haskin L. A.
*Geophysical Evidence for the Existence of the Lunar "Procellarum KREEP Terrane"* **[#1548]**
Remote sensing, sample, and geophysical data all suggest that the Procellarum/Imbrium region of the Moon is a unique geochemical province. We suggest that the crust in this province is largely composed of "KREEP-basalt."

Williams J. G. Boggs D. H. Ratcliff J. T. Dickey J. O.
*The Moon's Molten Core and Tidal Q* **[#1984]**
Analysis of Lunar Laser Ranges reveals signatures due to a liquid core as well as to solid-body tides. The estimated upper limit for core radius is 352 km for pure iron. Tidal dissipation is strong; Q at one month is 37.

Masarik J. Brückner J. Reedy R. C.
*Monte Carlo Simulations of Gamma Ray Emission from the Lunar Surface* **[#1655]**
Fluxes of the gamma rays from the lunar surface were simulated for chemical compositions characterized by high and low iron content. These fluxes can contribute to the interpretation of experimental neutron and gamma-ray data from Lunar Prospector.

Yingst R. A.   Head J. W. III
*Jules Verne Mare Soils as Revealed by Clementine UVVIS Data* **[#1684]**
To determine the nature of potentially low-Ca pyroxene (noritic) spectra in six South Pole-Aitken basin mare deposits, we undertake a multispectral analysis of a representative of these deposits, that associated with Jules Verne crater.

Shkuratov Yu. G.   Ovcharenko A. A.   Kreslavsky M. A.
*Shadow-Hiding and Coherent Backscatter Effects in Opposition Surge of the Moon* **[#1033]**
Our laboratory photometric measurements have shown that a component of coherent backscatter can be important for surfaces even if their albedo as low as 5%. Hence, the opposition surge of the Moon is substantially formed by the coherent backscatter.

Starukhina L. V.   Shkuratov Yu. G.   Kreslavsky M. A.
*Theoretical Validation of Lucey's Approach to Composition and Maturity of Lunar Regolith* **[#1032]**
Spectral effects of iron reduction in lunar samples have been calculated. The linear maturation trends on A (0.75 μm) - C (0.95/0.75 μm) plot have been confirmed theoretically though the lines are shown to have no common origin.

Eliason E. M.   McEwen A. S.   Robinson M. S.   Lee E. M.   Becker T.   Gaddis L.   Weller L. A.   Isbell C. E.   Shinaman J. R.   Duxbury T.   Malaret E.
*Digital Processing for a Global Multispectral Map of the Moon from the Clementine UVVIS Imaging Instrument* **[#1933]**
The digital image processing used in the compilation of the global multispectral map of the Moon is described.

Rosiek M. R.   Kirk R.   Howington-Kraus A.
*Lunar Topographic Maps Derived from Clementine Imagery* **[#1853]**
This report provides a review of the photogrammetric techniques used to derive elevation information from Clementine imagery and a summary of the initial results. The study areas are the North and South Poles of the Moon.

Grier J. A.   McEwen A. S.   Strom R. G.   Lucey P. G.   Plassman J. H.   Winburn J. R.   Milazzo M.
*A Survey of Bright Lunar Craters — Developing a Relative Crater Chronology* **[#1935]**
We have conducted a survey of the apparent maturity of ejecta for a number of bright rayed lunar craters. A relative crater chronology based on this survey can be used to help constrain the recent flux of impactors.

Velikodsky Yu. I.   Kreslavsky M. A.   Shkuratov Yu. G.   Akimov L. A.   Korokhin V. V.
*An Empirical Photometric Function in Analysis of Clementine Data* **[#1039]**
It is shown that the empirical photometric function presented by Akimov L.A. (1988) give good results if applied to Clementine image data. It secures homogeneous photometric conditions and allows successful prognosis of the lunar surface composition.

Kaydash V. G.   Shkuratov Yu. G.   Kreslavsky M. A.   Opanasenko N. V.
*Composition and Maturity Degree of Reiner-Gamma Formation from Clementine Data* **[#1044]**
A method for determination of maturity degree and chemical composition (Fe and Ti content) of regolith is proposed. The Clementine data for Reiner Gamma is used to illustrate new technique and to built $I_s$/FeO and (Ti,Fe) maps for this region.

Yamamoto H.   Isobe T.   Homma K.   Shimizu M.
*Shape Recognition of Craters in Clementine Images* **[#1066]**
For automatic recognition of various shape of craters in Clementine images, effective methods using a relatively small type computer architecture have been developed.

Opanasenko N. V. Shkuratov Yu. G. Kreslavsky M. A. Kaydash V. G.
*A Comparison of Clementine and Earth-based Observations of the Moon* **[#1130]**
A systematic difference between the Clementine and Earth-based absolute calibrations have been found. It was shown that the striped structure of the Clementine mosaic image can be eliminated by a new photometric function and Earth-based albedo image.

Heather D. J. Dunkin S. K.
*Clementine Multispectral Analysis of Tsiolkovsky Crater, Lunar Farside* **[#1177]**
This study utilises Clementine multispectral data to investigate the geology of the farside lunar crater Tsiolkovsky.

## Venus Geology and Geophysics

Grosfils E. B.
*Constraining Models of Shield Field Formation on Venus* **[#2035]**
Data obtained from a study of the elevation distribution of 454 venusian shield fields are used to gain insight into the process of shield field formation.

Krause M. O. Grosfils E. B.
*The Altitude Distribution of Uncategorized Intermediate Volcanoes on Venus* **[#1685]**
We analyzed the distribution of one subset of intermediate-sized volcanoes on Venus, "uncategorized intermediate volcanoes" or UIVs, and found that they do not conclusively conform to the predictions of the NBZ theory of volcanic emplacement.

Addington E. A.
*Clusters of Small Volcanoes on Venus* **[#1281]**
Shield fields within Sappho Patera (V20) were analyzed in order to determine their ages relative to the regional plains. The results of this study indicate that the shield fields have a wide range of relative ages and were formed over a long period of geologic time.

Wichman R. W.
*Distribution of Volcanically-infilled Craters on Venus* **[#1156]**
Measuring crater floor brightness and floor morphometry provides an improved basis for identifying volcanically-floored craters on Venus. These craters show regional variations in distribution and some correlation with local volcanic centers.

Brian A. W. Stofan E. R. Guest J. E.
*A New Topographic Rise on Venus: Characteristics and Implications* **[#1579]**
A low plateau in north Navka Planitia is interpreted to be an early-stage volcanic rise characterised by large, volcanic edifices. This discovery has implications for the development of an evolutionary sequence among volcano-dominated rises.

Banks B. K. Hansen V. L.
*Intratessera Flood-Lava Basins (ITBs) Constrain Timing of Crustal Plateau Structures* **[#2053]**
Timing relations of crustal plateau structures.

Stewart E. M. Head J. W. III
*Stratigraphic Relations and Regional Slopes in the Baltis Vallis Region, Venus: Implications for the Evolution of Topography* **[#1173]**
Baltis Vallis, a 6800-km-long canali on Venus, is interpreted to have formed in one event, with a uniform gradient, but is presently highly deformed. It can therefore be used to illuminate the regional stratigraphy and tectonic history.

Head J. W. III   Stewart E. M.   Pratt S.
*Analysis of Global and Regional Slope Distributions for Venus* **[#1264]**
A global slope map of Venus was produced using Magellan GTDR data. The range, frequency distribution, variation with elevation, and geographic distribution of slopes are analyzed. Slopes are then correlated with classes of geologic features.

Aittola M.   Raitala J.
*Classification of Venusian Novae* **[#1102]**
The term "nova" is short and its definition is well established. 55 novae of the Venus Volcanic Feature Catalogue were classified based on their morphological features and geological environments.

Basilevsky A. T.   Raitala J.
*Morphology of Selected Novae Based on Analysis of the Magellan Images, Venus* **[#1565]**
A photogeological analysis of a few novae and their location in the Venusian stratigraphy.

Basilevsky A. T.   Burba G. A.   Ivanov M. A.   Bobina N. N.   Shashkina V. P.   Head J. W. III
*Photogeologic Map of Northern Venus: A Progress Report* **[#1295]**
Mapping of Venus above 34°N shows consistency of geologic units over 21% of the surface.

Ivanov M. A.   Head J. W. III   Basilevsky A. T.   Bobina N. N.   Burba G. A.   Kryuchkov V. P.   Pronin A. A.   Shashkina V. P.
*Topographic Distribution of Geologic Units in Northern Venus and in the 30N Geotraverse* **[#1614]**
The topographic distribution of the same geologic units in two large areas on Venus (around N. Pole and in the 30N geotraverse) is essentially the same, suggesting similar evolution of large-scale topography in both areas.

Ivanov M. A.   Head J. W. III
*Geologic Mapping in V-13 (Ganiki Planitia) Quadrangle, Venus: Preliminary Results* **[#1204]**
Preliminary mapping of the V-13 quadrangle reveals that the basic stratigraphic scheme developed for Lavinia and Atalanta Planitiae is also applicable to the territory of Ganiki Planiti.

Dohm J. M.   Tanaka K. L.
*Geologic Map of Metis Regio Quadrangle (V-6), Venus* **[#1449]**
Geologic mapping of V-6 indicates four major periods of activity, represented by tesserae, coronae, wrinkle-ridge plains, and large volcanoes. Our stratigraphy generally is consistent with current models of global stratigraphy and corona formation.

Senske D. A.
*Geology of the Tellus Tessera Quadrangle (V-10), Venus* **[#1668]**
Geologic mapping of the Tellus Tessera Quadrangle (V-10) is being performed. The results from this analysis are used to constrain the sequence of events in tessera formation along with evaluating the relations between tessera and adjacent plains.

Senske D. A.
*Geology of the Phoebe Regio Quadarangle (V-41), Venus* **[#1671]**
The sequence of events and the processes involved in the formation of of tessera and its relation to adjacent plains is being examined through geologic mapping of the Phoebe Regio Quadrangle.

Davis A. M.   Ghail R. C.
*An Extended Strike-Slip Zone in Aphrodite Terra* **[#1330]**
Mapping of lineaments has indicated sinistral strike-slip movement between two tesserae blocks in Aphrodite Terra. Fracture-pattern analysis demonstrates reidal-shear type strike-slip movement, along a ~500 km NE-SW oriented zone.

Ghail R. C.
*Aeolian Processes in South-East Thetis Regio* **[#1258]**
Erosional features are observed in South-East Thetis Regio and from these wind flow is inferred. Magellan and Pioneer Venus reflectivity data are merged to infer type and thickness of sediment deposited in the adjacent plains.

Kucinskas A. B.   Banerdt W. B.
*Constraints on Venusian Crustal and Lithospheric Properties from Magellan Data* **[#2050]**
Spherical harmonic derived Venus topography and gravity are used, along with the observed stress field to model lithospheric stresses.

Anderson F. S.   Smrekar S. E.
*Implications of Atmospheric Temperature Change for Surface Deformation on Venus* **[#1943]**
Lithospheric thermal stress from climatic temperature change readily explains short wavelength features such as polygonal and gridded terrains.

## Europa

Varnes E. S.   Jakosky B. M.
*Lifetime of Organic Molecules at the Surface of Europa* **[#1082]**
The purpose of this study is to analyze the effects of particle bombardment on organic molecules at the surface of Europa, and to determine whether such molecules can survive dissociation.

Blaney D. L.   Goguen J. D.   Veeder G. J.   Johnson T. V.   Matson D. L.
*Europa's Thermal Infrared Emission* **[#1657]**
Ground based telescopic observations of Europa at 8.7, 12.5, and 20 mm were taken. Europa's thermal emission has a relatively large amplitude light curve with a maximum around 345°W longitude and a minimum around 100°W longitude.

Milazzo M.   McEwen A. S.   Hoppa G. V.   Phillips C. B.   Tufts B. R.   Turtle E. P.   Greeley R.   Galileo SSI Team
*Medium Resolution Imaging of Europa: A View from Pole to Pole* **[#1979]**
Medium resolution imaging of Europa helps us put high resolution images into context. This helps us understand local processes shaping Europa.

Williams D. A.   Klemaszewski J. E.   Greeley R.   Moore J. M.   Pappalardo R. T.   Prockter L. M.   Head J. W. III
Geissler P. E.   Hoppa G.   Phillips C. B.   Tufts B. R.   Greenberg R.   Sullivan R. J.   Belton M. J. S.
Galileo Imaging Team
*Terrain Variation on Europa: Overview of Galileo Orbit E17 Imaging Results* **[#1396]**
This abstract provides an overview of preliminary scientific interpretations made from observations of Europa on Galileo's 17th orbit of Jupiter, obtained during October, 1998.

Kadel S.   Chuang F.   Greeley R.   Granahan J.   Fanale F.   Asphaug E.   Moore J.   Collins G.   Head J. W. III
Pappalardo R.   Prockter L.   Carlson R.   Galileo SSI and NIMS Teams
*Geomorphic Mapping of Europa: Clues to an Underlying Water Ocean from the Tyre Macula Region* **[#1975]**
We have produced a geomorphic map and outlined a general geologic history for the Tyre area of Europa. Regional and local morphology indicate that region geologic style changed over time from closely- then widely-spaced ridge formation to chaos and fracture formation.

Durand-Manterola H. J.   Oleschko K.   Ortega F.   Tolson G.
*Fractal Atlas of Europa Fault Offsets* **[#1452]**
In the present study, the static geometrical properties of the fault offsets were described by mass fractal dimensions (Dm), while the dynamics of studied network was estimated by the spectral (or fracton) dimension d.

Spaun N. A. Prockter L. M. Pappalardo R. T. Head J. W. III Collins G. C. Antman A. Greeley R. Galileo SSI Team

*Spatial Distribution of Lenticulae and Chaos on Europa* **[#1847]**

This study focuses on the spatial distribution of lenticulae and chaos of selected areas of varying longitude near Europa's equator. We find that the distribution of these features may support existing global thickness and convection models.

Head J. W. III Pappalardo R. T. Spaun N. A. Prockter L. M. Collins G. C.

*Chaos Terrain on Europa: Characterization from Galileo E12 Very High-Resolution Images of Conamara Chaos: 1. Polygons* **[#1285]**

Analysis of Conamara Chaos shows details of polygon movement.

Collins G. C. Head J. W. III Pappalardo R. T. Spaun N. A.

*Evaluating Models for the Formation of Chaotic Terrain on Europa* **[#1434]**

Chaotic terrain on Europa has been cited as evidence for a very thin ice shell overlying an ocean, but this model lacks a plausible energy source. Instead, combined warm ice diapirism and melting in a thicker ice shell may be more plausible.

Klemaszewski J. E. Greeley R. Prockter L. M. Geissler P. E. Galileo SSI Team

*Geologic Mapping of Eastern Agenor Linea, Europa* **[#1680]**

Agenor Linea is perhaps the youngest large linea on Europa's surface. Here we describe units based on geologic mapping of Agenor Linea using high-resolution Galileo SSI data.

Prockter L. M. Head J. W. Pappalardo R. T. Collins G. C. Klemaszewski J. E. Geissler P. E. Galileo SSI Team

*Geological Mapping of Central Agenor Linea, Europa (212°–226°)* **[#1299]**

We present a geological map of central Agenor Linea. Previously thought to be recently or currently active, we show that the band probably formed in three episodes and is deformed and disrupted by later features, hence is older than expected.

Prockter L. M. Pappalardo R. T. Sullivan R. Head J. W. III Patel J. G. Giese B. Wagner R. Neukum G. Greeley R.

*Morphology and Evolution of Europan Bands: Investigation of a Seafloor Spreading Analog* **[#1900]**

High resolution imaging of Europa's polygonal bands reveals morphological similarities with terrestrial mid-ocean ridges. Using a terrestrial seafloor spreading analog, we propose that these bands formed relatively rapidly, from viscous material.

Tufts B. R. Greenberg R. Hoppa G. Geissler P.

*Tidal Model for Lithospheric Dilation on Europa* **[#1909]**

A tidally-based model for lithospheric dilation on Europa accounts for the range of morphologies among dilational features, including Class 2 ridges (Greenberg taxonomy), bands, and various intermediate dilational lineaments.

Tufts B. R. Greenberg R. Hoppa G. Geissler P. E.

*Strike-Slip on Europa: Galileo Views of Astypalaea Linea* **[#1902]**

Galileo views of Asytpalaea Linea reveal the internal structure of the strike-slip fault, lend confirmation to tidally-induced "walking" as the driver, support the Greenberg et al. ridge model and the presence of a subsurface decoupling layer.

Hoppa G. V. Tufts B. R.

*Formation of Cycloidal Features on Europa* **[#1599]**

Here we propose a model for the formation of cycloidal features on Europa as tension cracks due to diurnal tidal stress that can explain cycloidal segments, cusps, length, orientation, skewness, termination, and curvature that are commonly observed.

Hoppa G. V. Greenberg R. Tufts B. R. Geissler P. E.

*Plume Detection on Europa: Locations of Favorable Tidal Stress* **[#1603]**

Here we assess the possibility of detecting plumes during the E19 encounter with Europa based on a diurnal tidal stress model, and identify potential target areas for future plume searches.

Fagents S. A. Greeley R. Sullivan R. J. Pappalardo R. T. Prockter L. M. Galileo SSI Team

*A Cryomagmatic Origin for Low Albedo Features on Europa* **[#1296]**

Theoretical modeling suggests that certain low-albedo features on Europa might represent lag deposits of dark non-ice material resulting from enhanced ice sublimation in response to conductive heating by subsurface cryomagmatic intrusions or diapirs.

Ogawa Y. Yamagishi Y. Kurita K.

*Evaluation of Cryovolcanism on Europa* **[#1575]**

On Europa, liquid water magma must go up through the ice to the surface. Extra driving force is needed to overcome negative buoyancy. Supposing an isolated water magma chamber, we estimate the magnitude of solidification-induced overpressure.

Turtle E. P. Phillips C. B. Collins G. C. McEwen A. S. Moore J. M. Pappalardo R. T. Schenk P. M. Galileo SSI Team

*Europan Impact Crater Diameters and Inferred Transient Crater Dimensions and Excavation Depths* **[#1882]**

We have measured the diameters of all Europan craters observed to date that are larger than 4 km. We tabulate these with estimates for their transient crater diameters and depths and excavation depths. We discuss their implications for Europa.

Giese B. Wagner R. Neukum G. Moore J. M. Galileo SSI Team

*The Local Topography of Europa's Crater Cilix Derived from Galileo SSI Stereo Images* **[#1709]**

The topography of Europa's crater Cilix is derived from Galileo stereo images by methods of photogrammetry. Implications for the impact process and crust properties are discussed.

Prieto O. Kargel J. S. Quilez E. Martinez M. P.

*Reflectance Spectrum of $MgSO_4 \cdot 12H_2O$: Compositional Implications on the Surface of Europa Jovian Satellite* **[#1762]**

Studies on NIMS Galileo spectra show that mineral composition of the surface of Europa includes some hydrated salts. Preliminary spectral diffuse reflectance data for $MgSO_4 \cdot 12H_2O$ mineral are presented in this study.

Kargel J. S.

*Aqueous Chemical Evolution and Hydration State of Europa's Salts* **[#1851]**

Evidence for salts on Europa interpreted in terms of plausible geochemical pathways starting from Europa's origin, ending in formation of either (a) Mg-Na-$SO_4$-ice crust/ocean, or (b) Na-$SO_4$-$CO_3$ crust/ocean. Data on the stability of hydrated salts also discussed.

Sullivan R. Moore J. Pappalardo R.

*Mass-Wasting and Slope Evolution on Europa* **[#1747]**

Highest resolution Galileo images show that debris generation and dry mass-wasting are pervasive wherever steep slopes are seen, and some slopes probably are still actively evolving.

## Small Bodies

Stooke P. J.

*Large Scale Asteroid Maps* **[#1021]**

A scheme for systematic large scale mapping of small bodies is proposed. The Morphographic Equidistant map projection applied to the best-fit triaxial ellipsoid creates useful map quadrangles which can also be fitted together as gores to create globes.

Ghosh A. McSween H. Y. Jr.
*Dependence of the Thermal History of Asteroids on Accretion Rate and Duration* **[#1121]**
This is the first attempt at evaluating the thermal history of a growing asteroid using idealized accretion models. Significant thermal heterogeneity can be produced in a scenario of heating by $^{26}$Al due to differences in the rate of asteroidal growth.

Wilson L. Keil K.
*The Internal Structure of Asteroids* **[#1244]**
Impact disruption and reassembly can produce asteroids denser and narrow at one end of the long axis than at the other. Aqueously altered asteroids 20 to 50 km in size may have up to ~50% void space due to explosive loss of interior material.

Cloutis E. A. Burbine T. H.
*The Spectral Properties of Troilite/Pyrrhotite and Implications for the E-Asteroids* **[#1875]**
The spectral properties of troilite-pyrrhotite minerals (FeS to Fe(1-x)S) were examined. It was found that spectral properties are related to variations in structure and/or composition and that it may be identifiable in the spectra of asteroids.

Burbine T. H. Binzel R. P. Bus S. J.
*Near-Infrared Spectra of Pyroxene- and Olivine-rich Asteroids* **[#1777]**
To try to mineralogically characterize small (diameters<20 km) asteroids, we have instituted a near-infrared (0.9 to 1.65 microns) observational program called SMASSIR. We have focused on bodies with visible spectra indicating pyroxene- or olivine-rich surface assemblages.

Ivanov B. A. Neukum G. Wagner R.
*Impact Craters, NEA, and Main Belt Asteroids: Size-Frequency Distribution* **[#1583]**
The comparison of impact crater and main belt asteroid size-frequency distributions (SFD) shows the relative stability of their SFD during the past 3.7 b.y. The NEA and main belt asteroids seem to be similar in main details.

Barnouin-Jha O. S. Cheng A. F.
*The Spatial Variation of Impact Flux on Asteroids* **[#1837]**
A method is presented for computing the spatial distribution of impact flux and impact angle on the surface of asteroids.

Merline W. J. Chapman C. R. Colwell W. B. Veverka J. Harch A. Bell M. Bell J. F. III Thomas P. Clark B. E. Martin P. Murchie S. Cheng A. Domingue D. Izenberg N. Robinson M. McFadden L. Wellnitz D. Malin M. Owen W. Miller J.
*Search for Satellies Around Asteroid 433 Eros from NEAR Flyby Imaging* **[#2055]**
A preliminary search for satellites of 433 Eros from the NEAR flyby of December 1998 has revealed no definitive detections of satellites larger than about 50 m diameter in the entire gravitational sphere of influence.

Starukhina L. V.
*Estimation of 3 Micrometer Light Absorption by Hydroxyl of Solar Wind Origin: Implication for the Problem of Water Detection on the Surfaces of Atmosphereless Celestial Bodies* **[#1194]**
Chemical trapping of solar wind protons and formation of OH groups in regolith particles on the surfaces of atmosphereless bodies can result in absorption bands near 3 micrometers of the same depth, width and position as the bands due to ice or hydrosilicates

Hiroi T. Sasaki S.
*Importance of Olivine in S-Asteroid Space Weathering* **[#1444]**
As the result of the S asteroid observations and laser-irradiation experiments, olivine on the S asteroids is like to be more subject to space wathering than pyroxene. No signature of glass formation was detected in laser-irradiated olivine spectra.

Yamada M. Sasaki S. Fujiwara A. Hiroi T. Hasegawa S. Nagahara H. Ohashi H. Ohtake H. Yano H.

*Simulation of Space Weathering by Nanosecond Pulse Laser Heating and Proton Implantation: Difference of Olivine and Pyroxene Samples* **[#1566]**

To simulate the surface alteration process called "space weathering", experiments of nanosecond pulse laser irradiation and proton implantation were performed. Reflectance of olivine is more easily changed than that of pyroxene.

## Origins of Planetary Systems

Ozawa K. Nagahara H.

*Chemical and Isotopic Fractionation During Diffusion-controlled Free Evaporation from a Condensed Phase* **[#1605]**

A diffusion-controlled evaporation model is examined to see the behavior of elements and isotopes during free evaporation from a binary condensed phase. Chemical and isotopic fractionation is decoupled for highly volatile elements in the strongly diffusion-controlled regime.

KenKnight C. E.

*Nebular Convection: Lessons from Meteorology* **[#1131]**

Convection whose fastest growing mode yields paired helices is the "cloud rows" of Earth and caused rings in the nebula. Hundreds of the latter formed a critical radial flow with a complex energy release controlled by opacity derived from the solids.

Prentice A. J. R.

*Origin and Bulk Chemical Composition of the Galilean Satellites of Jupiter and the Inner Planets* **[#1509]**

It is proposed that both the Galilean satellites and the inner planets formed by the same mechanism, namely by condensation and accumulation of grains within gas rings cast off from the equators of the contracting, turbulent proto-Jovian/solar clouds.

## Presolar Grains

Macke R. J. Bernatowicz T. Swan P. Walker R. M. Zinner E.

*Non-Chemical Isolation of Silica and Presolar SiC from Murchison* **[#1435]**

We report on a new non-erosive disaggregation method for the isolation of silica and presolar SiC grains from meteorites. This method does not involve acid digestion or polishing and thus leaves the grain surfaces intact for study.

Yoshida T. Emori H. Nakazawa K.

*Abundance Ratios of Light Elements Synthesized in 15, 20, and 25 $M_\odot$ Type II Supernovae* **[#1311]**

We pursue explosive nucleosynthesis in the He-layer and the H-envelope for 15, 20, and 25 $M_\odot$ supernova explosions considering synthesis after mixing of the layers and investigate common features and differences on abundance ratios of light elements.

Stadermann F. J. Walker R. M. Zinner E.

*Sub-Micron Isotopic Measurements with the CAMECA NanoSIMS* **[#1407]**

This new SIMS instrument is particularly well suited for the study of presolar grains and isotopic imaging of TEM slices. We present results of the first actual measurements to document its capabilities in real-life analytical situations.

Choi B.-G. Huss G. R. Wasserburg G. J.

*Isotopic Compositions of Refractory Oxide and SiC Grains in Qingzhen (EH3)* **[#2004]**

The O isotopes of 31 refractory oxides in Qingzhen were measured and no presolar oxide was found. The Si isotopes of 19 Si-rich refractory phases fall in narrow range near solar, while C isotopes are always enriched in $^{12}C$ relative to solar.

Kiyota K. Sugiura N.
*Graphite Aggregates in UOCs: Carriers of Isotopically Anomalous Nitrogen* **[#1240]**
Some UOCs contain graphite aggregates associated with metal, Fe oxides or Fe sulfides. Graphite in Mezo Madaras, Dimmitt and Yamato 74191 contains isotopically heavy N and H. The graphite is possibly related to graphite in Kohar.

Verchovsky A. B. Fisenko A. V. Semjonova L. F. Wright I. P. Pillinger C. T.
*Ion Implantation into Presolar Grains: A Numerical Model and Its Astrophysical Implications* **[#1757]**
A numerical model of ion implantation which can be used for calculations of concentration profiles and isotopic effects in presolar grains has been developed.

Davis A. M. Pellin M. J. Lewis R. S. Amari S. Clayton R. N.
*Light and Heavy Element Isotopic Compositions of Mainstream SiC Grains* **[#1976]**
We report Mo isotopic compositions of mainstream presolar SiC grains with measured C, N and Si isotopic composition and examine correlations among isotopic systems and their implications for nucleosynthetic processes.

Sahoo S. K. Yonehara H. Kurotaki K. Masuda A. Yoneda S.
*The Isotopic Composition of Zirconium in Terrestrial Samples* **[#1230]**
High precision measurement of zirconium isotope ratios from Silinjarvi zircon sample has been carried out by using a Sector thermal ionization mass spectrometer. Relative aberration pattern has been calculated and $^{96}Zr$ reveals a negative aberration of 2.2 $\varepsilon$.

Clayton D. D.
*Condensation of Carbon in Supernovae: 2. Graphite in Meteorites* **[#1048]**
Consequences for meteoritics of carbon condensation in radioactive supernova gases are: size spectrum and mass fraction of C SUNOCONs; surface area; infrared emission; chemical fractionation; C/O abundance ratio.

## Calcium-Aluminum-rich Inclusions (CAIs) and Chondrules

Bogdanovski O. Jagoutz E.
*Samarium-Neodymium Isotopic Systematics of CAIs from Efremovka and Allende Meteorites* **[#1891]**
The Sm-Nd isotopic study of coarse-grained and fine-grained CAIs of different types from Allende and Efremovka meteorites.

Ireland T. R. Zinner E.
*High Sensitivity Analysis of $^{41}K$ Abundances in Refractory Inclusions* **[#1455]**
We have used the high sensitivity of SHRIMP ion microprobes with $^{40}Ca+$ count rates of >100 MHz to assess the analysis of the $^{41}Ca$-$^{41}K$ system. At these count rates, the background can be quantified and interferences monitored dynamically during analysis.

Nagasawa H. Suzuki T. Ito M. Morioka M.
*Inter-diffusion in Melilite: Determination of Al+Al vs. Mg+Si Inter-diffusivities* **[#1530]**
Inter-diffusion of Al+Al vs. Mg+Si in the gehlenite($Ca_2Al_2SiO_7$)-akermanite(Ca2MgSi2O7) solid solution system of melilite along the a-axis has been studied in the temperature range of 1200° to 1350°.

Sakai T. Yurimoto H.
*Oxygen Isotope Distribution in CAIs of the Murchison CM2 Meteorite* **[#1528]**
We found 89 CAIs in a polished thin section of the Murchison, and analyzed O isotope ratios of individual mineral in CAIs by SIMS. The O-isotopic variations observed were divided into $^{16}O$-enriched and $^{16}O$-depleted groups.

May C. Russell S. S. Grady M. M.
*Analysis of Chondrule and CAI Size and Abundance in CO3 and CV3 Chondrites: A Preliminary Study* **[#1688]**
This is a survey of the abundance, type, size and distribution of CAIs and chondrules. CAIs are less well sorted and smaller on average than chondrules in COs and in CVs, pointing to a late injection of CAIs after the chondrule sorting process.

Reisener R. J. Goldstein J. I.

*Microstructural and Chemical Study of Fe-Ni Metal Inside Semarkona Chondrules* **[#1868]**

Fe-Ni metal inside Semarkona chondrules is a mixture of kamacite and tetrataenite. The basic microstructure is plessite. We interpret metal thermal history in terms of the plessite microstructure and metal phase compositions.

Benoit P. H. Symes S. J. K. Sears D. W. G.

*Chondrule Size Distributions: What Does It Mean?* **[#1053]**

The restricted range of chondrule size within each chondrite group has been interpreted as indicating a sorting mechanism. We suggest, however, that chondrule size distribution may be primary and reflect formation processes.

## Chondrites

Brearley A. J. Hanowski N. P. Whalen J. F.

*Fine-Grained Rims in CM Carbonaceous Chondrites: A Comparison of Rims in Murchison and ALH 81002* **[#1460]**

Fine-grained rims in the highly altered CM chondrites, ALH 81002 show significant compositional and textural differences from rims in Murchison. We attribute these differences to the effects of advanced alteration on rims which were similar prior to alteration.

Fagan T. J. Krot A. N. Keil K.

*FeO-rich Silicates in EH3 and EL3 Chondrites: Evidence for Variations in Redox Conditions in Enstatite Chondrite-forming Region?* **[#1523]**

Are the ferrous silicates in EL3s and EH3s foreign or native to the EC-forming solar nebular region? In situ ion probe measurements of O-isotopic compositions of CAIs and ferromagnesian silicates in ECs may resolve this issue.

Grossman J. N.

*The Chemistry and Structure of the Matrix of Semarkona on a mm- to cm-scale* **[#1642]**

X-ray maps for 5 elements were prepared for Semarkona. A method was developed for masking all but fine-grained matrix out of the images. Rims, super-rims, and true matrix can all be observed. Elemental mobility during aqueous alteration can be documented.

Duke C. L. Brearley A. J.

*Experimental Low Temperature Aqueous Alteration of Allende Under Reducing Conditions* **[#1782]**

This abstract presents the results of a series of low temperature hydrothermal alteration experiments that were carried out in an anoxic environment. The results are compared with the results of previous experiments run under oxidizing conditions.

Bérczi Sz. Lukács B.

*Thermal/Aqueous (2.): Competition to Obscure Chondrules in the Van Schmus-Wood Sequence, on a New Scheme* **[#1275]**

In studying consequences of the reclassification of some portions of CM2 chondrites to CM1 (Zolensky et al., 1997) we made a new scheme to represent competition of thermal and aqueous metamorphism, where different chondritic evolutionary pathways can also be represented.

Buchanan P. C. Zolensky M. E.

*Nonporous Silicate Rims Around Dark Inclusions in Allende* **[#1830]**

Nonporous silicate rims around type B and some type A/B dark inclusions may be formed by diffusion of aqueous fluids out of these xenoliths into hot, dry Allende matrix.

Gounelle M. Zolensky M. E. Maurette M.

*Submillimeter Carbonaceous Chondrite in HED Achondrites: Small is Another World* **[#1134]**

Lonesome saponite as well as other mineralogical oddities set the submillimeter carbonaceous chondrites clasts in HED meteorites as a peculiar solar system population distinct either from their larger counterparts or from Antarctic micrometeorites.

Nazarov M. A. Brandstätter F. Kurat G.
*Phosphorian Sulfides from Banten and Boriskino CM Chondrites* **[#1260]**
P-sulfides in Banten are compositionally similar to those in Murray and Murchison, and in Boriskino two different types: one similar to those found in other CM chondrites (with a large compositional range) and a new one similar to $Fe_7Ni_3P_3S_3$.

Solt P.
*Different Trends of Spherule Distributions at the Kaba Meteorite Fall Area* **[#1269]**
Recovering the Kaba strewn field we could measure the distribution of ~600 spherules on the ~40 square kilometer area. We defined three zones of spherule occurrence. A spectacular cinober-red spherule (also in Tübingen University Kaba sample) was found.

Calvin W. M. Hamilton V. E. King T. V. V.
*Infrared Observations of Carbonaceous Chondrites: Petrologic Diversity Expressed in Reflectance and Emittance* **[#1495]**
Infrared wavelengths offer a better opportunity to deconvolve the spectra of carbonaceous chondrites into their constituent minerals. We will compare reflectance and emittance measurements with known mineral endmembers of the carbonaceous chondrites.

Meibom A. Hicks T. Scott E. R. D. Norman M. Krot A. N. Keil K.
*Search for Nebular Fractionation of Moderately Volatile Siderophile Elements in Metal Grains in CR-Clan Chondrites* **[#1419]**
To explore and distinguish between primary signatures imparted during condensation from the nebula and secondary redistribution of moderately volatile siderophile elements, we will do in situ ICPMS studies of metal in CH, CR, and Bencubbin-like chondrites.

Hoffman E. Seifu D. Oliver F. W.
*Axtell and Allende: A Mössbauer Spectroscopic Comparison* **[#1950]**
The CV3 chondrites Axtell and Allende were examined by Mössbauer spectroscopy. Each showed doublets for $Fe^{2+}$ ion in olivine and for paramagnetic $Fe^{3+}$ phases that served to distinguish them.

Saitow A. Ohsumi K. Zolensky M. E. Ivanov A. V.
*Identification of Micro-crystal in the Kaidun Meteorite by Polychromatic Laue Method Using Synchrotron Radiation* **[#1521]**
The unknown phase which has the chemical composition of FeTiP was discovered in the Kaidun meteorite. In this study, identification of the unknown phase was done by polychromatic Laue method using synchrotron radiation.

Chikami J. Miyamoto M.
*Zn Content of Chromites in Different Petrologic Type LL Chondrites* **[#1167]**
We studied Zn behavior of chromites in various petrologic types of LL chondrites. The Zn content in their chromites does not show any trend with petrologic type. Different Zn behavior between enstatite and LL chondrites suggests their different formation processes.

Aoyama H. Reid A. M.
*Heterogeneity of Silicates in Antarctic LL4 Chondrites* **[#1791]**
LL4 Antarctic chondrites contain a mix of relict primary and metamorphic secondary characteristics. The metamorphic effects probably relate to short-lived high temperature impact events rather than to prolonged burial metamorphism.

Consolmagno G. J. Bland P. A. Strait M. M.
*Weathering and Porosity: A Preliminary SEM Study of Weathered Meteorites* **[#1158]**
We examine SEM images of meteorites in varying stages of weathering to see how weathering affects porosity. First results support a "two stage" hypothesis for weathering and the practicality of estimating model pristine (pre-weathered) porosities for ordinary chondrites.

Bérczi Sz. Holba Á. Lukács B.

*On the Topology of the Urey-Craig Field* **[#1014]**

From thermal evolutionary paths of chondrite groups we map the topology of the Urey-Craig field. We suggest a point of inflexion (repulsion) between E & H regions, having balanced $C/H_2O$ ratio, not to run to reduction, like E-s and not to run to oxidation, like H-s.

Lukács B. Holba Á. Bérczi Sz.

*Gradistic vs. Cladistic Views in the Classification of Chondrites: The (L,H) Dichotomy and the Missing L/LL Precursors (NIPR Statistics VI.)* **[#1337]**

Chondritic parent body evolutionary trends were projected — on the basis of the NIPR Antarctic dataset (Yanai et al., 1995) — in multicomponent functions (i.e. $Fe$-$C$-$H_2O$ race) of chondrite types for all groups. We looked for the possible precursors of L/LL chondrites.

Norman M. D.

*Impact Processing of Chondritic Planetesimals: A Geochemical Study of the Chico L Chondrite* **[#1097]**

Impact melt in the Chico L chondrite is depleted in volatile lithophiles, and siderophiles due to metal-silicate fractionation. Chico provides an example of how impacts can modify chondritic planetesimals and influence the composition of the Earth and Moon.

Ruzicka A. Bennett M. E. III Patchen A. D. Snyder G. A. Taylor L. A.

*Widmannstätten Texture in the Portales Valley Meteorite: Slow (But Not Unusually Slow) Cooling at Low Temperatures* **[#1616]**

We present the results of petrographic and mineral-chemical data for the coarse metal fraction in Portales Valley that have implications for a low-temperature cooling history.

McHone J. F. Killgore M. Killgore E.

*Portales Valley, New Mexico Fall of 13 June 1998: Anomalous Fragment Distribution and Composition* **[#1964]**

A meteorite shower over Portales New Mexico occurred on 13 June 1998. 50 recovered specimens are larger and fewer in the direction of projectile arrival.

Krot A. N. Brearley A. J. Kallemeyn G. W. Hutcheon I. D. Petaev M. I. Keil K.

*In Situ Growth of Fayalite and Hedenbergite in the Ungrouped Carbonaceous Chondrite MAC88107 with Affinities to the CM-CO Clan* **[#1514]**

The ungrouped carbonaceous chondrite MAC88107 contains secondary fayalite ($Fa_{90-100}$), hedenbergite ($\sim Fs_{50}Wo_{50}$), phyllosilicates, magnetite, and Ni-bearing sulfides. Fayalite and hedenbergite formed during aqueous alteration in an asteroidal environment.

## Astrobiology: Precursors, Origins, and Martians

Stephan T. Heiss C. H. Rost D. Jessberger E. K.

*Polycyclic Aromatic Hydrocarbons in Meteorites: Allan Hills 84001, Murchison, and Orgueil* **[#1569]**

Relative abundances of different PAHs in TOF-SIMS spectra from Murchison and Orgueil resemble those from ALH 84001. They don't show indications for heterocycles or alkylation as expected for biogenic PAHs. A similar, non-biogenic origin is deduced.

Becker L. Bunch T. E. Allamandola L. J.

*C60, C70 and the Higher Fullerenes (C100 to C400) in the Allende Meteorite* **[#1805]**

Here, we report on a new suite of stable C clusters (C100 to C360) in the Allende meteorite. These large ET C clusters are either the first indication of higher fullerenes or we have identified an entirely new group of carbon-rich molecules that appear to be aromatic.

Schilling E. A. Schneider M. N.

*The Airborne Molecular Organic and Microbiological Content of Meteorite Curation Facilities at NASA Johnson Space Center* **[#1046]**

Measurable levels of molecular organics and bacteria were detected in various locations of the Meteorite Processing Lab. While approximating the organics to which meteorites are often exposed, limited sample size suggests the preliminary nature of these results.

Steele A. Westall F. McKay D. S.

*The Contamination of Murchison Meteorite* **[#1293]**

A chip of Murchison meteorite was found to be contaminated. Further studies cultures this contamination both on and off the sample. SEM imaging of the formed biofilm on the sample showed a wealth of mineral growth.

Toporski J. K. W. Steele A. Stapleton D. Goddard D. T.

*Contamination of Nakhla by Terrestrial Microorganisms* **[#1526]**

Using scanning electron microscopy, probable terrestrial fungal contaminants were observed on the fusion crust of Nakhla. Additional studies on samples from the interior of the meteorite also revealed probable fungal contaminants.

Burde S. Hersman L. E. Marrone B. L. Farmer J. D. McKay D. S.

*Fluorescent Staining of Microfossils Using Biological Stains* **[#1811]**

Known terrestrial microfossils were labeled with the fluorescent nucleic acid stain propidium iodide. The fossil microorganisms exhibited bright labeling with this dye. The approach may provide unequivocal verification of the presence of microfossils in martian samples.

Westall F. Steele A. Allen C. C. McKay D. S. Gibson E. K. Morris P.

*Biofilms as Biomarkers in Terrestrial and Extraterrestrial Materials* **[#1414]**

Biofilms consisting of microbial mucoidal substances and cells are more readily preservable in the fossil record than the bacteria, themselves, making them potentially ideal biomarkers in the search for extraterrestrial life.

Guidry S. A. Chafetz H. S.

*Preservation of Microbes in Geyserite and Siliceous Sinter: Yellowstone National Park, Wyoming* **[#1152]**

Siliceous hotsprings in Yellowstone sustain a wide variety of microbes and, when coupled with analyses of progressively older specimens, aid in the establishment of criteria to recognize microbes after successive iterations of diagenetic alteration.

Kivett S. J. Allen C. C.

*Biomarkers in Thermal Springs: Jemez, New Mexico* **[#1498]**

Thermal springs in Jemez, NM, were examined for biomarkers. The springs contain diverse microbes whose presence is recorded in mineralized deposits. Evidence includes organically mediated precipitation, bioerosion, and living and fossil biofilms.

Allen C. C. Albert F. G. Combie J. Graham C. R. Kivett S. J. Steele A. Taunton A. E. Taylor M. R. Wainwright N. Westall F. McKay D. S.

*Biomarkers in Carbonate Thermal Spring Deposits: Implications for Mars* **[#1436]**

Submicron organisms and mineralized biofilms in carbonate thermal spring deposits resemble possible biogenic features in ALH84001. The preservation of physical and chemical biomarkers at our four field sites supports a Mars sample return strategy based on thermal springs.

Robbins L. L. Van Cleave K. Ryan J. G.

*Comparison of Carbonate Textural Features in ALH84001 and Microbially Induced Textures in Orthopyroxene* **[#1464]**

To assess the possibility of microbially precipitated carbonates in ALH84001, we are conducting detailed petrographic studies of ALH84001 and studies of bacterial interactions with terrestrial orthopyroxene.

Gibson E. K. Jr. McKay D. S. Thomas-Keprta K. Westall F. Romanek C. S.

*Criteria for Evidence of Ancient Life: How Does the Data from ALH84001 Compare with Accepted Requirements?* **[#1174]**

Evidence exists in ALH84001 carbonate globules to support the accepted criteria for determining the presence of fossil life. Some features are assuredly martian in origin, but it is still necessary to evaluate the degree of Antarctic influence.

Zhang C. Vali H. Romanek C. S. Roh Y. Sears S. K. Phelps T. J.

*Chemical and Morphological Characterization of Siderite Formed by Iron-reducing Bacteria* **[#1855]**

Biogenic siderite formation was examined under laboratory conditions. Results showed that different microbial processes had significant but different impacts on the chemical evolution of the fluids and the mineralogical transformation of the solids.

Taunton A. E. Welch S. A. Banfield J. F.

*Phosphate Minerals as Sites for Localization of Biosignatures* **[#1748]**

In this paper, we discuss the effect of microorganisms on the weathering of apatite and secondary phosphates and the implications this has for searching for extraterrestrial biosignatures.

Morris P. A. Wentworth S. J. Allen C. C. Thomas-Keprta K. Westall F. Bell M. S. Gibson E. K. McKay D. S.

*Methods for Determining Biogenicity in Archean and Other Ancient Rocks* **[#1952]**

Identifying biogenic and syngenetic structures in ancient rocks can be aided with SEM and EDS. Rods and spheres can be formed by physical processes, but biogenic processes appear to leave unique geochemical signatures.

Ferris J. P. Delano J. W. Gaffey M. J. Nierzwicki-Bauer S. Roberge W. G. Whittet D. C. B. Hagan W.

*New York Center for Studies on the Origins of Life* **[#1625]**

A NASA Specialized Center of Research and Training (NSCORT) has been established by investigators from four departments at the RPI, SUNY Albany, and the College of Saint Rose. The research and education effort covers many areas relevant to the origin of life.

## Cosmic Dust

Sutton S. R. Flynn G. J. Rivers M. Eng P. Newville M.

*Trace Element Analyses of L2011 Cluster Particles with the New X-Ray Microprobe at the Advanced Photon Source* **[#1656]**

We report here our first use of the new x-ray microprobe at the Advanced Photon Source (APS), Argonne National Laboratory, for trace element analyses of IDPs. The APS microprobe has a sensitivity enhancement of about a factor of 100 over the NSLS microprobe.

Landgraf M. Liou J.-C. Zook H. A. Grün E.

*Multi Spacecraft Data on Dust in the Outer Solar System* **[#1427]**

Dust data from Pioneer 10/11, Ulysses, and Galileo is used to find physical sources of dust in the outer Solar System. Dust from Kuiper belt objects is needed to explain the Pioneer 10 measurements and it is not in contradiction with the data from the other spacecraft.

Feng H. Jones K. W. Stewart B. Herzog G. F. Schnabel C. Brownlee D. E.

*Internal Structure of Two Type-I Deep-Sea Spherules by X-Ray Computed Microtomography* **[#1209]**

X-ray tomographs of two submillimeter type-I deep-sea spherules reveal the presence of oxide rims, intergrown oxides in the interior, branched holes emanating from the surface, and micrometer-size nuggets rich in platinum-group elements.

Graham G. A. Kearsley A. T. Wallis D. McDonnell J. A. M. Grady M. M. Wright I. P.

*Residues from Hypervelocity Mineral Shots into Brittle and Ductile Substrates* **[#1629]**

Back-scattered electron images and X-ray maps of craters from light-gas-gun hypervelocity impacts of natural mineral grains on solar cells and aluminum sheets show distinctive residue textures and composition, comparable to those in LEO impacts.

Yano H. Arakawa M. Michikami T. Fujiwara A.
*Sub-Millimeter-sized Ice Grain Impacts on Aerogels: Implications to a Cometary Dust Sample Return Mission* **[#1961]**
Hypervelocity impacts of a sub-millimeter ice grains on aerogels at –10°C demonstrated distinctive morphological differences between "stubby" by ice and classic, long "carrot" by glass beads at the same impact condition.

Phelps A. W.
*Interstellar Diamond. II. Growth and Identification* **[#1753]**
Opinions regarding the formation mechanism(s) of meteorite and interstellar diamond grains have changed over the years as new methods of making synthetic diamond were developed.

Földi T. Ezer R. Bérczi Sz. Tóth Sz.
*Creating Quasi-Spherules from Molecular Material Using Electric Fields (Inverse EGD Effect)* **[#1266]**
We made spherules from gaseous phase, in isothermal conditions, using strong electrostatic fields. The electrostatic field coagulated the molecular components which behaves like cosmic powders, therefore our experiments may have consequences on the origin of cosmic powders.

Messenger S.
*Oxygen Isotopic Imaging of Interplanetary Dust by TOF-SIMS* **[#1600]**
The study of circumstellar grains preserved in primitive meteorites has become an exciting new branch of astrophysics, providing constraints on stellar nucleosynthesis, galactic chemical evolution, and physical and chemical conditions in stellar atmospheres in unprecedented detail.

## Planetary Interior Processes

Rushmer T. Jones J. H.
*Core Formation Under Dynamic Conditions: Initial Results of Silicate-Metal Distribution with Differential Stress* **[#1369]**
Deformation experiments have been performed on an H6 chondritic meteorite (Kernouve) to investigate the possibility of metallic melt mobilization with differential stress. Results suggest that deformation can enhance migration of molten metal and sulfide.

Agee C. B. Shannon M. C.
*Effect of Pressure on Dihedral Angle of Molten Fe-S with Magnesiowüstite: Implications for Planetary Core Formation* **[#1905]**
Experiments to determine the effect of pressure on the dihedral angle formed by molten iron-sulfur alloy.

Jaeger W. L. Capobianco C. J. Drake M. J.
*Metal-Silicate Partitioning of Co, Ga, and W: Dependence on Silicate Melt Composition* **[#1454]**
We have investigated the effect of silicate melt composition on metal/silicate partitioning of Co, Ga and W. D(W) decreases rapidly with increasing melt basicity, D(Ga) decreases moderately, and D(Co) behaves independently of the silicate composition.

Ertel W. Sylvester P. J. Drake M. J.
*Experimental Constraints on the Accretion of the Earth: Pt* **[#1480]**
Pt equilibrium solubilities in An-Di eutectic silicate melt was determined at 10 to 20 kbars and 1450° to 1850°C in piston cylinder experiments. Results are compared to previous work at 1 atm and 2 to 4 kbar.

Jacobs K. E. Colson R. O. Hendrickson T. R. Floden A. M. Holder D. Malum K. M. Nermoe M. K. B.
*The Effects of Phosphorous on Ni and Fe Activity in a Silicate Melt* **[#1486]**
Phosphorous in a silicate melt strongly affects the activity of Fe. The affect on the activity of Fe is due to interaction between P and Fe and not to indirect effects resulting from changes in melt polymerization.

## Impacts I

Takayama H. Tada R. Matsui T. Iturralde-Vinent M. A. Oji T. Tajika E. Kiyokawa S. Garciaanmd D. Okada H. Hasegawa T. Toyoda K.

*Origin of a Giant Event Deposit in Northwestern Cuba and Its Relation to K/T Boundary Impact* **[#1534]**

We investigated the Penalver Formation in northwestern Cuba, which is a <180 m thick, normal-graded calcareous clastic deposit. This formation must have been formed by a grain flow and huge tsunami waves caused by the K/T boundary impact.

Kiyokawa S. Tada R. Matsui T. Tajika E. Takayama H. Iturralde-Vinent M. R.

*Extraordinary Thick K/T Boundary Sequence; Cacarajicara Formation, Western Cuba* **[#1577]**

Cacarajicara Formation of western Cuba is the thickest K/T boundary sequence in the world. It is an upward-fining carbonate clastics, at least 300m in thickness. It might be a distal part of the ejector blanket of Chicxulub impact crater or a giant tsunami deposit.

Ward S. N. Asphaug E.

*Impact Tsunami: A Probabilistic Hazard Assessment* **[#1475]**

We apply linear tsunami theory to the NEO flux to investigate the generation, propagation, and hazard of tsunami spawned by oceanic asteroid impacts.

Matsui T. Imamura F. Tajika E. Nakano Y. Fujisawa Y.

*K/T Impact Tsunami* **[#1527]**

Numerical simulation of generation and propagation of the tsunami caused by the impact at the K/T boundary predicts that unusually gigantic tsunami attacked the coast of the Gulf of Mexico and the tsunami further propagated worldwide.

Nakamura Y. Christeson G. L. Buffler R. T. Morgan J. Warner M. Chicxulub Working Group

*Structure of the Chicxulub Impact Crater as Determined from Large-Offset Onshore-Offshore Seismic Data* **[#1288]**

Onshore-offshore seismic data over the Chicxulub impact crater revealed for the first time its deep structure. Major features include a central basement uplift and inward-dipping low-angle faults well outside the collapsed transient cavity.

Poag C. W.

*Secondary Craters from the Chesapeake Bay Impact* **[#1047]**

I document 23 secondary craters on two seismic reflection profiles north of the Chesapeake Bay primary crater (85-km-diameter). Seismostratigraphic analysis is calibrated with lithostratigraphy and biostratigraphy from nearby outcrops and bore holes.

Plescia J. B.

*Mulkarra Impact Structure, South Australia: A Complex Impact Structure* **[#1889]**

The Mulkarra impact structure in South Australia is interpreted as a complex crater having a diameter of ~20 km with a 9 km central pit or peak ring. This interpretation differs from that of Flynn (1988) who interpreted it as a simple 9 km bowl shaped crater.

Henkel H. Reimold W. U.

*Magnetic Model of the Central Uplift of the Vredefort Impact Structure* **[#1336]**

The negative magnetic anomalies occurring within the area of the central uplift of the Vredefort impact structure have been analyzed. The final model shows the extent of post-impact thermal re-magnetization and reveals structures related to the collapse of the central rise.

Popov Y. Pohl J. Romushkevich R.

*Geothermal Investigations of the Ries Impact Structure* **[#1623]**

Thermal conductivity measurements of the 1206 m Ries 1973 drill core characterize and differentiate impact formations. From temperature gradients and the new conductivity data, inferences about heat flow and fluid movements can be drawn.

Pohl J. Geiss E.
*Investigations of the Ries Crater Ejecta Using a Digital Geological Map, DEM and GIS* **[#1531]**
A digital edition of the Ries crater geological map allows, together with digital elevation data, a new investigation of the statistical geological and morphological characteristics of the ejecta and their radial and azimuthal distribution.

Herkenhoff K. E. Giegengack R. Kriens B. J. Louie J. N. Omar G. I. Plescia J. B. Shoemaker E. M.
*Geological and Geophysical Studies of the Upheaval Dome Impact Structure, Utah* **[#1932]**
Detailed geologic mapping and geophysical data indicate that Upheaval Dome in Canyonlands National Park (southeastern Utah) originated by collapse of a transient cavity formed by impact, not by salt diapirism as previously proposed.

Kenkmann T. Ivanov B. A.
*Low-Angle Faulting in the Basement of Complex Impact Craters: Numerical Modelling and Field Observations in the Rochechouart Structure, France* **[#1544]**
Low-angle normal faults generate during crater modification in acoustically-fluidized rocks. Faulting is a result of an impact-induced rheological stratification of the crater floor and a passive rotation due to the uplift of the central peak.

Buchanan P. C. Koeberl C. Reimold W. U.
*Petrogenetic Modeling of the Dullstroom Formation, South Africa* **[#1290]**
The Dullstroom Formation was the first phase of a magmatic episode culminating in the formation of the Bushveld Complex. This study models available geochemical data to determine whether impact or endogenic terrestrial processes were responsible.

Hough R. M. Vishnevsky S. Abbott J. I. Pal'chik N. Raitala J. Gilmour I.
*New Data on the Nature of Impact Diamonds from the Lappajärvi Impact Structure, Finland* **[#1571]**
New data is presented on the characteristics of impact diamonds from the Lappajärvi impact structure, Finland.

Wolbach W. S. Widicus S. French B. M.
*Carbon-bearing Impactites from the Gardnos Impact Structure, Norway: No Evidence for Soot* **[#1043]**
To test the idea that combustion of the impactor or carbon-bearing rocks could have occurred during the impact that produced the Gardnos crater, we searched for soot in Gardnos impactites and related rocks. No detectable soot is observed in any of these Gardnos samples.

King D. T. Jr. Neathery T. L. Petruny L. W.
*Impactite Facies Within the Wetumpka Impact-Crater Fill, Alabama* **[#1634]**
This paper summarizes initial findings from drilling two 190-m deep holes within the Late Cretaceous Wetumpka impact crater, Alabama. Five intercalated impactite facies from the crater fill unit are described: sands; sandy and cataclastic diamictites; breccias; and blocks.

Komatsu G. Olsen J. W. Baker V. R.
*Field Observation of a Possible Impact Structure (Tsenkher Structure) in Southern Mongolia* **[#1041]**
In 1998 summer, we visited the Tsenkher Structure, a possible impact structure in southern Mongolia. The structure's rim to rim diameter is 3.6 km, and a raised outer rim was observed. Prehistoric stone artifacts were found near the structure.

Master S. Diallo D. P. Kande S. Wade S.
*The Velingara Ring Structure in Haute Casamance, Senegal: A Possible Large Buried Meteorite Impact Crater* **[#1926]**
A new 48 km-diameter postulated impact crater, the Velingara structure, discovered on satellite images (centred on 14°7'40" W, 13°02'13.2" N, in Senegal), is developed in Mid-Eocene sediments, has a central uplift of metamorphic basement, and is buried by Neocene rocks.

Arday A(t). Bérczi Sz. Don Gy. Lukács B.
*Preliminary Report of Szilvágy-Patkó (Horseshoe): A New (Possible) Impact Crater Remnant in Hungary* **[#1384]**
In the last autumn during aerial photographing a central symmetric form was found 250 km SW from Budapest, in Hungary. We consider it to be a crater remnant, it is 500 m diameter and 25 m deep, and its southern wall is missing. Yet no transformed matter proves its origin.

## Special Session
## Future Missions: Science and Technology

Crisp D. Raymond C.
*The NASA New Millennium Program: Advanced Technologies for Future Science Missions* **[#2067]**
The New Millennium Program (NMP) identifies and flight-validates revolutionary spacecraft and instrument technologies that could enhance the science return of future missions, while reducing their cost and risk.

Butterworth A. L. Franchi I. A. Pillinger C. T.
*Solar Wind Sample Return from Genesis: A Technique for the Extraction of Carbon Implanted into Silicon-on-Sapphire Wafers* **[#1796]**
Thin layer growths of silicon on sapphire are proposed as a collector for carbon on the Genesis solar wind sample return mission. An evaluation of the collectors and a laser extraction technique for the sample analysis is given.

Cabrol N. A. Kosmo J. J. Trevino R. C. Stoker C.
*Astronaut-Rover Interaction for Planetary Surface Exploration: 99' Silver Lake First ASRO Experiment* **[#1069]**
During planetary surface missions, EVA crewmembers and rovers will have a significant role in performing surface tasks. The ASRO project provides the early assessment of EVA crewmembers and rover interaction to support decisions in surface reference mission development.

Gregg T. K. P. Fornari D. J.
*Looking for a Needle in a Haystack: Lessons for Extraterrestrial Geologic and Biologic Discovery from Deep Submergence Vehicle Surveys* **[#2011]**
Exploration of the deep sea is similar to exploration of other planetary surfaces. Techniques developed for site selection and data integration at Earth's mid-ocean ridges are applicable to future rover missions.

Eppler D. B. Kosmo J. Rajula S. Kakavand A. Washington C.
*Mobility Testing of a Hybrid Composite/Fabric EVA Suit in a Field Geology Setting: Implications for Mars Surface Suit Design* **[#1050]**
A series of planetary exploration EVA suit mobility tests were conducted during the period of 2–17 May 1998, in Flagstaff, AZ, to evaluate the use of the Mark III hybrid composite/fabric suit by a trained field geologist in a relevant geologic setting.

Solomon S. C. McNutt R. L. Jr. Gold R. E. Santo A. G. MESSENGER Team
*MESSENGER: The Rediscovery of Mercury* **[#1410]**
MESSENGER, a Discovery mission to flyby and orbit Mercury, will answer key questions about the planet's formation, crustal composition, geological history, magnetic field, core structure, polar deposits, volatile inventory, and magnetosphere.

Clark P. E. Curtis S. Giles B. Marr G. Eyerman C. Winterhalter D.
*JANUS: Fast, Low Cost, Low Risk Mission for Exploring Mercury* **[#1036]**
In response to the growing realization that largely unexplored Mercury holds important keys to the origin of the solar system, we developed JANUS, an extremely fast, low cost, low risk, four platform, multiple flyby pathfinder mission to Mercury.

Campbell B. A. Greeley R. Stofan E. R. Acuña M. H. Chutjian A. Crisp D. Cutts J. Fegley B. Guest J. Head J. W. Klaasen K. Mustard J. P. Senske D.
*The VEVA Mission: Exploration of Venus Volcanoes and Atmosphere* **[#1667]**
We propose VEVA, a novel new mission to study in detail the surface morphology and lower atmosphere chemistry of Venus using balloon platforms, atmospheric probes, and imaging sondes.

Pedersen L. Apostolopoulos D. Whittaker W. Cassidy W. Lee P. Roush T.
*Robotic Rock Classification Using Visibile Light Reflectance Spectroscopy: Preliminary Results from the Robotic Antarctic Meteorite Search Program* **[#1340]**
A method for automatically identifying rocks, particularly meteorites, from their visible light reflectance spectra is presented. Results from Antarctic field trials of the system, mounted on a robot to look for meteorites, are described.

Aulesa V. Casanova I.
*Construction Materials for Planetary Outposts: A Review* **[#1562]**
Different kinds of construction materials for planetary outposts are evaluated including concrete, sintered regolith, cast basalt, ceramics, ice. and metals.

Roush T. L. Gulick V. Morris R. Gazis P. Benedix G. Glymour C. Ramsey J. Pedersen L. Ruzon M. Buntine W. Oliver J.
*Autonomous Science Decisions for Mars Sample Return* **[#1586]**
Robotic explorers, e.g. rovers, need to make crucial science decisions autonomously that are distinct from control, health, and navigation issues. We have investigated potential tools that can be applied to imaging and near-infrared spectral data.

Arvidson R. Backes P. Baumgartner E. Blaney D. Dorsky L. Haldemann A. Lindemann R. Schenker P. Squyres S.
*FIDO: Field Test Rover for 2003 and 2005 Mars Sample Return Missions* **[#1201]**
FIDO is a prototype Mars rover equipped with an Athena-like payload. This rover will be used in a set of field trials to simulate finding, characterizing, collecting, caching, and finally depositing samples at a base station for later return to Earth.

Pieters C. Calvin W. Cheng A. Clark B. Clemett S. Gold R. McKay D. Murchie S. Mustard J. Papike J. Schultz P. Thomas P. Tuzzolino A. Yeomans D. Yoder C. Zolensky M. Barnouin-Jha O. Domingue D.
*Aladdin: Exploration and Sample Return of Phobos and Deimos* **[#1155]**
Aladdin has been selected as a finalist in the 1999 Discovery competition. Aladdin addresses two of NASA's high priority science objectives: the composition and nature of small bodies (the building blocks of the solar system), and the martian systems' origin and evolution.

Mustard J. F. Pieters C. M. Murchie S. L. Calvin W. M.
*Mapping the Mineralogy of Environments of Mars with Aladdin* **[#1479]**
The Aladdin Discovery mission will have an imaging spectrometer (ISPEC) capable of visible through near infrared measurements. An overview of the capabilities and the opportunity to provide unique data for mapping the mineralogy of environments on Mars is presented.

Marshall J. Anderson M. Buehler M. Frant M. Fuerstenau S. Hecht M. Keller U. Markiewicz W. Meloy T. Pike T. Schubert W. Smith P.
*The MECA Payload as a Dust Analysis Laboratory on the MSP 2001 Lander* **[#1163]**
The MECA payload for MSP 2001 Lander is described in terms of its capabilities for acquiring data on the origin and properties of dust on Mars — of importance to human exploration and planetary geology

Brunkhorst E. J. Choi J. M. Davis H. J. Ho W.
*Biological Barriers for Mars Mission* **[#1654]**
When martian samples return to Earth, one of the main concerns is biological contamination of the Earth from Mars and vice versa. The purpose of these experiments was to prove the biological barrier efficiency of traditionally used seals and filters.

Greeley R. Cutts J. A. Arvidson R. Blamont J. Blaney D. L. Cameron J. Kerzhanovich V. Smith I. S. Yavrouian A.

*Mars Aerobot Micromissions* **[#1282]**

Aerobots would be capable of providing near ground-truth observations over 1000s of km traverses, obtaining high resolution data on remnant magnetic fields, in-situ atmospheric measurements, and 10 cm/pixel images.

Miralles C. MacCready P. B.

*Mission Concepts Utilizing Gliders for Atmospheric and Surface Science* **[#1506]**

Aerial platforms can fill the gap between the spatial resolution and coverage achievable from orbit and from surface vehicles for planetary exploration. We introduce glider flight as a new approach to planetary mobility.

Yen A. S. Smrekar S. E. Murray B.

*Future Mars Micropenetrators Based on New Millennium Deep Space 2 (DS2)* **[#1870]**

The Deep Space 2 spacecraft has the unique capability of providing easy access to the martian subsurface, and many different scientific investigations based on future versions of this vehicle are possible.

Haldemann A. F. C. Jurgens R. F. Slade M. A. Thompson T. W. Rojas F.

*Mars Delay-Doppler Radar Observations with GSSR: Global Analysis for Landing Site Selection and Characterization* **[#1517]**

Earth-based radar data remain a key information set to select landing sites on Mars. Future Mars robotic exploration includes rovers, and rover trafficability, as determined by surface roughness is provided by radar echo modeling.

Young D. T. Waite J. H.Jr. Miller G. P. Bass D. S.

*A Method for the Determination of Isotopic and Elemental Abundances for Volatiles and Noble Gases in the Martian Surface Layer and Atmosphere* **[#1215]**

We describe a prototype gas enrichment device that, when coupled with a mass spectrometer, can be used for the *in situ* measurement of volatiles and noble gases in the martian atmosphere and surface layer.

Agresti D. G. Wade M. L. Wdowiak T. J. Armendarez L. P. Farmer J. D.

*A Mössbauer Study of an Iron-rich Hydrothermal Vent Mound, with Implications for Mars Exploration* **[#1840]**

Mossbauer study of an iron-rich vent mound finds ferrihydrite, nontronite, hematite, nanophase goethite, and siderite. The Mars-bound technique can help find hydrothermal mineral deposits on Mars and identify samples for later transport to Earth.

Gilmore M. S. Castaño R. Roush T. Mjolsness E. Mann T. Saunders R. S. Ebel B. Guinness E.

*Effects of Distance and Azimuth on Spectroscopic Measurements at Silver Lake, CA* **[#1886]**

VIS/NIR absorption features taken at a Mars analog site seem to vary with distance.

Sears D. W. G.

*Multiple Asteroid Sample Return: The Next Step* **[#1432]**

It is argued that with abundant spectral classifications for asteroids, recent success in the discovery of NEA and the realization that meteorites are not representative asteroid samples, asteroid sample return should be the next step in meteorite and asteroid studies.

Waite J. H. Jr. Bagenal F. Bolton S. J. Connerney J. E. C. Drossart P. Gautier D.

*Jovian Auroral and Inner Magnetosphere Explorer (JAIME) Mission* **[#1210]**

Two concepts are presented for JAIME, a post-Galileo Jupiter polar orbiter mission that will address key questions about Jupiter's inner magnetosphere and its coupling with the upper atmosphere that Galileo will leave unanswered.

Grimm R. E.

*Natural Electromagnetic Exploration for Water on Mars and Europa* **[#1442]**

Water is a near-ideal low-frequency EM target, and abundant natural sources exist for Jupiter and probably Mars. Frequencies <10 Hz to 1 kHz are highly diagnostic of water at depths of several km.

Castracane J. Schultz P. H. Gutin M.

*MEMS-based Ultra-Spectrometer (MEMUS) for Planetary Surface Analysis* **[#1860]**

Microelectromechanical systems (MEMS) technology has been applied to the development of an adjustable diffractive grating. Such a grating allows capturing different spectral passbands at different dispersions.

Thakoor S. Miralles C. Martin T. Kahn R. Zurek R.

*Cooperative Mission Concepts Using Biomorphic Explorers* **[#2029]**

Inspired by the variety of natural explorers (insects, birds etc.), their well-integrated biological sensor-processor suites, efficiently packaged in compact, dexterous forms, and their cooperative behavior, we present "Biomorphic Explorers."

Gruen E. Landgraf M. Svedhem H. Horanyi M.

*Galactic Dust Measurements Near Earth* **[#1405]**

Recently, galactic dust has been identified by the Ulysses dust detector outside 1.8 AU. Up to 30% of the dust flux with masses above $10^{-13}$ g at 1 AU may be of interstellar origin. A mission is proposed that detects and analyses interstellar dust in high-Earth orbit.

Reed K. L.

*A Comprehensive Plan for Investigation of Near-Earth Asteroids Using a Ground-based and Spacecraft-based Synthesis* **[#1261]**

Asteroid missions are problematic in that synoptic data at high resolution cannot be had with just one spacecraft to one body. Synoptic data may be had for the near-Earth asteroids using coordinated assets to increase the data acquisition efficiency.

Binzel R. P. Clark B. C.

*New World Explorer Mission to Vesta: The Most Ancient Terrestrial World* **[#1218]**

Vesta is the smallest surviving planetary body to have undergone the terrestrial processes of heating and differentiation. New World Explorer's one-year orbital mission at Vesta will reveal unique clues to the early evolution of terrestrial planets.

Weissman P. R. Smythe W. D. Muirhead B. K. Tan-Wang G. H. Sabahi D. Grimes J. M.

*The Deep Space 4/Champollion Comet Rendezvous and Lander Technology Demonstration Mission* **[#1142]**

The Deep Space 4/Champollion comet rendezvous and lander mission will be launched in April, 2003 and will orbit and land on periodic comet Tempel 1 in 2006. DS-4/Champollion is part of the New Millennium Program and is a joint project of NASA and CNES.

Lorenz R. D.

*To Fly or to Float? Heavier-than-Air and Dirigible Balloon Titan Explorer Concepts* **[#1088]**

Post-Cassini exploration of Titan will require close access to the surface and global coverage to inventory organic compounds and their geological context. Aeroplanes and airships appear to be the most attractive platforms.

Moss C. E. Ianakiev K. D. Prettyman T. H. Reedy R. C. Smith M. K. Sweet M. R. Valentine J. D.

*Performance of High Efficiency CdZnTe Gamma-Ray Detectors for Planetary Missions* **[#1478]**

Results from large-volume CdZnTe semiconductor detectors for ambient-temperature gamma-ray spectroscopy are presented. Our new multi-element-array design is a good low-mass and low-power candidate for elemental mapping on future planetary missions.

Terrile R. J. Klaasen K. P. Lunine J. Johnson T. V.

*Outer Planets/Solar Probe Project: Pluto Kuiper Express* **[#1988]**

The Pluto-Kuiper Express mission is designed to provide the first reconnaissance of the solar system's most distant planet, Pluto, and its moon Charon. This mission will launch in 2004 and arrive at Pluto about 9 years later.

Johnson T. V. Chyba C. Klaasen K. P. Terrile R. J.
*Outer Planets/Solar Probe Project: Europa Orbiter* **[#1423]**
The Europa Orbiter mission is planned for a 2003 launch, arriving at Jupiter in 2006–07. It's objectives are to determine the presence or absence of a liquid ocean and to characterize the surface and subface for future missions. Investigations will be selected in 1999.

Gulick V. C. Morris R. L. Ruzon M. Roush T. L.
*Autonomous Science Analyses of Digital Images for Mars Sample Return and Beyond* **[#1994]**
We are developing autonomous image analyses algorithms for future Mars missions that coupled with appropriate navigational software, decrease both data volume and command cycle bottlenecks that limit both rover and science yield.

**Wednesday, March 17, 1999**
**MARTIAN METEORITES I: THE NEWEST AND THE OLDEST**
**8:30 a.m. Room A**

**Chairs: A. H. Treiman**
**G. Dreibus**

Zipfel J.* Spettel B. Palme H. Dreibus G.
*Petrology and Chemistry of Dar Al Gani 476, a New Basaltic Shergottite* **[#1206]**
Dar al Gani 476 is classified as a basaltic shergottite. It is the most mafic member of this meteorite group. Here we report its petrology, chemistry and results of mixing calculations.

Mikouchi T.*
*Preliminary Examination of Dar Al Gani 476: A New Basaltic Martian Meteorite Similar to Lithology A of EETA79001* **[#1557]**
This abstract presents the preliminary result of petrology and mineralogy of a new Mars meteorite, Dar al Gani 476. It is very similar to EETA79001 (lithology A), but seems to have experienced a slightly more equilibrated crystallization history.

Nishiizumi K.* Masarik J. Welten K. C. Caffee M. W. Jull A. J. T. Klandrud S. E.
*Exposure History of New Martian Meteorite Dar Al Gani 476* **[#1966]**
A basaltic shergottite, Dar al Gani 476 was found May 1, 1998, in the Libyan part of the Sahara. This fragment represents the thirteenth individual martian meteorite. We report here preliminary results of cosmogenic $^{14}$C, $^{41}$Ca, $^{36}$Cl, $^{26}$Al, and $^{10}$Be.

Scherer P. Schultz L.*
*Noble Gases in the SNC Meteorite Dar Al Gani 476* **[#1144]**
The exposure age of DaG 476 calculated from cosmogenic $^{3}$He, $^{21}$Ne, and $^{38}$Ar is (1.2±0.2) Ma. This possibly shows another ejection event of martian shergottites. Trapped noble gases resemble those observed in Chassigny.

Jagoutz E.* Bogdanovski O. Krestina N. Jotter R.
*Dag: A New Age in the SNC Family, or the First Gathering of Relatives* **[#1808]**
Isotope systems in new SNC meteorite Da al Garni.

Boctor N. Z.* Wang J. Alexander C. M. O'D. Hauri E. Bertka C. M. Fei Y.
*Hydrogen Isotope Studies of Feldspathic and Mafic Glasses in Martian Meteorites ALH 84001 and EETA 79001* **[#1397]**
Hydrogen isotope data on the feldspathic and mafic glasses are presented and confirm the presence of an indigenous extraterrestrial H component in ALH 84001 and EETA 79001.

Borg L. E.* Connelly J. N. Nyquist L. E. Shih C. -Y.
*Pb-Pb Age of the Carbonates in the Martian Meteorite ALH84001* **[#1430]**
The Pb-Pb age of the carbonates in the martian meteorite ALH84001 is 4.02±0.02 Ga. This age is based on analysis of carbonate-rich leachates and agrees well with our previous Rb-Sr age of 3.90±0.04 Ga.

Schwandt C. S.* McKay G. A. Lofgren G. E.
*FESEM Imaging Reveals Previously Unseen Detail and Enhances Interpretations of ALH84001 Carbonate Petrogenesis* **[#1346]**
A high resolution Field Emission Scanning Electron Microscope (FESEM) povides new observations of the martian meteorite ALH84001. These new images impact hypotheses for carbonate petrogenesis.

Bell M. S.* Thomas-Keprta K. L. Wentworth S. J. McKay D. S.
*Microanalysis of Pyroxene Glass in ALH84001* **[#1951]**
Nanometer-sized regions of pyroxene glass in ALH84001 are examined by TEM, SEM, and electron microprobe to characterize relationships between glass and crystalline materials. Glassy pyroxene may represent incipient shock melting at pressures of ~50 GPa.

Kent A. J. R.* Hutcheon I. D. Ryerson F. J. Phinney D. L.
*The Temperature of Formation of Carbonates in Martian Meteorite ALH84001: Constraints from Cation Diffusion* **[#1473]**
Calculations based on our measurements of the diffusivities of Mg in calcite and Ca in magnesite indicate that carbonate rosettes in martian meteorite ALH84001 formed at temperatures that are at least below 400°C, and most likely less than 200°–250°C.

Golden D. C.* Ming D. W. Schwandt C. S. Morris R. V. Yang S. V. Lofgren G. E.
*An Experimental Study of Kinetically-driven Precipitation of Ca-Mg-Fe Carbonates from Solution: Implications for the Low-Temperature Formation of Carbonates in Martian Meteorite ALH84001* **[#1973]**
Carbonate globules similar in composition, zonation, and size to the ALH84001 globules were precipitated inorganically from aqueous solutions at temperatures <150°C.

van der Bogert C. H.* Schultz P. H. Spray J. G.
*Experimental Frictional Heating of Dolomitic Marble: New Insights for Martian Meteorite Allan Hill 84001* **[#1970]**
Experimental frictional heating of carbonate along with petrographic observations suggest that some carbonates in ALH84001 may have been melted and remobilized during impact-related high strain-rate deformation rather than a severe shock event.

Mojzsis S. J.* Coath C. D. Bunch T. Blake D. Treiman A. H. Amundsen H. E. F.
*Carbonate "Rosettes" in Xenoliths from Spitzbergen: SIMS Analysis of O and C Isotope Ratios in a Potential Terrestrial Analogue to Martian Meteorite ALH84001* **[#2032]**
We have studied the microdomain oxygen and carbon isotopic compositions by high-resolution SIMS (ion microprobe) of complex carbonate rosettes from spinel lherzolite xenoliths that may be of useful in understanding the origin of similar carbonate minerals on Mars.

**Wednesday, March 17, 1999**
**IMPACTS II**
**8:30 a.m. Room B**

**Chairs: J. B. Plescia**
**M. J. Cintala**

Housen K. R.* Holsapple K. A.
*Impact Cratering on Porous Low-Density Bodies* **[#1228]**
Impact experiments indicate that large craters on porous bodies form primarily by compaction with little deposition of ejecta exterior to the crater. This may explain the fact that large craters formed on Mathilde without destroying nearby craters.

Stewart S. T.* Ahrens T. J.
*Porosity Effects on Impact Processes in Solar System Materials* **[#2020]**
We are developing a model to explain the effect of porosity on impact processes. We will present calculations and experiments on the effect of porosity on the shock wave attenuation, dynamic strength and fragment distribution of porous, brittle materials.

Head J. N.* Melosh H. J.
*Effects of Layering on Spall Velocity: Numerical Simulations* **[#1761]**
We model 12 km/sec impacts into layered targets composed of gabbroic anorthosite and one of two different low-velocity versions of that material. Calculated peak spall velocities can exceed those achieved in either material alone.

Ivanov B. A.*
*Transient Crater Modification Due to Gravity Slumping* **[#1574]**
We present results of the numerical modeling of the slumping process with the simplest mechanical model of the rock behavior, assumed to be a cohesionless media with a dry friction.

O'Keefe J. D.* Ahrens T. J.
*Deep Seated Faulting in the Formation of Complex Impact Craters* **[#1304]**
We have found that deep seated faulting occurs early in the formation of complex impact craters. This was observed in modeling the rheological effects of damage in geologic materials due to impact-induced brecciation and comminution.

Warner M. R.* Morgan J. V.
*Transient Crater Collapse and Peak Ring Formation at Chicxulub* **[#1386]**
Seismic reflection data across Chicxulub reveal a topographic peak ring; surprisingly, this lies above the slumped transient cavity rim. The peak ring appears to have been formed by thrusting of the central uplift over the collapsed rim.

Morgan J. V.* Warner M. R.
*Kinematics of Multi-Ring Formation at the Chicxulub Impact Crater* **[#1367]**
Recent seismic reflection data over the Chicxulub impact structure reveal a multi-ring basin in which the whole crust has collapsed to form the outer ring. Multi rings appear to form by the normal collapse of excavation-stage thrusts.

Pierazzo E.* Melosh H. J.
*Melt Production in Oblique Impacts* **[#1223]**
Numerical simulations of oblique impacts indicate that peak shock pressures inside an asymmetric isobaric core decrease with impact angle. Melt volumes produced in the target do not seem to have a simple dependence on impact angle.

Skála R.* Hörz F. Jakeš P.

*X-ray Powder Diffraction Study of Experimentally Shocked Dolomite* **[#1327]**

Experimentally shocked dolomite was investigated by powder X-ray diffraction. Changes in the unit-cell size and crystal structure are discussed.

Rietmeijer F. J. M.* Bunch T. E. Schultz P. H.

*A Preliminary Analytical Electron Microscope Study of Experimentally Shocked Dolomite with Emphasis on Neoformed Carbon Phases* **[#1051]**

Oblique impact of dolomite yields disordered dolomite, degassing, carbon mantled CaO and MgO nanograins, soot, onion-shells, "bubbles" with a graphitic skin, and amorphous (vesicular) sheets. Neoformed carbons are sensitive to variations in carbon vapor compositions.

Dahl J. M.* Schultz P. H.

*In-Target Stress Wave Momentum Content in Oblique Impacts* **[#1854]**

Impact experiments indicate that stress waves generated in oblique impacts have greater momentum content downrange relative to momentum content in other target directions. This has implications for asymmetries in target damage from oblique impacts.

Ekholm A. G.*

*Crater Features Diagnostic of Oblique Impacts: The Central Peak Offset* **[#1706]**

From a study of Venusian craters, I find that there is no empirical evidence for a systematic uprange offset of the central peak in craters formed by oblique impacts, and such offsets therefore cannot be used as a measure of obliquity.

Alpert A. J.* Melosh H. J.

*Fragment Sizes of High Speed Ejecta from a Large Impact on Europa* **[#1881]**

The size-velocity distribution of ejecta from the Pwyll impact is estimated. As suggested by spallation models, it can be expressed as a power law. Comparison with distributions for other impacts show how they differ for silicate and icy bodies.

**Wednesday, March 17, 1999**
**MARS GLOBAL SURVEYOR (MGS): VOLCANICS AND SURFACES**
**8:30 a.m. Room C**

**Chairs: P. J. McGovern**
**L. Keszthelyi**

McEwen A. S.* Malin M. Keszthelyi L. Lanagan P. Beyer R. Hartmann W.
*Recent and Ancient Flood Lavas on Mars* **[#1829]**
MOC images have revealed extensive areas of young flood lavas on Mars, some perhaps younger than 10 My. This and other evidence such as deep layering in Valles Marineris show that flood volcanism has been voluminous throughout geologic time.

Keszthelyi L.* McEwen A. S. Thordarson Th.
*Terrestrial Analogs and Thermal Models for Martian Flood Lavas* **[#1227]**
Well-preserved flood lavas seen by the Mars Orbital Camera appear to be rapidly-emplaced channel-fed flows, with eruption rates 2–3 orders of magnitude higher than the fastest observed terrestrial eruptions.

McGovern P. J.* Solomon S. C. Faulkner S. E. Head J. W. Smith D. E. Zuber M. T.
*Extension and Volcanic Loading at Alba Patera: Insights from MOLA Observations and Loading Models* **[#1697]**
MOLA altimetry profiles of the large volcano Alba Patera call for a critical re-examination of edifice growth scenarios. Surface loading models are untenable; late sublithospheric loading is most consistent with observed topography and tectonics.

Jager K. M.* Head J. W. III Thomson B. McGovern P. J. Solomon S. C.
*Alba Patera, Mars: Characterization Using Mars Orbiter Laser Altimeter (MOLA) Data and Comparison with Other Volcanic Edifices* **[#1915]**
New topography data on Alba Patera provide data on edifice and caldera shape and origin.

Garvin J. B.* Sakimoto S. E. H.
*Near-Polar Cratered Cones on Mars: MOLA Measurements and Implications for Volcanic Origins* **[#1492]**
MOLA topographic cross-sections indicate that martian near-polar cratered cones and pitted domes are geometrically similar to low-relief lava shield volcanoes. Measured geometry parameters suggest that they are not hydromagmatic, and are geologically recent.

Zimbelman J.* Hooper D. Crown D. Grant J. Sakimoto S. Frey H.
*Medusae Fossae Formation, Mars: An Assessment of Possible Origins Utilizing Early Results from Mars Global Surveyor* **[#1652]**
The enigmatic MFF in the equatorial portion of Elysium-Amazonis Planitiae has numerous very different proposed hypotheses for its origin. Released MOC and MOLA data and Viking data are compared to predicted hypothesis-specific attributes.

Hamilton V. E.*
*Linear Deconvolution of Mafic Igneous Rock Spectra and Implications for Interpretation of TES Data* **[#1825]**
Successful linear deconvolution of laboratory thermal emission spectra provides an indication of the applicability of the technique to deconvolution of atmospherically corrected TES surface spectra.

Wyatt M. B.* Hamilton V. E. McSween H. Y. Jr. Christensen P. R. Patchen A. Taylor L. A.
*Comparison of Microprobe and Thermal Emission Spectroscopy Derived Modal Mineralogies of Basalt and Andesite* **[#1754]**
To apply mineralogic data from TES in the classification of martian rocks, modes of terrestrial analogs must be determined. This study addresses pertinent questions and develops the experience needed to map and interpret martian rocks from orbit.

Lane M. D.* Morris R. V. Christensen P. R.
*An Extensive Deposit of Crystalline Hematite in Terra Meridiani, Mars* **[#1469]**
A large deposit of crystalline hematite has been identified in the Terra Meridiani region of Mars using data from the MGS Thermal Emission Spectrometer. No other similar deposits, to-date, have been identified elsewhere on the planet.

Bell J. F. III* Morris R. V.
*Identification of Hematite on Mars from HST* **[#1751]**
New HST observations are presented that support previous telescopic and spacecraft identification of coarse-grained hematite on Mars.

Cooper C. D.* Mustard J. F.
*Topography and Roughness Signatures of Erosion of Crusted Soils on Mars* **[#1999]**
MOLA slope and roughness data shed light on the erosion of regional duricrust and suggest it follows pre-existing topography. This implies that cementation of the duricrust was likely due to atmosphere-surface interactions or *in situ* alteration.

Kirkland L. E.* Herr K. C. Forney P. B. Salisbury J. W.
*1969 Mariner 7 Infrared Spectrometer: Data Recovery and Comparison to TES* **[#1693]**
High quality 1969 Mariner Mars 7 Infrared Spectrometer (IRS) spectra have recently been recovered and calibrated. We will show newly recovered IRS spectra, and compare IRS and TES spectra.

Mitchell D. L.* Lin R. P. Crider D. Law C. Walker P. Cloutier P. Acuña M. H.
*Solar Wind Interaction with Martian Crustal Magnetic Anomalies* **[#2061]**
The magnetometer/electron reflectometer experiment on Mars Global Surveyor has made observations of the interaction of the solar wind with martian crustal magnetic anomalies.

## Wednesday, March 17, 1999
## ORIGINS OF PLANETARY SYSTEMS
## 8:30 a.m. Room D

**Chairs: J. F. Kerridge**
**H. A. T. Vanhala**

Liou J.-C.* Zook H. A.
*Signatures of Giant Planets on the Solar System Kuiper Belt Dust Disk and Implications for Extrasolar Planet in Epsilon Eridani* **[#1698]**
We show that giant planets produce large scale features on the Solar System Kuiper Belt dust disk. The features are similar to those observed on Epsilon Eridani. Numerical simulations on Epsilon Eridani dust disk suggest that there is a Neptune-size planet in the system.

Stepinski T. F.*
*Layered Accretion in the Solar Nebula* **[#1205]**
Evolutionary model of the solar nebula based on the concept of layered accretion is presented. Layered accretion leads to a highly episodic nebula evolution marked by a progression of outbursts and quiescent states.

Boss A. P.*
*Giant Planet Formation by Disk Instability* **[#1049]**
3D hydro models suggest that a protoplanetary disk with a mass of about 0.1 solar masses could quickly lead to the formation of two giant gaseous protoplanets, one at 6 AU and one at 12 AU.

Wetherill G. W.* Kortenkamp S. J.
*Asteroid Belt Formation with an Early Formed Jupiter and Saturn* **[#1767]**
The early formation of Jupiter (via disk instability) does not prevent runaway growth of planetary embryos near 1 AU, but may have important consequences for theories of asteroid belt formation.

Nagasawa M.* Ida S. Tanaka H.
*Three-dimensional Orbital Evolution of Asteroid Due to the Sweeping Secular Resonances* **[#1235]**
We studied three-dimensional orbital evolution of asteroids due to sweeping secular resonances with three types of nebula dissipation models. Non-uniform dissipation of the nebula can explain large eccentricities and inclinations of asteroids.

Weidenschilling S. J.* Marzari F.
*Supersonic Planetesimals in the Solar Nebula* **[#1713]**
Planetesimals in resonances with Jupiter can reach supersonic velocities within the solar nebula. Their surfaces can experience wide temperature variations on the timescale of an orbital period. Bow shocks can melt chondrule-sized particles.

Agnor C. B. Canup R. M.* Levison H. F.
*The Impact Phase of Terrestrial Planet Accretion: Implications for Lunar Origin* **[#1878]**
Direct integrations of the final stages of terrestrial planet accretion are used to determine impactor masses and angular momenta, and the evolution of planetary spins. Implications for lunar formation from a giant impact are discussed.

Cameron A. G. W.* Canup R. M.
*State of the Protoearth Following the Giant Impact* **[#1150]**
Optimum conditions for the giant impact: protoearth roughly half accumulated, becoming roughly two-thirds accumulated. It is then highly rotationally flattened, has internal mixing over most of the volume, and has substantial surface waves.

Nuth J. A. III*

*Constraints on Nebular Dynamics Based on Observations of Annealed Magnesium Silicate Grains in Comets and in Disks Around Herbig Ae and Be Stars* **[#1726]**

Observations of "crystalline olivine" grains in comets and in the disks surrounding Herbig Ae & Be stars indicate the action of a continuous flow of material from the inner to the outer regions of protoplanetary nebulae not accounted for in current nebular models.

Mendybaev R. A.* Beckett J. R. Grossman L. Stolper E.

*Effect of $f(O_2)$ on SiC Volatilization Rate* **[#1990]**

The rate of SiC volatilization has been measured in $H_2$-$CO_2$ with log $f(O_2)$ from IW-3 to IW-10. The results show that possible variations in the composition of a nebular gas do not increase lifetimes of interstellar SiC grains reported previously (several months at 1200°C).

Ozima M.*

*Primordial Noble Gas in the Earth* **[#1096]**

Comparative studies of Earth's atmospheric and mantle noble gases show that the primordial terrestrial noble gases are different from the solar components, and they were derived from the solar noble gas by fractionation which took place prior to the Earth's accretion.

Davis D. R.* Farinella P. Weidenschilling S. J.

*Accretion of a Massive Edgeworth-Kuiper Belt* **[#1883]**

We study accretion in the region of 24–50 AU to find a self-consistent scenario for the formation of Neptune and the E-K population. Using a 50 Me initial population, QB1-sized bodies form in a reasonable time but Neptune does not grow to terminate accretion in the E-K belt.

Vanhala H. A. T. Boss A. P.

*Injection of Radioactivities into the Presolar Cloud: The Effect of Shock Structure and Resolution* **[#1433]**

We present results from our study of the structure of interstellar shock waves, which is expected to influence the injection of radioactivities into the presolar cloud. The effect of the resolution of the calculations is also discussed.

**Wednesday, March 17, 1999**
**CHONDRULES**
***Session dedicated to the memory of Elbert King***
**1:30 p.m. Room A**

Elbert King was known to most of the space research community with his love for the finer things in life, which also included minerals, gemstones, tektites, meteorites, and planetary exploration. Following his undergraduate and graduate career at the University of Texas and Harvard, Elbert served as a staff scientist at NASA Manned Spacecraft Center from 1963 to 1967, where he helped plan and design the Lunar Receiving Laboratory, train Apollo astronauts, and was the first Curator of Lunar Samples, 1967–1969. In 1969 he became a Professor of Geology at the University of Houston, where he continued his research on tektites, meteorites, and lunar samples, directed graduate students, taught mineralogy and space-related courses, and with his insight and enthusiasm inspired many students to research careers. Among his many publications were a textbook on Space Geology in 1976, a personal recollection of the Apollo program entitled Moon Shot, and more than 100 scientific articles. He died on December 12, 1998, following a prolonged illness that had kept him from full participation in the many activities for which he was known and loved.

**Chairs: R. D. Ash**
**G. Libourel**

Ash R. D.* Young E. D. Alexander C. M. O'D. Rumble D. III MacPherson G. J.
*Oxygen Isotope Systematics in Allende Chondrules* **[#1836]**
Allende chondrules have undergone varying degrees of alteration in the meteorite parent body or the nebula. This has resulted in some chondrules lying along a slope 1 line and others on a slope 0.5 line on an oxygen 3 isotope plot.

Sears D. W. G.* Lyon I. C. Saxton J. M. Symes S. Turner G.
*Oxygen Isotope Heterogeneity in the Mesostasis of a Semarkona Group A1 Chondrule* **[#1406]**
Oxygen isotopes in a large group A1 chondrule with compositionally zoned mesostasis show a large spread along a slope one fractionation line with a radial trend of light oxygen increasing toward the edge. The chondrule formation process appears to have produced this trend.

Bridges J. C.* Li C. Franchi I. A. Hutchison R. Sexton A. S. Pillinger C. T. Ouyang Z.
*The Relative Effects of Mineralogy and Chondrule Size on Oxygen Isotopic Exchange in Bo Xian (LL3.9)* **[#1774]**
Oxygen isotopic compositions of chondrules separated from Bo Xian (reclassified as LL3.9) show that mineralogically controlled rates of diffusion, rather than chondrule size, control the extent of isotopic exchange in ordinary chondrites.

Wang J.* Yu Y. Alexander C. M. O'D. Hewins R. H
*The Influence of Oxygen and Hydrogen on the Evaporation of K* **[#1778]**
We show that K evaporation is not suppressed by high $fO_2$, and K isotopic mass fractionation during evaporation is not supressed by enhance evaporation rates in the presence of $H_2$.

Georges P. Libourel G.* Deloule E.
*Potassium Condensation Experiments and Their Bearing on Chondrule Formation* **[#1744]**
To test the role of K-volatilization or back-diffusion in chondrules, new experiments have been performed under controlled PK, $PO_2$ and T. K condensation is found efficient enough to produce on a short time the K contents observed in UOC chondrules.

Tsuchiyama A.* Tachibana S.
*Evaporation Rates of Elements, Such as Sodium, from Melts Under Solar Nebula Conditions* **[#1535]**
Evaporation rates of elements from melts under nebula conditions were formulated by quasi-equilibrium model. This explains previous experimental results, especially for Na evaporation. Evaporation regimes were discussed from the experimental data.

Nagahara H.* Kita N. T. Ozawa K. Morishita Y.

*Condensation During Chondrule Formation: Elemental and Mg Isotopic Evidence* **[#1342]**

Evidence for condensation of Mg, Si, Fe, Na, and K due to temperature decrease during chondrule formation is found in two Semarkona chondrules. The evidence includes compositional zoning in glass and heavier Mg isotopic composition in forsterite core.

Lofgren G. E.* Le L. Schatz V.

*Partial Melting of WSG95300: A Type 3 UOC* **[#1742]**

Partial melting experiments on a type 3 unequilibrated ordinary chondrite, WSG95300 at near solidus temperatures show that a large number of chondrules are produced with modest amounts of partial melting and subsequent crystallization.

Symes S. J.* Lofgren G. E.

*Distribution of FeO and MgO Between Olivine and Melt in Natural and Experimental Chondrules* **[#1869]**

FeO and MgO partitioning between olivine and melt for UOC chondrules has been investigated in order to understand their crystallization behavior. In addition, cooling rate experiments on synthetic chondrules have helped define the limits of the Fe-Mg exchange coefficient.

Jones R. H.*

*Isolated Pyroxene Grains in ALHA77307: Derivation from Chondrules* **[#1420]**

Isolated pyroxene grains in ALHA77307 have very similar compositions to chondrule pyroxenes. They appear to be derived from chondrules, albeit a slightly different chondrule suite than that currently observed.

Hewins R. H.*

*Relict Pyroxene — Constraint on Chondrule Melting??* **[#1678]**

Chondrules containing relict enstatite did not exceed 1577°C for more than a few seconds, but literature examples formed at low temperatures and do not prove a flash melting origin. The scarcity of relict pyroxene suggests that chondrules had relatively long melting times.

Cuzzi J. N.* Hogan R. C. Paque J. M.

*Chondrule Size-Density Distributions: Predictions of Turbulent Concentration and Comparison with Chondrules Disaggregated from L4 ALH85033* **[#1274]**

The size distributions predicted by turbulent concentration are free of adjustable parameters. Predictions and data from disaggregated chondrites are well fit by the same lognormal function.

Desch S. J.*

*Generation of Lightning in the Solar Nebula* **[#1962]**

We present a new model of solar nebula lightning based on triboelectric charging and turbulent concentration of dust. Unlike previous models, it is not limited by energetics or charge leakage, provided several Myr have elapsed since CAI formation.

**Wednesday, March 17, 1999**
**LUNAR STRUCTURE, EVOLUTION, AND HIGHLANDS**
**1:30 p.m. Room B**

**Chairs: G. Ryder**
**K. Righter**

Khan A.* Mosegaard K. Rasmussen K. L.
*A Reassessment of the Apollo Lunar Seismic Data and the Lunar Interior* **[#1259]**
Elucidation of the interior velocity structure of the Moon using an inverse Monte Carlo sampling method on the travel times measured by the four-station seismic array placed on lunar surface during the Apollo missions.

Nimmo F.* McKenzie D.
*Crustal and Elastic Thickness Estimates for the Moon* **[#1325]**
The crustal thickness of non-mascon lunar areas is about 45 km, assuming isostasy. The elastic thickness of the South Pole-Aitken Basin is about 5 km. These areas are weak, implying they must have formed early in the Moon's history.

Hood L. L.* Lin R. P. Mitchell D. L. Acuna M. A. Binder A. B.
*Initial Measurements of the Lunar Induced Magnetic Moment in the Geomagnetic Tail Using Lunar Prospector Data* **[#1402]**
Using data from the April 1998 tail lobe pass, an induced moment of $-2.6 \pm 1.2 \times 10^{22}$ G-cm$^3$ per Gauss of applied field is estimated. The corresponding preferred core radius is 375 +50/–75 km, representing 1–3% of the lunar mass for an Fe composition.

Pritchard M. E.* Stevenson D. J.
*How Has the Moon Released Its Internal Heat?* **[#1981]**
We have used conductive thermal models with melting to determine that under certain compositional, rheological, and initial conditions, mantle convection could be inhibited or weakened on the Moon.

Righter K.* Drake M. J.
*Partitioning of W Between Liquid Metal, Solid Silicates, and Liquid Silicates at High Pressures and Temperatures: Implications for the $^{182}$W Isotope Anomalies in Lunar and Martian Samples* **[#1381]**
New high pressure and temperature experiments on partially molten basalt and chondrite show that the $^{182}$W anomalies measured in lunar and martian samples must be interpreted with a full undertsanding of metal-silicate and clinopyroxene-silicate liquid partitioning.

Palme H.*
*The Lunar Hf/W Ratio and the Significance of $^{182}$W/$^{184}$W Ratios in Lunar Samples* **[#1763]**
It is shown that the W/Hf ratios of the Moon and the Earth's mantle are indistinguishable and that the excess of $^{182}$W/$^{184}$W in lunar samples is not compatible with formation of the Moon by the giant impact model in its simplest form.

Morgan J. W.* Walker R. J. Brandon A. D.
*Siderophile Elements in the Earth's Upper Mantle and the Moon's Ancient Impact Breccias: Manifestations of the Same Late Influx?* **[#1207]**
Earth's mantle contains siderophile elements because of a late influx of planetesimals. On the Moon, the same late influx is found preserved in ancient lunar breccias formed by early basin-forming impacts. Element patterns are similar on Earth and Moon.

Ryder G.*
*Meteoritic Abundances in the Ancient Lunar Crust* **[#1848]**
Meteoritic material added to the Moon between crustal formation and late basin formation, based on samples and crustal structure, is equivalent to only ~50 m. This is less than common estimates, suggesting a lower bombardment intensity than assumed.

Parmentier E. M.* Hess P. C.

*On the Chemical Differentiation and Subsequent Evolution of the Moon* **[#1289]**

Solidification of the magma ocean generates dense, incompatible element rich ilmenite cumulate. We examine the gravitational differentiation of this material and its implications for the subsequent evolution of the Moon.

Shearer C. K.* Newsom H. E.

*A Short-lived Lunar Magma Ocean. Implications for the Evolution of the Early Lunar Crust* **[#1362]**

Complexities in lunar sample geochemistry are not easily explained by the standard models for the evolution of the lunar crust. Evidence from W isotopes for a short-lived magma ocean could help in deciphering these complexities.

Ganguly J.* Domeneghetti M. C. McCallum I. S.

*Complex Cooling History of Lunar Mg Suite Gabbronorite 76255: Record in Exsolution-Diffusion and Fe-Mg Ordering in Pyroxenes* **[#1476]**

We determined cation ordering in orthopyroxenes from the gabbronorite 76255 and calculated the cooling rates from these data at ~500°C. Comparison with the earlier study of cooling rate at 800°C suggests a complex thermal history for this sample.

Masuda A.* Takahashi K.

*Origin of a Lunar Meteorite Asuka 881757: REE Geochemistry* **[#1338]**

Asuka 881757 is an earlier-stage cumulate from the primary magma. Pattern for the conjugate melt is estimated. It is likely that this meteorite was ejected from the depth of the non-mare area like the Decartes region.

Eugster O.*

*Chronology of Dimict Breccias and the Age of South Ray Crater at the Apollo 16 Site* **[#1007]**

Six Apollo 16 rocks with South Ray crater origin yield a cosmic-ray exposure age of 2 Ma, contemporaneous with 15 additional South Ray crater rocks. All dimict breccias dated until now originate from this crater and have a formation age of 3.97 Ga.

**Wednesday, March 17, 1999**
**MARS TECTONICS, VOLCANISM, AND INTERIOR**
**1:30 p.m. Room C**

**Chairs: D. L. Turcotte**
**F. S. Anderson**

Turcotte D. L.*
*Tectonics and Volcanism on Mars: What Do We and What Don't We Know?* **[#1187]**
Many fundamental questions concerning the tectonics and volcanic evolution of Mars remain unanswered. Two of the most significant are the cause of the global dichotomy and the origin of the Tharsis structure.

Anderson F. S.* Grimm R. E.
*Rifting of Valles Marineris, Mars: A Finite Element Analysis* **[#1954]**
A visco-elastic-plastic finite-element model is used to examine linked constraints on Valles Marineris trough width, depth, and flank uplift as functions of extension rate, crustal thickness, heat flux, and geometry of initiating asperities.

Anderson R. C.* Haldemann A. F. C. Dohm J. M. Golombek M. P. Franklin B. J. Lias J.
*Significant Centers of Tectonic Activity as Identified by Wrinkle Ridges for the Western Hemisphere of Mars* **[#1972]**
Two centers of tectonic activity were identified by projecting compressional (wrinkle ridge) features for the western hemisphere of Mars. This agrees with the primary Hesperian center of tectonic activity (Stage 3) identified by Anderson et al. (1998).

Mege D.*
*A Method for Estimating 2D Horizontal Shortening at Wrinkle Ridges from Remote Sensing Data: Results from the Yakima Fold Belt (Columbia Plateau)* **[#1838]**
Field data and length/displacement scaling laws applied to the Yakima fold belt on the Columbia Plateau are used to demonstrate a method for estimating surface shortening of wrinkle ridge areas. Application to martian wrinkle ridges is given in another abstract.

Mangold N.* Allemand P. Thomas P.
*Datation of Compressional Deformation on Mars: Evidence for a Single and Global Origin* **[#1017]**
Datation of compressional deformation on Mars is done using intersections between craters and structures. These datations and related observations conclude to a single and global phase. An age of Late Hesperian is deduced for this global phase.

Weitz C. M.*
*A Volcanic Origin for the Interior Layered Deposits in Hebes Chasma, Mars* **[#1277]**
We have examined the interior layered deposits in Hebes Chasma and compared them to terrestrial pyroclastic deposits. We propose that the layered deposits represent ignimbrites that formed by collapsed plinian columns erupted inside Hebes.

Howard A. D.*
*Simulation of Lava Flow Inundation on Martian Cratered Terrain* **[#1112]**
Lava inundation of a cratered surface is simulated by spreading from a few sources. Unlike equipotential flooding, lava covers intercrater plains but high-rimmed craters escape flooding or are partially filled, as on ridged plains and subdued cratered units.

Montési L. G. J.*
*Concentric Dike Swarm and Internal Structure of Pavonis Mons (Mars)* **[#1251]**
The morphology of the grabens and fractures on the flanks of Pavonis Mons indicates an underlying concentric dike swarm related to the rift zones. We address the origin of the required radial extension and the general evolution of martian shields.

Plescia J. B.*

*Geology of Uranius Patera, Mars* **[#1638]**

Uranius Patera is a Late Hesperian basaltic shield in northeast Tharsis. It has a large complex caldera, radial flanks flows, and low shields; concentric faulting is minimal. Eruptions seem to be purely effusive.

Choblet G. Grasset O. Parmentier E. M. Sotin C.*

*Mars Thermal Evolution Revisited* **[#1556]**

Models describing the thermal evolution of Mars are revisited on the basis of 3D numerical experiments on thermal convection with variable viscosity. Cooling of Mars is studied and the evolution of the lithospheric thickness is discussed.

Neal C. R.* Ely J. C. Jain J. C. Sedlar A.

*Differentiation of Mars Investigated Using High Field Strength (HFS) and Platinum Group Elements (PGEs)* **[#1002]**

The geologic history of Mars is investigated. A full suite of trace element data was produced and reservoirs are defined using PGE and high field strength elements (HFSEs).

Breuer D.* Spohn T. Yuen D. A.

*The History of the History of the Martian Dynamo Generated Magnetic Field as Implied by the Results of 2D and 3D Convection Calculations* **[#1676]**

The history of the martian dynamo generated magnetic field is calculated using 2D and 3D mantle convection models. It is found that the magnetic field could be a relatively recent phenomenon with dynamo action starting at about 2 Ga b.p. and operating for another Ga.

**Wednesday, March 17, 1999**
**SMALL BODIES**
**1:30 p.m. Room D**

**Chairs: K. L. Reed**
**J. L. Hinrichs**

Asphaug E.* Thomas P. C.
*Modeling Mysterious Mathilde* **[#2028]**
We model impacts into asteroid Mathilde, as imaged by the NEAR flyby en route to Eros.

Hinrichs J. L.* Lucey P. G. Meibom A. Krot A. N.
*Temperature Dependent Near-Infrared Spectra of Olivine and H5 Ordinary Chondrites* **[#1505]**
The dependence of olivine and ordinary chondrite spectra on temperature is presented. Meteorite data show that spectra of asteroidal materials are different at terrestrial and main belt temperatures.

Bottke W. F. Jr.* Rubincam D. P. Burns J. A.
*Delivery of Meteoroids from 6 Hebe Via Yarkovsky Thermal Drag* **[#1504]**
Yarkovsky thermal drag, a radiation effect which can modify meteoroid semimajor axes, can transport ejecta from 6 Hebe to Earth via the v6 resonance. We can show that their estimated delivery timescales are consistent with the cosmic-ray exposure ages of stony meteorites.

Gaffey M. J.*
*Improving Methodologies for Quantitative Interpretation of S(IV)/OC Type Aateroidal Spectra with Applications for the NEAR Eros Mission* **[#1375]**
The interpretive methodology for S(IV) spectral data, such as Eros, can be improved by use of spectral parameters derived from computed chondrite mineral abundances. Each chondrite subtype has a specific correlation function between mineralogy and spectral parameters.

Kelley M. S.* Gaffey M. J.
*The High Albedo, Odd Spectrum, and Compositional Possibilities of Asteroid 434 Hungaria* **[#1772]**
New spectral data from 0.4–2.5 microns have been obtained for 434 Hungaria. The near-IR spectrum is smooth, featureless, and agrees well with previous visible region data. However, the new visible region data exhibit broad spectral absorption features near 0.5 and 1 microns.

Reed K. L.* Lebofsky L. A. Gaffey M. J.
*Topographic Features of Asteroids Without Imaging: 4 Vesta as "Spacetruth"* **[#1710]**
Simultaneous reflected and emitted lightcurves of an asteroid can be used to deduce large topographic asperities on an asteroid's surface. Combined with rotational spectral variation data these can aid in defining a geologic context for the features.

Binzel R. P.* Bus S. J. Burbine T. H.
*The Orbital Distribution of Vesta-like Asteroids* **[#1216]**
More than 40 small (D < 10 km) Vesta-like asteroids are now known. Vesta is found to be at the locus of their distributions in all three dimensions of orbital space. This non-random distribution is a strongly compelling dynamical link implying a Vesta origin.

Malhotra R.
*Neptune's 2:1 Orbital Resonance in the Kuiper Belt* **[#1998]**
The peculiar character of stable orbits at the 2:1 Neptune resonance is described. We discuss how it affects the identification of 2:1 librators amongst observed Kuiper Belt objects.

Moore L. B.* Flynn G. J. Klock W.

*Density and Porosity Measurements on Meteorites: Implications for the Porosities of Asteroids* **[#1128]**

We measured porosities of 33 meteorite samples, and found porosities ranging from 6 to 29% among the stone meteorite falls. Meteorite finds generally have lower porosities, but two finds, Ozona and Muslyumovo, have 8 to 10% porosity.

Consolmagno G. J.* Britt D. T.

*Turning Meteorites into Rock: Constraints on Asteroid Physical Evolution* **[#1137]**

The relatively low porosity of meteorites puts serious constraints on their formation. It is difficult to find an adequate scenario for meteorite lithification consistent with standard models for parent body accretion.

Sunshine J. M.* Cloutis E. A.

*Absorption Bands in Spinels: Comparisons of Laboratory and Asteroid Spectra* **[#1640]**

Analysis of spectra of compositional end members of spinel are examined with the modified Gaussian model and compared to spectra of spinel-rich asteroids.

Britt D. T.*

*What Can Ordinary Chondrite Meteorites Tell Us About "Space Weathering"?* **[#1649]**

"Space weathering" in ordinary chondrite meteorites does not seem to mimic the red slope increases on plausible ordinary chondrite parent bodies. It may be that, as in the Lunaites, the red-slope carrying species in ordinary chondrites are relatively fragile.

**Thursday, March 18, 1999**
**MARTIAN METEORITES II: SHERGOTTITES, NAKHLITES, AND CHASSIGNY**
**8:30 a.m. Room A**

**Chairs: J. S Delaney**
**R. C. F. Lentz**

Berkley J. L.* Treiman A. H. Jones J. H. Mittlefehldt D. W.
*Highly Magnesian Orthopyroxenite Xenoliths in EETA79001: Implications for Martian Magmas and Differentiation* **[#1588]**
martian meteorite EETA79001 contains a xenolith with the highest Mg#(=86)known in martian materials. Calculated magma Mg#=60 is consistent with extreme mantle differentiation on Mars. High Si+Al glass inclusions in OPX may be magmatic or mineral relics.

Mittlefehldt D. W.* Lindstrom M. M.
*Petrology and Geochemistry of Martian Meteorites EETA79001 and ALHA77005* **[#1817]**
Petrologic and chemical data for martian meteorite EETA79001 show that lithology A groundmass is a hybrid mixture of solid and melted materials derived from xenoliths and lithology B. The lithology A groundmass is not a melt formed by martian igneous processes.

Lentz R. C. F.* McSween H. Y. Jr.
*Crystal Size Distributions of Basaltic Shergottites* **[#1126]**
CSD analyses of pyroxene grains in basaltic shergottites provide insights into their crystallization histories. Preliminary interpretations agree with previously suggested one- and two-stage crystallization scenarios.

Sharp T. G.* El Goresy A. Dubrovinsky L. Chen M.
*Very-dense Silica Minerals in the Shergotty SNC Meteorite: Evidence for Exteme Shock Pressures* **[#1827]**
Electron and X-ray diffraction confirm that $SiO_2$ in Shergotty consists of two very dense polymorphs in addition to stishovite. All three of these high-density structures are quench phases from post-stishovite structures stable at 47 to >80 GPa.

Herd C. D. K.* Papike J. J.
*Nonstoichiometry in SNC Spinels: Implications for the Determination of Oxygen Fugacity from Phase Equilibria* **[#1503]**
Application of electron microprobe oxygen analysis to spinels in the SNC meteorites has demonstrated that nonstoichiometry has an effect on the determination of oxygen fugacity using the spinel-ilmenite and spinel-olivine-orthopyroxene systems.

Delaney J. S.* Dyar M. D. Sutton S. R. Polyak D. Stefanis M.
*Mineralogical $Fe^{3+}/\Sigma Fe$ Measurements as Proxies of Volatile Budgets: III Oxidation State Zoning in Martian Basalt* **[#1861]**
Ferric/ferrous zoning has been documented in martian basalts QUE94201 and Shergotty. Ferric/ferrous ratio decrease with crystallization but abundance of each species increases. Magma fractionation under total constant composition conditions is inferred.

Farquhar J.* Thiemens M. H. Jackson T. L.
*$\Delta^{17}O$ Anomalies in Carbonate from Nakhla and Lafayette and $\Delta^{33}S$ Anomalies in Sulfur from Nakhla: Implications for Atmospheric Chemical Interactions with the Martian Regolith* **[#1675]**
Here we report measurements of $\Delta^{17}O$ and $\Delta^{18}O$ from 150°C acidification of Nakhla.23 and Lafayette USNM 1505. We also report the results of $\Delta^{33}S$ and $\Delta^{34}S$ measurements of Nakhla.23, Nakhla USNM 426, and EET 79001.341.

Jull A. J. T.* Klandrud S. E. Schnabel C. Herzog G. F. Nishiizumi K. Caffee M. W.
*Cosmogenic Radionuclide Studies of the Nakhlites* **[#1004]**
Due to their apparent origin on Mars, the nakhlites are of great interest. Scattered radionuclide data paint an incomplete picture of the histories of meteorites. In this study, we tried to confirm earlier radionuclide data on these meteorites from various sources.

Chaussidon M.* Robert F.
*$^{7}Li/^{6}Li$ and $^{11}B/^{10}B$ Ratios of SNC Meteorites* **[#1592]**
Basaltic SNCs have Li and B isotope compositions rather homogeneous and close to that of the Earth mantle, but up to 15‰ difference is present for both isotope systems in ALH84001 and in Chassigny.

Bridges J. C.* Grady M. M.
*Siderite and Gypsum Intergrown with Magnetite-Ilmenite in Governador Valadares* **[#1545]**
Governador Valadares contains a siderite-gypsum-apatite assemblage intergrown with magnetite-ilmenite. Ilmenite exsolved at 700°C — possibly a lower temperature limit for a CO3-rich fluid that originated by melt mixing with ice-rich sediment.

Treiman A. H.*
*Bad Water: Origin of Phoenicochroite-Lanarkite Solid Solution, $Pb_2O(CrO_4,SO_4)$, in Martian Meteorite EETA79001* **[#1124]**
EETA79001 contains grains of phoenicochroite-lanarkite, $Pb_2O(CrO_4,SO_4)$, deposited from martian groundwater with pH >8, low $(CO_3)_{2-}$, moderate $(SO_4)_{2-}$, [Pb] ~ $10^{-5}$M and [Cr] ~ $10^{-4}$M. The water, though a possible mineral resource, was not fit for human consumption.

El Goresy A.* Kong P. Palme H.
*Discovery of Cu-, Ni, Zn-, Fe-Metal Alloy Impregnations in the SNC Meteorite Chassigny: Fingerprints of a Pristine Metallogenic Activity on the SNC Parent Body?* **[#1078]**
Very thin sheaths of a Cu-, Ni-, Zn-, Fe-alloy occur as straight impregnations in olivine and "maskelynite" in Chassigny.These metal sheaths are probably fingerprints of metallogenic activity on the Chassigny parent body.

Kong P.* Ebihara M. Palme H.
*Highly Siderophile Elements in Martian Meteorites* **[#1570]**
Results of analyses of highly siderophile elements in six martian meteorites are reported. Mars has, as the Earth, obtained its inventory of these elements by a late veneer. Variable Os/Ir ratios in Nakhla and ALH84001 may be the result of aqueous activity on Mars.

## Thursday, March 18, 1999
## CHONDRITES I: ALTERATION AND PROCESSING
## 8:30 a.m. Room B

**Chairs:** **D. S. Lauretta**
**J. N. Grossman**

Goreva J. S.* Burnett D. S.
*Th/U Variations in Chondritic Materials. An Ubiquitous U-Rich Component?* **[#1467]**
A linear correlation of Th/U vs. 1/U suggests a 2-component mixing for all chondrites. The simplest global interpretation is a 3-component mixture, involving CAI, Low and High U components. Although ubiquitous, the presence of the High U component has gone largely unnoticed.

Hutcheon I. D.* Weisberg M. K. Phinney D. L. Zolensky M. E. Prinz M. Ivanov A. V.
*Radiogenic $^{53}Cr$ in Kaidun Carbonates: Evidence for Very Early Aqueous Activity* **[#1722]**
Kaidun carbonates contain large excesses of radiogenic $^{53}Cr$, corresponding to an initial $^{53}Mn/^{55}Mn$ of $\sim 9 \times 10^{-6}$. This value is similar to that measured in chondrules and much higher than in CI carbonates. Kaidun carbonates formed within ~1 Ma of CAI.

Brearley A. J.* Saxton J. M. Lyon I. C. Turner G.
*Carbonates in the Murchison CM Chondrite: CL Characteristics and Oxygen Isotopic Compositions* **[#1301]**
We have investigated the CL characteristics and oxygen isotopic compositions of carbonate grains from the Murchison CM chondrite. The oxygen isotopic compositions of 7 different calcite grains have $\delta^{18}O$ from 27.4 to 37.2‰ and lie along the terrestrial fractionation line.

Li J.* Hua X. Buseck P. R.
*Mineralogy of Fine-grained Rims in LEW90500 by Transmission Electron Microscopy* **[#1271]**
In this presentation, we report TEM results about the mineralogy of a fine-grained rim (FGR) from LEW90500. Our results show that the FGR contains cronstedtite, serpentine, tochilinite, pentlandite, and calcium sulfate (probably gypsum or anhydrite).

Hua X.* Wang J. H. Li J. Buseck P. R.
*Evidence for Both Pre- and Post-Accretionary Alteration in LEW90500* **[#1161]**
Results of BEI, EMPA, SIMS, and TEM studies of an unusual calcite-spinel-titanofassaite inclusion from the Antarctic CM meteorite LEW90500 and the surrounding fine-grained rim show evidence for both pre- and post-accretionary aqueous alteration.

Clayton R. N.* Mayeda T. K.
*Links Among CI and CM Chondrites* **[#1795]**
Oxygen isotopic compositions of Bells, Essebi and Niger-I suggest that they are intermediate between CM2 and CI1, having undergone incomplete parent-body conversion to phyllosilicates and magnetite at temperatures characteristic of CI, 100°–150°C.

Meibom A.* Petaev M. Krot A. N. Hicks T. Scott E. R. D. Keil K.
*Condensation Origin of Some Metal Grains in CH Chondrites: Implications for the Formation of Metal in the CR-Clan* **[#1411]**
We report findings of large metal grains (~150 μm) with distinct zoning patterns in Ni, Co, Cr, and Si in CH chondrites which are consistent with a condensation origin from a gas of solar composition.

Petry C.* Chakraborty S. Palme H.
*NiFe-Olivine Exchange Thermometer and Diffusion Coefficients in Olivine as a Tool for Determining the Thermal History of Meteorite Parent Bodies* **[#1248]**
A NiFe-olivine exchange thermometer has been calibrated and cation diffusion data in olivine have been determined experimentally. Data are applied to calculate the thermal history of meteorite parent bodies.

Zolensky M. E.* Bodnar R. J. Bogard D. D. Garrison D. H. Gibson E. K. Gounelle M. Nyquist L. E. Reese Y. Shih C.-Y. Wiesmann H.

*Fluid Inclusion-bearing Halite and Solar Gases in the Monahans 1998 H5 Chondrite* **[#1280]**

The Monahans 1998 H5 breccia contains indigenous halite and sylvite. We describe here noble gas analyses of Monahans lithologies, Rb/Sr systematics of halite separates, and aqueous fluid inclusions present within the halite.

Krestina N.* Jagoutz E. Kurat G.

*The Interrelation Between Core and Rim of Individual Chondrules from the Different Meteorites in Terms of Sm-Nd Isotopic System* **[#1918]**

The stepwise technique of chondrule abrasion has been used to investigate the relationship between rim and core of single chondrules from different meteorites in terms of Sm-Nd isotope system.

Lauretta D. S.* Zega T. J. Buseck P. R.

*Experimental and Petrographic Studies on the Origin of Chondritic Fayalite* **[#1160]**

The presence of endmember fayalite in chondritic meteorites is a relatively recent discovery. Several models have been proposed for its origin. We investigate oxidation of Si bearing metal and apply our results to fayalite-rimmed metal in Bishunpur (LL3.1).

Grossman J. N.* Rubin A. E.

*The Metamorphic Evolution of Matrix and Opaque Minerals in CO Chondrites* **[#1639]**

We examined a suite of CO chondrites using large, 10-element X-ray maps. S changes dramatically between types 3.1 and 3.2, and migrates out of matrix. P and Cr are very mobile during metamorphism. Y-81020 is one of the most primitive COs.

Hsu W.* Huss G. R. Wasserburg G. J.

*An Ion Probe Study of Al-Mg Systematics in the Ningqiang Carbonaceous Chondrite* **[#1488]**

We studied Al-Mg systematics in one CAI, one POI, and two chondrules in Ningqiang. The CAI shows a $(^{26}Al/^{27}Al)_0$ ratio close to the canonical value. The POI has a ratio one order of magnitude lower. Two chondrules show no clear excesses of $^{26}Mg^*$.

## Thursday, March 18, 1999
## MARS CLIMATE, POLAR CAPS, AND HYDROLOGY
## 8:30 a.m. Room C

**Chairs:** **N. G. Barlow**
**P. Lee**

Craddock R. A.* Maxwell T. A. Howard A. D.
*The Evidence for Climatic Variations on Early Mars* **[#1977]**
Modified craters on Mars provide strong evidence of warmer, wetter conditions. A distinct class of modified crater suggests that the intensity of rainfall events waned with time on early Mars and, perhaps, that a transitional periglacial climate preceeded today's.

Bills B. G.*
*Climate-Rotation Feedback on Mars* **[#1794]**
A new model of the coupled evolution of climate and rotation of Mars is presented. Obliquity influences polar ice mass and the spin axis precession rate is influenced by polar ice mass and viscous mantle flow. Dissipation qualitatively changes the system evolution.

Zent A. P.*
*An Open, Snow-based, Hydrologic System as an Analog for Noachian Mars* **[#1803]**
An open, snow-based, hydrologic system may explain the presence of valley networks on Noachian Mars. Water is delivered to the surface by volcanos or craters, and temperature and pressure varaitions allow temporally and spatially sparse melting and drainage.

Arthern R. J.* Winebrenner D. P. Waddington E. D.
*Modeling the Near Surface Density of the Martian Northern Hemisphere Ice Cap* **[#1487]**
Modeling the sintering of granular water ice under conditions typical of the martian northern hemisphere polar cap. Notes implications for gas bubble entrapment within the ice cap, as well as for the interpretation of thermal inertia measurements.

Mangold N.* Allemand P. Duval P. Geraud Y. Thomas P. G.
*Ice Content of Martian Permafrost Deduced from Rheology of Ice-Rock Mixtures* **[#1016]**
Experimental results on ice-rock mixtures show that a minimal ice content of 28% is needed to produce a viscous deformation like that observed in martian softened terrains. A global inventory of water of about 200 m is deduced from this high proportion of ice.

Schenk P. M.* Moore J. M.
*South Polar Cap and Layered Deposits of Mars: High-Resolution Stereo Topographic and Geologic Mapping* **[#1819]**
Stereo-derived topography of the South Pole of Mars reveals a 450-km-wide polar cap that is 3 km high. Layered deposits surrounding the cap are 1–2 km high. Evidence suggests that these deposits were once more extensive but have retreated.

Nye J. F. Durham W. B.* Schenk P. M. Moore J. M.
*Decay of a Carbon Dioxide Mars South Polar Ice Cap* **[#1965]**
Decay of a pure $CO_2$ south polar cap of Mars is calculated based on experimentally determined $CO_2$ rheology and an ice cap model. The maximum ice cap thickness allowed is about 2000 m.

Barlow N. G.* Perez C. B. Saldarriaga P. C.
*Distribution of Subsurface Volatiles Across the Equatorial Region of Mars* **[#1679]**
We are conducting a study of ejecta morphology variations within the martian equatorial region in order to constrain the regional distribution of subsurface volatile reservoirs.

Clifford S. M.* Parker T. J.
*Hydraulic and Thermal Arguments Regarding the Existence and Fate of a Primordial Martian Ocean* **[#1619]**
The existence of a primordial ocean in the northern plains of Mars is shown to have been an inevitable consequence of the hydraulic and thermal conditions that existed during the Early Noachian.

Lee P.* Rice J. W. Jr. Bunch T. E. Grieve R. A. F. McKay C. P. Schutt J. W. Zent A. P.
*Possible Analogs for Small Valleys on Mars at the Haughton Impact Crater Site, Devon Island, Canadian High Arctic* **[#2033]**
We present possible analogs for small valleys on Mars found at the Haughton impact crater site, Devon Island, NWT, Canada. Implications for Early Mars climate are discussed.

De Hon R. A.* Washington P. A.
*Bahram Vallis, Mars: A Brief History of a Long Term Discharge* **[#1928]**
Outflow from Juventae Chasma ponded on Lunae Planum. After drainage of the lake, ground water seepage carved Bahram Vallis. Preliminary modeling of ground water discharge and headward erosion indicates that the valley was active for 5,000 to 50,000 terrestrial years.

Emrick C. M.* De Hon R. A.
*Flood Discharge Through Labou Vallis, Mars* **[#1893]**
Labou Vallis extends 270 km across Terra Sirenum. Three stages of discharge through the Labou Vallis sytem are recognized. Preliminary estimates of flow velocity through the gorge near the mouth of the channel ranges from 32 m/2 to 8.9 m/s.

Ori G. G.* Baliva A.
*Large Bulges at the Center of Impact Craters on Mars* **[#1758]**
A few large bulges in the central part of some impact craters have been observed. They can be the product of 1) hydrothermal activity, or 2) mud volcanisms. The latter reason is the most probable and the associated gas could be methane or carbon dioxide.

**Thursday, March 18, 1999**
**LUNAR POLES AND REGOLITH**
**8:30 a.m. Room D**

**Chairs: D. B. J. Bussey**
**L. P. Keller**

Cook A. C.* Spudis P. D. Robinson M. S. Watters T. R. Bussey D. B. J.
*The Topography of the Lunar Poles from Digital Stereo Analysis* **[#1154]**
Digital Elevation Models of the Moon's poles have been produced using Clemetine UVVIS stereo imagery. Topographic features are described including two newly discovered pre-Nectarian and Nectarian basins: Sylvester-Nansen and Schrodinger-Zeeman.

Bussey D. B. J.* Robinson M. S. Spudis P. D.
*Illumination Conditions at the Lunar Poles* **[#1731]**
We have produced an illumination map of the lunar south pole. It shows the percentage of time that a point on the surface is illuminated during a lunar day. We identify regions that experience illumination extremes.

Margot J. L.* Campbell D. B. Jurgens R. F. Slade M. A.
*Locations of Cold Traps and Possible Ice Deposits near the Lunar Poles: A Survey Based on Radar Topographic Mapping* **[#1897]**
Detailed topographic maps of the lunar poles have been obtained via Earth-based radar interferometry. These digital elevation models were used to locate regions which are in permanent shadow from solar illumination and which may harbor ice deposits.

Nozette S.* Spudis P. D. Robinson M. Bussey B. Lichtenberg C. Bonner R.
*Integration of Lunar Polar Datasets* **[#1665]**
We continue our studies of the environment and the deposits of the poles of the Moon. In this paper, we describe our integration of Clementine, Lunar Prospector, and groundbased radar data to provide additional insight into the nature of the lunar polar ice deposits.

Taylor L. A.* Pieters C. Morris R. V. Keller L. P. McKay D. S. Pachen A. Wentworth S.
*Integration of the Chemical and Mineralogical Characteristics of Lunar Soils with Reflectance Spectroscopy* **[#1859]**
Remote analysis of the Moon depends upon modeling of reflectance spectra with the modes and chemistry lunar soils, in order to unravel the over-printing by space weathering. This is the premise underlying our Lunar Soil Characterization Consortium.

Staid M. I.* Pieters C. M.
*Integrated Spectral Analysis of Mare Soils and Craters: Characterization of Lunar Basalt Types* **[#1724]**
The composition of basalts from Mare Serenitatis, Tranquillitatis, Frigoris and Lacus Somniorum are compared. The effects of maturity and space weathering on spectral parameters are defined.

Keller L. P.* Wentworth S. J. Gezo J. McKay D. S. Taylor L. A. Pieters C. Morris R. V.
*Space Weathering Alteration of Lunar Soil Grains* **[#1820]**
Through combined electron microscopy and reflectance spectroscopy studies of individual lunar soil grains, we have identified petrographic features of the grains which give rise to the optical effects known as space weathering.

Li L.* Mustard J.
*Lateral Transport of Materials Across the Lunar Surface: An Anomalous Diffusion Model* **[#2012]**
Discontinuous ejecta may travel great distance due to lateral transport; classical diffusion model does not apply, an anomalous diffusion model required.

Basu A.* Wentworth S. J. McKay D. S.

*A Petrologic Comparison of Apollo 11 Soil 10084 and Disaggregated Regolith Breccia 10068* **[#1873]**

The proto-regolith of breccia 10068 is finer and agglutinate-deficient than soil 10084. Breccia 10068 was likely assembled in post-mare basalt time but much earlier than the formation of soil 10084.

Urquhart M. L.* Jakosky B. M.

*Lunar Near-Surface Thermal Gradients: Implications for Subsurface Temperatures and Regolith Properties* **[#1799]**

We have included radiative transfer in the top few mm of a diurnal thermal diffusion model for the lunar regolith and find near-surface thermal gradients to have a significant effect on lunar subsurface temperatures and derived regolith properties.

Hashizume K.* Marty B. Wieler R.

*Single Grain Analyses of the Nitrogen Isotopic Composition in the Lunar Regolith — In Search of the Solar Wind Component* **[#1567]**

Stepwise N and Ar isotope analyses of single mineral grains of lunar regolith have been performed. Among the low temperature steps, $\delta^{15}N$ values ranging from –200 to +100‰ have been observed. The $^{36}Ar/^{14}N$ ratios were 0.03–0.4× solar.

Kerridge J. F.* Mathew K. J. Marti K.

*Covariation of Nitrogen and Neon Isotopes in Lunar Regolith Grains: Insights into SEP-Nitrogen and the "Excess Nitrogen" Problem* **[#1059]**

Stepwise etching of lunar ilmenite reveals that deeply implanted (SEP) N is light-isotope enriched relative to solar wind, in contrast to SEP-Ne which is heavy-isotope enriched. Implications for the "nonsolar-N" controversy are critically discussed.

**Thursday, March 18, 1999**
**ASTROBIOLOGY: PRECURSORS, ORIGINS, AND MARTIANS**
**1:30 p.m. Room A**

**Chairs: I. Gilmour**
**K. L. Thomas-Keprta**

Glavin D. P.* Bada J. L.
*The Sublimation and Survival of Amino Acids and Nucleobases in the Murchison Meteorite During a Simulated Atmospheric Heating Event* **[#1085]**
The Murchison meteorite was heated to 1100°C for a few seconds under reduced pressure. We found that a large fraction of amino acids and nucleobases present in the meteorite (40–80%) survived after heating which is much higher than previously estimated.

Cody G. D. III Alexander C. M. O'D.* Tera F.
*New Insights into the Chemistry of Murchison Organic Macromolecule Using High Field $^{13}C$ Solid State NMR* **[#1582]**
The organic matter within the Murchison Meteorite is analyzed using high field solid state $^{13}C$ NMR. Carbon aromaticity equals 60%, carbonyl, carboxyl, methyl, methylene, methine, and ether/alchohol are present. Spatial heteogenity in organic composition is suggested.

Gilmour I.* Sephton M. A. Pillinger C. T.
*The Fate of Meteoritic Macromolecular Organic Material on Wet Planets* **[#1701]**
Hydrous pyrolysis of macromolecular organic material from the Murchison meteorite has been used as a tool to investigate the fate of extraterrestrial macromolecules on wet planets in the early solar system.

Cody G. D. III* Boctor N. Z. Brandes J. A. Filley T. R. Hazen R. M. Yoder H. S. Jr.
*The Catalytic Activity of Transiton Metal Sulfides and Their Role in Primitive Terrestrial and Extraterrestrial Biochemistry* **[#1615]**
Organosynthesis related to the emergence of biochemistry in the primordial Earth required effective catalysts. The catalytic activity of a range of transition metal sulfides in hydroformylation chemistry under high temperature, high pressure conditions is studied.

Brandes J. A.* Boctor N. Z. Cody G. D. Hazen R. M. Yoder H. S. Jr.
*A New Role for Minerals in Prebiotic and Extraterrestrial Nitrogen Chemistry* **[#1284]**
A new preservative role for minerals in hydrothermal systems is discussed. We show that the lifespans of amino acids under high temperature and pressure conditions can be greatly extended by the presence of certain mineral sulfide buffers.

Gilmour J. D.* Whitby J. A. Turner G.
*Comparative Iodine Geochemistry of Earth and Mars: A Possible Biomarker* **[#1661]**
Iodine geochemistry on Earth is dominated by the actions of life, and thus may act as a biomarker on other planets. To begin to address this question we review our data on iodine in ALH84001 carbonate and Nakhla and outline some areas for future research.

Zolotov M. Yu.* Shock E. L.
*Abiotic Origin for PAHs and Aliphatic Hydrocarbons in ALH84001 and Nakhla Martian Meteorites: Synthesis in Trapped Magmatic and/or Impact Gases* **[#1879]**
We argue that hydrocarbons in ALH84001 could have formed metastably from CO ($CO_2$) and $H_2$ in cooling magmatic and/or impact gases. The origin of hydrocarbons in Nakhla is unclear, but the trapped-gases hypothesis seems to be possible.

Flynn G. J.* Keller L. P. Jacobsen C. Wirick S.
*Organic Carbon in Mars Meteorites: A Comparison of ALH84001 and Nakhla* **[#1087]**
We compare C-XANES and FTIR spectra of organic matter associated with carbonate globule and rim material from ALH84001 and material consisting of phyllosilicate, carbonate and sulfate from Nakhla.

Steele A.* Westall F. Goddard D. T. Stapleton D. Toporski J. K. W. McKay D. S.
*Imaging of the Biological Contamination of Meteorites: A Practical Assessment* **[#1321]**
This abstract is an important summary of all the contamination issues we have discovered imaging meteorites. This includes references to contamination of Murchison, ALH84001, 4 Antarctic chondrites, and Nakhla.

McKay D. S.* Wentworth S. W. Thomas-Keprta K. Westall F. Gibson E. K. Jr.
*Possible Bacteria in Nakhla* **[#1816]**
0.2–1 micrometer-size spheres embedded in secondary deposits of martian origin in martian meteorite Nakhla show strong bacterial characteristics.

Kirschvink J. L.* Vali H.
*Criteria for the Identification of Bacterial Magnetofossils on Earth or Mars* **[#1681]**
Magnetite crystals produced by the magnetotactic bacteria and left as magnetofossils are distinctive enough to be used as biomarkers, either on Earth or Mars.

Thomas-Keprta K. L.* Wentworth S. J. McKay D. S. Bazylinski D. Bell M. S. Romanek C. S. Golden D. C. Gibson E. K. Jr.
*On the Origins of Magnetite in Martian Meteorite ALH84001* **[#1856]**
We suggest that the ALH84001 meteorite contains evidence of inorganic, low temperature, aqueous processes and biogenic activity based on the morphology and chemistry of the magnetite and the association with carbonate, which most likely formed at low temperature.

Vali H.* Sears S. K. Ciftcioglu N. Kajander E. O.
*Nanofossils and the Size Limits of Life* **[#1890]**
The existence of organisms at the nano-scale range is controversial, but nano-scale features observed on mineral surfaces such as biominerals (nanofossils) are used as evidence of biological activity. Thus, size limitations of living organisms can be neglected.

**Thursday, March 18, 1999**
**ACHONDRITES AND ANOMALOUS METEORITES**
**1:30 p.m. Room B**

**Chairs: C. Floss**
**M. K. Weisberg**

Longhi J.*
*Angrite Petrogenesis Revisited* **[#1953]**
New low-pressure experiments have located a psuedo-invariant point relevant to angrite petrogenesis. Refractory element ratios demonstrate that the formation of the angrite parent body cannot be attributed to "chondritic fractionations".

Buchanan P. C.* Lindstrom D. J. Reimold W. U. Koeberl C.
*Mineralogy and Composition of an Unmetamorphosed Basaltic Clast from the Polymict Eucrite Macibini* **[#1647]**
The present study compares texture, mineralogy, and composition of eucrite clast A/B from the meteorite Macibini with the "pristine" eucrite clast Y75011,84.

Liermann H. P.* Ganguly J.
*Orthopyroxene-Spinel Cosmo-Geothermometer: Experimental Calibration and Applications to Meteorites* **[#1765]**
We determined the $Fe^{2+}$-Mg fractionation between spinel and orthopyroxene as a function of temperature and composition in the Fe-Mg-Cr system, formulated a thermometric expression using these data, and applied it to a number of meteorite samples.

Fogel R. A.*
*Two-Pyroxene Thermometry of Aubrites* **[#1871]**
Diopside-enstatite thermometry is applied to the Norton County, Khor Temiki, LEW87294 and LEW87020 aubrites. Average T's for individual aubrites span 700°–1050°C. Enstatite and diopside crystals show variations to T's > 1200°C. Zonation patterns were also detected.

McCoy T. J.* Rosenshein E. B. Dickinson T. L.
*A Unique Oxide-Bearing Clast in the Aubrite Allan Hills 84008: Evidence for Oxidation During Magmatic Processes* **[#1347]**
A forsterite-sulfide clast in the ALH 84008 aubrite contains grains of perovskite ($CaTiO_3$) and geikielite ($MgTiO_3$) and a diopside-troilite-perovskite intergrowth. These oxides likely formed by oxidation of reduced phases typically found in aubrites.

Floss C.*
*Trace Element Constraints on the Origin of QUE 93148* **[#1149]**
Trace elements (e.g., Ti, Zr) in orthopyroxene from QUE93148 are systematically depleted relative to acapulcoites/lodranites. Melting calculations indicate that QUE93148 did not originate as a partial melting residue on their parent body.

Ruzicka A.* Boesenberg J. S. Snyder G. A. Prinz M. Taylor L. A.
*Rare-Earth-Element Abundances of Clasts and Matrix in the Lamont Mesosiderite: Complex Spatial Variations* **[#1516]**
We obtained petrologic constraints on the evolution of the Lamont mesosiderite by studying rare-earth-element abundances in various pyroxene clasts and matrix grains.

Goodrich C. A.* Fioretti A. M. Molin G. Zipfel J. Tribaudino M.
*Primary Trapped Melt Inclusions in Olivine in a Ureilite — II. Reconstruction of Liquid Composition and Implications* **[#1027]**
We reconstruct the original composition of trapped melt inclusions in olivine in a ureilite. Assuming that this represents the magma with which the host was in equilibrium at the time of entrapment, it permits us to evaluate whether this ureilite is a cumulate or residue.

Molin G. M.* Pasqual D. Tribaudino M. Goodrich C. A.
*Thermometric and Microtextural Study of $P2_1/c$ Pigeonite from Ureilite PCA82506 (En 76) and an Fe-rich Terrestrial Pigeonite (En 47)* **[#1140]**
Calibration of the $Fe^{2+}$-Mg intracrystalline geothermometer for pigeonite from ureilite PCA82506 and Parana rhyodacite shows no compositional dependence. PCA82506 pigeonite shows a closure T of 756 C indicating a very high cooling rate.

Tribaudino M.* Fioretti A. M. Goodrich C. A. Molin G. M.
*A TEM and Single-Crystal X-Ray Investigation of Silicate Phases in the Ureilite Hughes 009* **[#1170]**
TEM microtextures in the silicate phases of ureilite Hughes 009 indicate a low shock level and fast cooling. The latter, in the range of volcanic orthopyroxenes, is confirmed by Fe-mg intracrystalline ordering in orthopyroxene.

Chikami J.* McKay G. A. Le L.
*Partitioning of Zn Between Spinel and Liquid: An Experimental Study* **[#1310]**
We have conducted experiments to study partitioning of Zn between spinel and liquid. Zn spinel/liquid partition coefficient is around 3–5, while the pyroxene/liquid partition coefficient is much less than the spinel/liquid partition coefficient.

Weisberg M. K.* Prinz M. Clayton R. N. Mayeda T. K. Sugiura N. Zashu S. Ebihara M.
*QUE 94411 and the Origin of Bencubbinites* **[#1416]**
Bencubbinites are a new metal-rich chondrite group in the CR clan. They greatly increase the range of metal-silicate fractionation in chondrites. QUE94411 is a new member. GRO95551 is not directly related, based on mineral and isotopic compositions.

Sugiura N.* Zashu S. Weisberg M. K. Prinz M.
*H, C and N Isotopic Compositions of Bencubbinites* **[#1329]**
H, C, and N isotopic compositions of bencubbinites were measured by stepped combustion and by SIMS. It was found that the carriers of N isotopic anomalies are not pristine presolar grains.

**Thursday, March 18, 1999**
**IO**
**1:30 p.m. Room C**

**Chairs: A. G. Davies**
**J. A. Stansberry**

Smythe W. D.* Lopes-Gautier R. Kamp L. Davies A. G. Carlson R. W. Soderblom L. A. Galileo NIMS Team
*Io Thermal Output Distribution Maps from Galileo's Near-Infrared Mapping Spectrometer (NIMS)* **[#2044]**
Thermal output maps of Io are presented using data from Galileo NIMS.

Turtle E. P.* McEwen A. S. Keszthelyi L. Schenk P. M.
*Formation and Evolution of Ionian Mountains* **[#1971]**
We are using finite-element models to investigate formation mechanisms for Ionian mountains, focusing on motions of crustal blocks that may be subsiding, tilting, or overriding other blocks due to local differences in density or resurfacing rates.

Stansberry J. A.*
*Thermal Emission from Io's Lava Flows: Spectral Dependence on Emission Angle* **[#2009]**
The thermal emission from cracks in lava flows dominates the spectrum in the near-IR. Using a new model I show that the near-IR spectrum is a strong function of emission angle.

Goguen J. D.* Veeder G. J. Blaney D. L. Matson D. L. Johnson T. V.
*Io's Mid-IR Volcanic Thermal Emission During 1998* **[#1934]**
Mid-IR radiometric rotational lightcurves of Io from IRTF are presented for four epochs between June and November 1998. These data fill in an important gap in the GEM spectral coverage and they are discussed in the context of other recent data sets.

Howell R. R.*
*The Long Duration 1998 Brightening at Loki* **[#2010]**
Infrared observations of Io show that a volcanic brightening in the Loki region, which began in late May 1998, is continuing as of December, although perhaps at a reduced level. The infrared data are analyzed in terms of simple volcanic flow models.

Blaney D. L.* Johnson T. V. Matson D. L. Davies A. G. Veeder G. J.
*The Distribution of Volcanism on Io in the Galileo G2 Data* **[#1913]**
We have examined the G2 NIMS data to search for thermal emission from non-hotspot regions of the planet. Our analysis has shown that at least 27% of the spectra collected have clear evidence of thermal emission.

Soderblom L. A.* Becker K. J. Becker T. L. Carlson R. W. Davies A. G. Kargel J. S. Kirk R. L. Lopes-Gautier R. C. Smythe W. D. Torson J. M.
*Deconvolution of Galileo NIMS Day-Side Spectra of Io into Thermal, $SO_2$, and Non-$SO_2$ Components* **[#1901]**
Deconvolution of Galileo NIMS spectra of Io are used to explore thermal emission characteristics and compositional components of Io in the 4 to 5 micron region.

McEwen A.* Geissler P. Lopes-Gautier R. Keszthelyi L. Simonelli D. Belton M. Breneman H. Magee K. Galileo SSI Team
*Io Results from Galileo SSI and Plans for the Close Flybys* **[#1843]**
New results from Galileo lead to important questions about the volcanism, interior structure, plumes, and atmosphere of Io. The close flybys in late 1999 may provide some answers.

Lopes-Gautier R.* Smythe W. D. McEwen A. S. Geissler P. E. Davies A. G. Kamp L. Soderblom L. A. Carlson R. W. Keszthelyi L. Spencer J. R. Galileo NIMS Team

*The Temporal Activity of Io's Hot Spots* **[#1741]**

Results from NIMS and SSI during Galileo and GEM are used to investigate the temporal variability of Io's hot spots in terms of variation in power output, presence of plumes and red deposits, and magma temperature.

Davies A. G.* Keszthelyi L. P. Lopes-Gautier R. M. C. McEwen A. S. Smythe W. D. Soderblom L. Carlson R. W.

*Thermal Signature, Eruption Style and Eruption Evolution at Pele and Pillan Patera, on Io* **[#1462]**

Pele and Pillan Patera are volcanoes on Io. Analysis of Galileo NIMS and SSI data has allowed the modeling of the eruptions at these two sites. Pele appears to be a disrupted lava lake. Pillan Patera is the site of a massive (though brief) eruption.

Keszthelyi L.* McEwen A. S. Taylor G. J.

*Does Io Have a Mushy Magma Ocean?* **[#1224]**

Recent observations suggest that Io has widespread ultramafic volcanism, which is not expected in a highly differentiated, solid, Io. A partly crystallized (i.e., mushy) magma ocean provides the simplest alternative explanation.

Zolotov M. Yu.* Fegley B.

*Oxidation State of Volcanic Gases on Io* **[#1132]**

We infer a relative oxidized, terrestrial-like redox state of volcanic gases on Io based on available data on the composition of a volcanic plume, the atmosphere, plasma torus, and surface, as well as observed temperatures of hot spots.

Williams D. A.* Wilson A. H. Greeley R.

*Komatiites from the Commondale Greenstone Belt, South Africa: A Potential Analog to Ionian Ultramafics?* **[#1353]**

Recent studies of Io suggest some vents erupt high temperature lavas (>1430°C) with a spectral signature indicating Mg-rich opx. We found a komatiite from Africa containing opx phenocrysts, derived from a high MgO liquid, that may be a useful analog for these lavas.

**Thursday, March 18, 1999**
**PLANETARY SURFACE PROCESSES**
**1:30 p.m. Room D**

**Chairs: T. K. P. Gregg**
**A. Snyder Hale**

Bulmer M. H.* Campbell B. A.
*Topographic Data of a Silicic Lava Flow — A Planetary Analog* **[#1446]**
We have obtained high-precision topographic profiles over an andesitic lava flow on Sabancaya volcano (15.47°S, 71.51°W) in southern Peru. These data may be useful in the interpretation of emplacement mechanism for thick lava flows on Mars [1], Venus [2], and the Moon [3].

Gregg T. K. P.* Smith D. K.
*How to Make a Dome: Puna Ridge Seamounts as Analogs for Venusian Domes?* **[#1784]**
We present results of a detailed study of a large seamount on the axis of the Puna Ridge. Results from a detailed survey, using side-scan sonar, video and still imaging, allow us to constrain the genesis of this seamount.

Lescinsky D. T.* Fink J. H.
*Long Lavas with Narrow Flow Widths: A Case of External Flow Confinement?* **[#2051]**
Some long lava flows have narrow widths not adequately explained by lava transport models. We use experimental simulations to test whether subtle topographic features will confine lava, both directing and facilitating flow in a single direction.

Byrnes J. M.* Crown D. A.
*Relationships Between Pahoehoe Surface Texture, Topography, and Lava Tubes at Mauna Ulu, Kilauea Volcano, Hawaii* **[#1298]**
GIS analysis of the Mauna Ulu compound flow field demonstrates that the distribution of pahoehoe surface textures is related to pre-flow topography and not directly dependent on the major lava tube network.

Crown D. A.* Baloga S. M. Byrnes J. M.
*Emplacement of Pahoehoe Flow Fields: Scale-Dependent Characteristics of Mauna Ulu Flows* **[#1379]**
Statistical analyses of lengths and orientations of toes, channels, and lava tubes and observed transitions between pahoehoe features suggest that scale-dependent differences in distributary networks occur at Mauna Ulu with variability increasing at smaller scales.

Fagents S. A. Williams D. A. Greeley R.
*Factors Influencing Planetary Lava Flow Dynamics and Heat Transfer: Implications for Substrate Melting* **[#1823]**
Numerical simulations of lava-substrate heat transfer suggest that substrate melting and the formation of erosional channels is promoted by topographic irregularities, komatiite lava compositions, and lunar and venusian lava and substrate properties.

Snyder Hale A.* Hapke B.
*A Time Dependent Model of Radiative and Conductive Thermal Energy Transport in Planetary Regoliths* **[#1252]**
We present preliminary results of the first solution of the fully time dependent model of radiative and conductive thermal energy transport in planetary regoliths.

Nelson R. M.* Hapke B. W. Smythe W. D.
*The Opposition Effect in Simulated Planetary Regoliths: Circular and Linear Polarization Ratio Change with Phase Angle* **[#1314]**
We report the results of phase curve measurements of particulate materials which simulate planetary regoliths. We note that the size and shape of the linear and circular polarization ratio variation with phase are dependent on particle size.

Cabrol N. A.*

*Amazonian Fluvial Activity on Mars: Combination of Volcano-Tectonic Environment and Possible Sub-Glacial Drainage in the Generation of Flow in Durius Valles* **[#1022]**

The Durius Valles system is one of the most dense and varied hydrologic systems on Mars, showing an abundant and recent diversity of hydrologic styles and lacustrine types. We envision its origin and duration.

Sieger M. T. Simpson W. C. Orlando T. M.*

*Production of $O_2$ on Icy Satellites by Electronic Excitation of Low-Temperature Water Ice* **[#1394]**

$O_2$ has been reported in measurements of the Jovian moons Ganymede and Europa. We report laboratory measurements of the threshold energy, cross section, and temperature dependence of $O_2$ production by electronic excitation of ice in vacuum.

King T. V. V.* Rye R. O. Ridley W. I. Clark R. N.

*Exploring the Use of Infrared Spectroscopy to Examine Stable Isotopic Ratios: Preliminary Systematics of D/H Ratios in Kaolinite* **[#2013]**

Laboratory infrared spectroscopy measurements have been used to examine the D/H ratios in kaolinites.

**Thursday, March 18, 1999**
**POSTER SESSION II**
**7:00 p.m. UHCL**

## Education: Fun in the Classroom

Allen J. S. Grymes R. A. Lindstrom M. M.
*Overview of NASA Astrobiology Institute Education and Public Outreach* **[#2030]**
Astrobiology is the study of the origin, distribution, and future of life in the universe. The NASA Astrobiology Institute is carrying out innovative Education and Public Outreach initiatives to keep the public informed and involved with new research.

Heather D. J. Dunkin S. K. Martin P. Balme M.
*Mars in the Classroom* **[#1243]**
Mars in the Classroom is a project designed to provide a stimulating program of extra-curricular science activities to year 10 and 11 school children in the UK.

Cabrol N. A.
*The Martian Impact Crater Lakes Database: A Web Resource for the Planetary Science Community and for Educational and Public Outreach* **[#1024]**
The Catalog of Impact Crater Lakes on Mars features 179 crater lakes and is the result of a global survey using the Viking data. The Catalog provides information such as location, morphological and morphometrical data, sedimentary record.

Cabrol N. A. Briggs G. A. Gulick V. C.
*Educational Outreach Products at ARC's Center for Mars Exploration* **[#1070]**
CMEX is developing Concept Maps to provide a new information navigation tool in order to make Web or CD-based information about the exploration of Mars more meaningful and more easily navigable.

Klug S. L. Christensen P. R.
*Using Space Education to Bridge Worlds and Generations: The ASU Mars K–12 Education Outreach Program* **[#1708]**
The ASU Mars K–12 Education Outreach Program encompasses a wide variety of educational opportunities aimed at promoting science literacy by using the real-time experience of Mars exploration to engage teachers, students, and parents.

Friedman L. D. Hyder L. A. Klug S. L. Oslick J. S. Powell G. E. Thomas E. L. Vaughn J. L.
*Red Rover Goes to Mars: An Exploration Education Experiment for the Mars Surveyor* **[#1831]**
Red Rover Goes to Mars will be an exploration education experiment on the Mars Surveyor 2001 lander mission, providing student participation operating the lander robotic arm and Marie Curie rover, and in collecting data using the science instruments.

Bérczi Sz. Drommer B. Cech V. Hegyi S. Herbert J. Tóth Sz. Diósy T. Roskó F. Borbola T.
*New Programs with the Hunveyor Experimental Planetary Lander in the Universities and High Schools in Hungary* **[#1332]**
We continuously develop an experimental planetary lander (Hunveyor). The last year results: a) stereo and 3D camera, b) Website for students to observe and manipulate Solar System rock types around the lander, c) construction and planetary robot building in high school.

Drommer B.   Blénessy G.   Hanczár G.   Gránicz K.   Diósy T.   Tóth Sz.   Bodó E.

*The 3D System and Operations with Hunveyor (and Its Rover): Web Site for Students to Use Lander Instruments on a Simulated Planetary Surface* **[#1606]**

We made viewing and operating (3D camera, rover and arm manipulation) possibilities to the Hunveyor experimental lander on a simulated planetary surface configuration and opened a web site for education in planetary robotics to be used by students and teachers.

Bérczi Sz.   Józsa S.   Kabai S.   Kubovics I.   Puskás Z.   Szakmány Gy.

*NASA Lunar Sample Set in Forming Complex Concepts in Petrography and Planetary Petrology* **[#1038]**

Three branches of complex concepts were developed on courses using the NASA lunar thin section set: a) material maps, b) cell-mosaic automata description of petrographical textural transformations, and c) extended igneous petrography of the solar system.

Bérczi Sz.   Kabai S.   Hegyi S.   Cech V.   Drommer B.   Földi T.   Fröhlich A.   Gévay G.

*TUTOR on the Moon: A Discovery Type Multiple Lunar Probe (Improved Surveyors) Constructing and Research Program for Universities* **[#1037]**

Twenty Universities Teach and Operate Research (TUTOR) on the Moon project imagines 20 Surveyor type landing units, each equipped with special instrumentation (i.e.rover) and all Surveyors travel to the Moon on an icosahedral mother-ship, which later serves as relay.

Wood C.   Heldmann J.   Gerszewski M.   Mattern A.   Schmidt C.   Rydell J.   Langwost P.

*ACIT: An Internet-Controlled Telescope for Asteroid and Comet Research* **[#1839]**

To observe the sky during North Dakota's long cold winters we built an observatory controllable by Internet browsers. We solved many logistics problems using software to remotely operate the observatory. Research will focus on comet and NEA studies.

Leake M. A.

*Progress Report on Spectroscopic Search for Aqueous Alteration on Minor Planet Surfaces Involving the NASA/JOVE and NSF/REU Programs* **[#2034]**

Progress is reported on spectroscopic survey of primitive C-class asteroids for the presence of water of hydration in clay-type minerals. Student research is encouraged by NASA/JOVE and NSF/REU grants.

Lindstrom M. M.   Allen J. S. B.

*Rocks From Space: Astromaterials Education and Public Outreach at JSC* **[#2045]**

The Rocks from Space E/PO program at JSC focuses on the process of science inquiry and knowledge from Astromaterials research. Development of products is based on partnerships between scientists and educators.

Schneider D. M.   Sears D. W. G.   Benoit P. H.   Akridge D. G.   Akridge J. M. C.

*Space Science Educational/Public Outreach at the University of Arkansas* **[#1439]**

We have developed a multi-faceted outreach program to heighten public awareness of space science research at the University of Arkansas. Outreach activities include space science laboratories, public speakers, museum displays, and an internet home page.

Funk A. E.   Wallin L. B.   Ricke M. B.   Annexstad J. O.   Melchior R. C.

*Cosmic Spherules in Glacio-Lacustrine Sediments: An Undergraduate Research Endeavor* **[#1371]**

We search for cosmic spherules in glaciogenic sediments from fluvial and lacustrine environments. Undergraduates are used for sample gathering and initial analysis of samples.

Newsom H. E.   Hagerty J. J.   Spilde M. N.   Adcock C. T.   Sorge C.

*Introducing Planetary Science and Technology to Students from Grades 6–12* **[#1220]**

Our outreach program involves changing the student's attitudes about careers in science, and uses inquiry-based activities to introduce the students to planetary science, and the instruments (SEM) used in planetary materials research.

Coles K. S.

*Planetary Science Workshops for Indiana K–12 Teachers* **[#1447]**

Updates for teachers are free, Saturday workshops. Updates emphasize a mix of background, activities, and resources for teachers. Examples from a recent Update about Mars illustrate this successful, low-budget program.

Kenealy R. Baker R. W. Betts B. H.

*Successful Off-Site Planetary Science Field Trips* **[#1413]**

Over 16,000 students in the 3rd to 8th grades have come to the San Juan Institute (SJI) over the last five years to attend SJI's field trip programs.

Croft S. K. McGee S. M. Hornyak J. Coffield J. Stoffel D.

*Astronomy Village: A Multimedia Educational Interface for Communicating New Results in Space Science* **[#1780]**

Astronomy Village is a multimedia educational interface for presenting new scientific results in a problem-solving format. Two content packages exist, one highlighting research problems and data in Earth and space science, and one in stellar and galactic astronomy.

## Outer Planet Satellites

Piatek J. L. Zimmerman S. B. Byrnes J. M. Snyder Hale A. Crown D. A.

*Color and Morphology of Lava Flows on Io* **[#1468]**

Analyses of Voyager images of lava flows on Io show morphologic variations and changes in blue/orange reflectivity ratio that are inconsistent with the simple, progressive cooling of sulfur flows.

Phillips C. B. McEwen A. S. Galileo SSI Team

*Active Volcanism and Change Detection on Io from Galileo SSI* **[#1448]**

Changes occuring on Io are illustrated using an iterative coregistration technique on Galileo images. Ratio images show new plume deposits and lava flows corresponding to telescopic observations of active hot spots.

Leone G. Wilson L.

*The Geothermal Gradient of Io* **[#1358]**

We reassess the balance between conductive and advective heat transport on Io and find that the temperature gradient should lie between 30 and 60 K/km depending on the lithosphere thickness.

Cataldo V. Wilson L.

*Volcanic Eruption Plumes on Io: $SO_2$ Condensation on Tiny Glassy Volcanic Particles* **[#1246]**

We model the dispersal of mixtures of condensing volatiles and small pyroclasts from volcanic eruption plumes on Io fed from explosive vents which incorporate near-surface volatiles in erupting magmas.

Glaze L. S. Baloga S. M.

*Application of a Stochastic-Ballistic Emplacement Model for Io Plume Deposits* **[#1159]**

A stochastic-ballistic model is used to study the effects of variable ejection velocities on volcanic deposits on Io. At Prometheus, we predict a velocity distribution with an RSD% of 3% and a maximum plume height equivalent to 15–18 pixels.

Collins G. C. Pappalardo R. T. Head J. W. III

*Surface Stresses Resulting from Internal Differentiation: Application to Ganymede Tectonics* **[#1695]**

The formation of grooved terrain on Ganymede may have been driven by interior differentiation. We examine the implications of differentiation for surface stresses, and whether these predictions are consistent with observations of grooved terrain.

Pappalardo R. T. Collins G. C.

*Extensionally Strained Craters on Ganymede* **[#1773]**

We analyze four tectonized craters in Galileo Ganymede images and infer the craters were extensionally strained by 4 to 42% and horizontally sheared. Extension of tens of percent may be common on Ganymede and may efficiently resurface some dark terrain.

Denk T. Khurana K. K. Pappalardo R. T. Neukum G. Head J. W. III Rosanova T. V. Galileo SSI Team

*The Global Colors of Ganymede as Seen by Galileo SSI* **[#1822]**

The abstract gives a summary of global color properties of Ganymede which are partly correlated to its magnetic field. Areas on the surface which are exposed to charged particles from the Jovian field are often redder than shielded terrain.

Figueredo P. H. Greeley R. Galileo SSI Team

*Fracture Patterns on Ganymede and the Initiation of Tectonic Resurfacing* **[#1832]**

We have studied the orientation and linkage of fractures in areas of incipient deformation on Ganymede. With this information we determined stress fields in Nicholson Regio and reconstructed the structural evolution during the initial stages of tectonic deformation.

Kay J. E. Head J. W. III

*Geologic Mapping of the Ganymede G8 Calderas Region: Evidence for Cryovolcanism* **[#1103]**

Galileo imaging of Ganymede has revealed an apparent dearth of morphologic evidence for bright terrain cryovolcanism. However, morpho-stratigraphic mapping in one area, the G8 Calderas region in Sippar Sulcus, shows evidence for embayment and source vents.

Becker T. Rosanova T. Cook D. Davies M. Colvin T. Acton C. Bachman N. Kirk R. Gaddis L.

*Progress in Improvement of Geodetic Control and Production of Final Image Mosaics for Callisto and Ganymede* **[#1692]**

This report summarizes the recent efforts of USGS and RAND toward improved geodetic solutions and final digital mosaics for the Galilean moons Callisto and Ganymede.

Wagner R. Wolf U. Neukum G. Galileo SSI Team

*Ages of Individual Craters on the Galilean Satellites Ganymede and Callisto* **[#1818]**

Craters, palimpsests and multi-ring basins are important stratigraphic markers in establishing sequences of geologic events by stratigraphic relationships. In this paper, we present ages for craters on Ganymede and Callisto, based on two impact cratering chronologies.

Chuang F. C. Greeley R. Moore J. M. Galileo SSI Team

*Callisto: Large-scale Mass Movements Observed from the Galileo Nominal Mission* **[#1292]**

Large-Scale mass movement which infills craters with rim and/or wall material appears to be an important mechanism in degrading craters on the surface of Callisto. A re-analysis of nominal mission images have revealed several new landslides.

Denk T. Neukum G. Jaumann R. Roatsch T. Noll K. S. Porco C. C. Squyres S. W.

*Iapetus — Summary of Recent Work, Prospects for Cassini* **[#1841]**

Faint surface features within the dark Cassini Regio have been detected in Voyager data. On 1 Nov 1998, 13 disk-resolved images of Iapetus's dark hemisphere were taken by the HST's WFPC2 camera at wavelengths from 0.33 to 1.02 μm.

Jarvis K. S. Vilas F. Larson S. M. Gaffey M. J.

*Hyperion, Iapetus, and Phoebe: Linear Mixing Model Suggests Link* **[#1400]**

A dark material near-IR spectrum for Hyperion, a Saturnian satellite, has been calculated with a linear mixing model. Its spectrum is similar to the dark material spectrum of Iapetus, strongly suggesting their dark material is from the same source.

Lorenz R. D.

*Radar Absorptivity of Planetary Materials Measured Using a Microwave Oven* **[#1197]**

I report measurements of the 2.45 GHz absorptivity of rocks and ices, important to understand radar returns from planetary surfaces, using a microwave oven. Ammonia-rich ices, likely in the Saturnian system, are 10-1000 times more absorbing than pure water ice at 200K.

## Small Icy Bodies

Komitov B. Bonev B.
*The Cometary CN-Parent Molecules Scale Lengths in Relation with the Heliocentric Distance and Solar Activity: A Two-Factor Regression Analysis* **[#1429]**
A statistical analysis has been done of the observed Haser scale lengths of CN parent molecules in cometary atmospheres with respect to heliocentric distance and solar activity. The solar activity level proves to be an important complementary factor.

Colwell W. B. Festou M. C. Stern S. A. Parker J. Wm. Tamblyn P. M. Slater D. C. Weissman P. R. Paxton L.
*SWUIS Measurements of the Post-Perihelion $H_2O$ and Dust Production in Comet Hale-Bopp (C/1995 O1)* **[#1153]**
The Southwest Ultraviolet Imaging System (SWUIS) obtained $4.3 \times 10^5$ images of C/1995O1 (Hale-Bopp). At 2.33 AU from the Sun, Hale-Bopp's $H_2O$ production rate was $2.6 \pm 0.4 \times 10^{29}$s and Afrho was $2.0 \pm 0.8 \times 10^5$.

Garry J. R. C. Wright I. P. Pillinger C. T.
*Isotopic Fractionation of Cometary Volatiles by Drilling Operations* **[#1602]**
The degree to which drilling may influence the isotopic composition of vapour evolved from water ice in cometary surfaces is examined.

Shuvalov V. V. Artemieva N. A. Kosarev I. B. Nemtchinov I. V. Trubetskaya I. A.
*Small Comets Impacting the Moon* **[#1045]**
Numerical simulations of small comet (20 t, 30 km/s) impacts against lunar surface using cometary EOS and detailed opacities have shown high luminous efficiency of these events. Light flashes associated with postimpact gases can be detected by Earth-based equipment.

Hahn J. M. Brown L.
*Interpreting the Kuiper Belt Luminosity Function* **[#1888]**
The Kuiper Belt luminosity function is analyzed in order to assess whether the KBO radial surface density is primordial, meaning that it decreases with heliocentric distance, or eroded such that it increases with distance.

Ekholm A. G. Dahlgren M. Lagerkvist C.-I. Lagerros J. Lundström M. Magnusson P. Warell J.
*VRI Photometry of Kuiper Belt Objects and Centaurs* **[#1714]**
We present VRI photometry of seven Kuiper-belt objects and three Centaurs. We find no color-color or color-absolute magnitude correlations, but our data do show redder KBO colors with increasing semimajor axis, at a confidence level of 99%.

Doressoundiram A. Weissman P.
*Physical Properties of Some Spacecraft Mission Targets* **[#1129]**
We present results from photometric observations of asteroids and comets which are targets of upcoming spacecraft missions. We will give estimates of the size, axial ratio, and rotation period for 9P/Tempel 1, 140 Siwa and 4979 Otawara.

## Achondrites

Heim N. A. Wadhwa M. Davis A. M.
*Rare Earth Element Abundances in Vapor Deposited Minerals in Ibitira Vesicles* **[#1908]**
We report REE abundances in vapor deposited minerals in Ibitira vesicles. The aim of this study was to obtain constraints on the formation process of these minerals and the composition of the vapor phase that deposited them.

Rosenshein E. B. McCoy T. J. Dickinson T. L.
*Sulfide-bearing Clasts in Aubrites: Clues to Partial Melting* **[#1344]**
We have studied a number of sulfide±metal±feldspar clasts in aubrites. These clasts probably formed by incomplete migration of low-temperature partial melts, silicate-sulfide liquid immiscibility and silicate fractional crystallization.

Ruzicka A. Boesenberg J. S. Snyder G. A. Prinz M. Taylor L. A.

*Petrogenesis of the Lamont Mesosiderite: Evidence from Petrography and Pyroxene Clast Zoning Systematics* **[#1513]**

We evaluate the petrogenesis of the Lamont mesosiderite utilizing petrography and microchemical (EMP) data. The petrogenesis was complex, and included different types of interactions between pyroxene clasts and the surrounding melt-matrix.

Mittlefehldt D. W.

*Geochemistry and Origin of Pallasite Olivines* **[#1828]**

Minor and trace element compositions of pallasite olivines suggest that main-group pallasites may be derived from more than one parent body, or that they are not simple cumulus grains.

Bischoff A. Goodrich C. A. Grund T.

*Shock-induced Origin of Diamonds in Ureilites* **[#1100]**

We identify diamonds in ureilites by cathodoluminescence and evaluate their occurrence as correlated with shock level recorded by olivine (Stoeffler et al., 1991). Results support the model that ureilite diamonds formed by shock rather than chemical vapor deposition.

Goodrich C. A. Fioretti A. M. Molin G. Tribaudino M.

*Primary Trapped Melt Inclusions in Olivine in a Ureilite — I. Description* **[#1026]**

Primary trapped melt inclusions in olivine have been observed for the first time in a ureilite. A detailed petrographic description is given in this abstract. Modelling and implications are discussed in a companion abstract.

Smith C. L. Wright I. P. Franchi I. A. Grady M. M. Pillinger C. T.

*Attempts to Constrain Ureilite Petrogenesis Through the Study of the Role of Carbon in the Formation of Native Iron as Observed at Disko Island* **[#1715]**

Carbon isotope studies on sedimentary and graphite/metal-bearing basaltic rocks from Disko Island, Greenland have been used to infer the effect of reduction processes during ureilite formation and the origin of the graphite in the UPB.

Fioretti A. M. Goodrich C. A. Molin G. Tribaudino M.

*Associated Silicate-Metal-Sulfide Inclusions in Graphite of Ureilite FRO 95028* **[#1133]**

A new occurrence of a peculiar association of a silicate-rich phase, sulfide and metal, found to be widespread in the "book" graphite of low-shock ureilite FRO 95028, is described and chemically characterized (EMPA).

## Iron Meteorites

Skála R. Frýda J.

*Nickel-Dominant Schreibersite from Vicenice Iron* **[#1334]**

A nickel-dominant schreibersite was found in Vicenice iron meteorite. Its composition and comparison to other up to now known Ni-dominant schreibersites are provided.

Skála R. Drábek M.

*Fe/Ni-distribution over Crystallographically Non-Equivalent Sites in the Crystal Structure of Two Synthetic Schreibersites* **[#1553]**

Site occupancies over non-equivalent sites within the crystal structure of synthetic schreibersite-like phosphides were modeled and structures for models with best fit refined from powder X-ray diffraction data.

## Meteorite Mélange

Hamlin S. Garrison D. Bogard D.

*Chlorine Abundances in Meteorites* **[#1106]**

Chlorine concentrations determined in ~100 different meteorites of several types using the $^{37}$Cl (n,gamma) $^{38}$Ar technique have substantially increased the Cl data base and permit some resolution of terrestrial Cl contamination.

Wilkison S. L. Robinson M. S.
*Bulk Density Measurements of Meteorites* **[#1929]**
We present density measurements of meteorites detailing the precision and errors associated with the modified Archimedian method of Consolmagno and Britt. We find that the method is accurate to better than 1%.

Styrsa V. J. Weinbruch S. Müller W. F.
*A Transmission Electron Microscopy Study of Exsolution and Coarsening in Iron-free Clinopyroxene* **[#1111]**
Exsolved and coarsened lamellae in Fe-free clinopyroxene are studied experimentally in the range of 1100° to 1300°C. These data provide a reliable basis for the estimation of chondrule cooling rates derived from the microstructure of chondrule minerals.

Polyak D. E. Dyar M. D. Delaney J. S. Tegnar C.
*Mineralogical $Fe^{3+}/\Sigma Fe$ Measurements as Proxies of Volatile Budgets: V. Crystal Chemistry of Fe in Plagioclase from Four Heavenly Bodies* **[#1911]**
Mechanisms for substitution of ferric into plagioclase can be assessed because microanalytical data are now available. Substitution mechanisms for Fe in plagioclase are dominated by correlation with An content.

Zink A. J. C. Krbetschek M. R. Trautmann T. Singhvi A. K. Stolz W.
*Luminescence Spectrals Measurements of Meteorites* **[#1612]**
New spectral measurement of thermoluminescence and radioluminescence for 13 ordinary chondrite and one eucrite. In 11 cases, feldspar is the most intense phosphore.

Zink A. J. C. Krbetschek M. R. Trautmann T. Singhvi A. K. Stolz W.
*Thermoluminescence Measurements in Various Wavelengths: Potential for Meteorites Dating* **[#1596]**
The decay of the thermoluminescence in Esu (H6) ordinary chondrite and in Piplia Kalan eucrite depends on the emission spectral range.

Lee P. Cassidy W. A. Apostolopoulos D. Bassi D. Bravo L. Cifuentes H. Deans M. Foessel A. Moorehead S. Parris M. Puebla C. Pedersen L. Sibenac M. Valdés F. Vandapel N. Whittaker W. L.
*Search for Meteorites at Martin Hills and Pirrit Hills, Antarctica* **[#2046]**
We discuss the search for meteorites conducted at Martin Hills and Pirrit Hills, Antarctica, by the Robotic Antarctic Meteorite Search program.

Benoit P. H. Sears D. W. G.
*Pairing of Meteorite Finds: A Probability Approach* **[#1052]**
A quantitative probabilistic approach to pairing has been applied to 2200 literature pairings. For rare meteorites or those with unusual features, pairing certainties can be high but in most cases lack the relevant data.

Miller M. F. Franchi I. A. Pillinger C. T.
*High Precision Measurements of the Oxygen Isotope Mass-dependent Fractionation Line for the Earth-Moon System* **[#1729]**
High precision measurements of the oxygen isotope mass-dependent fractionation line for the Earth-Moon system, using laser fluorination of terrestrial silicate samples of diverse origin, indicate a well-constrained slope of $0.52461 \pm 0.00095$.

Tachibana S. Tsuchiyama A.
*Was Mg/Si Fractionation Caused by Incongruent Evaporation of Enstatite?* **[#1532]**
The evaporation behavior of enstatite in a closed system, which consists of enstatite and nebular gas, was evaluated numerically by using experimental results and a quasi-equilibrium evaporation model to discuss the Mg/Si fractionation in the nebula.

## Cosmogenic Nuclides

Sisterson J. M. Vincent J. Yen S. Zyuzin A. Y. Jull A. J. T. Donahue D. J. Cloudt S. Klandrud S. Jones D. T. L. Symons J. E. Schroeder I. Binns P. J. Brooks F. D. Buffler A. Allie M. S. Nchodu M. R. Ullmann J. Reedy R. C.

*New Neutron and Proton Production Cross Section Measurements for Cosmic Ray Studies* **[#1202]**

Cosmic rays produce nuclides in lunar rocks and meteorites. Good neutron and proton production cross sections are needed to analyze these cosmogenic nuclide archives. New cross sections reported here include $SiO_2(n,x)14C$ at 78.4 ± 1.9 MeV and $Ti(p,x)^{14}C$ for 100–500 MeV.

Sisterson J. M. Caffee M. W. Hudson G. B.

*New Neon Production Cross Section Measurements Needed for Cosmic Ray Studies* **[#1283]**

We present new proton production cross sections for $^{20}Ne$, $^{21}Ne$, $^{22}Ne$ and $^{22}TNe$ from Mg and Al. These cross sections are essential as input to models used to analyse the production of these isotopes in lunar rocks and meteorites.

Reedy R. C.

*Variations in Solar-Proton Fluxes over the Last Million Years* **[#1643]**

Average solar-proton fluxes from 1954–1996 and from lunar SCR-produced nuclides for 10 ka to 5 Ma ago are summarized. The good results for fluxes >30 MeV indicate a trend with higher fluxes recently than those averaged over the last million years.

## Martian Meteorites

Tsuchiyama A. Kawabata T. McKay G. A. Lofgren G. E.

*Three-dimensional Structure of Martian Meteorite ALH84001 by X-ray CT Method* **[#1539]**

The three-dimensional structure of ALH84001 was studied by X-ray CT method and image analysis technique. Plagioclase glass, cracks, and chromite form a foam-like structure of a few millimeters in size, which may be related to shock features.

Bishop J. L. Pieters C. M. Mustard J. F. Hiroi T.

*Spectral Identification of Major and Minor Constituents of Martian Meteorite ALH 84001 and the Importance for Remote Sensing on Mars* **[#2038]**

Spectroscopic analyses of martian meteorite ALH 84001 correctly identify low-Ca-pyroxene as the dominant mineral and the presence of Fe-Mg carbonate and magnetite in selected spots on chip surfaces.

Koziol A. M.

*Experimental Determination of Siderite (Iron Carbonate) Stability Under Moderate Pressure-Temperature Conditions, and Application to Martian Carbonate Parageneses* **[#1226]**

We must have an understanding of the equilibrium properties of magnesite-siderite (seen in ALH84001) under changing temperature, pressure, $O_2$ fugacity, and $CO_2$ fugacity conditions. Piston cylinder experiments on the reaction $FeCO_3 + Fe_2O_3 = Fe_3O_4 + CO_2$ will be presented.

Bodnar R. J.

*Fluid Inclusions in ALH84001 and Other Martian Meteorites: Evidence for Volatiles on Mars* **[#1222]**

Liquid and vapor fluid inclusions in ALH84001 and Nakhla martian meteorites provide direct evidence for the presence of liquid carbon dioxide and/or water at or near the martian surface in the geologic past.

Sugiura N. Hoshino H.

*Hydrogen Isotopic Compositions of Carbonate in Martian Meteorite ALH84001* **[#1324]**

H isotopic composition of carbonate in ALH84001 was measured by SIMS. The heaviest D/H ratio was 1344 permil, suggesting that the H in martian atmosphere was significantly fractionated at 3.9 Ga.

Olson E. K.   Swindle T. D.   Kring D. A.   Dettman D. L.   Rosenberg P. E.   Larson P. B.
*Can Carbonates be Dated Using K-Ar Techniques?* **[#1682]**
To determine the feasibility of K-Ar dating of carbonates, we analyzed four carbonates, using an electron probe and noble gas mass spectrometer. Early results are not promising. K contents were <100 ppm except for one sample with a K-rich inclusion.

Rao M. N.   Schwandt C.   McKay D. S.
*Trapped Argon and Xenon in EET79001 and ALH84001: Clues to Low Temperature Aqueous Activity on Mars* **[#1389]**
Using trapped Ar and Xe ratios in ALH84001 samples, we show that the martian atmospheric noble gases were incorporated at low temperatures by interaction of $CO_2$ rich solutions in the crushed zones of ALH84001.

Blake D. F.   Treiman A. H.   Amundsen H. E. F.   Mojzsis S. J.   Bunch T.
*Carbonate Globules, Analogous to Those in ALH84001, from Spitzbergen, Norway: Formation in a Hydrothermal Environment* **[#1683]**
Basalts and xenoliths from Spitsbergen (Norway) contain carbonate globules similar to those of ALH84001 in: mineralogy, chemical compositions, internal structures, and geological setting. The Spitsbergen globules formed in a hydrothermal environment.

Greshake A.   Stöffler D.
*Shock Metamorphic Features in the SNC Meteorite Dar Al Gani 476* **[#1377]**
Dar al Gani 476 is a newly discovered basaltic shergottite which is found to be heavily affected by shock metamorphism. Based on the shock defects observed a maximum shock pressure of 45 GPa is estimated.

Mikouchi T.   Miyamoto M.
*Micro Raman Spectroscopy of Amphiboles and Al-Ti-rich Pyroxenes in the Martian Meteorites Zagami and LEW88516* **[#1559]**
We analyzed amphiboles and Al-Ti-rich pyroxenes in Zagami and LEW88516 by micro Raman spectroscopy, which reconfirms that martian amphibole is kaersutite with Raman spectra similar to terrestrial kaersutite. Al-Ti-rich pyroxene has different peaks.

McHone J. F.   Kudryavtsev A. B.   Agresti D. G.   Wdowiak T. J.   Killgore M.
*Raman Imagery of Martian Meteorites* **[#1896]**
True Raman line-scan imaging has been exercised on the martian meteorites, Nakhla, Zagami, and the recently recognized Dar al Gani 476, to obtain micron-scale areal distributions of target materials keyed to particular selected spectral bands.

Kring D. A.   Gleason J. D.
*Siliceous Igneous Rocks on Mars* **[#1611]**
In this paper, we review how quartz-normative igneous rocks are produced and outline petrological and geochemical evidence for them on Mars based on analyses of SNC-related meteorites.

Boctor N. Z.   Fei Y.   Bertka C. M.   Alexander C. M. O'D.   Hauri E.
*Shock Metamorphic Effects in Martian Meteorite ALHA 77005* **[#1628]**
ALHA79005 was metamorphosed by impact at peak shock pressure of 80GPa.

Schwandt C. S.   McKay G. A.   Lofgren G. E.
*Silica in Martian Meteorites, There are Differences* **[#1637]**
Silica is preserved in ALH84001, Shergotty, and Zagami. It records petrogenetic information that predates ejection from Mars. ALH84001 silica indicates interaction with the martian hydrosphere.

Wentworth S. J.   McKay D. S.
*Weathering and Secondary Minerals in the Nakhla Meteorite* **[#1946]**
Secondary minerals in Nakhla are described using recently-developed FESEM techniques. The interior contains little evidence of terrestrial weathering. N is present in some terrestrial surface contaminants.

Vicenzi E. P. Heaney P. J.

*Examining Martian Alteration Products Using Insitu TEM Sectioning: A Novel Application of the Focused Ion Beam (FIB) for the Study of Extraterrestrial Materials* **[#2005]**

This represents the first known use of the focused ion beam (FIB) method of in situ TEM specimen preparation for the study of SNC secondary alteration. Microstratigraphy of "iddingsite" from the Lafayette meteorite has been examined.

Yanai K.

*Research for the Martian Meteorites from Diogenetic Achondrites* **[#1119]**

The twelve meteorites were identified as being of martian origin, and they were believed to originate from the Mars surface by recent impact events in the long history of solar system evolution.

Ashley G. M. Delaney J. S.

*If a Meteorite of Martian Sandstone Hit You on the Head Would You Recognize It?* **[#1273]**

Martian meteorites are igneous but Mars is Earthlike with sediments, igneous and maybe sedimentary rocks. Sedimentary meteorites should occur in proportion to the igneous/sedimentary ratio. Sedimentary meteorites would impact climatology and the search for life on Mars.

Mathew K. J. Marti K.

*Nitrogen and Xenon Isotopic Signatures in SNC's and the Interior of Mars* **[#1418]**

The N and Xe isotopic signatures in SNC samples presumably representing martian interior rocks are distinct from atmospheric components. The currently best N signature is -30‰ has been observed in Chassigny and is also observed in shergottites and nakhlites.

## Mars: General Science

Musselwhite D. S. Drake M. J.

*Early Outgassing of Mars: A Quantitative Assessment* **[#1541]**

We assess quantitatively the timing and extent of outgassing that can produce the $^{129}Xe/^{132}Xe$ ratio and total $^{132}Xe$ abundance in the present-day Mars atmosphere. A model with two stages of outgassing with atmospheric removal occurring before the 2nd stage is employed.

Durand-Manterola H. J. Perez-de-Tejada H.

*Theoretical Model of Evolution of the Martian Atmosphere* **[#1010]**

Our model examines the evolution of the Mars atmosphere by including processes related to the lost of mass to space, the oxidation of the planetary surface and degassing. The model depicts time variations of the atmospheric mass, pressure, and temperature.

Bass D. S. Siili T.

*Downslope Windstorm Effects and Raising Dust in Hellas Basin* **[#1058]**

We present observational evidence of dust storm activity in Hellas basin that supports the suggestion that slope angle has an effect on wind speed and subsequent atmospheric dust loading.

Cohen J. L. Treiman A. H.

*The Longitudinal Extent of a Layered Sequence in the Sub-Surface of Mars: Evidence for Diagenesis in the Hesperian* **[#1254]**

Horizontal rock layers are visible at wall tops throughout Valles Marineris, Mars. Similar layers are exposed by impact craters in the whole equatorial region, except under the Tharsis. So, these layers reflect a global process of rock formation.

Durham W. B. Kirby S. H. Stern L. A.

*The Rheology of Solid Carbon Dioxide: New Measurements* **[#2017]**

Experimental deformation of solid $CO_2$ at low stresses under hydrostatic confining pressure indicates a very weak material (10–15 times weaker than water ice at similar conditions) with an unusally high stress exponent of $n = 4.5$ to 7.

Mellon M. T.
*Martian Orbital Change and Its Effect on the Formation of Permafrost Polygons* **[#1118]**
Small-scale polygonal patterns have been observed on Mars and may have been formed by thermal contraction in ice-cemented permafrost. The seasonal tensile stress in martian permafrost is calculated at various climatic conditions to evaluate polygon formation.

Harrison K. P. Grimm R. E.
*A Conservative Approach to Hydrothermal Systems on Mars* **[#1941]**
Hydrothermal systems on Mars may have produced sufficient surface discharge to contribute to the formation of valley systems. A conservative approach to the study of groundwater mobilization and discharge due to hot magmatic bodies is presented.

Nicoll K. Komatsu G.
*Interpreting Martian Paleoclimates from Valley Network Morphologies: Insights from Terrestrial Analogues in Egypt* **[#1054]**
Wadi Mareef in S. Egypt, a paleovalley formed by spring-fed sapping and runoff processes, bears a striking resemblance to Nirgal Vallis. The concept of equifinality should apply to the modelling of martian landscape processes and paleoclimates.

Bourke M. C. Zimbelman J. R.
*Australian Paleoflood Systems: A New Earth Analogue for Martian Channels* **[#1804]**
Mapping and classification of Earth flood features, utilising TM and MSS imagery, enable a better understanding of land surface processes on Mars. Unconfined paleoflood channels and floodouts in arid central Australia provide a new perspective for studying martian channels.

Baliva A. Marinangeli L.
*Fan-shaped Features in Mangala Valles Region, Mars* **[#1764]**
A large variety of hydrologic patterns and interaction between sedimentary environments in Mangala Region allow the recognition of peculiar morphologies. We focused on the analysis of fan-shaped features outlining different sedimentary processes and environments.

Pranzini E. Zeoli A.
*Spiral Beaches on Mars: Evidence for a Long Lasting Liquid Ocean* **[#1178]**
Log-spiral significantly fit curvilinear ridges in the Cydonia Mensae region, just like occurs on equilibrium Earth beaches when offshore waves are diffracted by a headland and refracted by the sea-bottom. This proves the existence of an ancient liquid ocean on Mars.

Yen A. S. Murray B.
*A Dry Mars: Limited Chemical Weathering of Surface Deposits by Liquid Water* **[#1162]**
We present three sets of laboratory results that support the alternative viewpoint that liquid water never had significant chemical interactions with the surface that we see on Mars today.

Ramstad J. F.
*A Comparison of Fluidized Ejecta Impact Crater Morphology Between the Northern Lowlands and Southern Highlands of Mars* **[#1788]**
Fluidized ejecta craters are digitized and measured from high resolution imagery to determine if differences exist in the substrates of the northern lowlands and southern highlands.

Demura H. Kurita K.
*Formation of Fluidized Craters on Mars* **[#1630]**
The rampart crater, a kind of fluidized crater, is peculiar to Mars. A general view of formation of the fluidized craters is proposed on the basis of photogeological descriptions, classification, and photoclinometric survey.

Rosanova C. E.   Lucchitta B. K.   Hare T. M.   Velasco M.
*Observations of Candor and Ophir Chasmata in Valles Marineris, Mars, Using Merged Topographic, Geologic and Image Data* **[#1287]**
Images of Ophir and Candor Chasmata were draped over topographic data to produce perspective views, anaglyphs, and layered data sets. The 3-D views help determine the sequence of events. Slope and volume information is being obtained.

Chapman M. G.
*Enigmatic Terrain of North Terra Meridiani, Mars* **[#1294]**
Scrutiny of Viking and MOC images, a thickness estimate, and TESS results lead to new hypotheses for the origin of enigmatic terrain of north Terra Meridiani, west Arabia Terra, Mars.

Chapman M. G.
*Elysium Basin Lava Flows: New Interpretations Based on MOC Data* **[#1279]**
MOC images of Elysium Basin are interpreted by members of the Science Team to suggest fluid lavas formed in lakes. Details presented here suggest that a textural difference between lava types may be a more practical interpretation of the platey lava texture.

Lias J. H.   Tanaka K. L   Hare T. M.
*Geologic, Tectonic, and Fluvial Histories of the Eridania Region of Mars* **[#1074]**
The objectives of this study were to: (1) construct a geologic/geomorphic map of the Eridania region, (2) determine potential causes for tectonic structures in the region, and (3) determine potential sources for fluvial channels in the region.

Hiesinger H.   Head J. W. III
*Shorelines on Mars: Testing for Their Presence Using Mars Orbiter Laser Altimeter (MOLA) Data* **[#1370]**
MOLA data of the Deuteronilus Mensae area are used to test for the elevation of contacts interpreted to represent shorelines of an ancient northern ocean on Mars.

Franklin B. J.   Parker T. J.
*Geologic Maps of East Acidalia Planitia, Mars* **[#1785]**
Nine morphological units, 4 crater types and evidence of 3 shorelines are found in MTM Quads 45347, 45352, and 45357, Acidalia Planitia, Mars. We assess evidence for/against multiple shorelines.We await MOLA data as additional evidence regarding possible standing water.

McGill G. E.
*Evolution of the Dichotomy Boundary Zone, Arabia Terra, Mars* **[#1148]**
Mapping of 4 1:500K quadrangles (30-45N332) transecting the martian dichotomy boundary indicates that fretted channels and debris flows formed over finite intervals but at different times; thus the flow lobes do not necessarily imply that the channels formed by mass wasting.

Mege D.
*Surface Shortening at the Coprates Ridged Plain, Syria Planum Flood Basalt Province, Mars* **[#1876]**
Using a method developed in another paper, surface shortening is estimated at the Coprates ridged plain on Mars. Shortening is found to be 5.3–9.2% of the total 1.300,000 $km^2$ surface area, similar to estimates obtained at the Columbia Plateau on Earth.

Mege D.
*A Stress History Consistent with the Volcanic and Tectonic History of the Early Tharsis Flood Basalt Province on Mars* **[#2065]**
Based on comparison between early Tharsis evolution and evolution of terrestrial mantle plumes, a succession of logical and chronological relationships between stress and tectonic structures for the early stage of Tharsis evolution is proposed.

Hauber E. Kronberg P.
*Differences in Style and Age of Extensional Faulting — Examples from the Northern Tharsis Province, Mars* **[#1568]**
High-resolution mapping in the Alba and Tempe/Mareotis regions reveals differences in orientation, geometry, kinematics, and age of faulting. Both zones are believed to be related to plume activity, crustal extension, and associated volcanism.

Scott E. D. Wilson L. Head J. W. III
*Episodicity of Magma Supply to the Large Tharsis Volcanoes, Mars: Thermal Considerations* **[#1356]**
The presence of discrete magma reservoirs at various times during the formation of Tharsis volcanoes can only be made consistent with thermal constraints if the magma supply from the mantle varies episodically in time.

Bowling S. P.
*Modelling the Effusion Rates and Activity Phases of the Elysium Volcanics* **[#1185]**
The Elysium Volcanics can be considered to have occurred in two phases — volcano construction and flood lava production. Comparison with terrestrial flood lavas allows effusion rates and activity phases to be modelled for the Elysium Volcanic province.

Mitchell K. L. Wilson L. Wilson C. J. N.
*Consequences of Adiabatic Cooling Within Volcanic Conduits on Earth and Mars* **[#1716]**
The consequences of adiabatic rather than isothermal cooling in volcanic conduits are assessed for Earth and Mars using a new computational numerical model.

Moore J. M. Bullock M. A.
*Experimental Studies of Brines and Evaporites as Applied to Mars: Initial Results from the 1998–1999 Runs* **[#1922]**
This is the first ever report of results from our "full up," multi-variable, multi-control laboratory study of Mars brine chemistry. After two years of preparation, we now have results and analysis from the first few time-steps of the experiment.

Cooper C. D. Mustard J. F.
*Sulfates on Mars: Spectroscopic Evaluation of Analog Mixtures* **[#2042]**
Mixtures of sulfates and palagonite at levels comparable to martian soils have spectroscopic features in wavelength regions that should be detectable by TES. Cementation of the mixtures results in dramatic changes that should also be detectable.

Stooke P. J.
*Revised Viking 1 Landing Site* **[#1020]**
The position of the Viking 1 landing site in orbiter images has been revised to be consistent with Pathfinder and the new control network. Several horizon features can be matched at the new location including parts of a wrinkle ridge on the eastern horizon.

Kirkland L. E. Herr K. C. McAfee J. M. Salisbury J. W. Forney P. B.
*1969 Mariner Mars IRS Thermal Infrared Spectra of the Dark Side of Mars* **[#1687]**
Thermal infrared spectra of the martian night side have advantages over day spectra for examining the aerosol dust mineralogy because they contain weaker atmospheric gas and surface features. We will present and discuss IRS night spectra.

## Future Mars Missions

Kirk R. Barrett J. Howington-Kraus E.
*A Database of Viking Orbiter Image Coverage for Cartographic and Scientific Use* **[#1857]**
We have built simple but effective tools to manipulate geometric data for the ~46,000 Viking Orbiter images of Mars to evaluate mapping and science coverage. Coverage maps and statistics for resolution, lighting, stereo quality, etc., will be shown.

Kirk R. Becker K. Cook D. Hare T. Howington-Kraus E. Isbell C. Lee E. Rosanova T. Soderblom L. Sucharski T. Thompson K. Davies M. Colvin T. Parker T.

*Mars DIM: The Next Generation* **[#1849]**

The USGS part of a joint effort to revise geodetic control and map products for Mars in support of missions is described. As control is improved, more accurate versions of the global image mosaic will be released, superseding the current 6-CD set.

Farmer J. D. Nelson D. M. Greeley R. Klein H. P.

*The Elysium Basin-Terra Cimmeria Region of Mars as a Target for Mars Exopaleontology* **[#1833]**

Exopaleontology and identifying aqueous mineral deposits are key elements for the upcoming Mars missions. Using set engineering constraints, areas in Elysium Basin have been targeted for geologic mapping as possible landing sites.

Saunders R. S. Arvidson R. E. Weitz C. M. Marshall J. Squyres S. W. Christensen P. R. Meloy T. Smith P.

*Mars 2001 Mission: Addressing Scientific Questions Regarding the Characteristics and Origin of Local Bedrock and Soil* **[#1734]**

The Mars Surveyor Program 2001 Mission will carry instruments on the orbiter, lander and rover that will support synergistic observations and experiments to address important scientific questions regarding the local bedrock and soils.

Zimbelman J. R. Johnston A. K. Patel A. N.

*Geologic Evaluation of Two Candidate Landing Sites on Mars* **[#1662]**

Geologic maps of candidate landing sites (2.5°S, 249.5°W; 8.8°S, 214.7°W) in the Noachian highlands of Mars were prepared at 1:2M scale. Geologic history and engineering constraints for the target areas are summarized in the poster.

Lucchitta B. K. Chapman M. G. Weitz C. M.

*Potential 2001 Landing Sites in Melas Chasma, Mars* **[#1736]**

Four sites on interior layered deposits in southern Melas Chasma meet the 2001 mission's engineering requirements. The lander and rover would be able to study the deposits and provide important insights into the history of Valles Marineris.

Gulick V. C. Briggs G. Saunders R. S. Gilmore M. Soderblom L.

*Mars Surveyor Project Landing Site Activities* **[#2039]**

A key aspect of the program is the selection of landing sites. This abstract reports on status of landing site selection process beginning with the 2001 mission and outlines opportunities for the Mars community to provide input into the selection process.

Schultz R. A.

*Mars Surveyor Landing Sites in Valles Marineris: Highland Rocks from the Basement Using the Marie-Curie Lander* **[#1057]**

Two potential landing sites in the central Valles Marineris for the 2001 lander-rover mission emphasize geologic context and trough location for examining Noachian rocks. Mission results would favorably impact local, regional, and global issues.

Golombek M. Bridges N. Gilmore M. Haldemann A. Parker T. Saunders R. Spencer D. Smith J. Weitz C.

*Preliminary Constraints and Approach for Selecting the Mars Surveyor '01 Landing Site* **[#1383]**

Engineering and safety considerations limit the MS '01 landing site to a <2.5 km elevation equatorial area that appears hazard free in <50 m/pixel Viking images and has low slopes, low rock abundance and a competent surface (relatively little dust).

Beyer R. A. McEwen A. S. Malin M. C.

*Mars Orbital Camera (MOC) Observations of Possible Mars Surveyor 2001 Landing Sites* **[#1474]**

This poster will present MOC narrow angle images of possible Mars Surveyor 2001 landing sites along with their Viking context. We hope that this poster will generate discussion about possible future MOC imaging targets.

Squyres S. W. Arvidson R. Bell J. F. III Carr M. Christensen P. Des Marais D. Economou T. Gorevan S. Klingelhöfer G. Haskin L. Herkenhoff K. Knoll A. Knudsen J. M. Malin M. McSween H. Morris R. Rieder R. Sims M. Soderblom L. Wänke H. Wdowiak T.

*The Mars 2001 Athena Precursor Experiment (APEX)* **[#1672]**

The Athena Precursor Experiment (APEX) is a suite of scientific instruments for the Mars 2001 lander mission. It includes a panoramic color imager, an IR spectrometer, an APX spectrometer, and a Mössbauer spectrometer.

Boynton W. V. d'Uston C. Arnold J. R. Trombka J. I. Feldman W. C. Mitrofanov I. Englert P. A. J. Metzger A. E. Reedy R. C. Squyres S. W. Wänke H. Bailey S. H. Brückner J. Evans L. G. Starr R. Fellows C. W.

*Scientific Investigations on the Elemental Composition of Mars by Means of the Mars Surveyor 2001 Gamma-Ray Spectrometer* **[#1991]**

The Mars Surveyor 2001 Gamma-Ray Spectrometer will map the elemental composition of the surface of Mars. This work describes the instrument.

Boynton W. V. Bailey S. H. Bode R. Hamara D. K. Kring D. A. Lorenz R. D. Ward M. Williams M. S.

*The Thermal and Evolved Gas Analyzer (TEGA) on the Mars Polar Lander* **[#1914]**

The Thermal and Evolved Gas Analyzer (TEGA) on the 1998 Mars Polar Lander will use differential scanning calorimetry and evolved gas analysis to identify minerals and volatiles in the martian polar layered terrain.

Lorenz R. D. Moersch J. E. Smrekar S. E. Stone J. A. Keaton R. M.

*Impact Penetration of the DS-2 Mars Microprobes* **[#1042]**

We determine an empirical penetration equation from airgun tests of the DS-2 Mars Microprobes and estimate that they will reach a depth between 0.38 and 0.85 m for martian surface S-numbers between 4 and 20, for the expected 200 m/s impact speed.

Jolliff B. Wang A. Kuebler K. Haskin L. Arvidson R.

*Raman Analysis of Weathered Rocks from the FIDO Mars Rover Test Site, Silver Lake, California* **[#1512]**

We present results of laser Raman spectroscopy of rocks from the FIDO field test site for the Mars 2003 mission. Results include spectra taken under simulated field conditions of coated (varnished) natural rock surfaces for a diversity of rock types.

Shelfer T. D. Morris R. V.

*Mössbauer Spectroscopy on Mars: Effects of Sample Structure on Spectral Interpretation* **[#1813]**

The interpretation of Mössbauer spectra of geologic materials using backscatter geometry is more complicated than transmission spectra due to crystal orientation and texture effects. We present the results of a backscatter Mössbauer investigation.

Knight A. K. Scherbarth N. L. Cremers D. A. Ferris M. J. Wiens R. C. Blacic J. D. Nordholt J. E. Calvin W. M.

*Quantitative Elemental Analyses at Stand-Off Distances: Development of a Prototype Instrument for the Mars Rover Program* **[#1018]**

As part of the Mars Instrument Development Program, an instrument based on laser-induced breakdown spectroscopy (LIBS) is under development for stand-off (20 meters) elemental analysis of soil and rock samples.

Pillinger C. T. Wright I. P. Sims M. R.

*Science Activities with Beagle 2, the Mars Express Lander* **[#1560]**

The Beagle 2 lander, mass 25 kg, has been selected for the ESA Mars Express 2003 mission. In situ analyses of atmospheric and subsurface samples will search for evidence of past and present life and investigate whether conditions appropriate for life.

Ozorovich Y. R. Linkin V. M. Smythe W. D.

*MARS Electromagnetic Sounding Experiment — MARSES* **[#1549]**

The MARSES is the sounding instrument developed for searching for water, water-ice or permafrost layers existing in some depth under the visible surface of Mars.

Golden D. C. Ming D. W. Lauer H. V. Jr. Morris R. V. Galindo C. Jr. Boynton W. V.
*Differential Scanning Calorimetry of Hydrous Minerals Under Mars-like Conditions: Calibration Studies for the Mars '98 Lander Thermal and Evolved Gas Analyzer* **[#2027]**
The effects of reduced pressure and flow rates were determined on the thermal analysis of synthetic lepidocrocite using a modified differential scanning calorimeter in support of the Mars '98 Lander Thermal and Evolved Gas Analyzer (TEGA).

Lauer H. V. Jr. Ming D. W. Golden D. C. Boynton W. V.
*Effects of Reduced Pressure and Gas Flow Rate on Differential Scanning Calorimetry Analysis of Indium and Zinc: Implications for Remote Thermal Analysis* **[#1702]**
An experimental set up was constructed to emulate a set of Mars-based experiments on standard materials using laboratory based experiments performed at Mars-like conditions.

## Recipes for Lunar Rocks

Shervais J. W. McGee J. J.
*Ancient Crust Formation at the Apollo 14 Site* **[#1750]**
Mg-suite parent magma formed by partial melting of primitive lunar interior and buffering of the melts by ultramagnesian cumulates. The alkali suite parent magma may be related to the magnesian suite by AFC.

Schwartz J. M. McCallum I. S.
*Inferred Depths of Formation of Spinel Cataclasites and Troctolitic Granulite, 76535 Using New Thermodynamic Data for Cr-Spinels* **[#1308]**
New thermodynamic calculations of equilibria pertinent to spinel cataclasites and troctolites reveal that these assemblages formed at depths <25 km (cataclasites) and >45 km (troctolites). Calculations also suggest that symplectite textures formed from trapped melt.

Ojima K. Abe Y.
*Constraints on Formation History of Large Scale Lunar Topography from Observed Admittance: Viscous Relaxation with Lunar Thermal History* **[#1322]**
The scale- and age-dependence of topographic relaxation of a cooling viscoelastic sphere indicates that the 5000-km-scale (dichotomy scale) topography of the Moon should be external origin and formed later than 100 m.y. from the lunar formation.

Snyder G. A. Taylor L. A. Patchen A. Nazarov M. A. Semenova T. S.
*Mineralogy and Petrology of a Primitive Spinel Troctolite and Gabbros from Luna 20, Eastern Highlands of the Moon* **[#1491]**
We present petrologic and mineral-chemical data for several "new" highlands fragments from the Luna 20 landing site. These include a rare spinel troctolite, a troctolite, an anorthositic gabbro, and a gabbro.

Hidaka H. Ebihara M. Yoneda S.
*Samarium and Gadolinium Isotopic Compositions of Lunar Samples* **[#1316]**
Sm and Gd isotopic compositions in 10 lunar samples taken from two Apollo sites, A-12 and A-15, were measured by thermal ionization mass spectrometry to discuss the neutron capture effects on thelunar surface.

## Lunar Missions and Data

Foing B. H. Duke M. Galimov E. Mizutani H. ILEWG Team
*ILEWG Recommendations for Lunar Exploration* **[#2060]**
The International Lunar Exploration Working Group (ILEWG) was created in 1995 with the charter: 1. To develop an international strategy for the exploration of the Moon; 2. To establish a forum and mechanism for the communication and coordination of activities; and 3. To implement international coordination and cooperation.

Manifold J. D. Norris D. A.
*Commercial Lunar Geological Exploration: A Synergistic Model of Science and Private Enterprise* **[#1368]**
A program of unmanned sample-return missions to unexplored lunar sites is proposed. Applied Space Resources, Inc. plans a spacecraft similar in concept to the Soviet Luna series missions. The spacecraft can return at least 10 kg of regolith from the Nectaris basin.

Foing B. H. Racca G. SMART-1 Team
*ESA SMART-1 Mission to the Moon* **[#2052]**
SMART-1 is to be launched in 20001 as the first Small Mission for Advanced Research in Technology of the ESA Scientific Programme. It will use Primary Solar Electrical Propulsion in Deep Space and test new technologies for future missions.

Foing B. H. Hoffmann H. Grande M. Josset J. L. Cerroni P. Keller U. SMART-1 Team
*New Views of Lunar Terranes with SMART-1 Expected Data* **[#2057]**
Experiments on the ESA SMART-1 mission will provide new global and local data sets helpful to discriminate and characterize different lunar "terranes" multicolor imaging at medium and high resolution.

Hasebe N. Doke T. d'Uston C. Grande M. Kashiwagi T. Kikuchi J. Kobayashi M. N. Kubo K. Mitani S. Nishimura J. Okuno S. Reedy R. C. Shibamura E. Takashima T. Yoshida K.
*Gamma-Ray and Alpha-Ray Spectrometer Experiment on SELENE Mission* **[#1171]**
Present status of the development of Gamma-Ray Spectrometer (GRS) and Alpha-Ray Spectrometer (ARS) on Japanese lunar mission SELENE is reviewed.

Kruep J. M. Blase W. P. Olliver V.
*A Proposed Microlander for Low-Cost Lunar Missions* **[#1846]**
A low-cost "microlander" microspacecraft is described that is capable of carrying small payloads to the lunar surface and providing power and communications services for several months. Several possible missions are also described.

Isbell C. E. Eliason E. M. Adams K. C. Becker T. L. Bennett A. L. Lee E. M. McEwen A. S. Robinson M. S. Shinaman J. R. Weller L. A.
*Clementine: A Multi-Spectral Digital Image Model Archive of the Moon* **[#1812]**
A multi-spectral global Digital Image Model (DIM) containing Clementine Ultra-Violet Visible (UVVIS) images has been prepared. The 5-band DIM and phase angle information are each presented at 100 meters/pixel.

Gillis J. J. Spudis P. D. Hager M. A. Noel M. Rueb D. Cowan J.
*Digitized Lunar Orbiter IV Images: A Preliminary Step to Recording the Global Set of Lunar Orbiter Images in Bowker & Hughes* **[#1770]**
The complete set of Lunar Orbiter IV mission prints is recorded with an Olympus D-600L digital camera. A search engine is included with the image database to provide quick and easy location of images that fulfill query parameters set by the user.

Hiesinger H.
*The Lunar Source Disk: A New Compilation of Lunar Data Sets* **[#1200]**
We present a compilation of lunar data on CD. All data were transformed to a standard map projection to create an "image cube"-like data pool from which information of different data can be extracted on a pixel-by-pixel basis.

## Lunar Poles and Regolith

Riegsecker S. Basu A.
*Estimating the Composition of Apollo Landing Sites from Surface Soils* **[#1759]**
Estimates of average chemical and mineralogical compositions of lunar landing sites are calculated for terrane appreciation and the calibration of remote-sensing signals.

Assonov S. S. Mineev S. D. Polyakov V. B.

*On the Origin of Nitrogen Isotopic Variations in Lunar Regolith* **[#1834]**

This work considers whether various processes such as nitrogen chemical reactions and sorption operating at lunar conditions may account for huge nitrogen isotopic variations observed for lunar regolith samples.

Bondarenko N. V. Shkuratov Yu. G.

*Thickness of Lunar Regolith and Soderblom's Crater Parameter DL* **[#1196]**

Through comparison between DL data and regolith thickness there was shown the most acceptable mean regolith density is from 2.3 to 2.6 g/cm$^3$. The regolith densities for mare and highland appear to be very close.

Bussey D. B. J. Robinson M. S. Spudis P. D.

*Clementine High Resolution Imaging of the Lunar South Pole* **[#1738]**

We have produced a high resolution mosaic of the lunar south pole region. The resolution (40 m/pixel) allows features to be investigated in unprecedented detail, particularly areas previously discovered to receive large amounts of illumination.

Wählisch M. Hoffmann H. Wagner R. Wolf U. Hoffmeister A. Jaumann R.

*High Resolution Mosaic and Digital Terrain Model in the Lunar South Pole Region Derived from Clementine Data* **[#1636]**

We derived a small digital terrain model of part of the south pole region and a mosaic covering the region –86° to –90° using Clementine data.

Starukhina L. V.

*The Excess Hydrogen on the Lunar Poles: Water Ice or Chemically Trapped Solar Wind?* **[#1193]**

Concentration of hydrogen in lunar regolith due to chemical trapping of solar wind protons can be of the same value as found by Lunar Prospector. The excess hydrogen on the poles can be due to sharp decrease of mobility of atoms with temperature.

Vilas F. Domingue D. L. Jensen E. A. McFadden L. A. Coombs C. R. Mendell W. W.

*Aqueous Alteration on the Moon* **[#1343]**

One of the controversial issues concerning lunar science is the debate over the absence or presence of water at the poles. To add fuel to the fire of this debate we show additional indirect evidence supporting the presence of water-bearing minerals near the lunar South Pole.

Berezhnoi A. A.

*Determination of the Main Source of Water in Lunar Cold Traps* **[#1598]**

The determination of D/H ratio in lunar water can help us estimate the origin of water in lunar polar regions.

Noble S. K. Pieters C. M. Taylor L. Keller L. Morris R. McKay D. Wentworth S.

*The Optical Properties of the Finest Fraction of Lunar Soils: Initial Results and Implications for Weathering Processes* **[#1669]**

The finest fraction appears to contain rims of optically active weathering components. The products of space weathering are dependent on starting composition. Characterizing the finest fraction of lunar soils is sensitive to the processing method.

Hirata N. Haruyama J. Otake H. Ohtake M.

*Analysis of Dark Rings Around Lunar Craters Using Clementine Imaging Data* **[#1350]**

We investigated dark rings around lunar craters using Clementine image. Their spectral properties indicate that the ring material contains glassy impact melt. The mode of occurrence suggest that the impact melt are dispersed with ballistic ejecta.

## Mercury

Jurgens R. F. Rojas F. Slade M. A. Standish E. M. Haldemann A. F. C.
*Radar Images of the Kuiper Quadrangle (Mercury) from Goldstone Radar Data* **[#1524]**
From the currently processed radar data from 1989 to 1998, we have assembled crude radar images covering the Kuiper (H6) region on Mercury. Most of the radar features can be identified with structures seen in the Mariner 10 imaging.

Killen R. M. Potter A. E.
*Dynamic Changes in Mercury's Atmosphere Over a One Week Period* **[#1923]**
Images of Mercury's atmosphere obtained during Nov. 13–20, 1997, have been reduced to absolute abundance at 0.5" resolution. The abundance increased by roughly a factor of 2.5 during this week, beginning as a strong polar enhancement and spreading equatorward.

Cook A. C. Watters T. R. Robinson M. S.
*Examples of Mercurian Topography* **[#2066]**
A review of some selected features on Mercury is presented, based upon results of stereo matching Mariner 10 stereo imagery. These include craters, lobate scarps, basins, and the south pole area.

## Impacts II

Fiske P. S. Schnetzler C. C. McHone J. F. Chanthavaichith K. K. Homsombath I. Phouthakayalat T. Khenthavong B. Xuan P. T.
*Layered Tektites of Southeast Asia: Results of 1998 Expedition to Laos and Vietnam* **[#1937]**
We carried out a field investigation of layered tektite localities in Laos and Vietnam. We recovered 18 kg of tektite fragments from 10 sites, including 5 around the town of Muong Nong.

Albin E. F.
*Regional Stratigraphic Correlation of North American Tektites* **[#1357]**
In this investigation, North American tektite stratigraphic occurrence is considered in a regional context. An effort is made to correlate the parent tektite horizon between the sub-strewn fields.

Simonson B. M. Hornstein M. Hassler S. W.
*Are Irregular Clasts of Former Silicate Melt in the Carawine Dolomite (Late Archean, Western Australia) the Oldest Known Tektites on Earth?* **[#1481]**
Irregular clasts in the late Archean Carawine Dolomite have shapes and internal textures similar to Muong Nong-type tektites. This suggests they are the oldest tektites found to date and that textures in tektite glass can survive devitrification.

Pierazzo E. Schnabel C. Herzog G. F. Masarik J. Cresswell R. G. di Tada M. L. Liu K. Fifield L. K.
*Constraints on the Formation of Canyon Diablo Spheroids from Numerical Modeling and Nickel-59 Measurements* **[#1267]**
According to $^{59}$Ni measurements Canyon Diablo spheroids originated deeper in the impactor than the meteorites. This is in agreement with hydrocode modeling results, suggesting that an outer shell about 3m deep remained solid in the impact.

Rocchia R. Robin E. Smit J. Pierrard O. Lefevre I.
*Cosmic Markers in an Ammonite from the K/T Section of Bidart (French Basque Country)* **[#1576]**
In the K/T section of Bidart (France) an ammonite containing markers of the K/T event (iridium and Ni-rich spinel) has been found less than 5 cm below the boundary. This is consistent with the view that ammonites disappeared suddenly at the K/T boundary.

Miura Y. Fukuyama S. Gucsik A.

*New Impact Fragments of Fe-Ni-Si in Spherules at Takamatsu Crater, Japan* **[#1127]**

Fe-Ni-Si grains trapped in vacant regions formed by impact events on granitic rock are found in spherules included in glassy blocks on the surface of the buried Takamatsu crater, Japan.

Cintala M. J. Shelfer T. D. Hörz F.

*Growth Times of Impact Craters Formed in Fine-grained Sand* **[#1958]**

The times of growth of small impact craters have been estimated through use of a laser-based ejection-velocity measurement system. A dimensionless plot of growth time vs. scaled energy exhibits a possible nonlinearity; results are compatible with data from previous studies.

Sugita S. Schultz P. H.

*Impact Jetting: Comparison Between Spectroscopic Observations and a Standard Theory* **[#1842]**

Using a newly developed spectroscopic method, we measured jetting temperatures for blunt-body impacts. Comparison with a standard theory indicates that additional heating mechanisms other than shock heating may take place during impact jetting.

Flynn G. J. Klöck W. Krompholz R.

*Speed of Sound, Elastic and Shear Modulus Measurements on Meteorites: Implications for Cratering and Disruption of Asteroids* **[#1073]**

The longitudinal and shear wave velocities and elastic and shear moduli were measured for Richfield, Axtell, and Mt. Tazerzait. Mt. Tazerzait, which has visible porosity, has properties similar to concrete and distinct from terrestrial basalt.

Stewart S. T. Ahrens T. J. Lange M. A.

*Correction to the Dynamic Tensile Strength of Ice and Ice-Silicate Mixtures (Lange & Ahrens 1983)* **[#2037]**

We present a correction to the Weibull parameters for ice and ice-silicate mixtures (Lange & Ahrens 1983). These parameters relate the dynamic tensile strength to the strain rate. These data are useful for continuum fracture models of ice.

Kenkmann T. Greshake A. Schmitt R. T. Tagle R. Claeys P. Stöffler D.

*Naturally Shock-induced Phase Transformations in a Dolomite-Sandstone: An Example from the Popigai Impact Crater, Siberia* **[#1561]**

The study of a carbonate fragment from the Popigai crater demonstrates that the textural and phase reorganization induced by shock and post-shock melting occurred only at the micrometer scale and that about 22 wt.% $CO_2$ was released from the system.

Bass D. S. Murphy W. M. Miller G. P. Walker J. D.

*Smashing into Rock and Organic Molecules at 11.2 km/second: Preliminary Results Regarding the Stability of Organic Molecules Under Hypervelocity Impact Conditions* **[#1077]**

Impacting crustal rock and a PAH at 11.2 km/sec resulted in a distinct chemical and physical pattern away from the impact site that suggests that organic molecules may survive a hypervelocity impact.

Croskell M. S.

*Ejecta Dispersal and Infra-Red Pulse Generation by the Chicxulub Impact* **[#1745]**

The mass and trajectories of the material ejected from the Chicxulub impact structure are calculated, to quantify the heat pulse generated by the ejecta re-entry and its potential effect on the biosphere.

Pierazzo E.

*Projectile Melting in Impact Events: Shape Effects* **[#1677]**

Several 2D hydrocode simulations were carried out with constant impact velocity and projectile volume but different projectile shapes. The results show that impactor shape strongly affects the intensity of the shock inside the impactor.

Gerasimov M. V. Dikov Yu. P. Yakovlev O. I Wlotzka F.
*Nitrogen Impact-induced Outgassing and Ingassing During the Earth's Accretion Stage* **[#1593]**
The paper deals with the problem of impact-induced volatilization of nitrogen during Earth's accretion and the trapping of atmospheric $N_2$ during impacts by condensing silicates. Experiments prove the trapping of up to 0.3–0.6 wt.% of N in the condensates.

Kurita K. Sekine T. Hirata N.
*Mechanical Evolution of Primordial Materials by Impact Process* **[#1572]**
This report summarizes the shock-induced sintering process, which works to reduce porosity and acquisition of cohesive strength.

## Planetary Surface Processes

Ernst R. E. Buchan K. L.
*Paleo-Stress Patterns from Giant Dyke Swarms* **[#1737]**
Paleo-stress patterns and their causes on Earth and other planetary bodies can be efficiently determined from dyke swarms.

Crumpler L. S. Cashman K. Schultz R.
*Vesicles: A Fundamental Characteristic of Planetary Surface Rocks* **[#2002]**
Vesicles are the most abundant single characteristic of basaltic lava flows. The following (1) outlines what is known about vescle formation in lava flows and (2) their use as records of conditions at the time of emplacement.

Nettles J. W. Coombs C. R. Evans C. A.
*Use of Space Shuttle Imagery to Analyze Mudflow Patterns at Mount Pinatubo, Phillipines* **[#1520]**
Space Shuttle images were compiled and analyzed to determine how lahars from Mt. Pinatubo are changing spatially over time.

Peitersen M. N. Crown D. A.
*Effect of Flow Transitions on Martian and Terrestrial Lava Flow Morphologies: Implications for Modeling* **[#1203]**
Morphologic studies of lava flows demonstrate that flow width behavior changes at pahoehoe/aa transitions and is different in leveed and unleveed sections of flows. The derivation of rheologic parameters may be improved by modeling of flow subdivisions.

Radebaugh J. Christiansen E. H.
*Terrestrial Pluton Sizes: Defining the Relationship Between Planetary Calderas and Magma Chambers* **[#1466]**
Terrestrial pluton diameters are compared with terrestrial caldera diameters to further understand the link between magma chamber size and caldera diameter. A typical pluton diameter in Nevada is only 1 km; much less than a typical ash flow caldera.

Jock M. Smythe W. D. Keszthelyi L. P. Davies A. G.
*Analysis of Kilauea Field Data with Application to Io* **[#1723]**
Using NIMS- and SSI-like instruments, observations have been made of volcanism on Earth. Dual-filter images of active Hawaiian lava flows have enabled us to produce temperature/area histograms and synthesise thermal spectra for comparison to Io data.

Gregg T. K. P. Sakimoto S. E. H.
*Reality Check: Using Analytic Rectangular Channel Flow Solutions to Interpret and Predict Channelized Lava Flow Behavior on Earth and Mars* **[#1490]**
3-D analytic lava channel flow solutions provide more accurate and realistic viscosity and flow rate extimates. This study compares model with data for laboratory channel simulations, active Pu'u O'o and Mauna Loa channels, and MOLA topography of a Mars Elysium channel.

Koenig E. Fink J. H. Anderson F. S.

*Radial Dike Emplacement on Venus: The Effects of a Temperature-dependent Viscosity Structure on Volcanic Edifice Stresses* **[#1938]**

We are developing an elastoviscoplastic finite element model of edifice stresses related to volcano formation, as governed by a temperature dependent viscosity structure, in order to determine the conditions that allow radial dike formation on Venus.

Cabrol N. A. Grin E. A. Landheim R. Greeley R. Kuzmin R. O.

*About the "Non-Evidence" of a Paleolake in Gusev Crater, Mars* **[#1030]**

We show that the evidence for a paleolake in Gusev and intravalley lake in Ma'adim exists and is varied, that the statement of "non-evidence" of its existence and the discussion by the MOC team from one 15×35.5km-image are irrelevant.

Watters T. R. Robinson M. S. Schultz R. A.

*Comparative Studies of Displacement-Length Relations of Lobate Scarps on Mercury and Mars with Terrestrial Faults* **[#1826]**

The displacement-length ratios of thrust faults associated with mercurian and martian lobate scarps are similar and consistent with terrestrial faults. Differences between terrestrial thrust faults and lobate scarps may reflect a contrast in strain.

Christens-Barry W. A.

*Optical Polarimetry of In-Plane and Out-of Plane Scattering from Johnson Space Center Martian Soil Simulant Material* **[#2025]**

Scattered light polarimetry is used to evaluate the "opposition peak" using a martian soil simulant. Results are given for VV, HH, and crossed polarized scattering for various scattering geometries.

Preisinger A. Aslanian S.

*Timescale Calibration of Late Cretaceous and Early Tertiary Marine Sediments by Means of Milankovitch Cycles* **[#1660]**

Rhythmic sedimentation is demonstrated in continuous 100 m long Cretaceous/Tertiary section near Bjala, Bulgaria. The magnetic polarity zones go from C30N to C26R. The timescale is calibrated by 200 precessional Milankovitch cycles of 22.5 kyrs.

Zolotov M. Yu. Shock E.

*Speciation of Nitrogen Compounds in Planetary Volcanic Gases* **[#1895]**

We use thermochemical calculations to constrain the equilibrium abundances of 27 N-bearing gases in planetary volcanic gases under plausible ranges of T, P, $fO_2$ and bulk composition. The mole fractions of $NH_3$ and HCN can be as high as $10^{-5}$ and $10^{-8}$.

Ishiwatari M. Nakajima K. Takehiro S. Hayashi Y.-Y.

*A Numerical Study on the Appearance of Runaway Greenhouse State in a Three-Dimensional Gray Atmosphere* **[#1139]**

We determined the value of solar constant at which the runaway greenhouse state is realized in three-dimensional gray atmosphere and perform the numerical integration of the runaway greenhouse state by use of the atmospheric general circulation model (GCM).

## New Instruments and Techniques

Ocker K. D. Thonnard N.

*The Path to Krypton and Xenon Isotope Measurements from Few-Micron Sized Samples: II. Pulsed UV Laser Microprobing* **[#1622]**

Characterization of a high spatial resolution, low-blank UV laser microprobe system for ultra-sensitive Kr and Xe isotopic analyses using resonance ionization.

Delaney J. S. Dyar M. D. Sutton S. R.
*Mineralogical $Fe^{3+}/\Sigma Fe$ Measurements as Proxies of Volatile Budgets: I Preamble* **[#1704]**
Ferric/ferrous measurements of minerals can now be used to constrain magmatic volatile activities because synchrotron microXANES spectroscopy enables relevant measurements to be made. We introduce some of the problems to which SmX can be applied.

Dyar M. D. Delaney J. S. Sutton S. R.
*Mineralogical $Fe^{3+}/GFe$ Measurements as Proxies of Volatile Budgets: II. Comparison of Micro- and Macro-scale Data, and Applications Such as $K_D$ Derivation* **[#1445]**
Measurements of ferric/ferrous ratios at a petrologically relevant scale are compared with traditional bulk analysis techniques. Good correlation between techniques implies that the microanalysis of oxidation states can finally be made.

Brinckerhoff W. B. Managadze G. G. McEntire R. W. Cheng A. F.
*Characterization of Planetary Surfaces with In-Situ Laser Mass Spectrometry* **[#1752]**
The Laser Ablation Mass Spectrometer (LAMS) is a miniature instrument being developed for future landed missions. We describe LAMS and its elemental and isotopic accuracy with standard and unknown materials.

Vaniman D. Bish D. Chipera S. Sarrazin P. Blake D. Collins S.
*Sample Preparation and Mounting Strategies for Robotic XRD/XRF Analysis* **[#1431]**
Appropriate selection of sample preparation methods, mounting media and methods, and measurement geometry allows robotic X-ray fluorescence and diffraction analysis of soil, eolian, and rock materials.

George T. Tang W. Elliott D. Chang-Chien A. Tevuk D. Madsen L. Leskowitz G. Weitekamp D.
*Miniature Force-detected NMR Spectrometer for In-Situ Chemical and Mineral Characterization* **[#1453]**
This paper describes the development of a novel force-detected NMR spectrometer for in-situ chemical and mineral characterization. The use of MEMS fabrication technologies allow the construction of a sensor head with a mass <2 g and volume <0.2 cc.

Nelson R. M. Hapke B. W. Smythe W. D. Shkuratov Yu. Ovcharenko A. Stankevich D.
*The Reflectance Phase Curve at Very Small Phase Angle: A Comparative Study of Two Goniometers* **[#2068]**
A comparative study of two goniometers used in reflectance studies has begun. We find first order agreement, however we are investigating certain second order effects that we observe.

Reedy R. C. Frankle S. C.
*Neutron-Capture Yields for Obtaining Elemental Abundances from Planetary Gamma-Ray Spectra* **[#1658]**
Yields for gamma rays from neutron-capture reactions have been evaluated using new data, compiled, and compared to older compilations. These yields are needed to convert measured planetary gamma-ray fluxes to good elemental abundances and ratios.

Spohn T. Seiferlin K.
*MUPUS: A Thermal Probe for the Rosetta Lander* **[#1852]**
MUPUS is a thermal probe for the Rosetta lander designed to explore the thermal properties and the energy balance of the near surface layers of Comet P Wirtanen as it approaches the sun.

Okada T. Kato M. Shirai K. Yamamoto Y. Yamashita Y.
*Development of CCD-based X-Ray Spectrometer Onboard S310-28 Sounding Rocket and Its Future Applications to the Planetary Exploration* **[#2007]**
We developed the CCD-based X-ray spectrometer (XRS) onboard the S310-28 sounding rocket and performed its pre-launch tests. We present the main objectives and specification of the XRS and its future applications to planetary exploration.

Feldman J. Wilcox J. Z. George T. Barsic D. N. Scherer A.
*Atmospheric Electron X-Ray Spectrometer (AEXS) Development* **[#1422]**
This paper describes the development and current status of the JPL-proposed Atmospheric Electron X-ray Spectrometer (AEXS) for the in-situ elemental identification via electron beam-induced X-ray fluorescence of planetary rocks and minerals.

Wiens R. C. Blacic J. D. Cremers D. A. Ritzau S. M. Nordholt J. E. Funsten H. O.
*Laser Induced-Plasma Ion Mass Spectrometry for Characterization of Lunar and Planetary Surfaces* **[#1424]**
LIMS is being developed to perform isotopic and elemental analysis of lunar and planetary surfaces at standoff distances. It uses an advanced ion mass spectrometer to obtain mass and energy spectra from the ionized plume produced by a laser.

Davies A. G. Keszthelyi L. P. Smythe W. D. Jock M. Calis N.
*Field Experiments on Kilauea with SSI- and NIMS-like Instruments* **[#1458]**
A digital camera with motorized filter wheel, and an InSb detector, are used as analogs to SSI and NIMS on Galileo. These analog instruments have been used to observe volcanism on Earth, in order to better interpret Galileo data from Io.

Marshall J. Farrell W. Houser G. Bratton C.
*Radio Frequencies Emitted by Mobile Granular Materials: A Basis for Remote Sensing of Sand and Dust Activity on Mars and Earth* **[#1165]**
RF bursts emitted by grains of sand colliding with an antenna might be used to detect motion and composition of aeolian, volcanic, or other mobile granular materials on planetary surfaces.

Anderson W. W. Johnson M. Manker J. P. Askren D. R.
*X-Ray Diffractometer Using a Radioisotope Radiation Source* **[#1471]**
We have developed an X-ray diffractometer using a Fe-55 source. The data were collected with a scintillation screen and CCD. Tests confirm that diffraction patterns can be obtained, suggesting the feasibility of Fe-55 sources for flight instruments.

Slade M. A. Harmon J. K. Goldstein R. M. Jurgens R. F. Standish E. M.
*A New Technique for High-Accuracy Measurement of Mercury Obliquity and Wobble* **[#1143]**
A new technique is proposed for Earth-based high-precision measurements of the obliquity and libration in longitude. Mercury-Orbiter-based measurements of these quanitities will suffer from the large non-gravitational forces on such a spacecraft.

Musselman Z. A. Shepard M. K.
*A Test of a Common Super-Resolution Algorithm* **[#1157]**
We present results of a test of a super-resolution algorithm proposed and used by T. Parker (JPL).

## Digital Datasets

Hare T. M. Tanaka K. L.
*Planetary Geographic Information Systems (GIS) on the Web* **[#1456]**
We are producing a Web-based, user-friendly interface that will integrate powerful Geographic Information Systems (GIS) and Planetary Data System (PDS) graphical, statistical, and spatial relational tools for analyses of planetary datasets.

Acton C. H.
*SPICE Products Available to the Planetary Science Community* **[#1233]**
SPICE ancillary data and allied software are available for numerous NASA missions, with more to come. SPICE products are freely available to the planetary science community, provided by the NAIF node of the Planetary Data System.

Shepard M. K. Musselman Z. A.
*Geomorphology from Space — Radar* **[#1212]**
We present a dataset of optical and microwave images of diverse geological regions, based upon the text "Geomorphology from Space", NASA SP-486. Images are on CD-ROM in a simple HTML interface. The primary purpose of the data set is a teaching/learning tool.

**Friday, March 19, 1999**
**NEAR-FUTURE MARS MISSIONS**
**8:30 a.m. Room A**

**Chairs:** **R. E. Arvidson**
**S. M. Clifford**

Malin M. C. Bell J. F. III* Calvin W. M. Caplinger M. A. Clancy R. T. Haberle R. M. James P. B. Lee S. W. Ravine M. A. Thomas P. Wolff M. J.
*The Mars Color Imager (MARCI) Investigation on the Mars Climate Orbiter Mission* **[#1437]**
This abstract describes the instrumental characteristics and goals of the Mars Color Imager investigation, recently launched on the Mars Climate Orbiter mission.

Herkenhoff K. E.* Bridges N. T. Kirk R. L.
*Geologic Studies of the Mars Surveyor 1998 Landing Area* **[#1120]**
Preliminary photoclinometric analysis of a 33 m/pixel MOC narrow-angle image of the south polar residual cap shows a root-mean-square bi-directional slope at the limit of image resolution of 1.6 degrees and a maximum slope of 6 degrees.

Houben H.*
*Soil Moisture Predictions for Mars Polar Lander* **[#1884]**
Based on three-dimensional modeling of the seasonal water cycle, about 0.2–1 kg/cu-m or 150–750 ppm by mass of adsorbed water (but no near-surface water ice) is predicted in the martian soil at the sites of the Mars Polar Lander and Deep Space 2.

Saunders R. S.* Ahlf P. R. Arvidson R. E. Badhwar G. Boynton W. V. Christensen P. R. Friedman L. D. Kaplan D. Malin M. Meloy T. Meyer M. Mitrofonov I. G. Smith P. Squyres S. W.
*Mars 2001 Mission: Science Overview* **[#1769]**
The Mars 2001 mission — orbiter, lander and rover — completes global mapping lost with Mars Observer and begins the era leading to first sample return.

Arvidson R.* Bell J. F. III Kaplan D. Marshall J. Mishkin A. Saunders S. Smith P. Squyres S.
*Mars 2001 Lander Mission: Measurement Synergy through Coordinated Operations Planning and Implementation* **[#1428]**
The Science Operations Working Group, Mars 2001 Mission, has developed coordinated plans for scientific observations that treat the instruments as an integrated payload. This approach ensures maximum return of scientific information.

Christensen P. R.* Jakosky B. M. Kieffer H. H. Malin M. McSween H. Y. Jr. Nealson K. Mehall G. Silverman S. Ferry S.
*The Thermal Emission Imaging System (THEMIS) Instrument for the 2001 Orbiter* **[#1470]**
The Thermal Emission Imaging System (THEMIS) will acquire IR images in 8 spectral bands from 6.5 to 14.5 μm at 100 m resolution to determine surface mineralogy. It will also acquire 20 m resolution visible images in up to 5 spectral bands.

Mitrofanov I. G.* Anfimov D. S. Boynton W. V. Hundorin S. P. Kondabarov A. A. Litvak M. L. Litvin D. A. Pikel'ner L. B. Popov Yu. P. Shvetsov V. N. Strelkov A. V. Tonshev A. K.
*Russian High Energy Neutron Detector HEND for Mars Surveyor Orbiter 2001 Mission* **[#1550]**
HEND, as part of the Gamma-Ray Spectrometer facility of Mars Surveyor 2001, will provide the map of high-energy neutron albedo, which will allow identification of specific lines detected by GRS as well as surface regions with water ice deposits.

Marshall J.* Anderson M. Buehler M. Frant M. Fuerstenau S. Hecht M. Keller U. Markiewicz W. Meloy T. Pike T. Schubert W. Smith P.

*The MECA Payload as an Exobiology Laboratory on the MSP 2001 Lander* **[#1164]**

The MECA payload for MSP 2001 is a HEDS experiment for determining the properties of martian soil that may be detrimental to human exploration, but it is also well equipped to address a variety of exobiology questions.

Clifford S. M.* Marshall J.

*Characterization of Regolith Volatile Transport and Storage Properties by the MECA Payload on the MSP 2001 Lander* **[#1985]**

The MECA payload on the MSP 2001 Lander will provide significant new insights regarding the volatile transport and storage properties of the martian regolith.

Kaplan D. I.* Ratliff J. E. Baird R. S. Sanders G. B. Johnson K. R. Karlmann P. B. Juanero K. J. Baraona C. R. Landis G. A. Jenkins P. P. Scheiman D. A.

*In-Situ Propellant Production on Mars: The First Flight Demonstration* **[#1797]**

The Mars In-situ-propellant-production Precursor (MIP) Flight Demonstration is a payload onboard the MARS SURVEYOR 2001 Lander. MIP will demonstrate the production of propellant-grade oxygen using martian atmospheric $CO_2$ as feedstock.

Chicarro A. F.*

*The Mars Express Mission in 2003* **[#1646]**

The ESA Mars Express mission's scientific goals include high-resolution imaging, atmospheric circulation and composition, subsurface structure, and geochemistry and exobiology of the landing site.

Plaut J. J.*

*Probing the Crust of Mars with Orbital Sounding Radar: The MARSIS Experiment on Mars Express* **[#1136]**

The ESA Mars Express mission will carry an orbital sounding radar to Mars in 2003. The primary objective of the MARSIS experiment is to map the distribution of water, both liquid and solid, in the upper portions of the rust of Mars.

Allen C. C.*

*Effects of Sterilizing Gamma Radiation on Mars Analog Rocks and Minerals* **[#1195]**

A $^{60}Co$ gamma dose of 3 Mrad killed fungi and bacteria in basalt and Mars soil simulant. 30 Mrad yielded no changes in the isotope ratios or elemental composition of basalt, nor the crystal structures of 12 rocks and minerals. The only effects were changes in color and TL.

**Friday, March 19, 1999**
**IRON METEORITES AND PLATINUM-GROUP ELEMENTS**
**8:30 a.m. Room B**

**Chair: G. R. Huss**

Campbell A. J. Humayun M.*
*Microanalysis of Platinum Group Elements in Iron Meteorites Using Laser Ablation ICP-MS* **[#1974]**
Laser ablation ICP-MS was used to measure concentrations of PGEs, Re, and Au in 17 iron meteorites on a spatial scale of <20 microns. Data on bulk compositions and PGE microdistributions in irons are reported.

Huss G. R.* Hsu W. Wasserburg G. J.
*Ion-Probe Measurement of Os, Ir, Pt, and Au Abundances in Iron Meteorites* **[#1493]**
We describe an improved technique for obtaining abundances of Os, Ir, Pt, and Au in iron meteorites by ion probe. Data for five irons agree well with previous bulk measurements. Os, Ir, Pt, and Au are enriched in taenite and show M-shaped profiles.

McDonough W. F.* Horn I. Lange D. Rudnick R. L.
*Distribution of Platinum Group Elements Between Phases in Iron Meteorites* **[#2062]**
Platinum Group Elements (PGE: Ru, Rh, Pd, Os, Ir, and Pt), Re, Au and other trace siderophile elements in minerals from iron meteorites have been measured in situ by laser ablation ICP-MS (inductively coupled plasma-mass spectrometry).

Horan M. F.* Walker R. J. Morgan J. W.
*High Precision Measurements of Pt and Os in Chondrites* **[#1412]**
Platinum and osmium abundances were determined by isotope dilution for carbonaceous, ordinary, and enstatite chondrites. Preliminary data suggest that Pt/Os ratios in ordinary chondrites are higher by about 10% compared to enstatite and carbonaceous chondrites.

Wasson J. T.*
*The Trapped-Melt Model of Formation for IIIAB Irons: Ge-Au and Ga-Au Trends* **[#1477]**
Crescent-shaped Ge-Au and Ga-Au distributions in IIIAB iron meteorites are well simulated by a model involving fractional crystallization and the incorporation of trapped melt into the crystallizing solid.

Mathew K. J.* Marti K. Lavielle B.
*Nitrogen Isotopic Signatures of Chondritic Metal in Relation to Iron Meteorite Groups* **[#1426]**
The nitrogen isotopic signatures in iron meteorites and in chondritic metal are affected by spallation components. Corrected trapped N signatures can be used to assess origin, histories and genetic relations of parent objects.

Scott E. R. D.* Pinault L. J.
*Partial Melting and Incipient Segregation of Troilite and Metal in Winonaites, Acapulcoites, IAB and IIE Irons, and Fine-Grained H6 Chondrites* **[#1507]**
Fine-grained H6 chondrites like Portales Valley resemble primitive achondrites, acapulcoites and winonaites. Troilite and Fe,Ni were mobilized as Fe-Ni-S melts causing recrystallization of silicates.

Yin Q. Z.* Yamashita K. Jacobsen S. B.
*Investigating the Timescale of Metal-Silicate (Core-Mantle) Differentiation Using Hf-W and Tc-Mo Extinct Chronometers* **[#2049]**
We report new Mo isotope results in several group of iron meteorites with various Re/Mo ratios and the carbonaceous chondrite Allende. We also report the W isotopic composition of the 3.3 Ga scheelite from Malene, Greenland.

**Friday, March 19, 1999**
**EUROPA**
**8:30 a.m. Room C**

**Chairs:** **J. R. Spencer**
**L. Wilson**

Dalton J. B.* Clark R. N.
*Observational Constraints on Europa's Surface Composition from Galileo NIMS Data* **[#2064]**
Detailed spectral analysis of Galileo NIMS data reveals a number of spectral features which have been used to provide constraints on surface composition for use in mapping.

McCord T. B.* Hansen G. B. Matson D. L. Johnson T. V. Crowley J. K. Fanale F. P. Carlson R. W. Smythe W. D. Martin P. D. Hibbitts C. A. Granahan J. C. Ocampo A. Galileo NIMS Team
*Evidence for Hydrated Salt Minerals on Europa's Surface* **[#1508]**
Observations of hydrated salt minerals in well-defined areas on Europa's surface are reported based on distorted water absorption bands in Galileo-NIMS reflectance spectra. This is consistent with Europa models and a subsurface briny ocean.

Spencer J. R.* Tamppari L. K. Martin T. Z. Travis L. D.
*Nighttime Thermal Anomalies on Europa* **[#1968]**
Galileo PPR thermal observations of Europa show large, puzzling, variations in nighttime temperature: in some areas the equator is colder than mid-latitudes. Latitude-dependent thermal inertia, or surprisingly high levels of endogenic heat flow, are implied.

Van Cleve J. E.* Pappalardo R. T. Spencer J. R.
*Thermal Palimpsests on Europa: How to Detect Sites of Current Activity* **[#1815]**
The most recently active areas on Europa are the most interesting, and could be effectively located using thermal imaging. We show that eruptions of warm ice or liquid water would be detectable from orbit as thermal anomalies for time scales of decades to centuries.

Sullivan R.* Pappalardo R. Prockter L. Klemaszewski J. Galileo Imaging Team
*Europa: High Resolution Views of Spreading at Thynia Linea* **[#2059]**
In this work we analyze spreading at Thynia Linea, a 25 km wide band seen in 40 m/pixel Galileo SSI images obtained during orbit 17 of the Galileo Europa Mission.

Geissler P.* Greenberg R. Hoppa G. V. Tufts B. R. Milazzo M. Galileo Imaging Team
*Rotation of Lineaments in Europa's Southern Hemisphere* **[#1743]**
Succesive generations of lineaments in a newly imaged region of Europa's southern hemisphere appear to have rotated in an anticlockwise sense, consistent with the predictions of non-synchronous planetary spin.

Wilson L.* Head J. W. III
*Cryomagmatism: Processes of Generation, Ascent and Eruption and Application to Europa* **[#1689]**
Cryomagmatic processes are examined for Europa, particularly the cases of water mixed with impurities.

Greenberg R.* Hoppa G. V. Tufts B. R. Geissler P. Riley J.
*Chaos, Cracks and Ridges: Surface Effects of Thin Ice over Liquid Water on Europa* **[#1421]**
Formation of chaotic terrain by melt-through from below, and tectonic terrain (cracks, ridges, and bands) by tides have probably been the two dominant diachronous resurfacing processes over Europa's geological history.

Spaun N. A.* Head J. W. III Pappalardo R. T. Galileo SSI Team
*Chaos and Lenticulae on Europa: Structure, Morphology and Comparative Analysis* **[#1276]**
Micro-chaos material in lenticulae is morphologically similar to the internal texture of chaos. We find chaos forms and grows by fracturing and incorporation of lenticulae, suggesting a possible origin of chaos by coalescence of diapiric lenticulae.

Pappalardo R. T.* Head J. W. Galileo Imaging Team
*Europa: Role of the Ductile Layer* **[#1967]**
Europa's subsurface ductile layer may play the principal role in shaping the satellite's surface geology. Intense surface deformation may reflect high heat flow and a thin brittle lithosphere above a warm ice asthenosphere.

McKinnon W. B.* Gurnis M.
*On Initiation of Convection in Europa's Floating Ice Shell (And the Existence of the Ocean Below)* **[#2058]**
New numerical calculations of convection in Europa's icy shell are described, with implications for geology and radar sounding.

Moore J. M.* Asphaug E. Morrison D. Sullivan R. J. Bierhaus B. Chapman C. R. Greeley R. Klemaszewski J. E. Kadel S. Chuang F. Moreau J. Williams K. K. Turtle E. P. Phillips C. B. Geissler P. E. McEwen A. S. Head J. W. Pappalardo R. T. Collins G. C. Giese B. Wagner R. Neukum G. Klaasen K. P. Breneman H. H. McGee K. P. Senske D. A. Granahan J. Belton M. J. S. Schenk P. M. Galileo SSI Team
*Impact Features on Europa: Results of the Galileo Europa Mission (GEM)* **[#1485]**
GEM-era investigations of impact features on Europa have focused on: (1) the deposits of Mannann'an; (2) Tegid; (3) the topography of craters; (4) Pwyll secondaries; and (5) a survey and ordering of all primary impact features.

Neukum G.* Wagner R. Wolf U. Galileo SSI Team
*Cratering Record of Europa and Implications for Time-Scale and Crustal Development* **[#1992]**
Crater size-frequency distributions on the Galilean satellites have been examined using Galileo high-resolution images. In this paper we derive time-scales for impact events on Europa and implications for crustal development.

**Friday, March 19, 1999**
**CHONDRITES II: PORTALES VALLEY AND OTHERS**
**8:30 a.m. Room D**

**Chairs: K. C. Welten**
**A. Ruzicka**

Kring D. A.* Hill D. H. Gleason J. D.
*Portales Valley Meteorite: The Brecciated and Metal-veined Floor of a >20 Km Diameter Crater on an H-chondrite Asteroid* **[#1618]**
We describe a new meteorite, Portales Valley, which is the first known ordinary chondrite with Widmanstatten structure. The structure occurs in large metal-rich veins that appear to have been produced by an impact event on an asteroid.

Pinault L. J.* Scott E. R. D. Bogard D. D. Keil K.
*Extraordinary Properties of the Metal-Veined, H6 Portales Valley Chondrite: Evidence for Internal Heating Versus Shock-Melting Origins* **[#2048]**
The Portales Valley H6 chondrite is a unique unshocked ordinary chondrite, as it contains metal veins with Widmanstatten structure. All troilite was melted, probably not by shock.

Chen J. H.* Papanastassiou D. A. Wasserburg G. J.
*Re-Os and Pd-Ag Systematics in the Metal-Rich Chondrite Portales Valley* **[#1472]**
Both metal and WR in Portales Valley have similar $^{187}Os/^{188}Os$, but variable $^{187}Re/^{188}Os$. They are compatible with the iron meteorite evolution. The metal has a low $^{108}Pd/^{109}Ag$ and a normal Ag, indicating that the parent of PV did not have live $^{107}Pd$.

Bonino G.* Cini Castagnoli G. Taricco C. Bhandari N. Killgore M.
*Cosmogenic Radionuclides and Tracks in the Fresh Fall Portales Valley* **[#1355]**
On 13 June 1998, a shower fell in Portales, New Mexico. One fragment was used for measurement of the cosmogenic radionuclides. The results compared to those of Torino(1988) and Fermo(1996) show that the 3 meteorites were exposed to similar GCR flux

Ruzicka A.* Snyder G. A. Prinz M. Taylor L. A.
*Portales Valley: A New Metal-Phosphate-rich Meteorite with Affinities to Netschaevo and H-Group Chondrites* **[#1645]**
We report the results of petrographic, electron microprobe, and trace-element (SIMS) studies of the new meteorite Portales Valley that offer insights into its formation.

Rubin A. E.* Ulff-Møller F.
*The Portales Valley Meteorite Breccia: Evidence for Impact-induced Metamorphism of an Ordinary Chondrite* **[#1125]**
The Portales Valley H chondrite breccia was annealed, invaded by molten metal and partly melted during an impact event on its parent body. Its Widmanstatten pattern indicates slow cooling after the impact. Impact heating could account for metamorphism in all type 4–6 OCs.

Wolf S. F. Lipschutz M. E.*
*Contents of Highly Labile Trace Elements in H4–6 Chondrite Falls are not Affected by Post-Accretionary Heating* **[#1110]**
Contents of volatile trace elements in H4–6 chondrites were established during nebular condensation and accretion and the most thermally labile of these were unaffected by metamorphism of their parent bodies, shock heating or close solar approach.

Greenwood J. P.* Rubin A. E. Wasson J. T.
*Possible Oxygen-Isotopic Heterogeneity in R Chondrites* **[#1771]**
In this study, we have analyzed oxygen isotopes of individual olivine and magnetite grains by ion microprobe from an unequilibrated R(?) clast in PCA91241(R3.8) to investigate if further insights can be gained into the origin of elevated $\delta^{17}O$ in R chondrites.

Varela M. E.* Bonnin-Mosbah M. Métrich N. Duraud J. P. Kurat G.
*Carbon and Nitrogen Micro-Analysis of Glass Inclusions in Allende (CV) Olivine by Nuclear Reactions* **[#1341]**
C and N contents were determined by nuclear reactions in olivines and glass inclusions from the Allende (CV) chondrite. Olivine: C < 70 ppm, N up to 1.5 % at 20 µm depth. Glass inclusions: C = 600–1600 ppm, N up to 7000 ppm at 20 µm depth.

Polnau E.* Eugster O. Krähenbühl U. Gnos E.
*Solar Noble Gases in a Low Density Phase of the H Chondrites Kalvesta and ALH76008: Evidence for a Primitive Plagioclase Crust of the Chondrite Parent Asteroid(s)?* **[#1242]**
In an earlier work we observed solar noble gases in a plagioclase rich mineral phase of ALH76008. Therefore we prepared mineral separates of Kalvesta and found also solar gases in a plagioclase rich mineral phase of this meteorite.

Welten K. C.* Masarik J. Nishiizumi K. Caffee M. W. Wieler R.
*Neutron-Capture Production of $^{36}Cl$ and $^{41}Ca$ in Two H-Chondrite Showers from Frontier Mountain, Antarctica* **[#1899]**
We determined the neutron-capture component of $^{36}Cl$ and $^{41}Ca$ in the silicate phase of two Antarctic H-chondrite showers. The results are compared with model calculations to estimate the pre-atmospheric size and constrain the exposure history.

Patzer A.* Scherer P. Weber H. W. Schultz L.
*New Exposure Ages of Chondrites: Short Transfer Times from Asteroid Belt to Earth* **[#1145]**
Noble gases have been measured in 6 chondrites with exposure ages around/less than 1 Ma, including Galim (a) and (b) which belong to the same meteoroid. The delivery of meteorites from the asteroid belt to Earth can be as fast as 30 Ka.

Ferko T. E.* Schultz L. Francke L. Bogard D. D. Garrison D. H. Hutchison R. Lipschutz M. E.
*Cosmogenic Nuclides in a Large Meteoroid — Another Example of a Complex Exposure?* **[#1425]**
Cosmogenic radionuclide and noble gas measurement results are reported for ten samples from the Mocs meteorite strewnfield. While evidence of a simple exposure history is examined a more likely complex exposure is also described.

## PRINT ONLY PRESENTATIONS

### Future Planetary Missions

Armesto V. Belmar J. González C. Huete J. Ordóñez Y.

*A Mission Concept for the Search of Potential Microbial Activity in the Galilean Satellites* **[#1580]**
We propose a mission for the search of potential signs of microbial life in the Jovian system. The mission is composed of one orbiter and four landers, one for each of the Galilean satellites.

Stoker C. R. Cabrol N. Roush T. Gulick V. Hovde G. Moersch J. Marsokhod Rover Team

*1999 Marsokhod Field Experiment: A Simulation of a Mars Rover Science Mission* **[#1278]**
An experiment simulating a rover mission to Mars was performed at a field site representing an analog to a high priority Mars landing site. The experiment design, rover, science payload, science team, science interpretation, and ground truth results are described.

Lucchitta B. K.

*Mysteries of Valles Marineris: What Can We Learn from Future Exploration?* **[#1297]**
Summary of outstanding problems, with emphasis on history, wall-rock composition and morphology, interior deposits, landslides, and dark materials. Discussed are alternative hypotheses and solutions that may come from future exploration.

Avduevsky V. S. Akim E. L. Eflmov G. B. Eneev T. M. Marov M. Ya. Kulikov S. D. Papkov O. V. Konstantinov M. S. Popov G. A.

*Space Vehicle of New Generation: Missions to Phobos and Other Minor Bodies* **[#1219]**
Planetary exploration is a cornerstone of space science and technology development. To accommodate the new political and economical motivations and to recover with the Russian planetary program after the Mars 96 loss.

Tsurutani B. T. Klaasen K. P. Terrile R. J. Gloeckler G.

*Outer Planets/Solar Probe Project: Solar Probe* **[#1874]**
Solar Probe is the third mission of NASA's OP/SP Project. It will be the first mission to a star. The mission, its technological challenges, and its science objectives will be discussed.

### Impacts

Badjukov D. D. Raitala J. Petrova T. L.

*Metal and Sulfide Inclusions in the Lappajarvi Impact Melts* **[#1585]**
Impactites from the Lappajarvi crater are characterized both by enrichment in siderophiles and a presence of iron metal and sulfide inclusions. Composition metal droplets indicate a terrestrial source for the impactites and their origin to be by reduction processes.

Chicarro A. F. Zender J. J.

*Impact Cratering Pulses Throughout the Earth's History* **[#1653]**
The terrestrial cratering record is not constant over the last 600 million years but shows 4 peaks of impact activity (Ordovician, Carboniferous, Cretaceous, Eocene), most craters occurring at epoch boundaries.

De Carli P. S. Bowden E. Jones A. P.

*Evidence for Kinetic Effects on Shock Metamorphism of Quartz* **[#1563]**
This paper cites evidence for kinetic effects on the transformation of crystalline quartz to diaplectic glass. Kinetic effects must be quantified if we are to extrapolate from the microsecond regime of laboratory experiments to a second at pressure in a large impact.

Fel'dman V. I. Arbuzova E. E.
*Some Petrochemical Features of Impact Melt Rocks in Zhamanshin Astrobleme* **[#1182]**
Astrobleme Zhamanshin is a large and young impact structure. There are more than 700 chemical analyses of target rocks and impactites. Examination of these data let us show some characteristic features of impact melting of target rocks and degassing of impact melt.

Glotch T. Bottke W. F. Love S. G. Tytell D.
*The Elliptical Crater Populations on the Moon, Mars, and Venus* **[#1441]**
Asteroids striking a planetary surface at shallow angles produce elliptical-shaped craters. Our surveys of the Moon, Venus, and Mars show each have 5% elliptical craters, contrary to experimental predictions. We resolve this discrepancy in our abstract.

Hildebrand A. R. Brown P. Crawford D. Boslough M. Chael E. Revelle D. Doser D. Tagliaferri E. Rathbun D. Cooke D. Adcock C. Karner J.
*The El Paso Superbolide of October 9, 1997* **[#1525]**
The October 9, 1997 El Paso superbolide was recorded by satellite systems, seismographs, infrasound arrays and numerous video and still photographers. The terminal disaggregation released ~$2 \times 10^{12}$ J corresponding to a total mass of ~15 tonnes.

Hryanina L. P.
*The Bouquet of the Meteorite Craters in the Epicentre of Tunguska Impact 1908 Year* **[#1186]**
The Great Depression in the epicentre of impact 1908 is a bouquet of 3–4 meteorite structures of P-T age. It has signs of meteorite genesis.

Hryanina L. P. Vityasev A. V.
*Arkhys — The First Meteorite Crater in the Caucasus* **[#1183]**
The Arkhys meteorite crater is a depression in the valley of the Zelenchuk River. The break valleys were formed in the Lage Zelenchuk and Kisgych Rivers.

Kettrup B. Deutsch A.
*Chicxulub Impactites: Sr, Nd Isotope Composition of Melt Rocks and Basement Clasts* **[#1184]**
Basement clasts in Chicxulub drillcore samples show other Sr, Nd isotope composition than impact melt lithologies. The data set implies that more than two precursor components are essential to form Chicxulub impact melt.

Kotelnikov S. I. Feldman V. I.
*The Clinopyroxene X-Ray Maxima Broadering as Possible Geobarometer of Shock Metamorphism* **[#1138]**
The investigation of possibility of shock geobarometer construction on the basis of some characteristics of shocked (up to 44.9 GPa) clinopyroxene shows that the broadering of X-ray maxima is the most convenient effect for pressure estimation.

Langenhorst F. Pesonen L. J. Deutsch A. Hornemann U.
*Shock Experiments on Diabase: Microstructural and Magnetic Properties* **[#1241]**
Shock experiments have been performed on diabase to study the effect of shock on magnetic properties of minerals. TEM suggests that the change in magnetic properties is due to variations in crystal structure of titanomagnetite, the magnetic carrier in diabase.

Lorenz C. A.
*Trace Elements Geochemistry in Impact Melts of the Boltysh Crater, Ukraine* **[#1597]**
We analyzed 22 samples of Boltysh impactites for siderophile elements. The data confirmed low siderophiles abundances in this rock. The non-chondritic element pattern could have resulted from post-impact hydrothermal activity in the crater.

Masaitis V. L. Deutsch A.
*Popigai: Gneiss Bombs Coated with Impact Melt — Heating in the Fireball?* **[#1237]**
Glass coated gneiss bombs at Popigai record the whole impact history (pT path) from shock, ejection through the fireball, accretion of melt on the surfaces, until deposition as fragment in clastic or suevitic breccias.

Miura Y. Kobyashi H. Kedves M. Gucsik A.
*Carbon Source from Limestone Target by Impact Reaction at the K/T Boundary* **[#1522]**
Carbon found at the K/T geological boundaries can be explained by impact reaction between the K/T bolides and limestone target rocks, which are proved by other natural and artificial craters.

Miura Y. Kimura M.
*Investigations of Materials Related with Shock Effects on the Moon, Mars, Mercury and Asteroids* **[#1519]**
Shock-related materials of silica, feldspar, Fe and organic molecules will be found on the Moon, Mars, Mercury and asteroids in future explorations.

Miura Y. Fukuyama S. Gucsik A.
*Grains Formed by Impact Reaction Found at Spherules of Various Impact Craters, Meteoritic Showers and Geological Boundaries* **[#1533]**
New types of impact-related grains of Fe-Ni-Si or Fe-Si in composition found in spherules are collected at various impact craters, meteorite showers and geological boundaries.

Schultz P. H.
*Ejecta Distribution from Oblique Impacts into Particulate Targets* **[#1919]**
Oblique impacts into sand target generate enhancement in ejecta downrange due to the impactor-driven flow field reflecting early-time coupling processes.

Shevchenko V. V.
*On the Cometary Origin of Lunar Polar Ice* **[#1317]**
The results of fall of body with low density and huge mass (type of new giant comet) into lunar surface are considered.

Siebenschock M. Langenhorst F. Schmitt R. T. Stöffler D.
*Impact Diamonds in the Dike Suevite of Unterwilfingen, Ries Crater, Germany* **[#1172]**
Impact diamonds have been found in the strongly altered dike suevite at Lehberg quarry, Unterwilflingen, Ries Crater, Germany. They have formed strictly by martensitic transformation and are a perfect means for detecting impact features in deeply eroded impact structures.

Sokeland W. P.
*Elijah Papers: Three (Recent) Distinct Knocks (Impacts)* **[#1040]**
Impacts of the planet Earth are related in time by the Greenland Ice Cap Temperature Data and the disappearance of the mammoth. This abstract discusses the concept of a thermal model to explain the Triassic to end Cretaceous temperatures.

Spray J. G. Kelley S. P. Dence M. R.
*Geology and $^{40}Ar/^{39}Ar$ Laser Fusion Dating of the Strangways Impact Structure, Northern Territory, Australia* **[#1821]**
We present new ages from two impact melt samples and a granitoid from the central uplift of the Strangways impact structure of Northern Territory, Australia. The melt samples yield an age of 676±12 Ma, while the granitoid yields 1370±60 Ma.

## Interplanetary Dust Particles (IDPs)

Bernhard R. P. See T. H. Hörz F.
*Morphology of Impact Features in Space Exposed Aerogel* **[#1916]**
We interpret the diversity or morphologies of impact features in space-exposed aerogel, including deep tracks and shallow pits, to be the result of variable impact velocities.

Drummond J.   Gardner C.   Kelley M.
*Lasers on the Trail of Leonids* **[#1092]**
A video will be shown of the evolution of two kinds of lingering Leonid meteor trails. One produces great sodium enhancement at 100 km, as measured by lidar, is evanescent, and looks like a smoke ring. The other contains NO sodium, is turbid, and right-angled.

Gounelle M.   Maurette M.   Kurat G.   Hammer C.
*Comparison of the 1998 "Cap-Prudhomme" and "Astrolabe" Antarctic Micrometeorite Collections with the 1996 "South Pole" Collection: Preliminary Implications* **[#1564]**
A comparison of recent collections of large micrometeorites made in Antarctica at 3 distinct sites (Cap-Prudhomme and the Astrolabe ice field in 1998, and South Pole in 1996) gives the first evidence for a compositional change of the micrometeorite flux in recent time.

Hasegawa S.   Fujiwara A.   Morishige K.   Yano H.   Nishimura T.   Sasaki S.   Hamabe Y.   Ohashi H.   Nogami K.   Kawamura T.   Iwai T.   Kobayashi K.   Shibata H.
*Acceleration of Micro-Particles to Hyper Velocities by Using a 3.75 MV Van De Graaff Accelerator* **[#1543]**
A 3.75 MV Van de Graaff electrostatic accelerator was modified to accelerate microparticles, and acceleration testing was carried out. The velocity range is 1–20 km/s for micron or sub-micron particles.

Kearsley A. T.   Graham G. A.   Genge M. J.   Grady M. M.   Wright I. P.
*Measurement of Back-Scattered Electron Coefficient: A Novel Technique to Investigate Matrix in Unmelted Antarctic Micrometeorites* **[#1620]**
Hydrous minerals such as mafic phyllosilicates can be found within sections of Antarctic micrometeorites (and other extra-terrestrial samples?) by the use of electron back-scatter coefficient measurement in a scanning microscope.

Phelps A. W.
*Interstellar Diamond: I. Condensation and Nucleation* **[#1749]**
The formation mechanism(s) of meteoritic and interstellar diamond dust grains has been a subject of debate for many years but few explanations have provided the predictive tools with which to further explore and understand diamond grain formation.

Rietmeijer F. J. M.
*Energy for Dust Modification in the Solar Nebula, and in the First-Formed Protoplanets and Their Present-Day Survivors* **[#1065]**
Internal chemical and structural energy of metastable, vapor-condensed nonstoichiometric amorphous ferromagnesiosilica solids support modification in the earliest accreted protoplanets, viz (thermally-induced amorphization) and hydrocryogenic alteration.

Sasaki S.   Igenbergs E.   Ohashi H.   Münzenmayer R.   Naumann W.   Born M.   Färber G.   Fischer F.   Fujiwara A.   Glasmachers A.   Grün E.   Hamabe Y.   Hofschuster G.   Iglseder H.   Miyamoto H.   Morishige K.   Mukai T.   Nogami K.   Schwehm G.   Svedhem H.   Yamakoshi K.
*Initial Results of Mars Dust Counter (MDC) on Board NOZOMI: Leonids Encounter* **[#1581]**
Mars Dust Counter (MDC) is a lightweight impact-ionization type dust detector, which can determine the mass and velocity of a dust particle. MDC is on board Mars mission NOZOMI. Initial results during the circumterrestrial orbit are given.

## Mars

Bell J. F. III   Bustani D.
*Correlations Between Multispectral and Compositional Properties of Soils and Rocks at the Mars Pathfinder Landing Site* **[#1388]**
We are performing an exhaustive search for correlations between IMP multispectral parameters and APXS chemistry. Our results show the strongest correlations between red/blue and Mg, S, Cl, Si, and Al. Weaker correlations with red/near-IR are also noted.

Crooks J. L.

*Geology of Schroeter Impact Basin, Mars* **[#1312]**

A geological study of Schroeter impact basin, Mars. The current surface geology is studied and a possible basin history is proposed.

Crumpler L. S.

*Southwestern Isidis Basin Margin, Mars Surveyor Landing Site: Summary of Geologic Assessment and New Mgs Data* **[#2015]**

This study summarizes the results of geologic and surface engineering analysis of an area on the southwestern border of Isidis Planitia.

Crumpler L. S.

*MOLA Data for Arsia Mons: New Constraints on Caldera Formation* **[#2036]**

MOLA data for orbit 033 crossed the Arsia Mons edifice and the summit caldera. Review of some of the results anticipate some of relief details and structural insights to be expected during the primary phase of the MGS mission.

Greeley R.

*Mars Pathfinder Landing Site: Simulations of Wind Erosion and Deposition* **[#1300]**

The Mars Pathfinder site was simulated in a wind tunnel test which suggested that the site was subjected to a predominantly deflational (erosional) wind regime.

Greeley R.   Coquilla R.   Wilson G.   White B.   Haberle R.   Soriano J. F.   Bratton C.

*Mars Dust: Laboratory Experiments of Flux as a Function of Surface Roughness* **[#1189]**

The Mars Pathfinder landing site appears to have been subject to net deflation (erosion) by wind, based on wind tunnel simulations of the site which reveal distinctive morphological features for net deflation versus net deposition.

Hargraves R. B.

*Could Mars Dust be a Volcanic Aerosol Deposit?* **[#1364]**

Possibility that Mars dust is volcanic aerosol accumulation is explored.

Jolliff B. L.   Wang A.   Keubler K.   Haskin L. A.   Klingelhöfer G.

*Raman and Mössbauer Characterization of a Rock for Potential Use as an On-Site Calibration Target for In Situ Mineralogy Instruments on the Athena Rover for Mars Surveyor Missions* **[#1529]**

We describe laser Raman and Mössbauer analyses of an on-surface calibration rock target for the Athena Rover. The rock is a magnetite-rich calc-silicate that provides hydrated silicates for Raman calibration and Fe mineralogy for the Mössbauer.

Marshall J.   Bratton C.   Kosmo J.   Trevino R.

*Interaction of Space Suits with Windblown Soil: Preliminary Mars Wind Tunnel Results* **[#1239]**

Mars Wind Tunnel experiments at NASA Ames show that space suit materials are highly susceptibility to dust adhesion when exposed to windblown soil. Long-term function of space suits on Mars could be threatened by the tenacity of the dust contamination.

Michael G. G.   Rodionova J. F.

*The Difference Between the Crater Distribution on the Highland and Plains of Mars in Terms of Rim Degradation* **[#1361]**

A statistical analysis of a data bank of more than 19,000 martian craters shows that there is a difference in the density distribution of craters in terms of their preservation on the martian plains and highlands.

Morris R. V.

*Elemental Compositions of Local Rocks and Global Soil at Pathfinder and Viking Landing Sites: Evidence for Ongoing Comminution of Martian Rocks* **[#1151]**

Major-element correlations at Pathfinder and Viking landing sites are consistent with a model where local soils are two-component mixtures of fragments of local rock and globally-distributed average martian soil, implying ongoing comminution of rocks.

Nikolaeva O. V. Abdrakhimov A. M.

*Rocks of Andesitic Composition at the Mars Pathfinder Site Reveal Chemical Analogy with Subduction-related Andesites of Earth* **[#1376]**

According to McSween et al. (1998), Mars Pathfinder andesite composition is most similar to terrestrial andesites (icelandites) unrelated to subduction, rather than to subduction-related. Our conclusion here is the quite opposite.

Plescia J. B.

*Geology of Ceraunius Tholus, Mars* **[#1632]**

Ceraunius Tholus is a Late Hesperian age basaltic shield volcano in northeast Tharsis formed by both effusive lavas and pyroclastic eruptions. Pyroclastics are basaltic and formed by the interaction of ascending magma and ground water/ice.

Plescia J. B.

*Cerberus Plains — Source for the Young SNCs?* **[#1627]**

Cerberus Plains are interpreted to be the source for some SNCs. The plains are low-viscosity lavas erupted at high rates at 143±40Ma. Shergotty, Zagami, EETA79001, ALH77005 and LEW88516 are basaltic, have ages of 180 Ma and low viscosity and are consistent with a Cerberus source.

Plescia J. B.

*Geology of Uranius Tholus, Mars* **[#1648]**

Uranius Tholus is a small basaltic shield volcano in northeast Tharsis. It is the product of both effusive and pyroclastic eruptions. Based on the geology and regional volcanic context, Uranius Tholus is considered to be Late Hesperian rather than Noachian.

Rochelle W. C. Kirk B. Smith N. DeVall M. Hörz F.

*Atmospheric Entry and Survival of Small Meteorites on Mars* **[#1651]**

Computer calculations/models to determine minimum size, density, and velocity of meteorites that would permit such objects to survive passage through the martian atmosphere and impact the martian surface.

Schultz R. A.

*Planetary Fault Populations Revisited* **[#1056]**

Recent concepts of fault populations have revolutionized how geologists think about brittle deformation. The techniques are analogous to crater statistics and are useful for geologic mappers and those measuring brittle strain.

Stern S. A. Levison H. F.

*A Warm Early Mars and $CO_2$ Influx from the Late Heavy Bombardment* **[#1141]**

We find that a sufficient influx of $CO_2$ was imported to Mars by cometary bombardment during the Late Heavy Bombardment to have induced a one-to-several bar $CO_2$ atmosphere and its consequent warming to a state capable of allowing surface water to have existed on Mars.

Wang A.

*Some Grain Size Effects on Raman Scattering Intensity for In Situ Measurements on Rocks and Soils — Experimental Tests and Modeling* **[#1644]**

The major factors affecting the strength of Raman signals obtained from in situ measurements of rocks and soils are discussed. Experiments show that signal strength decreases with decreasing grain size but not drastically.

Watters T. R. Robinson M. S.

*Topographic Studies of Lobate Scarps Near the Martian Crustal Dichotomy Using MOLA Data* **[#1865]**

MOLA data is being used to study martian lobate scarps in the Amenthes region, near the crustal dichotomy. The dimensions and morphology of a lobate scarp crossed by a MOLA profile agree well with other scarps studied using photoclinometric data.

## Meteorites

Alexeev V. A. Gorin V. D.

*Radioactivity of Gursum H4 Meteorite* **[#1089]**

Contents of radionuclides in the Gursum H4 chondrite are: Aluminum-26 = 58 ± 6 dpm/kg, K = 1600 ± ppm, and Th = 200 ± 100 ppb. The Gursum meteorite fell February 10, 1981.

Alexeev V. A. Ustinova G. K.

*Radiogenic Ages of H- and L-Chondrites with Different Orbits: Some Inferences* **[#1114]**

A correlative analysis of ages and orbits of H- and L-chondrites shows that their parent bodies have been accumulated at ~2 AU from the Sun.

Bogard D. Takeda H. Mittlefehldt D. W. Garrison D.

*Petrology, $^{39}Ar$-$^{40}Ar$ and Exposure Ages, and Chemistry of a Gabbro Area from the Caddo Co. IAB Iron* **[#1253]**

Petrological, chemical and $^{39}$Ar-$^{40}$Ar age studies of silicate from the Caddo County IAB iron reveals a gabbroic area of feldspar and high-Ca pyroxene, enriched in incompatible lithophile elements, and last degassed of $^{40}$Ar 4.52–4.54 Gyr ago.

Bowman L. E. Papike J. J. Spilde M. N.

*Diogenites as Asteroidal Cumulates: Insights from Spinel Chemistry* **[#1008]**

Diogenites may be genetically linked through fractional crystallization in crustal intrusions. The composition of spinel was determined for a suite of 19 diogenites to determine if spinel retains signatures of its igneous history.

Chen J. H. Papanastassiou D. A. Wasserburg G. J.

*Re-Os Systematics in the Allende CAI: Big Al* **[#1483]**

A sample of coarse-grained Allende CAI, Big Al analyzed using reverse aqua regia, plots on the IIA iron meteorite reference isochron, suggesting a very small time difference between the formation of CAIs, chondrites, and iron.

Dyar M. D. Delaney J. S. McGuire A. V. Stefanis M. S. Polyak D. E.

*Mineralogical $Fe^{3+}/\Sigma Fe$ Measurements as Proxies of Volatile Budgets: IV. Crystal Chemistry of Iron in Extraterrestrial Pyroxene* **[#1712]**

The availability of microanalytical techniques for ferric/ferrous determination permits more complete assessment of pyroxene crystal chemistry than has been previously possible. We provide data for pyroxene from 4 bodies including the Earth.

Fisenko A. V. Semjonova L. F.

*P6 Component or Heterogeneous Distribution of Isotopes of Xe-H and Xe-L Components?* **[#1090]**

Explanation of isotopic composition of noble gas in presolar diamonds include the P6 component, a nearly isotopically-normal component that is released at higher temperatures than P3 and HL components.

Fisk M. R. Giovannoni S. J.

*Microbial Weathering of Igneous Rocks: A Tool for Locating Past Life on Mars* **[#1903]**

Some microbes are capable of living in terrestrial igneous rocks, and similar environments exist on Mars. Evidence for microbe on Mars could be found in volcanic glass in ejecta, quenched lavas, or shock melted meteorites.

Ipatov S. I. Mardon A. A.

*Delivery of Meteorites to the Earth from the Edgeworth-Kuiper Belt* **[#1147]**

About 20 percent of near-Earth objects with a diameter d>1 km may have come from the Edgeworth-Kuiper belt. The portion of smaller bodies that came from this belt may be larger, but most of these bodies cannot reach the surface of the Earth.

Kashkarov L. L. Korotkova N. N. Kalinina G. V. Ivliev A. I.

*Different Radiation Thermal History of the Erevan and Kapoeta Howardite Matters at the Regolith Stage* **[#1075]**

The detailed track and thermoluminescence investigation of radiation and shock thermal effects in individual silicate mineral grains of the Erevan and Kapoeta howardites lead us to further study of their radiation thermal history.

Klerner S. Palme H.

*Origin of Chondrules and Matrix in Carbonaceous Chondrites* **[#1272]**

New analytical data are presented that confirm a close genetic relationship of chondrules and matrix in carbonaceous chondrites. Both components must have formed from a single reservoir. Separate and independent formation of matrix and chondrules is not possible.

Krot A. N. Ulyanov A. A. Weber D.

*Al-Diopside-Rich Refractory Inclusions in CH Carbonaceous Chondrites* **[#2018]**

The Al-diopside-rich CAIs from CH chondrites contain Al-diopside as the major mineral; hibonite, grossite, melilite, and spinel are accessory; forsteritic olivine rims are commonly present. These CAIs crystallized from liquids under highly disequilibrium conditions.

Lavrukhina A. K.

*The Nuclear and Astrophysical Interpretations of Isotopic Anomalies in Oxygen of Meteorites* **[#1115]**

These data allow us to propose the presence in protoplanetic nebula of two types of primary matter with various oxygen isotopic compositions.

Lukács B. Bérczi Sz.

*Thermal/Aqueous: on the $H_2O$-$Na_2O$ Competition/Cooperation in Carbonaceous Chondrites (Kaba L., NIPR Statistics V.)* **[#1011]**

In aqueous/thermal metamorphism, during hydration and dehydration process of carbonaceous chondrites $H_2O$ and $Na_2O$ cooperates/competes in the nonterrestrial environment, which can be seen in composition of Kaba and Antarctic (NIPR data) chondrites.

Miyamoto M. Mikouchi T. Kaiden H.

*Diffusional Modification of Igneous Zoning During Crystal Growth: Analysis of Fe-Mg Zoning of Olivine in Semarkona (LL3.0) Porphyritic Olivine Chondrule* **[#1323]**

We computed diffusional modification of Fe-Mg zoning of olivine in Semarkona (LL3.0) porphyritic olivine chondrule formed by closed-system fractional crystallization as olivine crystal grows by solving the diffusion equation to study cooling history.

Nelson V. E. Rubin A. E.

*Size-Frequency Distributions of Chondrules and Chondrule Fragments in the Semarkona LL3.0 Chondrite* **[#1122]**

Chondrules in LL3.0 Semarkona are larger than chondrule fragments (560 vs. 340 micrometers) at a confidence level of >99.999%. This indicates that there was not a significant population of chondrules (larger than those preserved today) that were completely fragmented.

Nishiizumi K. Masarik J. Caffee M. W. Jull A. J. T.

*Exposure Histories of Pair Lunar Meteorites EET 96008 and EET 87521* **[#1980]**

The lunar basaltic breccia EET 96008 is the eighteenth fragment thought to represent fourteen lunar meteorites. We report here preliminary results of cosmogenic $^{14}C$, $^{41}Ca$, $^{36}Cl$, $^{26}Al$, and $^{10}Be$.

Noguchi T.

*Phyllosilicate Bearing Clasts and Dark Inclusions in Vigarano CV3 Chondrite* **[#1740]**

The author found clasts and dark inclusions that show distinct evidence for aqueous alteration predating the final agglomeration of the meteorite. They were investigated by SEM, electron microporobe, and TEM. Most of the phyllosilicate have about 1.0 nm fringe.

Petaev M. I. Meibom A. Krot A. N. Wood J. A.

*The Condensation Origin of Some Metal in CH Chondrites: A Thermodynamic Model* **[#1613]**

Thermodynamic modeling shows that zoned metal grains in the CH chondrite PAT91546 are pristine nebular condensates formed in the solar nebula. Isolation of condensing metal caused by grain growth resulted in condensation of Ni-poor metal in the grain rim.

Petaev M. I. Krot A. N.
*Condensation of CH Chondrite Materials: Inferences from the CWPI Model* **[#1775]**
The mineralogy and mineral chemistry of textural constituents of CH chondrites require their condensation in very different physical-chemical environments which cannot be produced in a classic, monotonically cooling solar nebula.

Podosek F. A. Nichols R. H. Jr. Brannon J. C. Dougherty J. R.
*Cr Isotopic Analyses of Undifferentiated Meteorites* **[#1307]**
We present Cr isotopic analyses of Semarkona leach fractions and of whole rock Orgueil and Allende. Detailed attention is given to mass spectrometric data reduction and error analysis. The results conflict with the monotonic heliocentric gradient interpretation for $^{53}Cr$.

Povenmire H. Wilson I.
*The June 13, 1998, Portales, New Mexico Meteorite Fall and Strewn Field* **[#1071]**
The dimensions of the June 13, 1998, Portales, New Mexico H6 meteorite strewn field are 12 by 2.5 km with an azimuth of 62 degrees.

Povenmire H. Liu W. Xianlin L.
*Australasian Tektites Found in Guangxi Province, China* **[#1072]**
Newly confirmed Australasian tektites have been found in Guangxi Province, China. This is some 500 km NW of Guangdong and represents an important extension of this strewn field.

Rao M. N. Wentworth S. J. Schwandt C. Yang S. R. McKay D. S.
*Molten Martian Soil in Shergotty Meteorite* **[#1626]**
Significant excesses of sulfur are found in Shergotty impact melt glasses.

Richter F. M. Davis A. M.
*Composition Dependence of Evaporative Isotope Fractionation Systematics* **[#1997]**
The trajectory of Si isotope fractionation vs. Mg isotope fractionation in evaporation residues may provide a way of determining whether the fractionated Si and Mg isotopes found in CAIs are due to processes that predate or postdate their formation.

Ruzicka A. Jerde E. A. Snyder G. A. Taylor L. A.
*A Large, Igneous-textured Inclusion Containing Co-Existing Enstatite and Ferroan Olivine in the LEW 86018 (L3.1) Chondrite* **[#1502]**
This abstract presents the results of a petrographic, microprobe, and trace-element study of a large, igneous-textured inclusion, designated LEW-1 in the LEW 86018 (L3.1) chondrite.

Schulze H.
*Mineralogy and Mineral Chemistry of Noble Metal Grains in R Chondrites* **[#1720]**
R chondrites are a highly oxidized chondritic group. Rarely these meteorites contain noble metal phases. In a detailed survey, five R chondrites were carefully examined for such phases which are described in detail.

Skála R. Císarová I.
*Crystal Structure of Schreibersite from Toluca Iron Meteorite* **[#1359]**
The crystal structure refinement of schreibersite single-crystal from Toluca is presented. Preferential occupancy of individual sites in crystal structure by nickel and iron is addressed.

Snyder G. A. Taylor L. A. Patchen A.
*Lunar Meteorite EET 96008, Part I. Petrology and Mineral Chemistry: Evidence of Large-Scale, Late-Stage Fractionation* **[#1499]**
We present petrologic and mineral-chemical data for lunar meteorite EET 96008 which indicates large-scale, late-stage fractionation and pairing with lunar meteorite EET 87521.

Steele A. Goddard D. T. Stapleton D. Toporski J. K. W. Sharples G. Wynn-Williams D. D. McKay D. S.
*Imaging of an Unknown Organism of ALH84001* **[#1326]**
A probable Antarctic contaminant has been found and imaged by SEM. Morphology has been used to try and characterize the organism, which seems to be an Antarctic Actinomycete.

Ustinova G. K.
*Generation of $^{41}$Ca in the Conditions of Shock Wave Propagation in the Early Solar System* **[#1351]**
The $^{41}$Ca generation, being considered in the standard conditions of the shock wave propagation in the early solar system, leads to the interval of the CAI formation in the carbonaceous chondrites of 0.79–0.91 Myr.

Ustinova G. K. Alexeev V. A.
*Galactic Cosmic-Ray Distributions in the Heliosphere During Four Solar Cycles as Evidenced by Radionuclides in Successively Fallen Chondrites* **[#1076]**
A picture of variation of the galactic cosmic ray integral gradients in 1955–1992 along the orbits of 14 fresh-fallen chondrites is presented. Some peculiarities of electromagnetic structure of the heliosphere are derived.

Warren P. H. Ulff-Møller F.
*A Compositional-Petrologic Study of Diverse Cumulate Eucrites, Including a Recent, as Yet Unnamed Fall from Argentina* **[#2054]**
We have studied the bulk composition and petrology of several cumulate eucrites, including a recent fall from Argentina. The Argentine meteorite is an adcumulate uncommonly depleted in incompatible elements, even by cumulate eucrite standards.

Wright I. P. Franchi I. A. Grady M. M. Pillinger C. T.
*Dar Al Gani 476— Lucky for Some, Unlucky for Others* **[#1594]**
The 13th SNC meteorite, Dar al Gani 476, has been analysed for C and $\delta^{13}$C. The sample contains 4.5 wt% carbonate, which is predominantly from desert weathering on Earth. There could be a small quantity of pre-terrestrial carbonate with $\delta^{13}$C of +20‰.

Zinovieva N. G. Mitreikina O. B. Granovsky L. B.
*Matrix Material of the Yamato-74417 Ordinary Chondrite (L3)* **[#1019]**
Three types of matrix material were recognized in the Yamato-74417 ordinary chondrite L3: fine-grained FeO-rich silicate, coarse-grained silicate, and sulfide-metallic. Reaction relations were revealed between the silicate matrix material and chondrules.

## Moon

Lindstrom D. J.
*Trace Element Analyses of Grain Size Separates from Disaggregated Soil Breccia 10068* **[#2014]**
INAA results on disaggregated soil breccia 10068 share some characteristics with lunar soils such as 10084, but differ in many compositional details.

Jolliff B. L Korotev R. L. Arnold S. A.
*Electron Microprobe Analyses of Dar Al Gani Lunar Meteorite, a Sample of the Feldspathic Highlands Terrane of the Moon* **[#2000]**
We report mineral, glass, and fusion crust compositions for the Dar al Gani 262 meteorite, and we compare these to QUE93069. DaG 262 is ferroan and represents another sample from the Feldspathic Highlands Terrane of the Moon, poor in magnesian components.

Haskin L. A. Korotev R. L. Jolliff B. L.
*Clast Provenance in Imbrium Impact-Melt Breccias* **[#1942]**
It is argued that feldspathic clasts in mafic impact-melt breccias produced by the Imbrium impact may derive mainly from outside the basin cavity at the point of impact of secondary molten ejecta.

Lindstrom D. J.
*Accuracy of Rastered-Beam Analysis (RBA) of Lunar Breccia Clasts by Electron Microprobe* **[#1917]**
A model is presented for calculating errors in matrix corrections for multi-phase systems. Errors are negative for elements concentrated in denser phases and vice-versa. Errors are larger for elements in the less abundant phase and for lighter elements.

Lin L. Mustard J. F. Pieters C. M.
*The Effects of Scattered Light in the Clementine UV-VIS Camera on Mixture Analysis* **[#1866]**
Observations across the lunar limb with the Clementine UV-VIS filters shows that there is a distinct stray-light component of scattered light. However, this scattered light does not significantly affect the nature of compositional boundaries due to mixing.

Basu A. Wentworth S. J. McKay D. S.
*Petrography of Disaggregation Products of Regolith Breccia 10068* **[#1850]**
Freeze-thaw disaggregation of the very mature regolith breccia 10068 produced a reasonable proto-regolith, which is fine grained (MZ = 33 mm) and has preserved many agglutinates (12%) and mature recycled regolith breccias (30%).

Snyder G. A. Taylor L. A. Patchen A. Nazarov M. A. Semenova T. S.
*Volcanism at Mare Fecunditatis: Mineralogy and Petrology of "New" Luna 16 Basalts* **[#1494]**
We present petrologic, mineral-chemical, and $^{40}Ar$-$^{39}Ar$ data on Luna 16 mare basalts.

Petrycki J. A. Wilson L.
*Photogeologic Observations of Lunar Nearside Graben* **[#1333]**
We have cataloged the sizes and geometric properties of most of the linear and arcuate rilles found in the Lunar Orbiter data set. Strong associations with specific maria and certain types of mare lavas are found.

Avsyik Yu. N. Alexandrov S. I. Galkin I. N. Gamburtsev A. G. Oleinic O. V.
*Spectral-Temporal Features of Tidal Lunar Seismicity* **[#1331]**
Spectral-temporal analysis of moonquake time series shows the existence of the known tidal rhythmical components and reveals the new ones. The space-time instability in the spectral structure of the lunar seismicity process has been found.

Shevchenko V. V.
*Clementine and Lunokhod-2: Iron Content in the Lunar Crater Le Monnier* **[#1315]**
The idea of calibration of Clementine data by means of Lunokhod-2 in situ measurement is presented.

Korotev R. L.
*A New Estimate of the Composition of the Feldspathic Upper Crust of the Moon* **[#1303]**
A new estimate of the composition of the feldspathic upper crust that is based on the composition of the five most feldspathic lunar meteorites is presented. This estimate (4.2% FeO) agrees well that obtained from the Clementine mission (4.2%).

Korotev R. L.
*Lunar Terranes and the Composition of the Regolith* **[#1302]**
The composition of Apollo soil samples is considered in the context of the lunar terrane concept. Figures are presented showing the relationship of the soils to the Procellarum KREEP Terrane, Feldspathic Highlands Terrane, and mare basalt.

Pugacheva S. G. Shevchenko V. V. Yakovlev S. G. Kibardin V. M.
*Calibration of the Moon's Infrared Images from Geostationary Satellite GOMS* **[#1247]**
A technique is described for the independent radiometric calibration of photometric measurements of the surface photometric brightness and radiation temperature of celestial bodies, based on the Moon as an external standard.

Dikov Yu. P. Wlotzka F. Ivanov A. V. Kantzel V. V. Buleev M. I.

*Auger Analysis of Apollo 17 Orange Soil Sample 74220* **[#1176]**

Two glass spherules analysed show Zn and S enriched on the very surface, but also between 400 and 800 Å a carbon-enriched layer and in the upper 600 Å enrichment of Si and Fe connected with a depletion in refractory Al, Ca, Mg and Ti.

Dikov Yu. P. Wlotzka F. Ivanov A. V.

*XPS Evidence for SiC on the Surface of LUNA-16 Regolith Particles* **[#1012]**

XPS spectra show the presence of SiC (up to 10 atom%) together with elemental carbon (nanodiamond or graphite, 3-8 atom%) between 0 and 1500 Å depth of LUNA-16 soil particles, probably formed by condensation from an impact cloud.

## New Instruments and Techniques

Hamabe Y. Kawamura T. Nogami K. Ohashi H. Shibata H. Sasaki S. Hasegawa S.

*Development of Dust Analyzer with TOF Mass Spectrometry* **[#1760]**

We designed a new dust analyzer with TOF (time-of-flight) mass spectrometer on board spacecraft, and perfomed preliminary experiments with pulsed IR laser irradiation and high velocity particles impact as ion source.

Hendrickson T. R. Colson R. O. Floden A. M. Malum K. M. Holder D. H. Nermoe M. K. B.

*An Improved Method for Measuring Electrode Surface Areas in Electrochemical Experiments in Silicate Melts* **[#1781]**

Uncertainty in the surface area of electrodes is one of the main limitations of electrochemical methods in silicate melts. This experimental technique allows surface areas to be measured and controlled more accurately.

Veres M. Greguss P. Gschwindt A.

*New Image Mapping Method in Planetary Research: Centric Minded Imaging* **[#1175]**

Centric Minded Imaging (CMI) is a new image mapping method with a 360-degree panoramic field of view. In space research it is beneficial to apply as a navigation instrument and a vision module. CMI could serve these subsystems of spacecraft and robots.

## Origins of Planetary Systems

Borisov A.

*Reaction of Palladium with Silica in Reducing Conditions Resulting in Melting of Initially Solid Metal: An Experimental Study* **[#1265]**

I present experimental results on t°-$fO_2$ dependence of pure solid Pd melting in pure solid silica and the implications of the results to the problem of composition of the refractory metal nuggets in CAIs of carbonaceous chondrites.

Humbert F. Marty B. Libourel G.

*Enhanced Solubility of Nitrogen in Basaltic Melt Under Reducing Conditions: A Way to Enrich Nitrogen Relative to Rare Gases During Planetary Formation* **[#1955]**

Incorporation processes of nitrogen in planetary systems was investigated by studying the N solubility in basaltic melt under varying oxygen fugacity.

## Outer Planets and Satellites

Cataldo V.

*Plume Fallout Deposits on Io, Their Colours, and Relationships with Other Coexisting Volcanic Features* **[#1245]**

I discuss the reliability with which silicate particles and condensed volatiles can be distinguished in volcanic deposits on Io's surface. Volatiles condensing on cooled silicate pyroclasts complicate the issues.

Cataldo V.

*The O-H Stretch Transition Inferred from the Observation of the 3.15 $\mu$ m Band in the Infrared Spectra of Io: Two Possible Interpretations* **[#1378]**

We explain the inferred existence of the O-H molecule on Io in two ways: by transport of the molecule to Io by comets, or by the presence of $H_2O$ in erupting magma.

Denk T. Neukum G. Pappalardo R. T. Head J. W. Greeley R. Galileo SSI Team

*Galileo-SSI Color Observations of the Icy Galilean Satellites During the Primary Mission: (1) General Comparison* **[#1872]**

SSI data of Europa, Ganymede and Callisto indicate at least two types of non-ice material spectra in addition to water ice on each moon. Color-ratio diagrams have been used to examine the surface color properties of the Galilean satellites.

Denk T. Neukum G. Wagner R. Greeley R. Galileo SSI Team

*Galileo-SSI Color Observations of the Icy Galilean Satellites During the Primary Mission: (2) Callisto and Europa* **[#1877]**

Callisto shows a planet-wide color dichotomy with presumably irregular boundaries. At least two non-ice components are observed in Europa's brown mottled terrain: a strong violet absorber and a reddish material with a constant spectral slope.

Head J. W. III Pappalardo R. T. Spaun N. A. Prockter L. M. Collins G. C.

*Chaos Terrain on Europa: Characterization from Galileo E12 Very High-Resolution Images of Conamara Chaos: 2. Matrix* **[#1587]**

Analysis of Conamara Chaos shows matrix may form from degraded polygons.

Head J. W. III Pappalardo R. T. Denk T. Spaun N. A. Prockter L. M. Collins G. C. Phillips C. B.

*Conamara Chaos Region: Analysis of Color Variations and Relationship to Geologic Processes* **[#1440]**

Analysis of Europa color data for Conamara Chaos suggests a three stage thermal process: heating and sublimation, disaggregation, and recondensation of frost.

Head J. W. III Pappalardo R. T.

*Brine Mobilization During Lithospheric Heating on Europa: Implications for Formation of Chaos Terrain, Lenticulae Texture, and Color Variations* **[#1664]**

Brine mobilization is proposed as a potentially important process for terrain disaggregation and destruction on Europa.

Head J. W. III Pappalardo R. T. Prockter L. M. Spaun N. A. Collins G. C. Greeley R. Klemaszewski J. Sullivan R. Chapman C. Galileo SSI Team

*Europa: Recent Geological History from Galileo Observations* **[#1404]**

The series of features on Europa and their sequence suggests significant changes in its recent geological history.

McCord T. B. Hansen G. B. Orlando T. M. Sieger M. Crowley J. K. Hibbitts C. A. Van Keulen L.

*Properties of Hydrated Salts Including Under Europa Conditions* **[#1510]**

Laboratory measurements are reported to determine the properties and behavior of hydrated salt minerals including under Europan conditions. These include at low temperatures, for ranges of particle sizes and under electron and ion irratiation.

Ruiz J. Tejero R.

*Heat Flow and Brittle-Ductile Transition in the Ice Shell of Europa* **[#1031]**

Application of rheological profiles technique to ice lithosphere of Europa indicates heat flows, for ~2 km depth brittle-ductile transition (after Galileo observations of Conamara Chaos regio), much higher than obtained from tidal heating models.

Stern S. A. Canup R. Durda D. D.
*Pluto's Family: Debris from the Binary-forming Collision in the 2:3 Resonance?* **[#1213]**
We hypothesize that some fraction of the Edgeworth-Kuiper Belt objects orbiting with Pluto in the 2:3 mean-motion resonance is debris from the Pluto-Charon binary formation event.

Sullivan R. Greeley R. Klemaszewski J. Moreau J. Tufts B. R. Head J. W. III Pappalardo R. Moore J.
*High Resolution Geological Mapping of Ridged Plains on Europa* **[#1925]**
We map ridge morphologies seen in the bright, ridged plains observed by Galileo at 21 m/pixel on the spacecraft's sixth orbit, and discuss possible ridge formational mechanisms.

Tejfel V. G.
*Comparative Study of Latitudinal Zonal Variations of the Methane Absorption and Atmospheric Structure on Jupiter and Saturn* **[#1211]**
The latitudinal variations of the methane absorption bands and the limb darkening on the disks of Jupiter and Saturn were studied by CCD photometry and spectrophotometry.

Thomas C.
*Is Global Expansion of Ganymede Still Required Given New Thermal Evidence from Callisto?* **[#1635]**
The implications of new evidence of an ocean in Callisto are discussed and it is proposed that global expansion may no longer be required to explain the origin of Bright Terrain on Ganymede.

Yamagishi Y. Kurita K.
*The Singularity of the Evolution of the Icy Satellites* **[#1552]**
By investigating the thermal history of icy satellites, we obtained evolutional models that indicate the existence of a molten layer in Europa and a metallic core in Ganymede and the origin of endogenic activities regardless of size.

## Planetary Surface Processes

Cabrol N. A. Grin E. A.
*Sedimentary Record in Martian Impact Crater Paleolakes as Indicators of Past Climate, Hydrogeologic Processes, and Environment Evolution* **[#1023]**
We study how the presence of deltas, terraces, shorelines, mounds and evaporite deposits reveals the past climate, hydrogeology, and environmental evolution with extension to favorable niches for life on Mars.

Grin E. A.
*Predictive Analysis of Groundwater Inflow into Deep Martian Impact Craters* **[#1025]**
We propose a quantitative method for the prediction of groundwater inflow into deep impact craters on Mars derived from civil-engineering methods for the design of hydrograph of groundwater circulation between deep excavations and drained unconfined aquifers.

Homan K. S. Figueredo P. H. Greeley R.
*Latitudinal Distribution of Morphologic Features on Europa Based on Galileo Europa Mission (GEM) Data: Orbits E15 and E17* **[#1960]**
A north to south mosaic of Europa has shown the distribution and orientation of surface features to be consistent with the location of the thinnest part of the ice shell, areas of compressional stress fields, and models of non-synchronous rotation.

Kozak R. C.
*Digital Geologic Maps* **[#1948]**
Digital versions of thirty-three published geologic maps of Mercury, Moon, Mars, Io, Ganymede, and Callisto will be released in various formats on a single CD shortly. The original text and figures will be included.

Marshall J.

*The Enigmatic Longevity of Granular Materials on Mars: The Case for Geologically Episodic Dune Formation* **[#1168]**

Processes mitigating sand attrition are ultimately defeated by the vast time available on Mars. Sand longevity results from long-term climatic cycling. Dune fields undergo relatively brief periods of activity, then lapse into protracted periods of aeolian stasis.

Marshall J. Sauke T.

*Computer Modeling of Electrostatic Aggregation of Granular Materials in Planetary and Astrophysical Settings* **[#1234]**

Computer modeling of natural particulate clouds enables aggregate formation rates and morphology, and cloud collapse or dispersion, to be predicted from initial cloud conditions of density and charge.

Marshall J. Sauke T. Buehler M. Farrell W. Green R. Birchenough A.

*"EGM" (Electrostatics of Granular Matter): A Space Station Experiment to Examine Natural Particulate Systems* **[#1236]**

Microgravity will test an electrostatic dipole model of grain interactions, and provide knowledge of grain-aggregation effects on the behavior and longevity of natural particulate systems.

Marshall J. Smith P. White B. Farrell W.

*"Dust Devils": Gardening Agents on the Surface of Mars, and Hidden Hazards to Human Exploration?* **[#1166]**

Dust devils may be important aeolian agents on Mars. Vortices may "garden" the top centimeters of material — disturbing uniform surface layers, and causing compositional mixing, albedo, color, and spectroscopic changes.

Marshall J. Stratton D.

*Computer Modeling of Sand Transport on Mars Using a Compartmentalized Fluids Algorithm (CFA)* **[#1229]**

On Mars, saltating grains can cause hundreds of secondary reptation trajectories and a consequent ballistic cascading transport effect. We developed a computer model to address this phenomenon using "fluid" compartments defined by grain motion and momentum transfer.

Shevchenko V. V. Skobeleva T. P. Kvaratskhelia O. I.

*A New Lunar Catalog: Spectropolarimetric Parameter of the Lunar Soil Maturity* **[#1318]**

The spectropolarimetric parameter is a unique characteristic that may be used by the remote sensing technique.

Sunshine J. M. Pieters C. M. Pratt S. F. McNaron-Brown K. S.

*Absorption Band Modeling in Reflectance Spectra: Availability of the Modified Gaussian Model* **[#1306]**

The modified Gaussian model, a physically based description of absorption bands in spectra, has been updated to provide compatibility with most computer systems. These new versions, written in MATLAB and IDL, are available at the RELAB Website (www.planetary.brown.edu).

## Small Bodies

Belskaya I. N. Shevchenko V. G.

*Albedo Dependence of Asteroid Opposition Effect* **[#1374]**

The amplitude and width of asteroid opposition effect were shown to depend on albedo in a non-monotonic way with maximum for moderate albedo asteroids. It is impossible to explain neither by coherent backscatter nor shadow hiding effect alone.

Golubeva L. F. Shestopalov D. I.

*On S-Asteroid Surface Material* **[#1061]**

We have emphasized that theoretical simulation of S-asteroid reflectance spectra permits to judge on the very total properties of regolith composition of these minor planets.

Hasegawa S. Abe M.

*Recalculation of IRAS Observed Asteroids Using Three Simple Thermal Models* **[#1546]**

We recalculated the geometric albedos and the diameters of IRAS asteroids with three simple thermal models. The average value of the albedos for this study, which uses all data except for 1 band observation, is about 35% smaller than those in IMPS.

Hicks M. D. Buratti B. J. Rabinowitz D. L. Weissman P. R. Doressoundiram A. Fink U.

*The Deep Space 1 Mission Target 1992 KD: A Connection to Stony Meteorites?* **[#1719]**

Three nights of photometric observations suggest a near-Earth object with extremely atypical colors: more similar to a sample of pure olivine and/or pyroxene than to the vast majority of main-belt asteroids.

Housen K. R. Holsapple K. A.

*A General Scaling Law for Strength-dominated Collisions of Rocky Asteroids* **[#1095]**

A collisional scaling model based on flaw coalescence has been verified through collision tests. This along with observations of faults in terrestrial rocks is used to estimate the specific energy required for fragmentation of rocky asteroids.

Krugly Yu. N. Shevchenko V. G.

*Magnitude Phase Dependence of Asteroid 433 Eros* **[#1595]**

Results of photometric observations of 433 Eros in 1993, 1995 and 1997 are presented. Magnitude phase dependence was obtained in the range 0.3°–31.4°.

Malhotra R.

*Kuiper Belt Objects 1997 SZ10 and 1996 TR66* **[#1810]**

We report on the results of long-term integrations of two KBOs that are likely 2:1 Neptune resonance librators.

Masarik J. Brückner J. Reedy R. C.

*Simulations of Expected Gamma-Ray Fluxes from Asteroids* **[#1663]**

The fluxes of cosmic-ray-produced gamma rays escaping from an asteroid's surface were calculated for 8 chemical compositions corresponding to particular meteorites of various types. Chemical composition strongly affects the fluxes of gamma rays.

Shestopalov D. I. Golubeva L. F.

*Calculations of Reflectance Spectra of S-Asteroids and Their Surface Minerals: Vicissitudes of the Method* **[#1062]**

We summarize our impressions about possibilities of the method of the calculation of diffuse reflectance spectra of polymineral powderlike surface imitating S-asteroid regolith.

## Venus

Basilevsky A. T. Head J. W. III

*Stratigraphy and Sequence of Geologic Events in the History of Venus* **[#1255]**

Two aspects of Venus global stratigraphy are discussed: 1) Unit definitions; and 2) Global synchronicity.

Burba G. A. Blue J. Campbell D. B. Dollfus A. Gaddis L. Jurgens R. F. Marov M. Ya. Pettengill G. H. Stofan E. R.

*Venus Nomenclature Progress Report: The New Names Introduced in 1998* **[#1366]**

19 new names were added on Venus in 1998 (6 craters, 5 fluctus, 1 patera, 3 tholi, 4 valles). All features, but craters, are at Aino Planitia area within 22°–46°S, 67°–105°E. The names are provisional until their final approval in 2000.

Burba G. A. Schaber G. G. Campbell D. B.

*Earth-based Arecibo Radar Data Reveal Two More Large Craters on Venus Beyond the Magellan Files* **[#1756]**

Two new craters, 41 and 19 km in diameter, revealed on Venus with Earth-based Arecibo radar image within the Magellan coverage gap on Lavinia Planitia. There is an inner ring on flat bottom at the larger crater, and a central peak at the smaller one.

Hamilton V. E.

*Structure and History of Taranga Corona: Relationship to Extension at Hecate Chasma, Venus* **[#1536]**
Taranga Corona straddles Hecate Chasma and displays complex structures unlike most other coronae on Venus. A detailed tectonic analysis may shed light on the interaction between this corona and the extensional forces that created Hecate Chasma.

Koronovsky N. N. Galkin V. A.

*Ridges and Crosscutting Grabens Forming in One Part of Thetis Tessera Region — Tectonophysical Modeling* **[#1779]**
Developed 3 stage model of ridges and grabens origin of Thetis tessera region.

Krassilnikov A. S.

*Stratigraphy and Tectonic Evolution of Nefertiti Corona on Venus* **[#1610]**
Study of corona Nefertiti stratigraphy and deformation structures lead to suggestion a scenario of its multistage evolution, including rejuvenation. Part of corona annulus is interpreted to be a landslide.

Krassilnikov A. S. Galkin V. A. Basilevsky A. T.

*Formation of Coronae on Venus. Preliminary Results of Tectonophysical Modeling* **[#1584]**
Coronae formation was modeled in experiments with sand, oil, and wet clay. Deformation of the model within the uplifted dome and after its downwelling was studied. The results are quite similar to those received in the computer modeling.

Perez-de-Tejada H.

*Solar Wind Erosion of the Venus Polar Ionosphere* **[#1005]**
The geometry of the Venus ionosphere is examined using plasma data obtained with the PVO and the Mariner 5 spacecraft. There is evidence that downstream from the magnetic polar regions there are ionospheric channels carved out by the solar wind in the nightside hemisphere.

Pronin A. A.

*Venus: Age Relationships Between Lakshmi Planum Units and Regional Plains* **[#1983]**
Detailed mapping of the western part of Danu mounts illustrates that regional plains with wrinkle ridges outside Lakshmi Planum are younger than smooth plain units inside Lakshmi structure.

Schaber G. G. Strom R. G.

*The USGS/U. of Arizona Database of Venus Impact Craters: Update for 1999* **[#1221]**
The USGS/U. of Arizona Database of Impact Craters on Venus now contains 965 entries that can be accessed via the Internet at http://wwwflag.wr.usgs.gov. Several additional categories of crater data will be added during 1999.

** Denotes speaker*
*UHCL – Bayou Building, University of Houston–Clear Lake*

## AUTHOR INDEX

| | |
|---|---|
| Chicxulub Wkg. Grp. | Impacts I Posters, Tue., p.m., UHCL |
| Chikami J. | Chondrites Posters, Tue., p.m., UHCL |
| Chikami J.* | Achondrites, Thu., p.m., Rm. B |
| Chipera S. | New Instruments...Posters, Thu., p.m., UHCL |
| Choblet G. | Mars Tectonics, Volcanism..., Wed., p.m., Rm. C |
| Choi B.-G.* | Early Solar System..., Tue., a.m., Rm. A |
| Choi B.-G. | Presolar Grains Posters, Tue., p.m., UHCL |
| Choi J. M. | Future Missions...Posters, Tue., p.m., UHCL |
| Christens-Barry W. A. | Surface Processes Posters, Thu., p.m., UHCL |
| Christensen P. | Future Mars Missions Posters, Thu., p.m., UHCL |
| Christensen P. * | MGS: A New Chapter, Tue., a.m., Rm. C |
| Christensen P. | MGS: Volcanics..., Wed., a.m., Rm. C |
| Christensen P. | Education Posters, Thu., p.m., UHCL |
| Christensen P.* | Near-Future Mars Missions, Fri., a.m., Rm. A |
| Christeson G. L. | Impacts I Posters, Tue., p.m., UHCL |
| Christiansen E. H. | Surface Processes Posters, Thu., p.m., UHCL |
| Chuang F. | Europa Posters, Tue., p.m., UHCL |
| Chuang F. | Outer Planet Satellites Posters, Thu., p.m. UHCL |
| Chutjian A. | Future Missions...Posters, Tue., p.m., UHCL |
| Chyba C. | Future Missions...Posters, Tue., p.m., UHCL |
| Chyba C. | Future Planetary Missions, Tue., p.m., Rm. C |
| Ciftcioglu N. | Astrobiology, Thu., p.m., Rm. A |
| Cifuentes H. | Meteorite Mélange Posters, Thu., p.m., UHCL |
| Cini Castagnoli G. | Chondrites II, Fri., a.m., Rm. D |
| Cintala M. J. | Mars Lander Science, Mon., a.m., Rm. C |
| Cintala M. J. | Impacts II Posters, Thu., p.m., UHCL |
| Císarová I. | Print Only: Meteorites |
| Claeys P. | Impacts II Posters, Thu., p.m., UHCL |
| Clancy R. T. | Near-Future Mars Missions, Fri., a.m., Rm. A |
| Clark B. | Future Missions...Posters, Tue., p.m., UHCL |
| Clark B. C. | Mars Lander Science, Mon., a.m., Rm. C |
| Clark B. C. | Future Missions...Posters, Tue., p.m., UHCL |
| Clark B. E. | Small Bodies Posters, Tue., p.m., UHCL |
| Clark P. E.* | Lunar Volcanos, Mon., a.m., Rm. B |
| Clark P. E. | Future Missions...Posters, Tue., p.m., UHCL |
| Clark R. | MGS: A New Chapter, Tue., a.m., Rm. C |
| Clark R. | Planetary Surface Processes, Thu., p.m., Rm. D |
| Clark R. | Europa, Fri., a.m., Rm. C |
| Clayton D. D. | Presolar Grains Posters, Tue., p.m., UHCL |
| Clayton D. D. | Presolar Grains, Mon., a.m., Rm. A |
| Clayton R. N. | Presolar Grains, Mon., a.m., Rm. A |
| Clayton R. N. | Presolar Grains Posters, Tue., p.m., UHCL |
| Clayton R. N.* | Chondrites I, Thu., a.m., Rm. B |
| Clayton R. N. | Achondrites, Thu., p.m., Rm. B |
| Clemett S. | Future Missions...Posters, Tue., p.m., UHCL |
| Clemett S.* | Cosmic Dust, Tue., p.m., Rm. D |
| Clifford S. M. | Mars Climate Posters, Thu., a.m., Rm. C |
| Clifford S. M.* | Near-Future Mars Missions, Fri., a.m., Rm. A |
| Cloudt S. | Cosmogenic Nuclides Posters, Thu., p.m., UHCL |
| Cloutier P. | MGS: A New Chapter, Tue., a.m., Rm. C |
| Cloutier P. | MGS: Volcanics..., Wed., a.m., Rm. C |
| Cloutis E. A.* | Mars Surface Chemistry, Mon., p.m., Rm. C |
| Cloutis E. A. | Small Bodies Posters, Tue., p.m., UHCL |
| Cloutis E. A. | Small Bodies, Wed., p.m., Rm. D |
| Coath C. D. | Martian Meteorites I, Wed., a.m., Rm. A |
| Cody G. D. III* | Astrobiology, Thu., p.m., Rm. A |
| Coffield J. | Education Posters, Thu., p.m., UHCL |
| Cohen J. L. | Mars: General Science Posters, Thu., p.m., UHCL |
| Coles K. S. | Education Posters, Thu., p.m., UHCL |
| Collins G. | Europa Posters, Tue., p.m., UHCL |
| Collins G. | Print Only: Outer Planets and Satellites |
| Collins G. | Outer Planet Satellites Posters, Thu., p.m. UHCL |
| Collins G. | Europa, Fri., a.m., Rm. C |
| Collins S. | New Instruments...Posters, Thu., p.m., UHCL |
| Colson R. O. | Print Only: New Instruments and Techniques |
| Colson R. O.* | Interior Processes, Mon., p.m., Rm. B |
| Colson R. O. | Interior Processes Posters, Tue., p.m., UHCL |
| Colvin T. | Outer Planet Satellites Posters, Thu., p.m. UHCL |
| Colvin T. | Future Mars Missions Posters, Thu., p.m., UHCL |
| Colwell W. B. | Small Bodies Posters, Tue., p.m., UHCL |
| Colwell W. B. | Small Icy Bodies Posters, Thu., p.m., UHCL |
| Combie J. | Astrobiology Posters, Tue., p.m., UHCL |
| Connelly J. N. | Martian Meteorites I, Wed., a.m., Rm. A |
| Connerney J. E. | Future Missions...Posters, Tue., p.m., UHCL |
| Connerney J. E. | MGS: A New Chapter, Tue., a.m., Rm. C |
| Connolly H. C. Jr.* | CAIs, Tue., p.m., Rm. A |
| Consolmagno G. J. | Chondrites Posters, Tue., p.m., UHCL |
| Consolmagno G. J.* | Small Bodies, Wed., p.m., Rm. D |
| Cook A. C.* | Lunar Poles and Regolith, Thu., a.m., Rm. D |
| Cook A. C. | Mercury Posters, Thu., p.m., UHCL |
| Cook D. | MGS and Pathfinder Posters, Tue., p.m., UHCL |
| Cook D. | Outer Planet Satellites Posters, Thu., p.m. UHCL |
| Cook D. | Future Mars Missions Posters, Thu., p.m., UHCL |
| Cooke D. | Print Only: Impacts |
| Coombs C. R. | Lunar Volcanos...Posters, Tue., p.m., UHCL |
| Coombs C. R. | Lunar Poles and...Posters, Thu., p.m., UHCL |
| Coombs C. R. | Surface Processes Posters, Thu., p.m., UHCL |
| Cooper C. D.* | MGS: Volcanics..., Wed., a.m., Rm. C |
| Cooper C. D. | Mars: General Science Posters, Thu., p.m., UHCL |
| Coquilla R. | Print Only: Mars |
| Cordua W. S. | Impacts I, Mon., a.m., Rm. D |
| Corrigan C. M. | Impacts I, Mon., a.m., Rm. D |
| Coustenis A. | Future Planetary Missions, Tue., p.m., Rm. C |
| Cowan J. | Lunar Missions...Posters, Thu., p.m., UHCL |
| Craddock R. A. | Mars Climate Posters, Thu., a.m., Rm. C |
| Crawford D. | Print Only: Impacts |
| Cremers D. A. | Future Mars Missions Posters, Thu., p.m., UHCL |
| Cremers D. A. | New Instruments...Posters, Thu., p.m., UHCL |
| Cresswell R. G. | Impacts II Posters, Thu., p.m., UHCL |
| Crider D. | MGS: A New Chapter, Tue., a.m., Rm. C |
| Crider D. | MGS: Volcanics..., Wed., a.m., Rm. C |
| Crisp D. | Future Missions...Posters, Tue., p.m., UHCL |
| Crisp J. A. | MGS and Pathfinder Posters, Tue., p.m., UHCL |
| Croft S. K. | Education Posters, Thu., p.m., UHCL |
| Crooks J. L. | Print Only: Mars |
| Croskell M. S. | Impacts II Posters, Thu., p.m., UHCL |
| Crowley J. K. | Print Only: Outer Planets and Satellites |
| Crowley J. K. | Europa, Fri., a.m., Rm. C |
| Crown D. | MGS: Volcanics..., Wed., a.m., Rm. C |
| Crown D.* | Planetary Surface Processes, Thu., p.m., Rm. D |
| Crown D. | Surface Processes Posters, Thu., p.m., UHCL |
| Crown D. | Outer Planet Satellites Posters, Thu., p.m. UHCL |
| Crumpler L. S. | Print Only: Mars |
| Crumpler L. S. | Surface Processes Posters, Thu., p.m., UHCL |
| Curtis S. | Future Missions...Posters, Tue., p.m., UHCL |
| Cutts J. | Future Missions...Posters, Tue., p.m., UHCL |
| Cuzzi J. N.* | Chondrules, Wed., p.m., Rm. A |
| Dahl J. M.* | Impacts II, Wed., a.m., Rm. B |
| Dahlgren M. | Small Icy Bodies Posters, Thu., p.m., UHCL |
| Dalton J. B.* | Europa, Fri., a.m., Rm. C |
| Dass J. D. | Impacts I, Mon., a.m., Rm. D |
| Daubar I. | MGS: Oceans, Basins..., Tue., p.m., Rm. C |
| Davies A. G.* | Io, Thu., p.m., Rm. C |
| Davies A. G. | New Instruments...Posters, Thu., p.m., UHCL |
| Davies A. G. | Surface Processes Posters, Thu., p.m., UHCL |
| Davies M. | Outer Planet Satellites Posters, Thu., p.m. UHCL |
| Davies M. | Future Mars Missions Posters, Thu., p.m., UHCL |
| Davies M. | Mars Lander Science, Mon., a.m., Rm. C |
| Davis A. M. | Print Only: Meteorites |
| Davis A. M. | Presolar Grains, Mon., a.m., Rm. A |
| Davis A. M. | CAIs, Tue., p.m., Rm. A |
| Davis A. M. | Early Solar System..., Tue., a.m., Rm. A |
| Davis A. M. | Presolar Grains Posters, Tue., p.m., UHCL |
| Davis A. M. | Venus Posters, Tue., p.m., UHCL |
| Davis A. M. | Achondrites Posters, Thu., p.m., UHCL |
| Davis D. R.* | Origins, Wed., a.m., Rm. D |
| Davis H. J. | Future Missions...Posters, Tue., p.m., UHCL |
| Daydou Y. H. | New Moon II: Major Lunar..., Tue., p.m., Rm. B |
| Deans M. | Meteorite Mélange Posters, Thu., p.m., UHCL |
| De Carli P. S. | Print Only: Impacts |
| De Hon R. A. | Mars Climate Posters, Thu., a.m., Rm. C |
| Del Genio A. | Future Planetary Missions, Tue., p.m., Rm. C |
| Delaney J. S. | Print Only: Meteorites |
| Delaney J. S.* | Martian Meteorites II, Thu., a.m., Rm. A |
| Delaney J. S. | New Instruments...Posters, Thu., p.m., UHCL |
| Delaney J. S. | Meteorite Mélange Posters, Thu., p.m., UHCL |
| Delaney J. S. | Martian Meteorites Posters, Thu., p.m., UHCL |
| Delano J. W. | Astrobiology Posters, Tue., p.m., UHCL |

| | |
|---|---|
| Deloule E. | Chondrules, Wed., p.m., Rm. A |
| Demura H. | Mars: General Science Posters, Thu., p.m., UHCL |
| Dence M. R. | Print Only: Impacts |
| Denk T. | Print Only: Outer Planets and Satellites |
| Denk T. | Outer Planet Satellites Posters, Thu., p.m. UHCL |
| Des Marais D. | Future Mars Missions Posters, Thu., p.m., UHCL |
| Desch S. J.* | Chondrules, Wed., p.m., Rm. A |
| Dettman D. L. | Martian Meteorites Posters, Thu., p.m., UHCL |
| Deutsch A. | Print Only: Impacts |
| DeVall M. | Print Only: Mars |
| di Tada M. L. | Impacts II Posters, Thu., p.m., UHCL |
| Diallo D. P. | Impacts I Posters, Tue., p.m., UHCL |
| Dickey J. O. | New Moon Views Posters, Tue., p.m., UHCL |
| Dickinson T. L. | Achondrites, Thu., p.m., Rm. B |
| Dickinson T. L. | Achondrites Posters, Thu., p.m., UHCL |
| Dikov Yu. P. | Print Only: Moon |
| Dikov Yu. P. | Impacts II Posters, Thu., p.m., UHCL |
| Diósy T. | Education Posters, Thu., p.m., UHCL |
| Dohm J. M. | Venus Posters, Tue., p.m., UHCL |
| Dohm J. M. | Mars Tectonics, Volcanism..., Wed., p.m., Rm. C |
| Doke T. | Lunar Missions...Posters, Thu., p.m., UHCL |
| Dollfus A. | Print Only: Venus |
| Dombard A. J.* | Icy Satellites, Tue., a.m., Rm. D |
| Domeneghetti M. C. | Lunar Highlands, Wed., p.m., Rm. B |
| Domingue D. | Future Missions...Posters, Tue., p.m., UHCL |
| Domingue D. | Small Bodies Posters, Tue., p.m., UHCL |
| Domingue D. | Lunar Poles and...Posters, Thu., p.m., UHCL |
| Don Gy. | Impacts I Posters, Tue., p.m., UHCL |
| Donahue D. J. | Cosmogenic Nuclides Posters, Thu., p.m., UHCL |
| Dones L. | Icy Satellites, Tue., a.m., Rm. D |
| Doressoundiram A. | Print Only: Small Bodies |
| Doressoundiram A. | Small Icy Bodies Posters, Thu., p.m., UHCL |
| Dorrer E. | MGS and Pathfinder Posters, Tue., p.m., UHCL |
| Dorsky L. | Future Missions...Posters, Tue., p.m., UHCL |
| Doser D. | Print Only: Impacts |
| Dougherty J. R. | Print Only: Meteorites |
| Dougherty J. R.* | Early Solar System..., Tue., a.m., Rm. A |
| Dowling T. | Future Planetary Missions, Tue., p.m., Rm. C |
| Drábek M. | Iron Meteorites Posters, Thu., p.m., UHCL |
| Drake M. J. | Interior Processes, Mon., p.m., Rm. B |
| Drake M. J. | Interior Processes Posters, Tue., p.m., UHCL |
| Drake M. J. | Lunar Highlands, Wed., p.m., Rm. B |
| Drake M. J. | Mars: General Science Posters, Thu., p.m., UHCL |
| Dreibus G.* | Mars Lander Science, Mon., a.m., Rm. C |
| Dreibus G. | Martian Meteorites I, Wed., a.m., Rm. A |
| Drommer B. | Education Posters, Thu., p.m., UHCL |
| Drossart P. | Future Missions...Posters, Tue., p.m., UHCL |
| Drummond J. | Print Only: IDPs |
| Dubrovinsky L. | Martian Meteorites II, Thu., a.m., Rm. A |
| Dubuffet F.* | Venus, Mon., p.m., Rm. A |
| Duke C. L. | Chondrites Posters, Tue., p.m., UHCL |
| Duke M. | Lunar Missions...Posters, Thu., p.m., UHCL |
| Dunkin S. K. | New Moon II: Major Lunar..., Tue., p.m., Rm. B |
| Dunkin S. K. | New Moon Views Posters, Tue., p.m., UHCL |
| Dunkin S. K. | Lunar Volcanos...Posters, Tue., p.m., UHCL |
| Dunkin S. K. | Education Posters, Thu., p.m., UHCL |
| Dupuis C. | Impacts I, Mon., a.m., Rm. D |
| Durand-Manterola H. J. | Europa Posters, Tue., p.m., UHCL |
| Durand-Manterola H. J. | Mars: General Science Posters, Thu., p.m., UHCL |
| Duraud J. P. | Chondrites II, Fri., a.m., Rm. D |
| Durda D. D. | Print Only: Outer Planets and Satellites |
| Durham W. B. | Mars Climate Posters, Thu., a.m., Rm. C |
| Durham W. B. | Mars: General Science Posters, Thu., p.m., UHCL |
| d'Uston C. | New Moon Views Posters, Tue., p.m., UHCL |
| d'Uston C. | Future Mars Missions Posters, Thu., p.m., UHCL |
| d'Uston C. | Lunar Missions...Posters, Thu., p.m., UHCL |
| Duval P. | Mars Climate Posters, Thu., a.m., Rm. C |
| Duxbury T. | New Moon Views Posters, Tue., p.m., UHCL |
| Dyar M. D. | Print Only: Meteorites |
| Dyar M. D. | Martian Meteorites II, Thu., a.m., Rm. A |
| Dyar M. D. | New Instruments...Posters, Thu., p.m., UHCL |
| Dyar M. D. | Meteorite Mélange Posters, Thu., p.m., UHCL |
| Ebel B. | Future Missions...Posters, Tue., p.m., UHCL |
| Ebel D. S.* | Impacts I, Mon., a.m., Rm. D |

| | |
|---|---|
| Ebihara M. | Martian Meteorites II, Thu., a.m., Rm. A |
| Ebihara M. | Achondrites, Thu., p.m., Rm. B |
| Ebihara M. | Recipes for Lunar...Posters, Thu., p.m. UHCL |
| Economou T. | Mars Lander Science, Mon., a.m., Rm. C |
| Economou T. | Future Mars Missions PostersThu., p.m., UHCL |
| Edgett K. | MGS and Pathfinder Posters, Tue., p.m., UHCL |
| Edgett K.* | MGS: A New Chapter, Tue., a.m., Rm. C |
| Eflmov G. B. | Print Only: Future Missions |
| Eiler J. M.* | Mars Surface Chemistry, Mon., p.m., Rm. C |
| Ekholm A. G.* | Impacts II, Wed., a.m., Rm. B |
| Ekholm A. G. | Small Icy Bodies Posters, Thu., p.m., UHCL |
| El Goresy A.* | Martian Meteorites II, Thu., a.m., Rm. A |
| Eliason E. | New Moon II: Major Lunar..., Tue., p.m., Rm. B |
| Eliason E. | MGS and Pathfinder Posters, Tue., p.m., UHCL |
| Eliason E. | New Moon Views Posters, Tue., p.m., UHCL |
| Eliason E. | Lunar Missions...Posters, Thu., p.m., UHCL |
| Elkins L. T.* | Lunar Volcanos, Mon., a.m., Rm. B |
| Elkins L. T. | Lunar Volcanos...Posters, Tue., p.m., UHCL |
| Elliott D. | New Instruments...Posters, Thu., p.m., UHCL |
| Elphic R. C.* | New Moon I: Hot Spots..., Tue., a.m., Rm. B |
| Ely J. C. | Mars Tectonics, Volcanism..., Wed., p.m., Rm. C |
| Emori H. | Presolar Grains Posters, Tue., p.m., UHCL |
| Emrick C. M.* | Mars Climate Posters, Thu., a.m., Rm. C |
| Eneev T. M. | Print Only: Future Missions |
| Eng P. | Cosmic Dust Posters, Mon., p.m., UHCL |
| Englert P. A. J. | Future Mars Missions Posters, p.m, UHCL |
| Engrand C.* | Cosmic Dust, Tue., p.m., Rm. D |
| Eppler D. B. | Future Missions...Posters, Tue., p.m., UHCL |
| Erard S. | New Moon II: Major Lunar..., Tue., p.m., Rm. B |
| Ernst R. E. | Surface Processes Posters, Thu., p.m., UHCL |
| Ertel W. | Interior Processes Posters, Tue., p.m., UHCL |
| Esquerdo G. A. | MGS: A New Chapter, Tue., a.m., Rm. C |
| Eugster O.* | Lunar Highlands, Wed., p.m., Rm. B |
| Eugster O. | Chondrites II, Fri., a.m., Rm. D |
| Evans C. A. | Surface Processes Posters, Thu., p.m., UHCL |
| Evans L. | Lunar Volcanos, Mon., a.m., Rm. B |
| Evans L. | Future Mars Missions Posters, Thu., p.m., UHCL |
| Eyerman C. | Future Missions...Posters, Tue., p.m., UHCL |
| Ezer R. | Cosmic Dust Posters, Mon., p.m., UHCL |
| Fagan T. J.* | CAIs, Tue., p.m., Rm. A |
| Fagan T. J. | Chondrites Posters, Tue., p.m., UHCL |
| Fagents S. A. | Europa Posters, Tue., p.m., UHCL |
| Fagents S. A. | Planetary Surface Processes, Thu., p.m., Rm. D |
| Fahey A. J.* | Presolar Grains, Mon., a.m., Rm. A |
| Fanale F. | Europa Posters, Tue., p.m., UHCL |
| Fanale F. | Europa, Fri., a.m., Rm. C |
| Färber G. | Print Only: IDPs |
| Farinella P. | Origins, Wed., a.m., Rm. D |
| Farmer J. D. | Astrobiology Posters, Tue., p.m., UHCL |
| Farmer J. D. | Future Missions...Posters, Tue., p.m., UHCL |
| Farmer J. D. | Future Mars Missions Posters, Thu., p.m., UHCL |
| Farquhar J.* | Martian Meteorites II, Thu., a.m., Rm. A |
| Farrand W. H.* | Mars Surface Chemistry, Mon., p.m., Rm. C |
| Farrell W. | Print Only: Surface Processes |
| Farrell W. | New Instruments...Posters, Thu., p.m., UHCL |
| Faulkner S. E. | MGS: Volcanics..., Wed., a.m., Rm. C |
| Fegley B. | Future Missions...Posters, Tue., p.m., UHCL |
| Fegley B. | Io, Thu., p.m., Rm. C |
| Fei Y. | Interior Processes, Mon., p.m., Rm. B |
| Fei Y. | Martian Meteorites I, Wed., a.m., Rm. A |
| Fei Y. | Martian Meteorites Posters, Thu., p.m., UHCL |
| Fel'dman V. I. | Print Only: Impacts |
| Feldman J. | New Instruments...Posters, Thu., p.m., UHCL |
| Feldman P. | Future Planetary Missions, Tue., p.m., Rm. C |
| Feldman V. I. | Print Only: Impacts |
| Feldman W. C.* | New Moon I: Hot Spots..., Tue., a.m., Rm. B |
| Feldman W. C. | Future Mars Missions Posters, Thu., p.m., UHCL |
| Fellows C. W. | Future Mars Missions Posters, Thu., p.m., UHCL |
| Feng H. | Cosmic Dust Posters, Mon., p.m., UHCL |
| Fenton L. | MGS: Oceans, Basins..., Tue., p.m., Rm. C |
| Ferko T. E.* | Chondrites II, Fri., a.m., Rm. D |
| Ferris J. P. | Astrobiology Posters, Tue., p.m., UHCL |
| Ferris M. J. | Future Mars Missions Posters, Thu., p.m., UHCL |
| Ferry S. | Near-Future Mars Missions, Fri., a.m., Rm. A |

| | |
|---|---|
| Kosmo J. | Print Only: Mars |
| Kosmo J. | Future Missions...Posters, Tue., p.m., UHCL |
| Kotelnikov S. I. | Print Only: Impacts |
| Kovach R. L. | Future Planetary Missions, Tue., p.m., Rm. C |
| Kozak R. C. | Print Only: Surface Processes |
| Koziol A. M. | Martian Meteorites Posters, Thu., p.m., UHCL |
| Kraft M. D. | MGS and Pathfinder Posters, Tue., p.m., UHCL |
| Krähenbühl U. | Chondrites II, Fri., a.m., Rm. D |
| Kramer G. M. | Mars Lander Science, Mon., a.m., Rm. C |
| Krassilnikov A. S. | Print Only: Venus |
| Krause M. O. | Venus Posters, Tue., p.m., UHCL |
| Krbetschek M. R. | Meteorite Mélange Posters, Thu., p.m., UHCL |
| Kreslavsky M.* | Venus, Mon., p.m., Rm. A |
| Kreslavsky M. | New Moon II: Major Lunar..., Tue., p.m., Rm. B |
| Kreslavsky M.* | MGS: Oceans, Basins..., Tue., p.m., Rm. C |
| Kreslavsky M. | New Moon Views Posters, Tue., p.m., UHCL |
| Kreslavsky M. | MGS and Pathfinder Posters, Tue., p.m., UHCL |
| Krestina N. | Martian Meteorites I, Wed., a.m., Rm. A |
| Krestina N.* | Chondrites I, Thu., a.m., Rm. B |
| Kriens B. J. | Impacts I Posters, Tue., p.m., UHCL |
| Kring D. A. | Future Mars Missions Posters, Thu., p.m., UHCL |
| Kring D. A. | Martian Meteorites Posters, Thu., p.m., UHCL |
| Kring D. A.* | Chondrites II, Fri., a.m., Rm. D |
| Krompholz R. | Impacts II Posters, Thu., p.m., UHCL |
| Kronberg P. | Mars: General Science Posters, Thu., p.m., UHCL |
| Krot A. N. | Print Only: Meteorites |
| Krot A. N.* | CAIs, Tue., p.m., Rm. A |
| Krot A. N. | Chondrites Posters, Tue., p.m., UHCL |
| Krot A. N. | Small Bodies, Wed., p.m., Rm. D |
| Krot A. N. | Chondrites I, Thu., a.m., Rm. B |
| Kruep J. M. | Lunar Missions...Posters, Thu., p.m., UHCL |
| Krugly Yu. N. | Print Only: Small Bodies |
| Kryuchkov V. P. | Venus, Mon., p.m., Rm. A |
| Kryuchkov V. P. | Venus Posters, Tue., p.m., UHCL |
| Kubo K. | Lunar Missions...Posters, Thu., p.m., UHCL |
| Kubovics I. | Education Posters, Thu., p.m., UHCL |
| Kucinskas A. B. | Venus Posters, Tue., p.m., UHCL |
| Kudryavtsev A. B. | Martian Meteorites Posters, Thu., p.m., UHCL |
| Kuebler K. | Mars Surface Chemistry, Mon., p.m., Rm. C |
| Kuebler K. | Future Mars Missions Posters, Thu., p.m., UHCL |
| Kuebler K. | Print Only: Mars |
| Kulikov S. D. | Print Only: Future Missions |
| Kurat G. | Print Only: IDPs |
| Kurat G. | Chondrites Posters, Tue., p.m., UHCL |
| Kurat G. | Chondrites I, Thu., a.m., Rm. B |
| Kurat G. | Chondrites II, Fri., a.m., Rm. D |
| Kurita K. | Print Only: Outer Planets and Satellites |
| Kurita K. | Europa Posters, Tue., p.m., UHCL |
| Kurita K. | Mars: General Science Posters, Thu., p.m., UHCL |
| Kurita K. | Impacts II Posters, Thu., p.m., UHCL |
| Kurotaki K. | Presolar Grains Posters, Tue., p.m., UHCL |
| Kuzmin R. O.* | Mars Lander Science, Mon., a.m., Rm. C |
| Kuzmin R. O. | Surface Processes Posters, Thu., p.m., UHCL |
| Kvaratskhelia O. I. | Print Only: Surface Processes |
| Lagerkvist C.-I. | Small Icy Bodies Posters, Thu., p.m., UHCL |
| Lagerros J. | Small Icy Bodies Posters, Thu., p.m., UHCL |
| Lanagan P. | MGS: Volcanics..., Wed., a.m., Rm. C |
| Lanagan P. | MGS and Pathfinder Posters, Tue., p.m., UHCL |
| Landgraf M. | Cosmic Dust Posters, Mon., p.m., UHCL |
| Landgraf M. | Future Missions...Posters, Tue., p.m., UHCL |
| Landheim R. | Surface Processes Posters, Thu., p.m., UHCL |
| Landis G. A. | Near-Future Mars Missions, Fri., a.m., Rm. A |
| Lane A. L. | Icy Satellites, Tue., a.m., Rm. D |
| Lane M. | MGS: A New Chapter, Tue., a.m., Rm. C |
| Lane M. | Mars Surface Chemistry, Mon., p.m., Rm. C |
| Lane M.* | MGS: Volcanics..., Wed., a.m., Rm. C |
| Lange D. | Iron Meteorites, Fri., a.m., Rm. B |
| Lange M. A. | Impacts II Posters, Thu., p.m., UHCL |
| Langenhorst F. | Print Only: Impacts |
| Langevin Y. | New Moon II: Major Lunar..., Tue., p.m., Rm. B |
| Langwost P. | Education Posters, Thu., p.m., UHCL |
| Larsen K. W.* | Mars Lander Science, Mon., a.m., Rm. C |
| Larson P. B. | Martian Meteorites Posters, Thu., p.m., UHCL |
| Larson S. M. | Outer Planet Satellites Posters, Thu., p.m. UHCL |
| LaTourrette T.* | CAIs, Tue., p.m., Rm. A |
| Lauer H. V. Jr.* | Interior Processes, Mon., p.m., Rm. B |
| Lauer H. V. Jr. | Future Mars Missions Posters, Thu., p.m., UHCL |
| Lauretta D. S.* | Chondrites I, Thu., a.m., Rm. B |
| Lavielle B. | Iron Meteorites, Fri., a.m., Rm. B |
| Lavrukhina A. K. | Print Only: Meteorites |
| Law C. | MGS: Volcanics..., Wed., a.m., Rm. C |
| Law C. | MGS: A New Chapter, Tue., a.m., Rm. C |
| Lawrence D. J.* | New Moon I: Hot Spots..., Tue., a.m., Rm. B |
| Lawson S. L.* | New Moon II: Major Lunar..., Tue., p.m., Rm. B |
| Le L. | Lunar Volcanos, Mon., a.m., Rm. B |
| Le L. | Chondrules, Wed., p.m., Rm. A |
| Le L. | Achondrites, Thu., p.m., Rm. B |
| Le Mouélic S. | New Moon II: Major Lunar..., Tue., p.m., Rm. B |
| Leake M. A. | Education Posters, Thu., p.m., UHCL |
| Lebofsky L. A. | Small Bodies, Wed., p.m., Rm. D |
| Lee E. | MGS and Pathfinder Posters, Tue., p.m., UHCL |
| Lee E. | Future Mars Missions Posters, Thu., p.m., UHCL |
| Lee E. | New Moon II: Major Lunar..., Tue., p.m., Rm. B |
| Lee E. | New Moon Views Posters, Tue., p.m., UHCL |
| Lee E. | Lunar Missions...Posters, Thu., p.m., UHCL |
| Lee P. | Future Missions...Posters, Tue., p.m., UHCL |
| Lee P. | Mars Climate Posters, Thu., a.m., Rm. C |
| Lee P. | Meteorite Mélange Posters, Thu., p.m., UHCL |
| Lee S. W. | Near-Future Mars Missions, Fri., a.m., Rm. A |
| Lefevre I. | Impacts II Posters, Thu., p.m., UHCL |
| Lefèvre I. | Impacts I, Mon., a.m., Rm. D |
| Lemmon M. | MGS and Pathfinder Posters, Tue., p.m., UHCL |
| Lemmon M. | Mars Lander Science, Mon., a.m., Rm. C |
| Lentz R. C. F.* | Martian Meteorites II, Thu., a.m., Rm. A |
| Leone G. | Outer Planet Satellites Posters, Thu., p.m. UHCL |
| Lescinsky D. T.* | Planetary Surface Processes, Thu., p.m., Rm. D |
| Leshin L. A. | Cosmic Dust, Tue., p.m., Rm. D |
| Leskowitz G. | New Instruments...Posters, Thu., p.m., UHCL |
| Levison H. | Icy Satellites, Tue., a.m., Rm. D |
| Levison H. | Print Only: Mars |
| Levison H. | Origins, Wed., a.m., Rm. D |
| Lewis R. | Presolar Grains, Mon., a.m., Rm. A |
| Lewis R. | Presolar Grains Posters, Tue., p.m., UHCL |
| Li Chunlai | Chondrules, Wed., p.m., Rm. A |
| Li J.* | Chondrites I, Thu., a.m., Rm. B |
| Li L.* | Lunar Poles and Regolith, Thu., a.m., Rm. D |
| Lias J. | Mars Tectonics, Volcanism..., Wed., p.m., Rm. C |
| Lias J. | Mars: General Science Posters, Thu., p.m., UHCL |
| Libourel G. | Print Only: Origins |
| Libourel G.* | Chondrules, Wed., p.m., Rm. A |
| Lichtenberg C. | Lunar Poles and Regolith, Thu., a.m., Rm. D |
| Liermann H. P.* | Achondrites, Thu., p.m., Rm. B |
| Lin D. | Future Planetary Missions, Tue., p.m., Rm. C |
| Lin L. | Print Only: Moon |
| Lin R. P.* | New Moon I: Hot Spots..., Tue., a.m., Rm. B |
| Lin R. P. | MGS: A New Chapter, Tue., a.m., Rm. C |
| Lin R. P. | New Moon Views Posters, Tue., p.m., UHCL |
| Lin R. P. | MGS: Volcanics..., Wed., a.m., Rm. C |
| Lin R. P. | Lunar Highlands, Wed., p.m., Rm. B |
| Lindemann R. | Future Missions...Posters, Tue., p.m., UHCL |
| Lindstrom D. J. | Print Only: Moon |
| Lindstrom D. J. | Achondrites, Thu., p.m., Rm. B |
| Lindstrom M. M. | Lunar Volcanos...Posters, Tue., p.m., UHCL |
| Lindstrom M. M. | Martian Meteorites II, Thu., a.m., Rm. A |
| Lindstrom M. M. | Education Posters, Thu., p.m., UHCL |
| Linkin V. M. | Future Mars Missions Posters, Thu., p.m., UHCL |
| Liou J.-C. | Cosmic Dust Posters, Mon., p.m., UHCL |
| Liou J.-C.* | Origins, Wed., a.m., Rm. D |
| Lipschutz M. E.* | Chondrites II, Fri., a.m., Rm. D |
| Litvak M. L. | Near-Future Mars Missions, Fri., a.m., Rm. A |
| Litvin D. A. | Near-Future Mars Missions, Fri., a.m., Rm. A |
| Liu K. | Impacts II Posters, Thu., p.m., UHCL |
| Liu W. | Print Only: Meteorites |
| Liu W.* | Presolar Grains, Mon., a.m., Rm. A |
| Llorca J. | Cosmic Dust, Tue., p.m., Rm. D |
| Lofgren G. E. | Martian Meteorites I, Wed., a.m., Rm. A |
| Lofgren G. E.* | Chondrules, Wed., p.m., Rm. A |
| Lofgren G. E. | Martian Meteorites Posters, Thu., p.m., UHCL |

# Notes